

IMPACT PRESSURES OF SEA WAVES

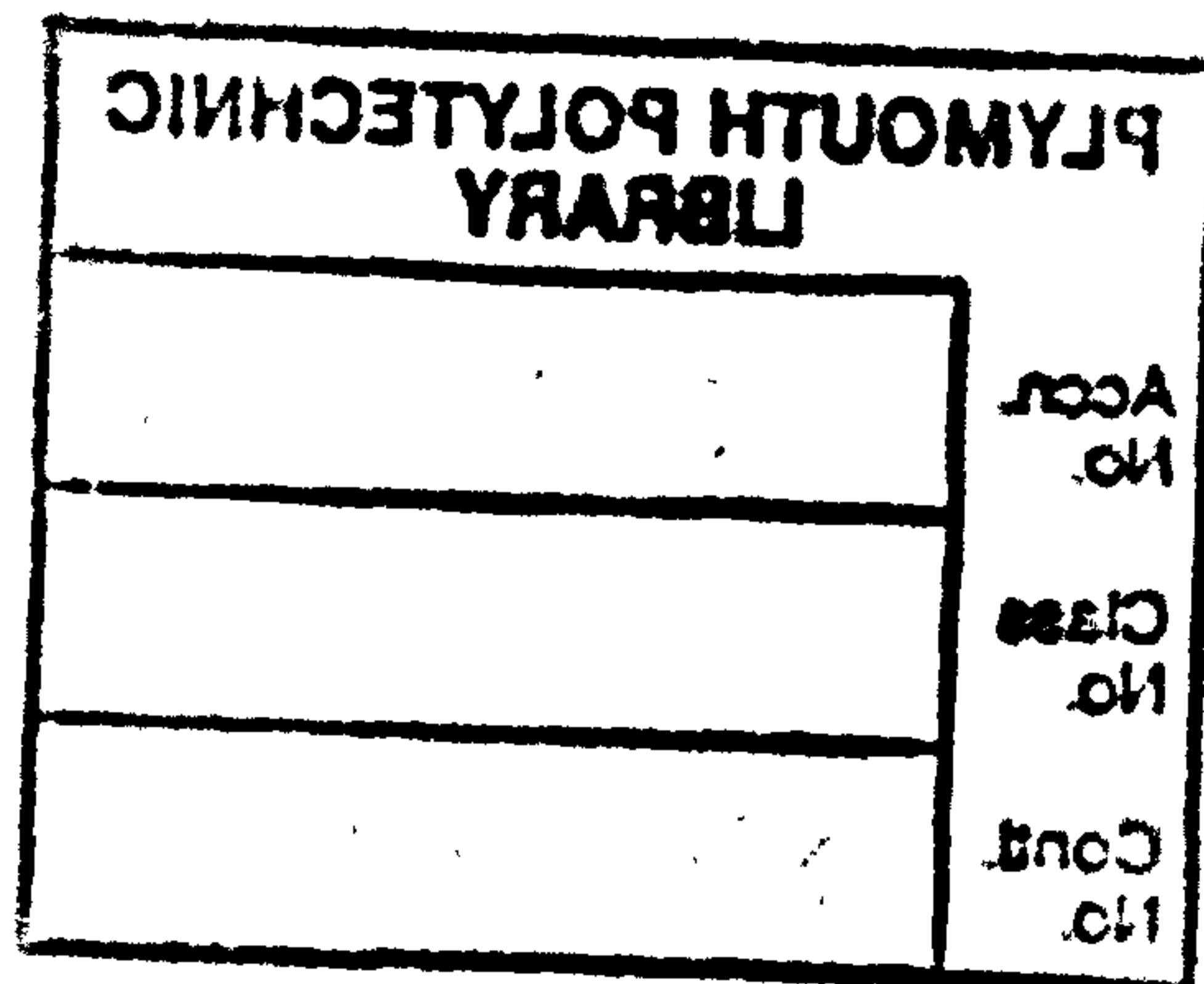
by

ALEXANDER L. ROSSI. B.E. & A., M.Sc. D.I.C.

This thesis is submitted in partial fulfilment of the requirements for the degree of Doctor of Philosophy

to

The Council for National Academic Awards



Department of Civil Engineering

Faculty of Technology

Plymouth Polytechnic

Plymouth

Collaborating Establishment

S.W.W.A.

November 1984

To Lexia ...

[Faint, illegible text, possibly bleed-through from the reverse side of the page]

CONTENTS	PAGE
ACKNOWLEDGEMENTS	i
DECLARATION	iii
ABSTRACT	iv
ABBREVIATIONS AND PRINCIPAL SYMBOLS	v
INTRODUCTION	1
HISTORICAL BACKGROUND	9
CHAPTER ONE	
1.0 INSTRUMENTATION	16
1.1 PRESSURE TRANSDUCERS	17
1.2 CALIBRATION	20
1.2.1 Static Calibration	21
1.2.2 Integral Properties	21
1.2.3 Dynamic Pressure Response	22
1.3 MODIFIED DESIGN	25
1.3.1 Balance Control	25
1.3.2 Signal-to-Noise Considerations	26
1.3.3 Amplification Control	27
1.3.4 Other Considerations	28
1.4 SITE ARRANGEMENT	29
1.4.1 Vertical Arrangement	29
1.4.2 Horizontal Arrangement	31
1.4.3 Beach Array	31
1.4.4 Single Recording	33
1.5 AMPLIFICATION	34
1.5.1 On Site Considerations	35
1.6 RECORDING	37
1.6.1 Characteristics Of The Recording Facility	37
1.6.2 Alignment Procedure	39
1.6.3 Field Considerations	39

	PAGE	
1.7	REMOTE MECHANISM	42
1.8	FACTORS OPTIMISING STRAIN MEASUREMENT	43
1.8.1	Gauge Bonding For Optimum Performance	45
1.9	ACCURACIES IN MEASUREMENT	47
1.9.1	Optimisation Of Results	48
 CHAPTER TWO		
2.0	SITE CONSIDERATIONS	58
2.1	THE SITE LOCATION	59
2.1.1	Fixing Considerations	61
2.1.2	The Alternative Site	62
2.2	TIDAL EFFECTS	65
2.2.1	Differences In Tidal Levels	65
2.2.2	Currents Associated With Water Movements	67
2.2.3	Tide As A Favourable Factor For The Chosen Site	68
2.2.4	Meteorological Influences On Tides. Surges	69
2.3	FREQUENCY OF USE. FORECASTING	70
2.3.1	Wave Height Distribution	70
2.3.2	Wave Period Distribution	72
2.3.3	Random Wave Field In Nature	73
2.3.4	Useful Spectra For Comparison	75
2.3.5	Values Obtained From Energy Spectra	77
2.3.6	Directional Influence	78
2.3.7	Forecasting	79
2.4	WIND DATA	82
2.4.1	General Pattern Of Winds	83
2.4.2	Wind Wave Field - Waves In A Generated Area	85
2.4.3	Applications Of Wave Climates	86
2.4.4	The Effects Of Wave Heights And Energy Of Waves On Leaving The Generated Area	87
2.5	VARIATIONS OF RECORDED WAVES WHEN COMPARED TO DEEP WATER WAVES	89
2.5.1	Wave Refraction	90
2.5.2	Diffraction	92
2.5.3	Reflection And Transmission	92
2.5.4	Currents. Type Of Wave Breakers	95
 CHAPTER THREE		
3.0	DATA ACQUISITION	129
3.1	RANDOM SIGNAL PROCESSING	130
3.1.1	Introduction To Concepts Included In Digital Process	135

	PAGE	
3.1.2	Discrete Time System	136
3.1.3	The Sequence	137
3.2	PREPROCESSING	139
3.2.1	Storing Data Temporarily	140
3.2.2	Preparation For Preprocessing	142
3.2.3	Reformatting And Conversion	144
3.3	PREQUALIFICATION	146
3.3.1	Trend Removal	147
3.4	QUALIFICATION	149
3.4.1	Probability Density Function	151
3.4.2	Standardisation Of Variable (Dependent)	152
3.5	ANALOGUE TO DIGITAL CONVERSION	154
3.5.1	Particulars Of Multiprogrammer For Conversion To Digital Output	154
3.5.2	Fundamentals Of Program Sequence	156
3.5.3	Other Uses For Computer Software	158
3.6	DIGITAL FILTERING	161
3.6.1	Filtering Design	161
3.6.2	Removal Of The DC Component	163
3.6.3	Filter Types	164
3.6.4	Windowing	166
3.6.5	Mechanics Of Windowing Function	167
3.6.6	Further Averaging For Resolution And Smoothing Improvements. Segmentation	169
3.7	TRANSIENT ANALYSIS	172
3.7.1	Triggering Mode	174
3.7.2	Digital Storage	176
3.7.3	Sources Of Error In The Digitisation Process	178
3.8	DEVIATION FROM NORMAL DISTRIBUTION	181
3.8.1	The Effect Of Amplitude Distribution by Linear Processing	
 CHAPTER FOUR		
4.0	WAVE THEORIES. TIME SERIES ANALYSIS	200
4.1	INTRODUCTION	201
4.2	WAVE THEORIES	204
4.2.1	Assumptions And Frame Of Reference	204
4.2.2	Equations Of Motion	205
4.2.3	Airy Theory	207
4.2.4	Stokes Theory	214
4.2.4.1	The Expansion Method	215
4.2.5	Cnoidal Theory	220
4.2.6	Solitary Wave Characteristics	224

	PAGE	
4.3	REAL TIME WAVE ANALYSIS	225
4.3.1	Pressure Attenuation With Depth	225
4.3.2	Significant Wave Period And Wave Height	226
4.4	WAVE VELOCITY AND DIRECTION OF APPROACH	230
4.4.1	Cross Correlation	232
4.4.2	Cross Correlation Of Two Random Signals	232
4.5	SURFACE ELEVATION POWER SPECTRA	237
4.6	MEAN WATER LEVELS ASSOCIATION WITH TIDAL CHANGE	238
4.7	WAVE PRESSURES ON A SEAWALL	241
4.7.1	Escalating Strengths Of Pressure On A Wall	242
4.7.2	Pressures Due To Standing Waves	244
4.7.3	Types Of Breakers	245
4.7.4	The Limiting Wave Height	247
4.7.5	Engineering Aspects Of Breaking Waves	248
4.7.6	Wave Measuring Investigation Of Breakers	253
4.7.7	The Breaking Sea	255
4.7.8	Breaking Wave Heights	256
4.8	WAVE FORCE ON RIGID VERTICAL WALLS	259
4.8.1	Pressures From Non Breaking Waves	259
4.8.2	Pressures From Breaking Waves	261
4.8.3	Pressures From Waves Following Impacts	266
4.9	MEASUREMENTS OF WAVE PROFILES	268
4.9.1	Wave Grouping	270
4.9.2	Parameters Of A Wave Group	272
4.9.3	Irregular Waveforms In Wave Groups	273
4.9.4	Group Velocity	274
4.10	DESCRIPTION OF WATER BEHAVIOUR ON IMPACT	276
 CHAPTER FIVE		
5.0	NUMERICAL ANALYSIS - WAVE PROPAGATION	386
5.1	INTRODUCTION	387
5.2	REGION	389
5.3	BOUNDARY CONDITIONS	391
5.4	GOVERNING EQUATIONS	393
5.4.1	The Velocity Potential	393
5.5	STATIONARY INITIAL CONDITIONS	396

	PAGE	
5.6	INDEPENDENT VARIABLES	398
5.6.1	Time Stepping Procedure	399
5.6.2	Values Of Coefficients	401
5.7	SMOOTHING CHARACTERISTICS	402
5.7.1	Smoothing The Instability	403
5.8	CONVERGENCE OF SOLUTION FOR ITERATIVE STEPS	405
5.9	VARIATIONS OF BOUNDARY CONDITIONS	406
5.9.1	Asymmetry	407
5.10	NUMERICAL RESULTS FROM A FULLY DEVELOPED SEA STATE	410
5.10.1	Induced Pressures To A Progressive Wave	410
DISCUSSION		415
CONCLUSION		429
SUGGESTIONS FOR FURTHER RESEARCH		430
REFERENCES		432

LIST OF FIGURES

FIGURE		PAGE
1.1	PRESSURE TRANSDUCER CAP AND STRAIN GAUGE.	51
1.2	STATIC CALIBRATION CURVE.	52
1.3	TYPICAL DYNAMIC CALIBRATION CURVE.	53
1.4	ELEVATION AND PROFILE OF SEAWALL AT ILFRACOMBE WITH TRANSDUCER POSITIONS.	54
1.5	TWO ARRANGEMENTS FOR POSITIONS OF THREE BEACH TRANSDUCERS AT ILFRACOMBE.	55
1.6	PLOT OF TEMPERATURE AGAINST STRAIN.	56
1.7	DIAGRAM OF BONDING AND DIN PLUG WIRING.	57
2.1	GENERAL LOCATION OF FIELD TESTING AT ILFRACOMBE AND BOVISANDS.	97
2.2	DETAILS OF TESTING SITE AT ILFRACOMBE.	98
2.3	MAP SHOWING LOCATION AT ILFRACOMBE.	99
2.4	SEA DEPTHS AROUND ILFRACOMBE SEAWALL.	100
2.5	ILFRACOMBE SEAWALL.	101
2.6	SEA SURROUNDING BOVISANDS SEAWALL.	102
2.7	MAP SHOWING LOCATION OF BOVISANDS.	103
2.8	DETAIL OF AREA AROUND BOVISANDS.	104
2.9	DETAIL OF SEA AROUND BOVISANDS.	105
2.10	VARIATIONS OF SPRING AND NEAP TIDES FOR ILFRACOMBE.	106
2.11	RAYLEIGH DISTRIBUTION FUNCTION.	107
2.12	RAYLEIGH PROBABILITY DISTRIBUTION.	108
2.13	THE BRETSCHNEIDER SPECTRUM.	109
2.14a	DIRECTIONAL SPREAD. COSINE SQUARED.	110
2.14b	DIRECTIONAL SPREAD. COSINE POWER.	110
2.15	GRAPH OF WIND VELOCITY AND DURATION FOR SHORT FETCHES.	111
2.16	RAYLEIGH PROBABILITY DISTRIBUTION WITH EXTREME WAVE HEIGHT PREDICTED.	112
2.17	FREQUENCY DOMAIN DIFFERENCE BETWEEN SWELL AND LOCAL SEA EFFECTS.	113

	PAGE
2.18a	WIND VELOCITY 'ROSE' BY DIRECTION ONLY. 114
2.18b	WIND VELOCITY 'ROSE' BY DIRECTION AND SPEED. 115
2.19	DYNAMIC RESPONSE. 116
2.20	GRAPH OF WAVE HEIGHT AGAINST WATER DEPTH. 117
3.1a	TYPICAL WAVE FORM DATA RECORDING. 183
3.1b	AMPLITUDE PROBABILITY DENSITY AGAINST GAUSS'S NORMAL DISTRIBUTION. 184
3.2	TIME DOMAIN SIGNAL WITH A SHIFTED MEAN. 185
3.3	STANDARDISED TIME DOMAIN SIGNAL. 186
3.4	TIME DOMAIN SIGNAL WITH UNDERLYING TREND. 187
3.5	TIME DOMAIN SIGNAL WITH TREND REMOVED. 188
3.6	WAVEFORM SAMPLE FOR CHARACTERISTIC MEASUREMENT. 189
3.7	IMPACT AND SECONDARY PRESSURE CHARACTERISTICS AS MEASURED ON SEAWALL. 190
3.8a	POLES AND ZEROS FOR FILTER A.1.0. 191
3.8b	FREQUENCY DOMAIN. TRANSFER FUNCTION FOR ABOVE FILTER. 191
3.9	FREQUENCY DOMAIN. SINGLE SEGMENT WITH ZERO PADDING. 192
3.10	FREQUENCY DOMAIN. THREE SEGMENTS WITH NO OVERLAP. 193
3.11	FREQUENCY DOMAIN. FIVE SEGMENTS WITH OVERLAP. 194
3.12	FREQUENCY DOMAIN SPECTRUM. SEGMENTING AND WINDOWING. 195
3.13	ERRORS DUE TO ALIASING. 196
3.14	ERROR DUE TO QUANTISATION. 197
3.15	AN EXAMPLE OF KURTOSIS AND SKEWNESS FOR AN AMPLITUDE DISTRIBUTION OF WAVELENGTH. 198
4.1	REFERENCE FRAME AND DEFINITION OF TERMS. 278
4.2	GRAPH OF $K(\kappa)$ VS. κ^2 . 279
4.3	GRAPH OF $E(\kappa)/K(\kappa)$ VS. κ^2 . 280
4.4	GRAPH OF U VS. κ^2 . 281
4.5	CNOIDAL FREE SURFACE ELEVATION WITH WAVELENGTH. 282
4.6	ATTENUATION FACTOR OF PRESSURE WITH WATER DEPTH. 283
4.7	FLOW DIAGRAM FOR THE DETERMINATION OF WAVE CHARACTERISTICS (H_s, T_s). 284

	PAGE	
4.8	CROSS CORRELATION OF TWO SIGNALS DELAYED BY AN UNKNOWN TIME DIFFERENCE.	285
4.9	VELOCITY AND DIRECTION OF WAVE ACTION RELATIVE TO SEAWALL.	286
4.10	POWER SPECTRUM OF WAVE PROFILE.	287
4.11	GRAPH OF THEORETICAL TIDAL CURVE VS. EXPERIMENTAL CURVE.	288
4.12	DYNAMIC PRESSURE MEASURED ON SEAWALL AGAINST WAVE VELOCITY.	289
4.13	THE LIMITING STEEPNESS OF EXPERIMENTAL AGAINST THEORETICAL WAVES.	290
4.14	WAVE PROFILE SHOWING DOUBLE PEAKS AT WAVE CREST.	291
4.15	WAVE STEEPNESS AGAINST BEACH SLOPE WITH TYPE OF BREAKER FORMATION.	292
4.16	STANDING WAVE PRESSURE DISTRIBUTION AT SEAWALL.	293
4.17	IMPACT AND SECONDARY PRESSURE CHARACTERISTICS AS MEASURED ON SEAWALL.	294
4.18	PRESSURE DISTRIBUTION OF A WAVE IMPACT ON THE SEAWALL.	295
4.19	WAVE GROUPING WITH AN UNDERLYING LOW FREQUENCY COMPONENT.	296
4.20 (a-e)	IMPACT PRESSURES WITH RISE TIMES MEASURED ON SEAWALL.	297
4.21	TYPICAL SECONDARY PRESSURE DISTRIBUTION AT THE SEAWALL.	302
4.22	3-D VARIATION OF IMPACT AND SECONDARY PRESSURE IN VERTICAL ARRAY.	304
5.1	ARBITRARY AXES FOR NODAL POINTS ON FREE WATER SURFACE.	413
5.2	STEEPNESS AND ASYMMETRICAL FACTORS OF A PROGRESSIVE WAVE.	414
6.1	TYPICAL IMPACT PRESSURE DISTRIBUTIONS AT THE SEAWALL.	427
6.2	COMPARISON OF TYPICAL EXPERIMENTAL TO THEORETICAL WAVEFORM	428

LIST OF PLATES

PLATE		PAGE
I	GENERAL VIEW OF ILFRACOMBE SEAWALL.	118
II	ROCK OUTCROPS SEAWARD OF ILFRACOMBE WALL.	118
III	VERTICAL ARRAY OF PRESSURE TRANSDUCERS.	119
IV	DETAIL OF CLAMPING OF CABLES ON TOP OF WALL.	120
V	VIEW OF CABLE FIXTURES.	120
VI	WAVE MAST.	121
VII	DETAIL OF FIXING FOR BEACH TRANSDUCER.	122
VIII	A FLOODING TIDE ACTING ON A TRANSDUCER.	122
IX	GENERAL VIEW OF BOVISANDS SEAWALL.	123
X	DETAIL OF FIXING FOR ALENCO HOSE.	123
XI	DETAIL OF PROFILE OF SEAWALL AT BOVISANDS.	124
XII	IMPACT PRESSURE MEASUREMENT AT ILFRACOMBE.	125
XIII	WAVE ACTION AT BOVISANDS.	125
XIV	IMPACT PRESSURE MEASUREMENT AT BOVISANDS.	126
XV	EXAMPLE OF SPILLING BREAKERS.	127
XVI	FORMATION OF A PLUNGING BREAKER.	127
XVII	EXAMPLE OF A LONG CRESTED WAVE.	128
XVIII	IMPACTS AND AIR ENTRAINMENT.	128

ACKNOWLEDGEMENTS

This research was financed by the M.A.F.F. and S.W.W.A. under the sponsorship of the Plymouth Polytechnic.

First, I would like to express my thanks to my main supervisor Mr. P.J. Hewson of the Plymouth Polytechnic for his support and encouragement towards this research. I would also like to extend my gratitude towards Dr. C. Williams for his useful comments on the subject.

Further, I am also grateful to Dr. C.K. Kennedy, Head of the Department of Civil Engineering, Plymouth Polytechnic, for his backing of this research project, and Dr. G.N. Bullock for his contribution to this research. I would also like to thank Mr. B. Pateman, the head of the technicians for his supervision in the technical aspects of the project.

I would also like to thank the technical staff of the department, in particular, Mr. J. Barker, Mr. K. Stott and Mr. S. Edmonds for their technical support in this research.

I also acknowledge the help of the following:

Mr. and Mrs. W.J. Clemence	The Quay, Ilfracombe.
Commander Bax	Fort Bovisands.
Dr. R. Motte	Weather Station, Dept. of Maritime Studies.
Mrs. H. Serpell	Weather Station, Dept. of Maritime Studies.
Mr. F.A. Ramage	Technimeasure, High Wycombe.
Dr. A. New	Institute of Oceanographic Sciences.

I would also like to thank the members of staff of the following establishments:

The Learning Resources Centre	Plymouth Polytechnic
The Media Services	Plymouth Polytechnic
R.A.F.	Chivenor
Hewlett Packard	Bristol
Gould Instrumentation	Ilford
School of Mathematics	Bristol University

I would also like to include in my thanks, the rest of the staff of the Department of Civil Engineering, Plymouth Polytechnic. Finally, I would like to express my thanks to my wife, Josette, for the typing of this thesis and for her dedicated support and help in seeing me through this research.

DECLARATION

I hereby certify that this work has not been
accepted for any degree and is not being concurrently
submitted in candidature for any degree other
than the degree of Doctor of Philosophy of
the Council for National Academic Awards.

Candidate:

Alexander L. Rossi

A handwritten signature in black ink that reads "Rossi". The signature is written in a cursive style with a prominent initial "R" and a horizontal line underlining the name.

Abstract

Following previous work (by P. Blackmore, 1982, at Plymouth Polytechnic) more detailed pressure measurements were taken at Ilfracombe, North Devon and at a new site, Bovisand, near Plymouth. In both cases a beach array of transducers was used to enable a determination of wave characteristics for correlation with impact pressures.

At both sites, the tidal variations were exploited to obtain depth dependent parameters such as wave steepness and their effect on impact pressure magnitude and variation. The bulk of the readings come from Ilfracombe, as storm damage brought a temporary halt to work at Bovisand.

The wave profile can be characterised by the relevant wave theory using a linear approximation for deep water waves, but requiring a non-linear approach for shallow water waves. Computer programs were developed to extract appropriate measurements from experimental data using digitally processed time series analysis for the purpose of comparing with values obtained from linear and non-linear modelling methods.

The main aspects studied included, the impact pressures with their magnitude, duration and frequency of occurrence. Probability distributions have been used to provide a prediction of the extreme value of wave height for the data analysed.

A dual loading pattern involving high intensity impacts together with prolonged secondary pressures was highlighted in this research as direct loading on the sea wall. The experimental results have shown that components of the loading pattern produce pressure distributions of equal importance.

ABBREVIATIONS AND PRINCIPAL SYMBOLS

AC	= Alternating Current
A/D	= Analogue to digital
ASCII	= American Standard Code Information Interchange
B	= Filter bandwidth
B_{eff}	= Effective bandwidth
BNC	= Bayonet connector
BSP	= British Standard Pipe
c	= Celerity
C_G	= Group Velocity
C_w	= Speed of sound in water
d	= Depth of mean water level
d_b	= Mean water level of breaking wave
DC	= Direct Current
D.O.E.	= Department of Environment
\overline{DTE}	= Data transfer enable
e	= Perturbation parameter or Bandwidth
E	= Energy
$E(f)$	= Spectral distribution
$E(\kappa)$	= Complete elliptical integral of the second kind
f_b	= Observed frequency
f_e	= Expected number of samples per frequency interval
f_i	= Observed number of samples that occur within incremental values
f_o	= Peak frequency
f_m	= Peak frequency
$\sqrt{f_m}$	= Dimensionless peak frequency
F_{cs}	= Force over wetted area
F_m	= Total dynamic force per unit length of wall
FFT	= Fast Fourier Transform
FM	= Frequency Modulation
g	= Acceleration due to gravity
$G(\theta)$	= Directional spectra

H	= Wave height
\bar{H}	= Average wave height
$H_{\frac{1}{3}}$	= Significant wave height
H_b	= Breaking wave height
H_g	= Maximum wave height in group of waves
H_i	= Incident wave height
H_{max}	= Maximum wave height
H_o	= Deep water wave height
$H_{r.m.s.}$	= Root mean square value of wave height
H.R.L.	= Hydraulics Research Limited
H_s	= Significant wave height
IFT	= Inverse Fourier Transform
I/O	= Input/Output
ISL	= Input select
I.S.S.C.	= International Ships Structures Congress
JONSWAP	= Joint north sea wave project
k	= Wave number
$K(\kappa)$	= Complete elliptical integral of the first kind
l	= Line segment length
l_b	= Virtual length of breaking wave
L	= Wavelength
L_b	= Breaking wavelength
L_o	= Deep water wavelength
LF	= Low frequency
LP	= Lowpass
m	= Beach slope
m_o	= Moment to first order
m_2	= Moment to second order
N	= Number of observations or number of nodal points
N_c	= Number of crests
N_{FFT}	= Number of samples used in the FFT size
N_z	= Number of zero up crossing points
P_m	= Maximum pressure
$p(H)$	= Probability density function(for wave height)
$p(T)$	= Probability density function(for wave period)

P	= Potential energy
P_m	= Dynamic pressure determined at seawall
$P(H/\bar{H})$	= Probability distribution function
P_s	= Pressure at air-water interface
q	= Argument of Cnoidal function
[Q],[R]	= Square matrices
(r,θ)	= Polar coordinates
r.m.s.	= Root mean square
R	= Twice the breaking wave height
RAM	= Random Access Memory
R.M.S.	= Root Mean Square
ROM	= Read Only Memory
R_s	= Run up on the wall
s	= Standard deviation or degree of spread
S_1, S_2	= The ends of a line segment
S.W.L.	= Still Water Level
\overline{SYE}	= System enable
t	= Time
t_m	= Rise time
T	= Wave period
\bar{T}	= Average wave period
$T_{\frac{1}{3}}$	= Significant period
T_b	= Wave period at point of breaking
T_g	= Average period of group of waves
T_o	= Peak period
T_s	= Significant period
T_z	= Number of zero up crossing points
TME	= Timing mode
u	= Horizontal velocity component
\dot{u}	= Horizontal acceleration component
u_b	= Phase velocity of breaking wave
U	= Ursell's number
$U_{19.5}$	= Wind speed at 19.5m above sea level
v	= Vertical velocity component
\dot{v}	= Vertical acceleration component

WMO	= World Meteorological Organisation
(x,y,z)	= Cartesian coordinates
x^*, y^*	= Arbitrary Cartesian coordinates
\bar{x}	= Mean value of data points
$\{x_n\}$	= Sequence set
α	= Angle of slope
β	= Angle free surface makes to the horizontal axis
γ	= Peak enhancement factor or ratio of $E(\kappa)$ to $K(\kappa)$
δ	= Partial differential
ζ	= Vertical particle displacement
η	= Free surface elevation
η^*	= Free surface relative to arbitrary coordinates
$\bar{\eta}$	= Mean of surface elevation
η_s	= Elevation of water surface of combined and reflected wave
θ	= Phase angle
$\theta_1, \theta_2, \theta_3$	= Weighting factors
κ	= Modulus of Cnoidal function
λ	= Vertical asymmetrical factor
μ	= Horizontal asymmetrical factor
ν	= Coefficient of Dean's Stream Function
ϵ	= Horizontal particle displacement
ρ	= Density
τ	= Imposed time shift
ϕ	= Velocity potential
ψ	= Stream function
ω	= Wave angular frequency
ω_m	= Peak frequency of wind speed and fetch
$\tan \beta$	= Slope of the beach

INTRODUCTION

INTRODUCTION

The research into impact pressures of sea waves aims at examining their characteristics and forces on coastal defences. It includes the determination of pressure distributions on seawalls. This distribution is time dependent in the case of dynamic loading of an impact pressure. The other type of distribution under consideration arose during this research and is due to a second peak pressure. In either case, the varying component of pressure and therefore the resultant force is expressed in terms of a vertical distribution.

The system set up for taking field measurements opted for uneven distances between recorded points. With this option, the area of maximum pressure around the mean water level was identified, and this research also takes into account the pressure distribution in the vertical movement of water after impact occurs.

The high frequency of occurrence of these second peaks, as a result of the movement of water mass after impact, forms an important source of loading which is investigated. With pressure measurements being associated with phase velocities, this gave rise to the possibilities of obtaining a detailed form of wave velocity and direction. The phase velocity is an unknown factor of the characteristic of the waveform as it approaches the wall. The random nature of the sea is described in more detail by other significant characteristics of period and wave height. This research takes into account energy redistribution processes, the more predominant being shoaling and reflection.

Having obtained a description of the sea state, individual waveforms are also described. The full theory treatment is applied to individual records at this stage to carry out the following steps of a progressive wave to the point of limiting steepness.

Thorough analysis of lengthy field records of waveform and pressure time histories was made viable through the practical extraction of the information in digital form. The extensive use of a microcomputer made this format the most suitable method for analysis. This facility allowed the use of prewritten programs as well as additional adapted programs developed during this research. The value of this method was appreciated when the completed work showed how it was possible to reach the above aims not only in a concise but also in an indicative way.

In order to carry out the work successfully, considerations had to be taken from the initial stage of measurement to the final stage of presentation of results. The prime factor of the measuring system was to achieve functioning field equipment together with the permanent magnetic recording of the data obtained. Obstacles that arose during the analysis stage took the form of uncertainties in interpretation of digital values. For this reason, quick decisions were taken during the field measurements to optimise the recorded data output. This preparatory work proved invaluable in the reduction of the obstacles mentioned earlier.

For this basic and important stage there were plenty of difficulties to overcome these constraints. The objective was to provide instrumentation for measurement. This was fulfilled by performing an up to date verification of the functioning system and the appropriate calibration. The situation involved the combination of sensitive electronic equipment with water under a hostile marine environment. Under these conditions, however much attention was given during the construction stage, drawbacks were inevitable. When a part of the system was laid up during the operation, contingencies were such, so as to require that the rest of the system remained unaffected. In some cases, the option of a suitable alternative such as stand-by gauges was also made available. With this principle maintained throughout the project, the losses in the form of time, and therefore opportunity, were kept to a minimum.

This idea of alternatives was extended by assessing the favourable conditions featured in an existing site and applying them to the choice and setting out of a new site. This fundamental choice was supplemented by supporting information at the new site. This information was in terms of weather conditions, which were studied as hindcast levels to be applied at forecast levels.

Continuous time signals were analysed by adaptation and development of existing methods. These were applied to the digitised data format. Special purpose designed software was developed to cater for the analysis requirements of the existing records. The various situations encountered during the analysis of the recorded signal indicated that the sample rate should be chosen to accentuate the parameter

being measured. From this point in the analysis, the removal of the mean shift in the recorded signal and underlying trends was carried out. The filtering of high frequencies by the use of low-pass filtering principles, was also required. Having accomplished this, the smoothing of discrete values became a problem in itself to reproduce the continuous signal as accurately as possible for presentation purposes.

Maxima, minima and mean locations in a given signal have been identified. This was done over the sample which incorporated a number of crests and troughs, and in the localised situation in order to isolate the similar elements from one another. In support of all this information, a comprehensive graphics display system was set up to generate a standard format for presentation work. Transients, due to impact pressures on the seawall, were identified from the relevant signals. In the process, removal of high frequency components of interference became critical when obtaining the real measurements of rise time and peak pressures. The amplitude distribution of continuous waveform signals was evaluated to test their randomness by determining their deviation from the normal distribution.

All the pressure related measurements were justified in terms of pressure dependence on water depths before actual values could be deduced. This attitude triggered off a degree of acceptance on the experimental values when checked against expected values obtained from the background theories. Besides giving guide lines as to the order of magnitude expected, background theories also specify limits

which render some experimental values as erroneous and therefore an untrue representative of a real situation.

The variation of the mean water level with time is determined as a tidal variation. The determination of this variable produced a solution to the water level as it appeared in different parts of the recording of wave measurements. The irregular random sea to the engineer is reduced to significant wave height and period values which is evaluated from the recorded signal.

The velocity components in terms of the direction of wave action obtained from a beach array of transducers were determined. The significance of this part was to identify the individual waveforms producing significant pressures detected on the seawall. Besides a one-to-one correspondence, the mean value of this data gives a general description of the wave characteristics. From a reasonable set of data, the main controlling parameters were obtained in an organised way suitable for use for design purposes. This objective was found necessary, in the case of a site which was conducive to haphazard forms of wave action. This was attributed to wave transformations such as shoaling due to an irregular seabed profile and reflections in the presence of outcrops.

The result of carrying out a number of tests was that for the cross-section of results obtained, an improvement on previous results was reached. This tendency in the deduction of results arose as randomness and appeared to be a main factor in the original wave loading conditions.

As the results obtained are particular to a specific type of seawall situation, an extension of this work was required to verify the approach at a different site. The advantage of the second site chosen was the occurrence of a regular train of waves to produce intense extreme values given the right conditions. This site was chosen in spite of a change in wall profile.

The overall approach to this project involves, besides a clear understanding of the wave characteristics, the investigation of the dynamic loading on the coastal structure. This takes the form of impact pressures which were seen as individual loading sources in time, but, of more significance, their distribution in a vertical direction relative to the mean water level. The impact pressure is seen in association with its corresponding rise time to produce a momentum change. The momentum change is given on the assumption that the final momentum of the water mass just after impact occurs is reduced to zero. This significant momentum change forms the basis of obtaining the dynamic response of the structure.

In addition to this dynamic type of loading, the values of the second peak pressure together with its prolonged duration provide a second source of loading on the structure. Although of a hydrostatic nature, the vertical distribution produces pronounced pressure magnitudes especially around the still water level. As the measurements of pressure are determined in detail for the distribution purposes, their validity is assessed by their comparison to a second variable. The phase velocity of the approaching wave was chosen as the second variable as pressure is a function of velocity.

From a number of pressure distributions measured, the distribution under extreme conditions may be predicted. The centre of action of this distribution gives a practical result. The result in this form produces a better understanding towards the design of the structure. The approach taken to the design problem gives an added engineering dimension over other empirical methods.

HISTORICAL BACKGROUND

HISTORICAL BACKGROUND

The reasons for the engineer's concern with waves originates from a curiosity inherent in man's intellect. His understanding of this phenomena is coupled to the way in which waves affect the structures and works built by man for the protection of man.

The understanding of waves may only be satisfied through the study of reliable information. The key factors involved in this information can only come from an adequate wave history. This fact becomes of prime importance in the construction stage of any major maritime structure, either coastal or offshore.

The process adopted for practical wave characteristic determination is based on numerical analysis of correspondingly digitised signals. The significant parameters required to describe the sea state are determined from maxima and minima and the zero-up crossings along the mean of the signal. This method was used by Tucker⁽¹⁾ (1961) and Draper⁽²⁾ (1966). The technique has now been developed on these original methods in the form of numerical analysis. In addition to this information, a knowledge of directional spectra is achieved through a detailed study of the wave direction and velocity of the sea. This work, started by Arthur⁽³⁾ (1949), was extended to ocean waves by Isaacs and Chin⁽⁴⁾ (1948) and Hall⁽⁵⁾ (1950). A suggested tri-system of detection for measurement by Snodgrass⁽⁶⁾ (1952), also formed a basis for the study of this aspect of waves.

In the measurement of free surface elevation by pressure transducer, the inclusion of hydrodynamics due to subsurface fluctuations cannot be avoided, as seen by Kim and Simons⁽⁷⁾ in 1973. However, this work developed under shallow water conditions and the associated attenuation provided a negligible contribution. The continual association of measured work with the more established theories required a thorough investigation of the development of these theories. The extent to which this was carried out was to cover the more fundamental concepts that deal with linear theories. On this basis, further theories verging into the non-linear field were investigated thus covering the shallow water in which measurements were carried out.

The study of the wave theories, covers the wave loading principles which provides the associated details of particle velocity, accelerations and pressure of the fluid motion in action. The linear theory (also called Airy's theory) is based on sinusoidal wave theory or small amplitude wave theory, and was first introduced by Airy (1845).

Work on theoretical derivation was further carried out in some detail by Stokes⁽⁸⁾ (1847, 1880). On this initiation, Stokes developed this theory into higher order theories by the introduction of perturbation parameters. These theories actually were a series of successive approximations, but fitted aptly to satisfy deep water, and of more importance, intermediate water conditions. This work was substantiated by contributions due to De⁽⁹⁾ (1955), Chappellear⁽¹⁰⁾ (1958) and later by Schwartz⁽¹¹⁾ (1974).

The extension of the linearity shown in the above cases begins to be suppressed in the shallow water extreme situation and is better

depicted by the solitary wave theory. This theory was first propounded by Boussinesq⁽¹²⁾(1871), after being described by Scott Russell⁽¹³⁾(1844). The practical application of this theory is to introduce periodicity to the shallow water wave. This was found successfully in the Cnoidal Theory due to Korteweg and deVries⁽¹⁴⁾(1895). However, no significant contributions to this theory were made before the introduction of numerical analysis. This was mainly due to the handling of non-linear simultaneous equations to a high order. Laitone⁽¹⁵⁾ in 1961, derived expressions for higher order Cnoidal and Solitary waves by using a method suggested by Friedrichs⁽¹⁶⁾(1948). This method applied a marked proportional difference between the variables associated with the horizontal and vertical (water depth) dimensions respectively.

Higher order Cnoidal theories were put forward by Fenton⁽¹⁷⁾(1974), where he applies non-dimensionless parameters, such as the number attributed to Ursell⁽¹⁸⁾(1953). The extensive use of these parameters led to the practical use of these theories as engineering solutions.

A direct application of wave motion comes about when instability of the free surface is considered. As far as this aspect is concerned, the study of maximum wave height approaching the state of a breaking wave is involved. Previous work in this field is limited to more recent attempts by Longuet-Higgins⁽¹⁹⁾(1976), Cokelet⁽²⁰⁾(1977) and Peregrine⁽²¹⁾(1979). Their work is based on computational methods with the total verification with actual measurements limited by the asymmetrical formation of a wavefront to the point of instability.

The conditions of the propagating medium which cause the waves to break and produce different types of breakers was given by Galvin⁽²²⁾ (1968). This led Tenaud and Graillet⁽²³⁾ (1975) to give an engineering slant in the design of coastal structures, bearing the breaking wave in mind. In the description of breaking wave formation, the wave characteristics take a more specific significance. In the case of an engineering solution, Weggel⁽²⁴⁾ (1972) produced empirical expressions over experimental work by Galvin⁽²⁵⁾ (1969) and Goda⁽²⁶⁾ (1970).

The prime importance of breaking waves' action on seawalls is their formation of impact pressures. Full scale testing of this nature has been limited to within the last century, with the more recently recorded in Britain in the late 19th century by F. Latham. By progression into the development of measuring devices, the detection of such pressures became more frequent and reliable. In the 1900's D.D. Gaillard⁽²⁷⁾ measured dynamic pressures with his diaphragm dynamometer. A few years later in Japan, Hiroi⁽²⁸⁾ used a spring dynamometer and detected pressures in excess of 300 KN/m². He produced an empirical formula for maximum pressure of,

$$1.5 \rho g H \quad \text{where } H = \text{wave height.}$$

which was distributed uniformly over the height of the wall for design purposes.

In 1915, Molitor⁽²⁹⁾ carried out his experiments on Lake Ontario in Canada where he incorporated other influencing factors such as beach slope and water depth. His extreme pressure measured was, however, only 30 KN/m².

In later work in Porto Valparaiso, Profs. Luigi⁽³⁰⁾ (1921) estimated maximum pressures of the order of 300 KN/m² around the mean water level. This value was reached at, by movement of purposely placed massive stones in this area.

In 1937, Rouville et al⁽³¹⁾ measured maximum pressures of 689 KN/m² for a 2.5 m wave using electronically based transducers in Dieppe, France. These values rate as the largest recorded on a real structure. In the 1950's at Le Havre, Cot⁽³²⁾ measured pressures to a maximum of 100 KN/m² with rise times of 10 ms. In 1966 Muraki⁽³³⁾ concluded on his earlier work together with other colleagues that the maximum possible pressure estimated for a 4.5 m wave was 150 KN/m².

In 1974, Millar et al⁽³⁴⁾ developed a system of pressure measuring devices fixed at known points. By this method, impact pressures measured around 45 KN/m² for a 1 m wave, were associated to the class type of wave, after Galvin's⁽²²⁾ description. In 1975, at Genoa, Marchi et al⁽³⁵⁾ operated with a vertical array of equidistant transducers, to conclude that pressures at the base of the caisson are independent of wave action. More recently in 1981, Blackmore⁽³⁶⁾ at Ilfracombe, measured impact pressures to a maximum of 27 KN/m² and while at Seaford, the maximum pressure recorded was 49 KN/m². For these tests, he used diaphragm pressure transducers as measuring devices.

In addition to impact pressures, secondary or second peak pressure measurement is necessary in the investigation of a probable cause to structural damage. Work in this direction was started by Larras⁽³⁷⁾

in 1937. He expressed that this pressure lasts for an appreciable portion of the wave period. The pressure diminished when the waves failed to break at the wall but occurred more frequently than impact pressure would. He also determined that this pressure increased with wave period but remained unaffected by bottom slope.

Further experiments in this respect were carried out by Salih Kirkgoz⁽³⁸⁾ (1983), to a variable slope of an impermeable beach. He expressed the importance of this type of pressure in structural design, otherwise a cause for serious damage in vertical faced walls.

The research in this field was counterbalanced by numerical work which has made significant progress within the last few years. This work is made possible by use of computers to the extent of even predicting the behaviour of steep waves. Work by Longuet-Higgins and Cokelet⁽³⁹⁾ (1976), showed a trace of progression of waves by time-stepping methods. Their results expressed a complete array of particle velocities and accelerations within the boundaries of a wave train of given height and wavelength. The extension of this type of modelling was taken to one reaching a steep wavefront situation.

More recently, in 1980 Salmon et al⁽⁴⁰⁾ applied numerical analysis to a simplified open boundary problem to incorporate a linear theory. The obtaining of data in the shallow water region, has however led to the requirement of extending this boundary integral method. The method used incorporates non-linear conditions similar to that carried out by Liggett and Liu⁽⁴¹⁾ in 1982.

CHAPTER ONE

INSTRUMENTATION

1.1 PRESSURE TRANSDUCERS

The principal instrument for measurement of impact and hydrostatic pressures for the beach and wall was the transducer. It directed stress via the diaphragm to a strain measuring gauge. The basic grid arrangement opted for was to accept maximum radial strain and tangential strain. The grid was eliminated in the area which identified the positions of points of contraflexure. This arrangement was confined to an optimum expected from a fixed ended thin walled diaphragm. The sagging moment over the central area was counteracted by a hogging moment at the rigid ends of the diaphragm. The latter value was evaluated at twice the central value for a uniformly distributed applied load⁽⁴²⁾. This theory gave a value of central deflection subject to dynamic pressure resulting from an impact load, acting over a small area. Strengthening of the diaphragm walls at the contact point to the plate was provided by eliminating the sharp edges between the two.

This was the basis of the design for the transducers used in the field measurements. Further requirements satisfied the physical limitations encountered during the measurements. The construction was lightweight and compact. It consisted of a stainless steel diaphragm of 25 mm diameter turned and milled from a 75 mm diameter cap. The thickness of the diaphragm was limited by the extent to which no permanent deformations were produced, and approximated 1 mm. This cap was attached to a stainless steel housing by means of four hold down bolts. The securing of bolts was carried out in a prescribed manner to avoid initial deformation of the diaphragm under no load conditions.

To the diaphragm was fixed the strain gauge. The gauge was made of a copper-nickel foil of thickness $0.007 \text{ mm} \pm 0.004 \text{ mm}$. The foil was precision etched onto an epoxy base. The gauge was of the TML range - FDFF - 24, being 24 mm in diameter (Fig. 1.1). Each gauge had an arrangement of two tangential and two radial resistance grids of $120 \text{ ohms} \pm 0.5 \text{ ohms}$. These four resistances made up the arms of a Wheatstone Bridge. The solder tabs were used to fix the printed circuit board to the strain gauge. The printed circuit board integrated the electronic circuitry.

A measure of the radial and tangential strains was obtained from small deflection theory in the elastic range. The tangential strains at the central area, with the radial strains at the periphery optimised the diaphragm response to a uniform pressure distribution.

The variability of the diaphragm thickness measured differences of between $\pm 0.2 \text{ mm}$. Since the sensitivity was proportional to the square of the thickness a variance of 30% between diaphragms was produced. The performance was also represented by the linearity and frequency response while operating over the working pressure range of 0 to 100 kN/m^2 . The capability of reaching the static pressure equivalent was supplemented by the minimum dynamic capacity of 200 Hz transient measurements.

This option of transducers has been shown to be cost effective with a facility of being easy to replace. This was found to be necessary to overcome the initial difficulties of waterproofing. The prime

physical consideration was flexibility and close proximity to the measured face. The first condition was satisfied by the transducers' interchangeability. The mere thickness of the housing was kept to a minimum. This meant that each transducer was fixed to a plate on the wall without affecting the distance of the measuring face to the wall.

1.2 CALIBRATION

The calibration of the transducers was carried out in two phases. The first phase included the measurement of the signal amplitude obtained by applying a load and allowing the transducer to reach static equilibrium. The second phase was a measure of the dynamic response of the gauge obtained by applying a transient load.

The procedure in each case, was carried out by first checking the resistance across adjacent and opposite arms of the Wheatstone Bridge. The values of resistance read 90 ohms and 120 ohms respectively. Over this value, the nominal resistance of the long length of cable (at most 60 m) had to be taken into consideration. A check was made to determine whether there was electric leakage between the 7 pin DIN plug and the transducer housing. Lack of leakage ensured adequate insulation and screening from external noise.

Each transducer was then connected to its corresponding amplifier module which was supplied by an 18V DC unit. At no load, the bridge excitation voltage was adjusted to read 5V. The reason for this value is explained later. By isolating the input from the bridge, the variable potentiometer was adjusted to zero the offset. The bridge was balanced at no load with optimum position at mid range value. This inferred that distortion was minimised for output signal.

1.2.1 Static Calibration

The balanced bridge was subjected to incremental pressures of 10 kN/m^2 and allowed to attain static equilibrium. The pressures were applied by an air line from an electric compressor having a storage tank capacity. An airtight adaptor with a pressure indicator was used, to ensure that the pressure was applied uniformly over the face of the diaphragm. While applying the pressure, the span control was adjusted to provide an output equivalent of 1 volt per 100 kN/m^2 . The output was monitored on a digital voltmeter. The gain was recorded and formed a measure of the sensitivity.

The excitation voltage was based on performance tests. These tests covered instabilities under zero load conditions. Instabilities were due to drift and temperature changes. The degradation of performance of the output was dependent on opting for the highest possible voltage within the safe power rating used. The calibration was best done at the operating temperature rather than the room temperature. The temperature response for the type of gauges used indicated a zero apparent strain for 25°C . For temperatures either above or below this standard, the apparent strain was proportionally lower. This relationship holds good for stainless steel mounting with P-2 for choice of adhesive.

1.2.2 Integral Properties

Each transducer had its own integral properties. However, the design was to cater for general values for which the limitations were not

exceeded. These properties fall under the heading of sensitivity, linearity, deflection and frequency response. The frequency response falls under the dynamic characteristics of the gauges.

The sensitivity was measured by the ratio of output voltage to the excitation voltage for the maximum rated pressure of 100 kN/m^2 .

The value was expressed before taking the gain factor into consideration. Typical values were 1.125 mV/V of excitation voltage. From this sensitivity the diaphragm thickness was estimated for completed transducers. The values obtained took into account that only small deflections were produced when pressure was applied to the transducer.

From the output for the 10 kN/m^2 increments, the linearity for the loading cycle within the elastic range was determined (Fig. 1.2). The direct proportionality between distributed pressures and voltage output was maintained throughout the range of transducers. The plot of these two variables showed that around the initial 20 kN/m^2 loading increment, the deviation from linearity was of the order of 3%. This was calculated from the residuals of the best line fit through coordinated points. This analysis showed that the system was unlikely to detect difference in pressure variations to within 30 cm of head. In any case, variations of this magnitude tended to become insignificant in the field of study concerned.

1.2.3 Dynamic Pressure Response

The dynamic response is a measure of the natural frequency of vibration of the diaphragm. This was further represented in the maximum allowable central deflection for the diaphragm.

A simple but effective test was carried out for the determination of the frequency response of the diaphragm. This was done by dropping a rubber weight from a known height. The response was recorded in digital format. The digital information was captured by the arming of a single shot in the quarter signal delay mode. The instrument in use for this exercise was the Gould Digital Storage Oscilloscope OS 4200.

The diaphragm was found to withstand a rise time of 2 ms (500 Hz) at approximately full range output. The frequency response of the diaphragm was coupled by a magnified dynamic response due to the damping character of the measuring device. The basis of the discussion was that the dynamic frequency of the transients should not exceed 20% of the natural frequency of the gauges. This value was gauged for a damping coefficient in air. As water provides a higher damping resistance, the resulting displacements took proportionally lower values. The frequency response had a critical value which is directly proportional to the diaphragm thickness. Therefore it followed that the diaphragm thickness could not be much further reduced without reaching a level of resonance which would have interfered with the measurements (See Fig. 1.3).

The estimated thickness of the diaphragm was its direct relationship to the maximum deflection permitted. With large deformations, the elastic strains turned to permanent plastic deformations. In order to avoid this condition, the centre deflection was limited to 25% of the diaphragm thickness. It follows that the thinnest diaphragm

gave the most critical condition. The amount by which the thickness differed from the limit was a measure of the extent to which the diaphragm was liable to sustain overloading.

Other requirements included, the repeated use and variations in temperature strain. This property was attributed to the characteristics of the epoxy resin used. This resin was necessary to bond the strain gauge to the diaphragm. As a design factor, the gauge chosen had a coefficient of expansion compatible to the stainless steel. This minimised the apparent strain due to temperature changes.

For the type of gauge chosen, the recommended adhesive P-2 allowed a temperature range of -30°C to 80°C in which to take stable static measurements. This range included the limits of operation for the system. The mode of application suggested involved a curing pressure of 2 kg/cm^2 . This pressure was applied for three hours at a temperature of 20°C above the rating for the use of the gauge. Further, this method of adhesion permitted a fatigue life of 10^6 applications at 40 Hz of cyclic loading and unloading.

1.3 MODIFIED DESIGN

The transducer as it performed initially, had shown a need of improvement. The aspects to take into consideration were the deficiencies due to balance, signal-to-noise ratio, amplification characteristic and prevention of water ingress into the system.

1.3.1 Balance Control

The balance of the Wheatstone Bridge used in strain gauge measurement appeared to be uneven in some of the transducers. This was partially due to the tolerance error of the resistors of each arm of the bridge. Another cause for balance control was the heat generated by long term use of the gauge which affected the foil characteristics by expansion. This is called the gauge self heating effect. This resulted in a degree of distortion to the output signal, giving an unrealistic representative of the measured parameter.

The method opted for to bring about this improvement was to incorporate a shunt resistor. The resistance was calculated to make good the lower value of the group of four resistances. The value that was used falls in the region of 47 kilo ohms ($k\Omega$). This resistance was suitable as it was readily available industrially. It was also provided with a specific tolerance of up to 10%.

The physical size of the resistor was suitable to be connected in parallel to the weakest resistance. This was essential for the limited space between the gauge and the printed circuit board. The

dimension of this space was predetermined by the necessity of keeping the distance of the diaphragm as near to the wall as possible. The other limitation was that the housing had to be removed from the fixing for regular maintenance.

1.3.2 Signal-to-Noise Considerations

The application to the addition of signal-to-noise consideration is that it provided an improved signal representation. The scope was further broadened by the reduction of drift evident in long stretches of recordings. The gradual zero drift was unwanted but was further overcome by the use of proper screening in the cables carrying the conductors.

The control of the noise level maximised the signal-to-noise ratio. Noise was generated in either electrostatic or magnetic form. The electrostatic was due to the voltage carrying conductor, where a group of connectors put together caused interference. The magnetic noise was due to a cut in the magnetic field or a rate of change of flux in current carrying conductors.

The method chosen for detecting and controlling the amount of high frequency noise components was carried out independently of the strain measurements. With the excitation voltage suppressed, the output represented a tolerable level of noise. The noise so generated was reduced by a gain increase. This effect was to be compensated by an increase in the excitation voltage.

The main noise source was from lead pickup. The shielding of the cable was in the form of a braided mesh and was an effective form of reducing noise from lead pickup. This was particularly essential for long runs of signal carrying conductors. The six core cable connected the gauge to a 7 pin DIN plug which provided a means for grounding off the screen at one end only. Discontinuity in the cabling produced leakage to ground which also generated noise and had to be avoided. The leakage was prone to temperature changes having the least resistance with high temperatures.

The optimum soldering technique was to connect directly to the tabs. Any excess wire between connectors was coiled up to act as a barrier to magnetic noise.

1.3.3 Amplification Control

The maximisation of signal-to-noise ratio can be affected through the application of a unit gain amplifier. The input noise signal was passed through two channels via a unit gain amplifier connected in the direction of one input opening onto two outputs. The output was a result of common source rejection, approaching the flat response of high frequency components. The amplifier component was small enough to be incorporated in the space of the transducer cap. This approach was the equivalent of an active filter circuit as it was applied before the signal was recorded. The gain constant of unity ensured that the signal response was not attenuated up to 200Hz.

1.3.4 Other Considerations

Water ingress into the system in the form of moisture condensation or direct entry was detrimental to signal capture. The water proofing of the submersed electronic parts had to be satisfactory. Care was taken when sealing the strain gauges to the stainless steel housing. This was achieved by inserting a greased O-ring in matching grooves to overcome the metal to metal contact.

Moisture condensation around the cable was overcome by the use of an alternative type of hose for the supporting structure. The type used was Alenco 6 mm nominal diameter of bore with $\frac{1}{4}$ BSP straight female and parallel male unions. Its use was justified in its protective role and inherent structural properties. The strength to overcome the catenary sag of long leads was attributed to the double walled reinforced section. Being black in colour, this hose superceded its translucent equivalent, in that it reduced the moisture condensation trapped between the cable and its cover.

1.4 SITE ARRANGEMENT

The positioning of the transducers on the site was split up into a spatial arrangement for the wall and one for the beach. The determining factor in either case was based on the objective for which the measuring device was put there. Other restrictions to take into consideration were due to the physical limitations of the site.

1.4.1 Vertical Arrangement

The wall arrangement was based on previous work carried out by P. Blackmore⁽³⁶⁾(1981). This initially traced back to field experiments carried out at Le Havre by Cot⁽³²⁾(1953). The main concept involved the cruciform arrangement to detect pressure distribution in both the horizontal and vertical direction. Cot was able to measure maximum dynamic pressures of 100 kN/m² with rise times of 10 ms below the Still Water Level (S.W.L.). The arrangement was for five transducers with 2 m centres in the horizontal direction and 2.5 m and 1.5 m centres in the vertical direction. Later work found it necessary to include a larger number of transducers in the vertical direction. This was reflected in the importance of obtaining a representative vertical distribution of pressure which is acting normal to the plane of the wall.

When dealing with a constructed seawall, its durability was based on being dense and well compacted, whether it was of reinforced concrete or of sandstone blocks. The result was that the face

could not easily receive a random arrangement of transducers without heavy plant machinery. Although being a physical limitation, it was at the time, overcome quite effectively by having the location of transducers at predetermined positions. This logically stemmed from the fact that any results obtained for a seawall had to be related to other walls in other situations. This flexibility was best achieved by introducing a 3.3 m by 50 mm by 6mm mild steel bar which was fixed directly to the wall at three locations. The array of six vertical transducers placed at 45 cm centres were then fixed to the bar by means of 20 mm threaded studs. This facilitated easy and rapid fixing of the transducers to the seawall (See Fig. 1.4, Plate III).

This principle was used on the two different cases of measurements. In any case, the largest activity in terms of pressure was centered around the S.W.L. The position of this level is tide and time dependent. This formed the basis for location of the bar carrying the transducers. The arrangement covered the range between the mean high water and the mean low water spring tides. At any time of the recording, the bulk of the transducers were located around this region. This emphasised the importance in configuration of the lower four transducers. Besides this, the upper level of the wall was shown to be equally important where measurements were concerned. From this upper level, the fundamental behaviour of a wave after the impact had struck the wall could be established. The two upper transducers served well for this purpose offering an increasing level of information in favour of the highest transducer. The highest transducer therefore appeared at twice the normal spacing of 90 cm from the batch of four.

1.4.2 Horizontal Arrangement

The previous objective had also a determining effect on the horizontal arrangement. Further studies of the results lead to the knowledge of pressures along a rectangular mesh. The mesh had nodes located at distances related to the degree of emphasis given to the variable in that direction, seen as a vector. This was even more so when the variations of the variable were non-linear. This meant that the closer the mesh size the nearer the discrete values were a representative of the true variation. The idea of the mesh size was carried throughout most numerical methods as a form of studying the behaviour of a parameter in terms of its independent variables.

This principle was coupled with the fact that horizontally, the wavefront tended to offer larger dispersed variations over short intervals. As a consequence, not much importance was given to the variations in this direction. However, to incorporate these reasons, the horizontal distance of 75 cm centres for an array of these transducers was changed to a multiple of mesh size. The horizontal mesh size chosen was twice that of the vertical mesh size at 90 cm centres.

1.4.3 Beach Array

The array of transducers for the beach was involved with the determination of wave characteristics, which were, wave height, velocity, direction and length. Although arbitrary to some extent, the relative positions and orientations had to be well surveyed for the purpose they were intended. The arrangement was built around three transducers at

the vertices of a triangle. The distance between them should preferably be a fraction of wavelength apart. This ensured that a wavefront in its passing over successive transducers did not vary out of character of its structure. This was necessary in the identification of the signal representing the wavefront both in the time domain and in the spectral representation.

Another deciding factor was that the distance of the transducer from the wall was to avoid the effect of the reflected waves. These waves had an additive effect on the oncoming train and lead to improper results. The elimination of this situation was however, only partial and may be used to its advantage in the measure of the reflective properties of the wall.

The arrangement opted for covered the determination of the velocity variations and the direction of approach on the wall. The mode of fixing was by embedded studs grouted in holes in the rock. The arrangement was of a right angled triangle of adjacent sides, 5.5 m and 8.9 m with only one transducer nearest the wall by 5.5 m (Fig. 1.5). The longer side ran square to the face of the wall. The other determining factor satisfied by this arrangement was that the maximum permitted length of cable was 60 m, to bring down the signal-to-noise ratio to an acceptable value.

The rest of the specific significant values for the wave characteristics were obtained from a beach transducer. For this purpose, a continuous well defined signal from one location was adequate to fulfil its requirements.

1.4.4 Single Recording

When only one recording is obtained from the beach, the method opted for was based on the energy response. The assumption for this theory, given by E.M. Bitner-Gregson & S.Gran⁽⁴³⁾(1983) was that the free surface flow was two dimensional with a substantial degree of linearity and covering a narrow band of frequency distribution.

The aspect of linearity was synonymous with small amplitude waves. As the waves entered a shallow area, they experienced a decrease in wave celerity and wavelength, but an increase in wave height. The transformation of the wave was covered by small amplitude wave theory until a more rigorous approach was required. In this case the theory would revert to one that dealt with finite amplitude waves.

The small amplitude wave theory was brought about when the bottom slope had only a negligible effect on the characteristics at any point. This was evident in the present situation of wave measurements which dealt with relatively flat slopes for seabeds. If seen as a basic concept, this assumption provided a means of retrieving data from a single signal record, especially at local level of interest.

When the waves measured a high level of steepness, care had to be taken to view the signal in a broader sense. What was meant by this approach was that initially, an evening out factor was applied to reduce the inherent steepness. The extraction of data was then carried out. Although the results showed signs of deviation from the expected values they were fundamental and still remain a representative of the real sea situation.

1.5 AMPLIFICATION

The signal output from strain gauge measurements was in a form of variation in voltage with time, measured across the bridge. These variations were in the order of millivolts. Suitable amplification also acted as a signal conditioner before it was recorded on magnetic tape.

The type of amplifier used was from RDP electronics of the DS2011 type. Besides conditioning the signal, the module provided a suitable bridge excitation voltage. The excitation voltage was predesignated at 5V to optimise the signal-to-noise ratio. The choice of these amplifiers was such that their contribution towards noise in the signal was minimal, (10 μ V p.t.p. above 10 Hz). They also maintained a linearity of 0.1% full scale output. The zero and temperature drift of the instrument was in the order of -25 μ V per $^{\circ}$ C, an amount that was negligible in its contribution towards the signal.

The amplifiers, in the form of modules, built up to form a multipoint facility for the scientific means of measurement. The connections were via terminal blocks to the rear panel. It formed a simplified control system which was supplied by an external DC voltage stabilised at 18V. The power unit had an analogue indicating monitor which gave a 5 volt output at full scale. This provided a reading for the excitation voltage.

These amplifiers were versatile in that they had a facility to incorporate a calibration resistor. With a resistor of 30 kilo ohms

(k Ω), fitted in the integrated circuit, the calibration switch activated a definite readout. The resistance required to act as a calibration resistor was based on the value of the excitation voltage. Another facility was the inclusion of an inactive gauge with the active gauge. The fitting of this gauge formed part of the module. The function of the gauge was to compensate for temperature and long lead effects evident in the type of experimentation the strain gauges were involved in.

The amplification of the output signals was also suitable for direct application to digital storage oscilloscopes. This technique was adopted when the immediate effect from the response of a transducer was required, and also for monitoring the measurements on site.

1.5.1 On Site Considerations

A general operational check on all the strain gauges was carried out once the system had been set up. The 7 DIN plugs, before connecting to the amplifiers, were connected to an adaptor box. Jacks were plugged into the box in a prescribed order corresponding to the pin number connections. The objective of this exercise was to check the continuity of the cabling, the efficiency of the screening and the resistance arrangement of the gauges. This also served to maintain the matched arrangements between the transducer and the amplifier.

A minimum resistance measured by a strain gauge indicator signified continuity of the connection. Proper insulation between the screen

and cabling was in the order of 10,000 mega ohms ($M\Omega$). The resistance across parallel arms of pins 3 - 4 ; 6 - 7 should read 120 ohms. The resistance across adjacent arms of 4 - 7 should read 90 ohms. To these values were added the nominal value of resistance to cover the cable length. Also, opposite arms of a full bridge carried two conductors per terminal. This ensured that the voltage variations along the cable were compensated when the readings were taken. The absolute check for each of these connections was that continuity was maintained at the plug output.

The resistance check was followed by connection to the amplifier rig. The main parameters to be adjusted were the zero and the balance. The variations were found to be due to environmental changes. The predominant factor was the temperature difference which provided a bias offset to the signal. The elimination of this factor in part, if not totally, reduced the consequence of drift likely to occur throughout the long duration of measurement. This was because the zero frequency components did not contribute in terms of gain of the amplified signal.

1.6 RECORDING

The DC output signals from the amplifiers were recorded on two high precision RACAL recorders. Each tape deck was loaded by 8 track magnetic tapes including a voice channel, and cover 2400 feet of tape. Recording was carried out by frequency modulation with an optimum intermediate band width of 0 to 313 Hz or 625 Hz. This was equivalent to the speed of recording of 0.925 to 1.875 inches/sec respectively. An option of operating a Tchebychef filter was found on the filter board. This condition provided a maximum flat band width with a minimum carrier breakthrough — a condition which optimised the signal-to-noise ratio.

1.6.1 Characteristics Of The Recording Facility

The speed control switch on the "TACH" mode operated with a stable internal system — ideal for temperature variations encountered on field measurements. The hazards were that the tape was affected by environmental changes of temperature and humidity which had a direct influence on the replay. The mode of operation ensured an accurate time base of operation.

Low tape speeds were required in the operation for the signal recording of long duration. The low speed recordings were carried out with a flutter compensation which provided the improvement towards the signal-to-noise ratio.

Playback speeds of a recording were varied according to the level of monitoring required. The choice was arbitrary unless a real time speed of recording was required. In this case, the value at which the recording was carried out was chosen. The facility of speeding up the playing back of a tape produced a condensed version of the signal. This option was taken to view the general trend of the signal. The implications of increasing the speed by a factor of two each time also attenuated the higher frequency components. This was justified in the aim of looking at the trend in which it usually was a result of a low time varying relationship.

Reduction of speed of the playback by half decreased the band width in terms of frequency response. Therefore a more detailed version of the signal was obtained by this method.

The frequency modulator board had an option switch for re-recording with an offset control. With the unipolar negative switch on, the zero point of the record board was shifted from zero to a maximum positive. This provided a 40% deviation in terms of the re-recording of a signal from one tape deck to another. The offset control on the FM record board had the power to remove a DC component from an AC signal.

A recording session required the coordination of simultaneous signals from various outputs. This formed a means of relating the signals to one another in the time domain. It was only successfully carried out once the signal circuits were aligned prior to the recording.

The alignment procedure was carried out by a maintenance team. It involved the sequential adjustment of the respective potentiometers on printed circuit boards.

1.6.2 Alignment Procedure

The "LOCAL ENABLE" mode was used before any modifications were carried out. Each channel was prepared to have its four switches on the record board and first two switches on the filter board on open circuit. The bandwidth switch was selected to an intermediate level. An application of a stabilised known voltage of 1V was monitored either on an external device, like a digital voltmeter, or on the incorporated monitor present on each recorder. The procedure involved the switching on of the input attenuator on positive to check for a full scale deflection. Adjustment was carried out on the filter board. With the attenuator on reference, the output should give an 18.5% input value with adjustment of the replay board. Set at 20V the output was expected to give a zero value with adjustment of the record board. Once again the sequential adjustment was finalised if the positive set attenuator gave a true value for the output voltage.

1.6.3 Field Considerations

With the tape recorders preset, the field procedure was carried out with a certain amount of supervision. The other aspect covered by this procedure was to overcome a certain amount of drifting inevitable throughout the duration of the recording.

Initial setting of the switches involved the loading of the tape spool, setting the selector to the appropriate speed, initial selection of the attenuation level and activating the recording mode. Occasional monitoring of the input signal was carried out via the monitor switch and monitor meter, with the response switch in DC mode. The control was necessary to ensure that distortion was minimised while obtaining the maximum amplitude to full scale deflection. The use of an ordinary scope helped to maintain a substantial level of signal.

The input attenuator provided the facility adjustment. The maximum amplitude to full scale deflection was given in terms of the output readout per unit volt input. The outputs of specific interest were of a 1 : 1 ratio for a 1V level and 2 : 1 for the 0.5V attenuation level. This holds for as long as the maximum value permitted by the signal is not exceeded.

Further considerations applicable to field recordings were, the duration of the recordings and the time of commencement of the recording. Sessions took as long as three to four hours duration. The starting time of the recording was contrived to cover its greater bulk in time before high tide was reached. This was justified by the observation that most of the impact pressures occurring on the wall were accentuated due to a flooding tide. The other determining factor was coupled with the vertical transducer arrangement. The significance of this condition was that the lower set of the transducers was immersed in part or in full when the recording was taking place. The final but more important aspect was the depth

limitation set by the tidal conditions. It can be seen that waves required specific depth conditions to allow the breaking situation of the wave to take place. These were major aspects taken into consideration to reproduce time dependent signals from the beach transducers together with those from the wall transducers. Two tape decks were used for a number of signals exceeding 7 but less than 14. The optimum way to overcome the slight discrepancy between the two capstan speeds was to record a single channel simultaneously on both recorders. The use of two way BNC connectors was indispensable for this sort of arrangement.

1.7 REMOTE MECHANISM

An additional mode of operation that was particularly suitable for on site measurements was the use of remote mechanism. The remote system was of greatest value at times which were inaccessible to the start of a recording. The system was adapted for recordings with a number of successive lengths of recording separated by specified intervals.

The system in operation consisted of a 7 day digital clock that operated the sequential switching process. The logic of the electronic contacts were repeated through a mechanical system and transmitted to the recorder through an interfacing cable. The clock was preset to the times the operation was required to be active. Both tape recorders were connected to the same parent system. The basic requirement for a satisfactory run was that the local controls were disengaged. The circuit was therefore modified by earthing the LOCAL ENABLE switch.

A recording session in remote operation required some preliminaries to be carried out. This involved the pre-engaging of the ON switch, loading to a tensioned tape and selection of both speed and input attenuator controls. At the predescribed times, the loading mechanism followed by the record mode then came into operation. The record indicator lit on each channel showed a positive run. The end of a recording was performed by a repetition of the switching process in reverse.

1.8 FACTORS OPTIMISING STRAIN MEASUREMENTS

When taking strain measurements, some basic attention had to be given to the behaviour of the strain measuring device. Considerations towards thermal effects, optimum excitation and heat dissipation produced improved strain results. This aspect was associated to the performance degradation of gauges. In many cases this was more apparent as a deficiency rather than as an absolute failure. Prevention of it happening necessitated an appropriate power rating and mechanical strain prevention. These factors were to form part of the total requirements to be met at each installation.

Power loss was determined in terms of dissipation of heat. A strain gauge operated at a higher temperature than the bonded material. The efficient conduction transfer was limited by the heat sink capacity of the transducer. The measure of this was given by the Gauge Factor. In turn, the transducer operated at temperatures greater than ambient. These temperature differences resulted in apparent strains unless overcome by the conduction process.

Another effect as a result of the excitation of the gauge in a lower temperature environment was the formation of hotspots. The heat was here localised in the area of the grid and was a cause of creep and instability. The importance of proper waterproofing cannot be overemphasised at the open face of the gauge. This was needed to prevent a loss in performance of the gauge.

The main factor for consideration was the power dissipation of the gauge. It was a direct function of the area of the grid. A mechanical barrier was provided through longer thermal paths of transfer. The barrier was a direct consequence of the thermal conductivity of the adhesive and affected the power rating of the gauge in this way. Loss of performance also resulted through mechanical debonding of the solder tabs and the debonding of the glue line.

The power rating was a direct measure of the operational requirements in terms of stability, accuracy and repeatability. In the dynamic measurements, the loss of performance in terms of power rating became less of a determining factor.

Strain measurement precision transducers were affected by zero shift variation with temperature. The stability was assessed under load at maximum operating temperatures. In determining the grid area, consideration had to be taken for the excitation voltage and power dissipation under heat sink conditions. As a typical example, stainless steel is said to offer fair heat sink conditions. On this basis, with moderate static and dynamic conditions, the typical power rating ($10E-3$ watts/mm²) required an equivalent grid area of 3.25 mm². This value was expressed in terms of the 5V excitation voltage. A larger excitation voltage would have required a larger grid area for the same power rating. The value given is for a 120 ohm bridge resistance. If the bridge resistance were substituted by one of 350 ohms, the equivalent area of grid was reduced by 40%. Therefore the bridge supply voltage could be increased.

Quantitative strain measurements have been expressed in previous work by P. Blackmore⁽³⁶⁾(1981). Their values were associated with the plate theory of small deflections. Based on a fixity and restriction within the elastic region, compatibility of radial strain and tangential strain was to be maintained⁽⁴⁴⁾. The equivalent grid area for a 25 mm diameter diaphragm was given in terms of radial to tangential strain in the ratio of 1 : 6⁽⁴⁵⁾.

Optimum static and dynamic strain measurements should involve high frequency changes relative to the frequency of the temperature change. This difference singled out the temperature apparent strain from the main measurement. In any case, measured strain was inversely proportional to the gauge factor. A temperature change was associated with a decrease in gauge factor, thus overestimating the strain measurement. This aspect was taken into consideration with sudden temperature changes liable to occur throughout the course of the measurements (See Fig. 1.7).

1.8.1 Gauge Bonding For Optimum Performance

Gauge bonding and gauge protection were two physical aspects that are directly related to its sustained performance. The efficiency of these parameters was emphasised to overcome the hazards of the hostile environmental measurements. The environment in this case, not only was water saturated but was also saline at that. The competence of the gauge under these conditions was a result of the attention taken at gauge preparation level.

A brief description of the preparation of the specimen is given in the steps that follow. The metal contact was precoated with a fine layer of adhesive including a surplus beyond the grid area. The adhesive mixed in the proper proportions was then applied on the precoated area to take the gauge. The precoating served to give better bond characteristics between the two layers.

The printed circuit board took the unprotected leads from the gauge. At this stage, care was taken to maintain electrical isolation for each lead. Any excess of adhesive was removed by means of a blade. The take out leads were vinyl lined and fixed tightly to protect against any outer loading. Finally, layers of micro crystalline wax were applied in the melted state. The wax is not a mechanical strength protector but it formed an excellent waterproofing barrier. Its flexibility allowed a degree of movement of the vinyl leads. In its application, care was taken to ensure proper contact between the wax and the surrounding surface of the cap.

The importance of the gauge bonding was emphasised, as a precaution against a common type of failure detected in gauges responding to imposed pressures.

1.9 ACCURACIES IN MEASUREMENTS

When the general measurements for analysis purposes contained extraneous elements, these had to be identified and eliminated. The quantities affecting the accuracy were classified deterministically or, where not possible, statistically in terms of trends of influence. This interference was classed as noise. The value of noise and how it can be reduced in the recording session of experimentation, has already been discussed. However, to say that it did not form part of the pure signal is not realistic. The knowledge of this fact made one aware of it and can therefore act against it at any stage of the expression of the results.

One of the prime influences of noise formation was the carrying out of measurements in a moist environment. This case of total submersion of measuring instruments produced a higher probability of it happening. Therefore, full attention to waterproofing the system was of paramount importance for successful results. The use of greased O-rings and sealing of cable entry, as mentioned earlier, became a major task in the assurance of a watertight system.

Besides the mechanical precautions, the electric and electronic precautions had also to be fulfilled. In spite of this, the inevitable interference in the measurements was present, but to what extent is not known exactly. The magnitude of this was termed signal-to-noise ratio. Where the ratio could not be maximised at source it was measured and eliminated or reduced during the processing of the results.

As a guide line, the acceptable signal was achieved when the apparent signal was not less than a third of the measured signal⁽⁴⁶⁾. In any case, the detection and removal of the noisy elements became part of the preprocessing requirements. The basic principle lies in the superimposition of signals where the frequency components from two random stationary signals were additive.

The value of noise expected from a set of signals was characteristic of the system. The magnitude was represented in terms of frequency range or a band width. The representation of this type of narrow band noise was defined through a constant power spectral density function.

In a wide band width it was necessary to assess the frequency distribution of the interference, and to give the Root Mean Square value of the amplitude for corrective purposes. This was also represented totally by a power spectral density function.

1.9.1 Optimisation Of Results

The power spectral density for a characteristic random signal was used in a practical context. The direct application was in the filtering of a noisy signal. The squaring and averaging of a noisy signal gave a Root Mean Square (r.m.s.) value for the signal.

The method adopted for the determination of a power spectrum in the frequency domain was via a Fast Fourier Transform (FFT) of the frequency components (cf. 4.5). The sum of random stationary processes,

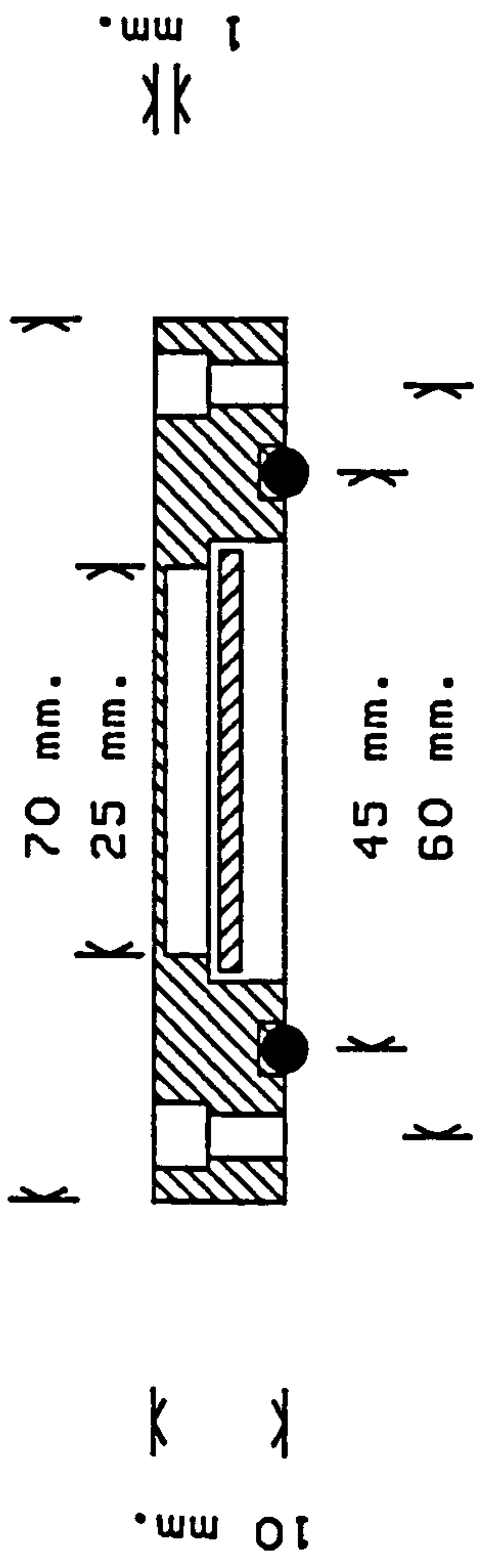
produced, in fact, a composite power spectrum. The composite picture was made up of components directly proportional to the square of the amplitude of the components of each of the separate power spectra.

The problem can be reduced in low frequency measurements. If the interference was restricted to high frequency, the error was contained in this band width. Thus, the low frequency periodic measurements were effectively isolated from the error source. This gave a high level of confidence in the results.

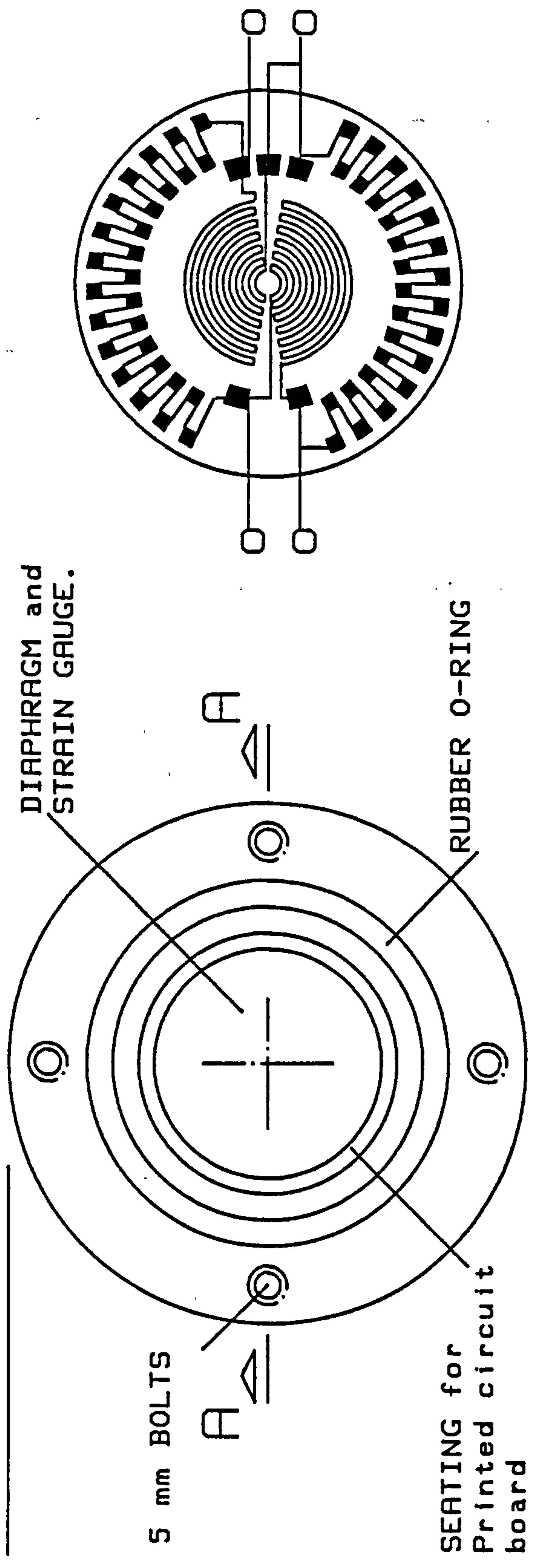
High frequency measurements, on the other hand, were sensitive to the high frequency components. Therefore elimination of extraneous material in the frequency domain became inconclusive. This was overcome by reverting the processing of the signal to the time domain. In this case, the structure of the signal became the main source of identification in a noisy environment. The use of correlation functions placed confidence in the results of time domain stationary random sequences.

The amplitude of the extraneous signal, at any rate, introduced the tolerance to which the results may be quoted. This was expressed by the variance as part of the normal distribution of a random signal. The normal distribution also expressed the mean of the signal which tends to be zero, or near to it, for randomly generated signals. By definition, the normal distribution was determined from the probability density function. The probability density function was a measure of the duration in the time domain of various levels of amplitude for a given sample.

A means of processing high frequency information was by slope detection in the time domain. The influence of interference for this process was overcome by the use of triggering at a level higher than was normally reached by the maximum amplitude — a value given by the normal distribution.



SECTION A - A



PLAN of TRANSDUCER CAP

TML STRAIN GAUGE. FDFPP-24

FIG 1.1 PRESSURE TRANSDUCER CAP AND STRAIN GAUGE

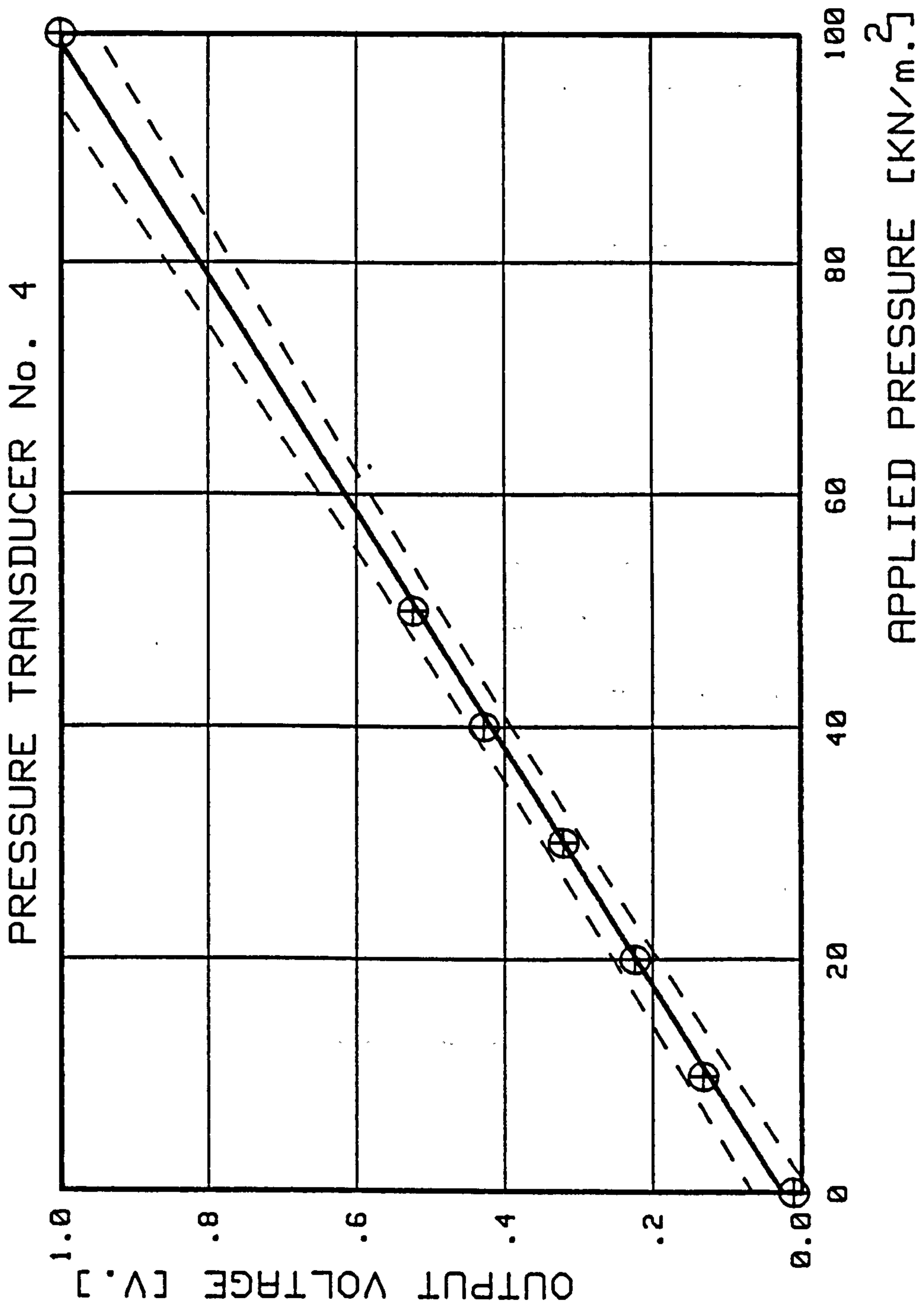


FIG 1.2 STATIC CALIBRATION CURVE

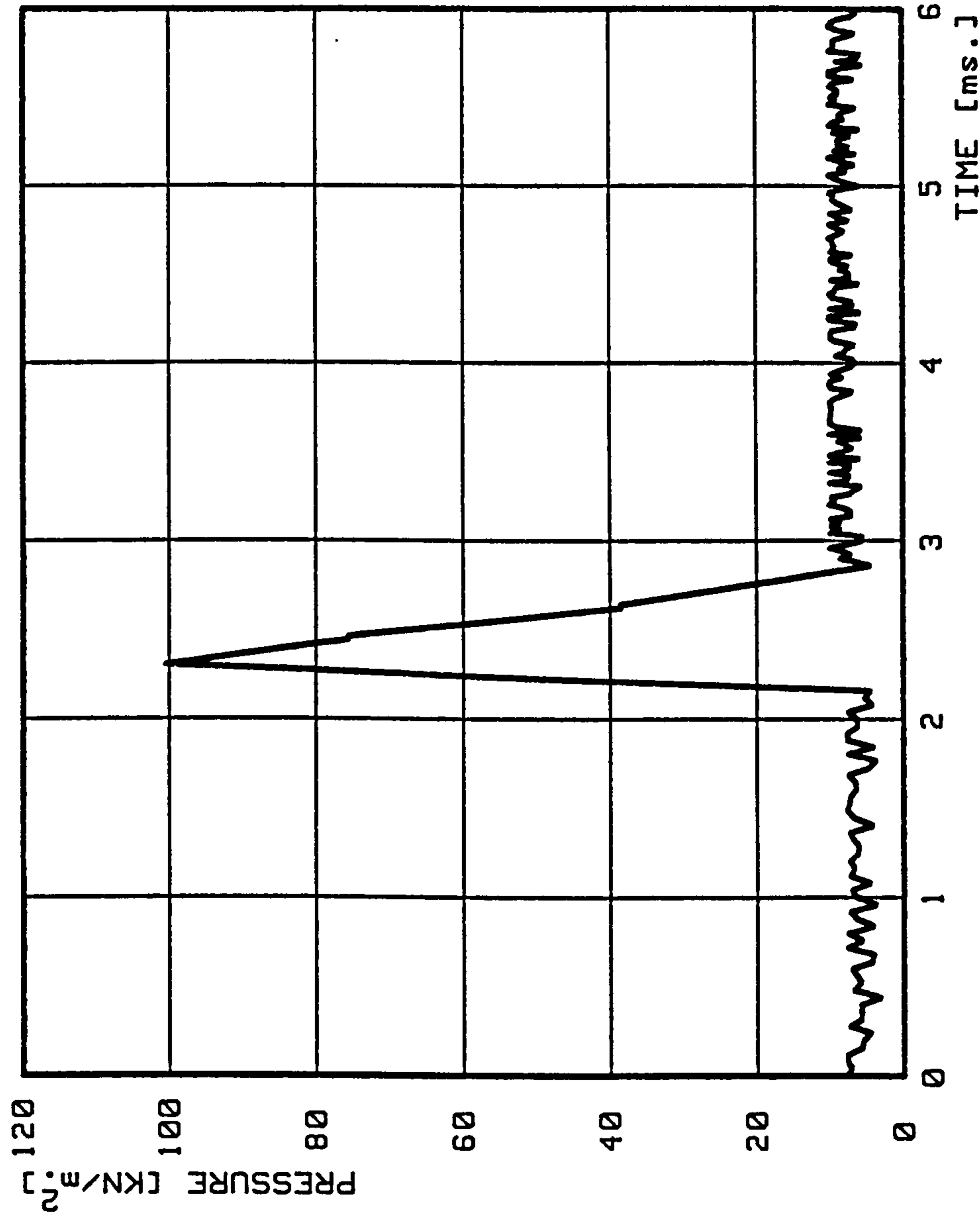


FIG 1.3 TYPICAL DYNAMIC CALIBRATION CURVE

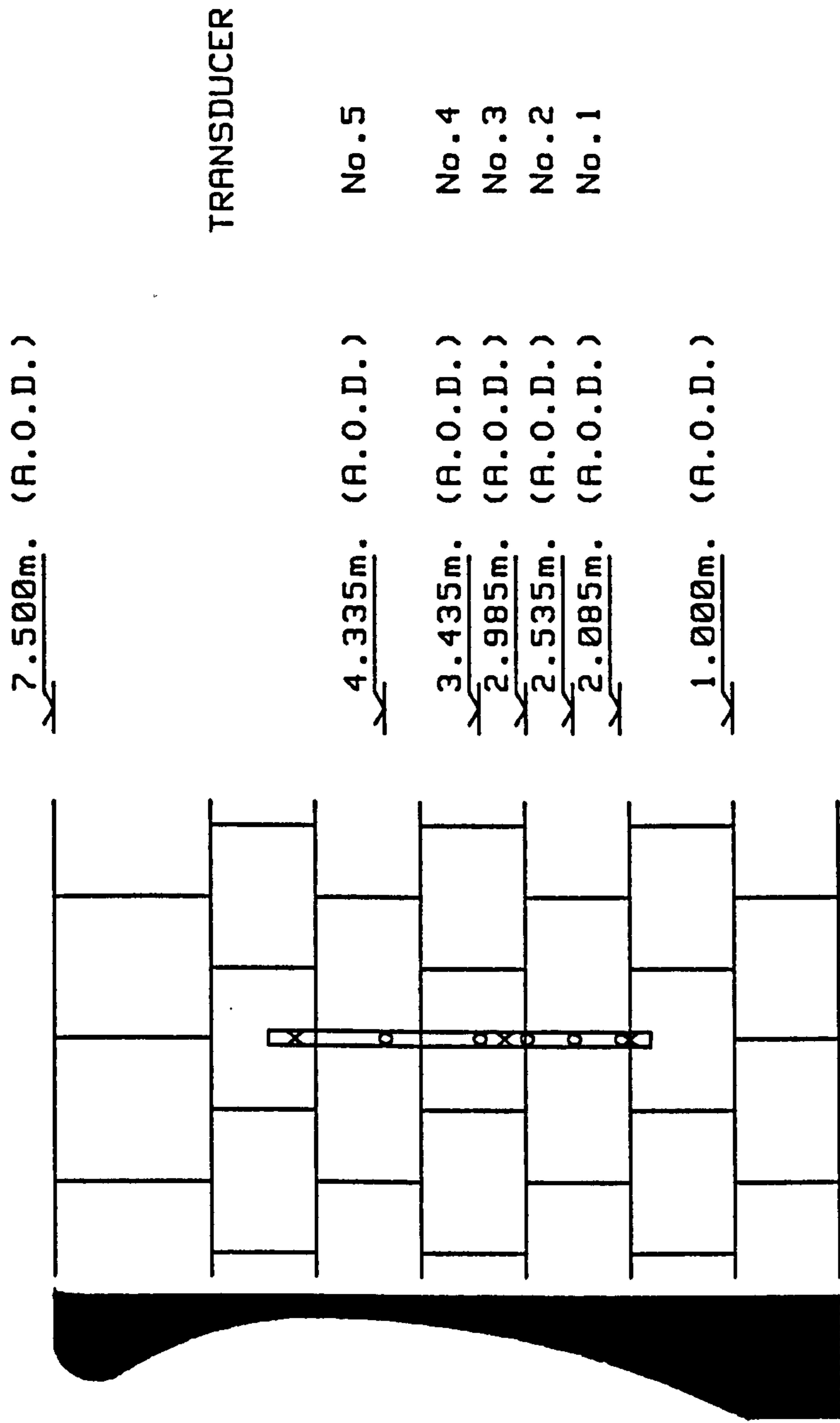


FIG 1.4 ELEVATION AND PROFILE OF SEAWALL AT ILFRACOMBE WITH TRANSDUCER POSITIONS

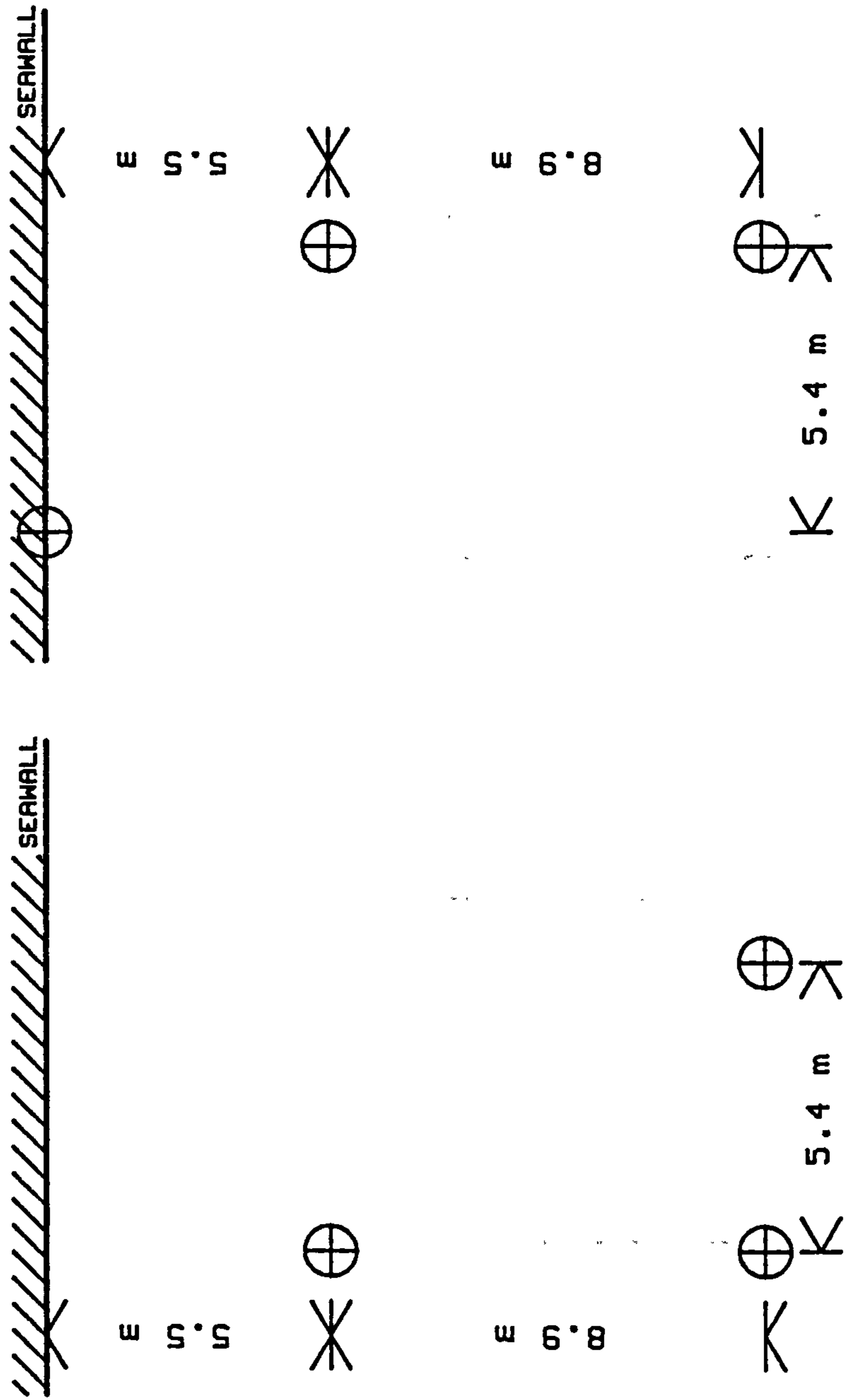


FIG 1.5 TWO ARRANGEMENTS FOR POSITIONS OF
THREE BEACH TRANSDUCERS AT ILFRACOMBE

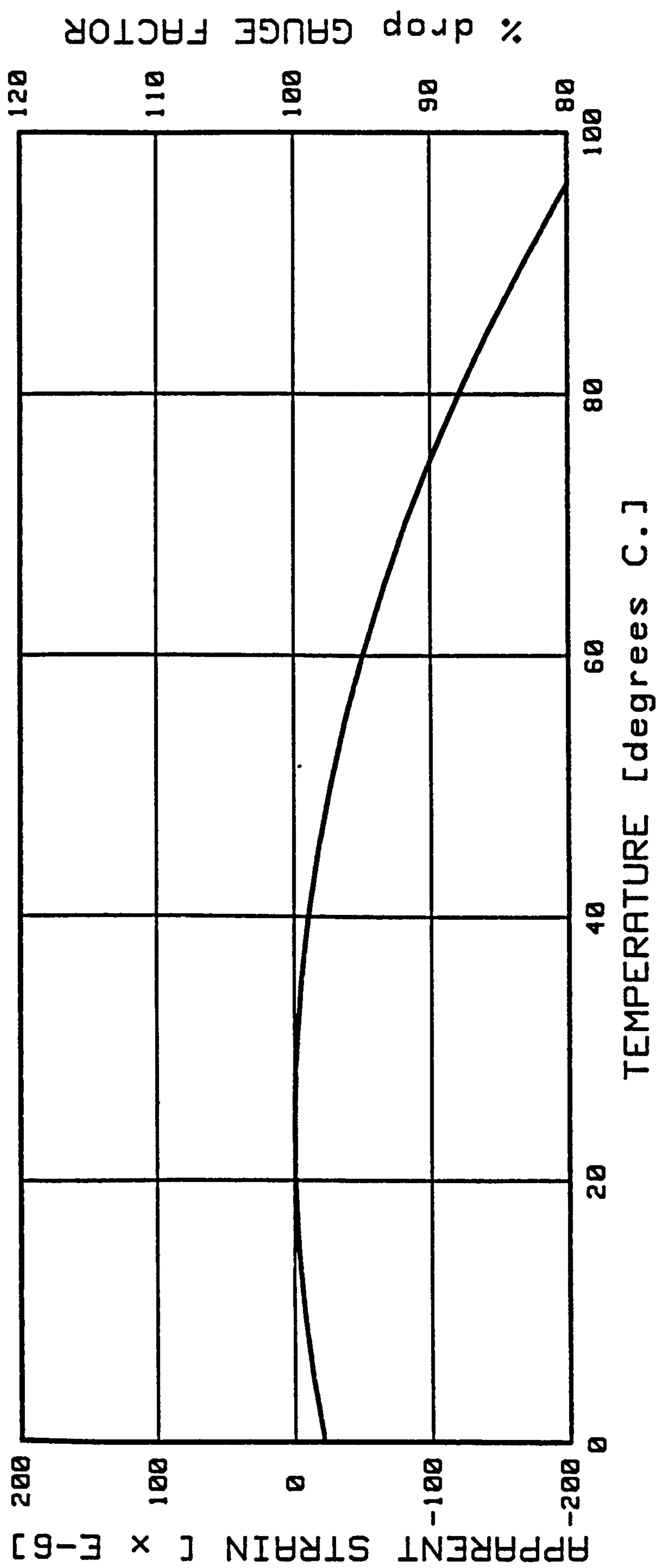
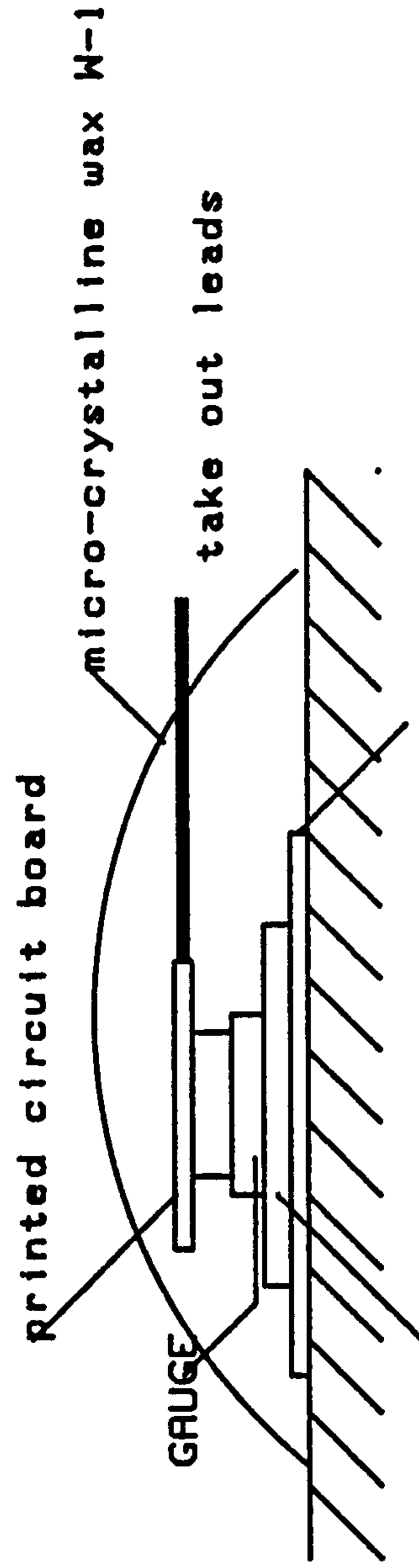
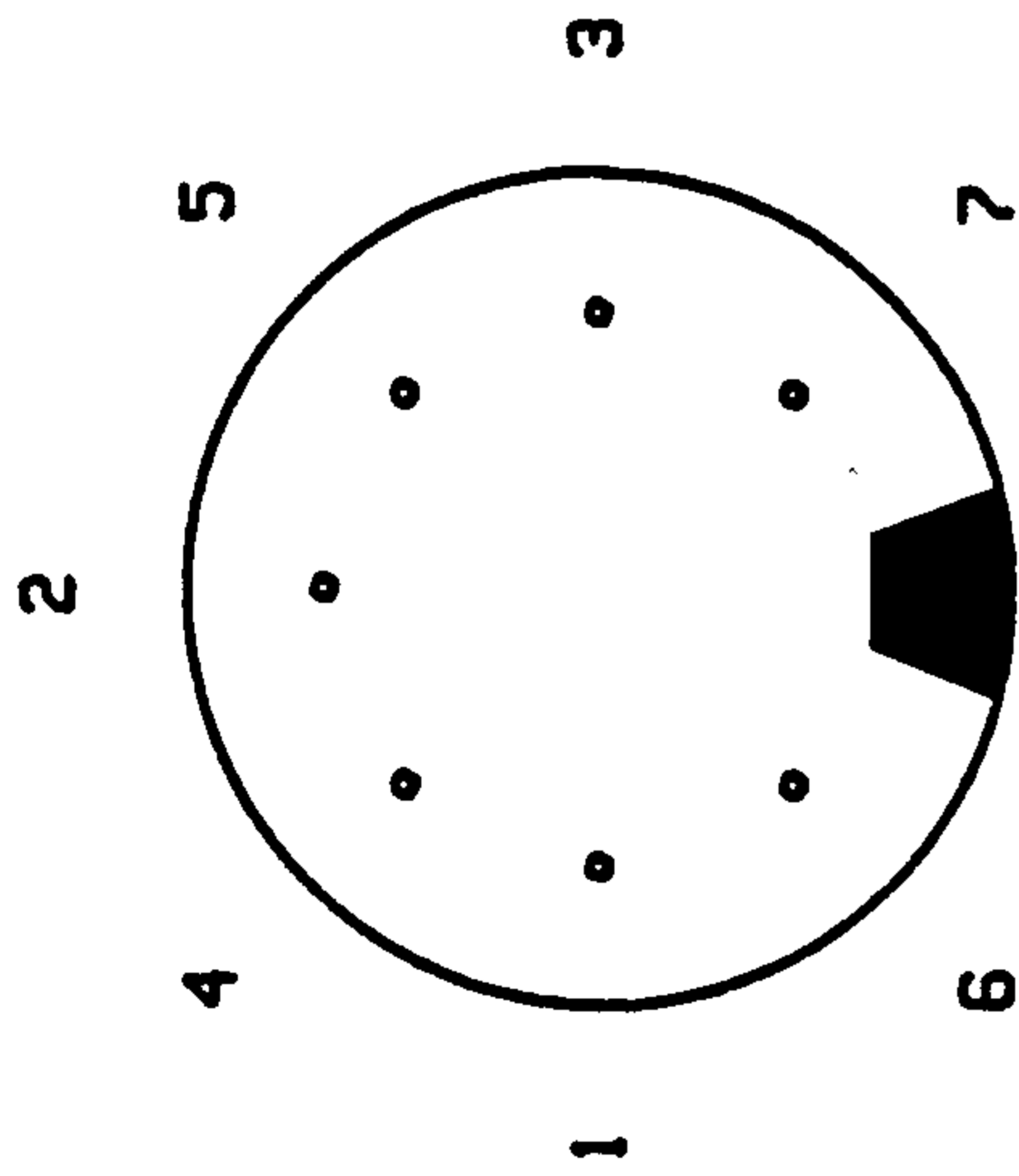


FIG 1.6 PLOT OF TEMPERATURE AGAINST STRAIN

COLOUR CODE

- 1 = yellow
- 2 = black
- 3 = red
- 4 = blue
- 5 = screen
- 6 = green
- 7 = white



Precoating P-2

P-2 adhesive

FIG 1.7 DIAGRAM OF BONDING AND DIN PLUG WIRING

CHAPTER TWO

SITE CONSIDERATIONS

2.1 THE SITE LOCATION

The site chosen for the field measurements was Ilfracombe on the North Devon coast of England. It is situated in the Bristol Channel and forms part of the outer reaches of the Severn Estuary (Figs. 2.1, 2.2, 2.3, 2.4).

A number of sea defences protect this coastline, and the one chosen for experimentation was rebuilt in 1973 (Plate I). The wall is made of precast reinforced concrete and replaces an older brick wall. The purpose of the wall is to protect the backyards of a number of residential and commercial buildings. These are situated on the north quay of the Ilfracombe harbour. As Ilfracombe is mainly a summer resort, the wall also protects an open area used for leisure purposes. The wall alignment rests at 20 m from the private property party walls. An insitu concrete ground slab and screed, laid to falls, ends at the superstructure of the wall. Overtopping from waves is drained through 100 mm diameter ducts laid at 1 m centres at the inner face of the wall. The inner face also serves as a parapet wall and stands 1.3 m above promenade level.

The precast concrete blocks are of 1.5 m x 1 m x 1 m basic dimensions and were laid in stretcher bond on the face of the wall. Bonding of the blocks was reinforced by grouted bars fixed to the starter bars at the toe foundations. The main characteristic of the wall is the shaped blocks in section. The overall profile forms part of a re-entrant curve with a bull nose finish at the crown (Fig. 2.5). The purpose of this design is that, under the impact of a wave,

the wall acts as a return on the oncoming momentum. Also the deflection of the water mass reduces the amount of overtopping. An overtopping reduction was a case for consideration for the site. A backing wind acting on the overtopping volume of water has detrimental effects on the property that is intended to be protected. The nominal height of the wall is 7.5 m above the toe.

The wall is stabilised through a volume of mass concrete and backfill. This construction gives a damping characteristic of the dynamic response that is more mass controlled than stiffness controlled. The foreshore consists of shale rock outcrops surrounded by shingle beach (See Fig. 2.5, Plate II).

The field tests were carried out about the centre of the complete 120 m length of wall. This location was in line with a let room in a private dwelling which served as a recording station. The determining factor on this option was, first, the dry roof over the instruments, and secondly, that the maximum suggested connecting cable runs at 60 m for minimised interference. The positioning of the fixing point on the wall and the steel pin fixed on the back wall were located at 20 m apart. The tensioning of the cable-cum-hose between these two fixing points provided a secure suspended set up. The provision for the underpassing of traffic made this option necessary. This suited the public use of the area when experimentation was carried out. The idea of keeping the general open space free from additional equipment also made it safe when the site was not in use for long periods of time. In this case, all permanent fixing points were positioned at inaccessible places.

For this reason they were also clearly identified in contrast to the surroundings.

Ilfracombe has proved to be a prime site for the fixing of the equipment and the siting of the recording station. The variability of the sea state occurring in most cases, has shown that the site itself provided suitable random information. It is this type of information that was sought after in the presentation of this work — a variability otherwise difficult to achieve under controlled conditions. In this case the data collected was extraneous as a result of other governing factors. These governing factors were not only local, as has been discussed but were due to more far reaching influences.

2.1.1 Fixing Considerations

The type of fixing required for the securing of the measuring equipment was required to withstand both tensile and shearing forces. The tensile forces were a result of the holding down strength as would be encountered in mooring forces. The shear forces were due to the lateral loading at the fixing points.

The tensile and shearing strength to meet the above requirements was satisfied by threaded studs. The material had to be stainless steel to withstand the high degree of corrosion present in the marine environment. The standard thread provided a quick but effective means of securing the superstructure to. Also a degree of flexibility had to be upheld when sensitive equipment was placed in long term rough conditions.

The chosen way of securing the holding down bolts was to grout them in 20 mm diameter holes bored by percussion hammer drill. The grouting was made from a mixture of rapid hardening cement and a low water content. This provided a slurry adequate for proper compaction into a restricted area. The limited time for setting of the grout also had to be taken into consideration. The bolts held both the beach (Plate VII) array and the wall array fitted on the fixing metal strip.

The initial fixing point of the transducers on the face of the wall required the need of an intermediate fixing point. This was situated on the top of the wall. It took the form of clamps cut out of 25 mm by 50 mm hardwood sections and bolted together. The clamps were fixed to an upright mild steel angle 64 mm by 51 mm which was anchored to the wall by Rawlbolts (Plate IV). This fixing overcame the lateral movement of the bulk of the hoses by water movement along the face of the wall.

The hoses maintained this distributed spread by adopting a similar suspended clamped device at the other fixing point (Plate V). The slack was taken up by means of a jack with a ratchet used for applying the tension gradually.

2.1.2 The Alternative Site

A second site was chosen for the extension of previous measurements and for providing a variation on the wall profile. This exercise involved a means for the verification of the determined results

from the previous site. It also served to present a set of readings that were capable of reaching higher levels in which the other site was lacking.

The site was at Bovisands which is situated on the East Coast of the Plymouth Sound (Figs. 2.6, 2.7, 2.8, 2.9). The wall used for the experimentation is of a breakwater type. It protects a small harbour which serves for launching seacraft and is a starting point for deep water diving exercises. The wall is constructed of small sandstone blocks of approximate height 0.5 m to 0.6 m. It is founded directly on rock. The wall stands 7.0 m high including the 3 m (wall) upstand on the face, buffeting severe storm activity. This face is straight (Plate XI) with a gentle inclination for most of the wall except for the top capping blocks.

The foreshore is rocky with parts of it lying below low water springs. This provided an ideal location for beach transducers which could be immersed immediately at the rise of the tide. The inclination of the wall did not create any difficulties in the fixing of the transducers. A similar technique as was used in the previous set up was adapted for this situation; maintaining the same regard for the level of fixing (above Ordnance Datum).

The proximity of the recording station meant that the cables could be run at ground level. The site benefits from its vicinity to the main laboratory at the research centre to which last minute modifications could easily be accommodated.

A favourable aspect of this site was that the wall faces Southwest. As the regular monitoring of the locality showed, gales arising from this orientation in the cyclonic configuration of pressure were quite frequent. The interest as regards the research was that the site provided a dramatic change from deep water to shallow water (Plate XIII). The result was that not much wave energy was dissipated during the shoaling process. Consequently, the site experienced a reduction in randomness in favour of better defined long crested waves. Also the location of the wall transducers, decided by a sharp rise in the beach level, provided an increase in the probability for the formation of potentially large breaking waves (See Plate XIV).

2.2 TIDAL EFFECTS

The Bristol Channel is one of the areas of interest in terms of coastal engineering. It covers one of the larger tidal ranges around the British Isles. The value of this has already been studied in great depth along the estuary of the Severn. The D.O.E. has commissioned feasibility studies for the designing of a tidal power barrage for the area⁽⁴⁷⁾. Work has been carried out by Hydraulics Research Limited from 1976. Information concerning tides in this area due to areas having further outreaching influences is therefore available. The extended area concerned with in this study is also bounded by the Irish Sea, the English Channel and the Continental Shelf.

This vast expanse of sea has an influence on the seas reaching the wall. The wall itself is facing North-North East. The tide is determined by the periodic rise and fall of the water level. The tidal regime for the Severn Estuary is semi-diurnal and has a cycle of about 12½ hours. The changes in sea level bring about horizontal movements of the water which generate the tidal currents. The variations in these tidal levels are seasonal and are maximised in equinoxal tides. These tides occur in the vernal and autumnal equinoxes during March and September.

2.2.1 Differences In Tidal Levels

The difference in level between high and low water is called the range of the tide. In this semi-diurnal cycle, there also exist

large ranges and low ranges. The larger range is called the spring tide occurring about once a fortnight on the new or full moon. This is in contrast to the lower end of the range and is called a neap tide.

Surveying of the tidal information is intended to produce a derivation of the tidal constituent values. By this is understood the rate of change of tidal movements with respect to the peak tides and the daily variations.

Sets of simultaneous spring and neap tidal level observations have been obtained from a tidal gauge at Ilfracombe. The temporal variations of sea level produced a set of tidal curves. These curves showed clearly the shape encountered for either a spring or a neap tide. The variation confirmed that the $12\frac{1}{2}$ hours repeated cycle applies to Ilfracombe. The 3 hour interval values also determined the level of the water relative to the surveying reference point of Ordinance Datum at Newlyn (see Fig. 2.5)

The maximum tidal range recorded in the Bristol channel is 9.29 m for springs and 4.01 m for neaps (See Fig. 2.10)⁽⁴⁸⁾. These relatively high ranges and the rate of change of the tide are subject to current changes. For flood and ebb currents that are well matched, they only produce a negligible amount of net transport of the loose material. However, the water movements generated by the current strength produce the flow properties of the water mass. Typical current strengths as a result of the flow pattern of the mean tide

is given as 0.8 ms^{-1} . General observations of the tidal motion increasing in the landward direction is due to the funnel shape of the estuary.

2.2.2 Currents Associated With Water Movements

The effect of currents on coastal structures is determined by the configuration of the coastline. A longshore current acting together with oncoming waves produces currents opposing the general movement of wave propagation. These currents are called rip currents and are mainly associated with movement of water along beaches. Their influence is to induce a steep vertical profile on the front of the wave when compared to the back of the crest of the wave⁽⁴⁹⁾.

Tidal currents in excess of 1.5 ms^{-1} have been measured as near bed velocities along coastal stations. These measurements were initially carried out on Langford Grounds, Cardiff⁽⁴⁷⁾ at the beginning and end of submersion during a spring tide. However, the coastal sites on the North Devon coast experience the same tidal regime with equally possible attainable currents. The fast currents are a direct effect of the large tidal range. This additional parameter affects deep water collected data. This is because of the physical difficulties in handling the instruments from vessels at anchor. Also, any velocity measurements have to be corrected for the current component.

2.2.3 Tide As A Favourable Factor For The Chosen Site

A large tidal range was sought in this type of experimentation. The low water mark exposed most of the structure. This, aided by the easy access to the foreshore, proved invaluable for setting out of the work initially. There are always a number of time consuming tasks that have to be carried out in the critical hours of low tide. Otherwise, the provision of more sophisticated and complicated means of access and supporting rig had to be devised. The difficulties of working under the stormy conditions meant that a greater degree of safety precautions had to be taken. Reducing the risks of a rough sea, which had to be coped with, made the tasks more manageable. The organisation of the work had to be maintained even for setting up the equipment when the readings were to be taken.

The tidal range meant that a variable water depth could be realised throughout the course of experimentation. This condition was required for the development of the free water surface into a potentially breaking zone. The other pre-requisite was that the waves had to break frequently, definitely and preferably at the wall. These conditions were satisfied readily at this chosen site because of the tidal range.

The tidal range most applicable to these requirements, was, in fact, the spring levels(which evidently showed the larger variability). This period of data reading was chosen to overcome the hazards from the rock outcrops. This meant that energy contained in wave motion did not dissipate before reaching the wall. Also, continuity

of the wave train was more evident in terms of maintaining a sense of stability in profile. The transformation of a wave into an unstable one was considered to be limited primarily to depth reduction, even before reaching inhibiting obstructions.

2.2.4 Meteorological Influences On Tides. Surges

The continual reference to change in atmospheric pressure is necessary when considering tides. The values of levels are given as mean levels. A sudden drop in barometric pressure has a prolonged effect on the general body of water. The tendency is to raise the average overall level of the water mass. This is most evident in the approaching of a storm. The change in level of as much as 1 m has been recorded and is called a tidal surge. In some cases, although a surge is likely, this is counteracted by an effective change in the wind direction. The backing wind will bring down a tidal surge to its original level.

2.3 FREQUENCY OF USE. FORECASTING

The frequency of use of the site is determined by the factors that generate the wave field. These factors put together according to their degree of influence, dictate the appropriate time for measurements to take place. Before describing the relevant technique of forecasting waves, an understanding of their associated distribution and representation is carried out. The type of distribution opted for was one that fitted the variabilities expected on site in terms of active acquired data⁽⁵⁰⁾.

2.3.1 Wave Height Distribution

A sample of wave heights plotted against their frequency of occurrence took the shape of a distribution attributed to Rayleigh. This was in keeping with the fact that wave heights are measured as positive quantities. To avoid the irrational and arbitrary spread of values taken from different samples, the data obtained in this field was normalised. The parameter chosen for any normalisation process is usually of the same calibre, or at least carries the same overall dimensions as the measured value.

In this case the mean value of the wave height, \bar{H} was chosen for the normalisation process and for plotting to the same scale.

The Rayleigh's Distribution is given as:

$$p(H) = \frac{\pi}{2} \frac{H}{\bar{H}^2} \left[\exp \left\{ -\frac{\pi}{4} \left(\frac{H}{\bar{H}} \right)^2 \right\} \right] \quad (2.1)$$

in terms of the probability density function $p(H)$ (Fig. 2.11).

The plot of the above was adapted to relate typical samples of a duration given by the product of the number of waves, N and the average period, T . This gave a specific statistical representation of the random sea.

The true significance of this representation was to plot the cumulative probability that a value of H is exceeded. On this basis all values of wave height above zero were included in this final significance, i.e. at zero, $P(H) = 1$. As wave height increases in incremental values, so the amount (number in population) exceeding this value is only a percentage of the overall amount. As the wave height increases, so this percentage reduces. This proceeds until the maximum wave height is reached to give no values of the total distribution larger than this.

The analysis was used to determine a wave height to any significance. The chosen value is usually termed the third of the highest. This was calculated from the Probability Distribution Function. The latter has been calculated as $P(H/\bar{H})$ as in the previous exercise.

Therefore, the area under the curve for 33% of the population – the extreme end of the curve, gave a distribution of the highest third waves, (an ascending order arrangement is automatically sorted out). The average value of this distribution was given as the significant wave height,

$$\text{or: } \int_H^{H_{\max}} p\left(\frac{H}{\bar{H}}\right) \cdot H \, dH \quad (2.2)$$

(Fig. 2.12)

The maximum value of wave height is also important.

The accuracy of the maximum value of wave height, when obtained from a random sample in terms of the significant wave height is a function of the number of samples, N . In turn, the number of samples are in terms of a function of the crossing-up period; for instance, for 200 waves, H_{\max} is given as $1.64 H_{\frac{1}{3}}$. Graphically, the significant wave height per unit \bar{H} is given as the centroid of the shaded area (Fig. 2.12).

In quantitative terms, the following relations were obtained for the unit mean wave height, \bar{H} :

$$\begin{array}{rcl}
 \text{Significant wave height, } H_{\frac{1}{3}} & = & 1.64 \bar{H} \\
 \text{Maximum wave height, } H_{\max} & = & 3.10 \bar{H} \\
 \text{Ratio} & = & 1.89
 \end{array} \tag{2.3}$$

The product of the probability density function and the square of wave height over the whole curve, gives, on taking its root, the root mean squared value of the height, H_{rms} .

2.3.2 Wave Period Distribution

The wave period is a result of a composite number of waves with a varying period distribution. This hierarchy of waves is due to the development and propagation of the general sea state. The period follows the same distribution as the wave height for the random sea. In this case, the governing term is the square of the period and this is used in comparing the number of samples in the population.

Here, the equivalent Rayleigh Distribution is made up of the square of its terms, i.e.

$$p(T) = \underbrace{\left(\frac{\pi}{2}\right)^2}_{[1]} \frac{T^3}{\bar{T}^4} \left[\exp \left\{ - \underbrace{\left(\frac{\pi}{4}\right)^2}_{[2]} \cdot \left(\frac{T}{\bar{T}}\right)^4 \right\} \right] \quad (2.4)$$

Approximate value of [1] is 2.7

Approximate value of [2] is 0.675, given for Nagoya Harbour

Significant Period, $T = 1.07 \bar{T}$ with 8% error, where \bar{T} is the average period ^(s1)(s2)

2.3.3 Random Wave Field In Nature

The random wave field in nature is usually described in terms of $T_{\frac{1}{3}}$ and $H_{\frac{1}{3}}$. The physical significance of this is that the wave field is represented by a number of sinusoidal waves with differing frequencies of oscillations. A quantitative representation of the same field is therefore given by a spectrum of the wave frequency components. This means that an energy representation of the sea may be given.

The wave generation may have a predominant direction, but in a real situation, the distribution of directions is evident. This implies that the spectrum in frequency terms will have to be evaluated for the different directions. This brings about the spatial quality of wave propagation.

Assuming the wave propagation may be reduced to a predominant direction, the energy spectrum is of a one dimensional type. The value of this, if given in $[L]^2.[T]$ units, may be used to evaluate the mean of the square value of elevation. The surface elevation η , mentioned here, is distinct from wave height H , in that it covers the whole of the continuous surface variation in discrete samples. In the case of wave height, the quantities are reduced to one value per wave defined between successive zero up crossing points. The integral of the spectrum in the frequency domain is equal to the mean of the square of the surface elevation, that is,

$$\int \text{SPECTRUM } df = \bar{\eta}^2 \quad (2.5)$$

This value represents the energy contained in the wave train.

This method depends on the representation of the wave train by a number of sinusoidal waveforms with:-

- (i) specific amplitudes
- (ii) specific frequency of oscillation
- (iii) phase difference

All three parameters are specific for each of the waveforms and in each case the surface elevation is reduced to a function of time only. The combined effect of the individual waveforms gives a value of the surface elevation at a given point in time. The identifying of the different parameters is grouped in the process of producing the energy spectrum. This is because, the spectrum evaluation takes into consideration the frequency components, the amplitude and the phase variations.

2.3.4 Useful Spectra For Comparison

The deterministic values obtained from sample energy spectra are directly compared to standard representative ones, namely:-

1. The Pierson and Moskowitz.
2. The Bretschneider.
3. The JONSWAP.

The first is wind speed dependent — a spectrum resulting from wind generated waves by the continual effect of a wind force acting along a main direction (and for a definite duration of application).

For a fully developed sea, the equation of the Pierson-Moskowitz is,

$$E(f) = \frac{8.10 \times 10^{-3} g^2}{(2\pi)^4 f^5} \exp \left[-0.74 \left(\frac{g}{2\pi U_{19.5} f} \right)^4 \right] m^2 s \quad (2.6)$$

Where $U_{19.5}$ is wind speed in ms^{-1} at 19.5 m above the mean water surface.

The second spectrum is dependent on the significant wave period and wave height. However, each of these are converted to mean values by previous formulation to evaluate the expected spectrum. This spectrum is Fetch definite and still is a direct consequence of wind generated waves. Representation of this most directly applicable and useful spectrum is,

$$E(f) = 0.430 \left(\frac{\bar{H}}{g\bar{T}^2} \right)^2 \frac{g^2}{f^5} \exp \left[-0.675 \left(\frac{1}{\bar{T}f} \right)^4 \right] \quad (2.7)$$

(Fig. 2.13)

A Fetch limited JONSWAP spectrum is given by the equation

$$E(f) = \frac{\alpha g^2}{(2\pi)^4 f^5} \exp \left[-1.25 \frac{f m^4}{f^4} \right] \gamma \exp \left[-\frac{(f-f_m)^2}{2 f m^2 \sigma^2} \right] \quad (2.8)$$

Where

$$\alpha = 3.26 \times 10^{-2} \tilde{f}_m^{6/7}$$

$$\gamma = 4.42 \tilde{f}_m^{3/7}$$

$$\sigma = 0.07 \quad f \leq f_m$$

$$= 0.09 \quad f > f_m$$

$$\tilde{f}_m = U f_m / g$$

γ is the peak enhancement factor

w_m is the peak frequency of wind speed and fetch

f_m is the peak frequency

\tilde{f}_m is the dimensionless peak frequency

α is a constant

σ is a constant

A peakier representation of the Pierson-Moskowitz spectrum is the JONSWAP spectrum⁽⁵³⁾, with γ being the ratio between two peaks.

The spectrum is characterised by the width of the frequency about the central frequency determining a narrow band width of significant frequency values — about which the bulk of energy is concentrated.

Any energy due to ripples is eliminated by its sheer negligible value in the spectrum.

2.3.5 Values Obtained From Energy Spectra

Spectrum in the right sort of units can produce a user with a selection of related data. The most useful parameters are called the moments, of which there are plenty, including the values,

$$m_0 = \eta^{-2} = \int_0^{\infty} \text{Spectra } df$$

and

$$m_2 = \int_0^{\infty} \text{Spectra} \cdot f^2 df \quad \text{etc.} \quad (2.9)$$

These particular values then give the average period.

$$\bar{T} = \left[\frac{m_0}{m_2} \right]^{\frac{1}{2}} \text{ which is also the zero up crossing period.}$$

This value is required to establish a frame of reference for the scales used. Other binding equations are, significant wave height and average wave height, obtained from theory and are given by,

$$\begin{aligned} \bar{H} &= 1.77 \sqrt{E} \\ H_{\frac{1}{3}} &= 1.6 \cdot 1.77 \sqrt{E} && (54) \\ &= 2.83 \sqrt{E} && (2.10) \end{aligned}$$

Where E is the area under the energy spectra in the frequency domain. From these known values of mean wave height or significant wave height, the order of magnitude for E can be established. This method serves as a means of standardisation of the variety in the results.

The peak frequency, f_0 and the peak period T_0 are self explanatory.

Then,

$$\begin{aligned} \text{mean period,} \quad \bar{T} = T_z &= 0.710 f_0^{-1} \\ \text{mean frequency,} \quad \bar{f} &= 1.296 f_0^{-1} \quad (52) \\ \text{significant period,} \quad T_s &= 0.946 f_0^{-1} \quad (2.11) \end{aligned}$$

2.3.6 Directional Influence

As mentioned earlier, the spectra are considered as being uni-directional. However, the interest in the spread may become evident when referring to the velocity of progression or celerity of the random sea waves.

Comparative directional spectra include:-

- i) Cosine Squared⁽⁵⁵⁾
- ii) Cosine Power⁽⁵⁶⁾

The first is defined for θ about zero limited by $\pm \pi/2$,

that is,

$$G(\theta) = \frac{2}{\pi} \cos^2 \theta \quad |\theta| < \pi/2 \quad (2.12)$$

(Fig. 2.14a)

The second involves a variable power, s , proportional to the velocity of progression, standard deviation of waves and acceleration due to gravity. It defines the degree of spread,

that is,

$$G(\theta) = C \cdot \cos^{2s} (\theta/2) \quad (2.13)$$

about the central direction. (Fig. 2.14b)

2.3.7 Forecasting

The wave climate at a site is determined in terms of deep water wind generated waves. The external effects on the resulting waves are then taken into consideration. This produces the waveform configuration with all its design parameters that will be relevant to the situation. The design parameters are average and extreme values.

The history of weather information is needed to generate a wave pattern likely to be encountered during the life of the structure. The general approach is to determine the deep water waves derived from the data obtained from the continuous numerical study and hindcasting. The arrangement may take the form of a series of graphs or even expressions. The acquired data is sifted through processes brought about by shallow water transformation. The difficulty to overcome is that accurate determinations deal with a specific system. A system applicable to this case, is one that deals with irregular waves and non-linear effects resulting from the depth reductions. The inclusion of design storm conditions is treated as the fundamental from which to start.

The value of wind speed direction and duration are used with a JONSWAP Spectrum, described previously, to determine the significant wave height and period (Fig. 2.15). If information of the fetch (otherwise known as the distance over which a wind has maintained its characteristics), is lacking, an alternative spectrum is used. The Pierson-Moskowitz Spectrum (see earlier description) utilises the fetch, wind velocity and duration to establish these same parameters⁽⁵⁷⁾.

A determination of the return period has to be made for the investigation. The return period being the reciprocal of 1 minus the probability that a value is not exceeded; given in years. This is related to the anticipated lifetime of a structure. The probability of the extreme event happening is inversely proportional to the return period. It is also related to the number of events of measured data per year — obtained from continual data monitoring, for example, "Datawell" or deep water buoy recording.

On a macro scale, elaborate pressure fields are used in the determination of wind speed and direction. The result is in a form of a wind field limited by the planetary layer at one end and the sea level at the other. However, of greater importance, are the surface winds which impart the energy at the sea interface⁽⁵⁸⁾.

The exceedence value curve is plotted for long term probability measurement. This curve is plotted as the percentage exceeding incremental values of significant wave height. This curve is used for prediction of extreme conditions of wave height. The curve is used with an appropriate data set to determine the best fit distribution of data and to determine the extreme value of wave height. This value is obtained by extrapolation of the tail end of the curve.

A more rigorous statistical method to determine the extreme value is by producing a Weibull Distribution⁽⁵⁹⁾. Data values are plotted against the log plot of the log of 1-probability. The best line fit is passed through the plotted points and the extreme value obtained by extrapolation (See Fig. 2.16).

Wave activity is defined in terms of a wind sea and a swell sea. The wind sea is the one described above. The swell sea is identified whenever the wind sea decreases in terms of energy content. The result is long period waves and, at times may be independent of the wind speed — a wave type being not so steep in character⁽⁶⁰⁾.

The distribution of the wind and swell sea is picked out in the spectral shape of the energy in the frequency domain. A study of the spectra shows a sharp peak (Fig. 2.17). This is dominated by swell components which are giving the energy content of the free surface variations. The wideband frequency range is due to the local sea state. The local waves give the steepness contribution and contain high frequency components. These waves are limited by their stability criteria. The narrowness of the band of swell components is a measure of the wave groupiness found in a random distribution⁽⁶¹⁾.

The forecasting of wind generated waves in deep water has its limitations. These include non-linear effects and the lateral distribution of energy (the 3-D effect). The basic assumption for this study is that the energy flux is transmitted from one wavefront to the next⁽⁶¹⁾.

2.4 WIND DATA

Winds are measured in terms of their velocity, and the direction is given in terms of where the wind is blowing from. The pressure associated with a wind may be "to windward" or "to leeward"; with the wind blowing behind and away from the observer respectively. Intense winds are associated with a marked density of isobars or lines of equal pressure. When the barometric pressure is low, the circular area describing this is cyclonic in nature (See Fig. 2.17).

Forces of winds are measured on the Beaufort scale of 1 to 12. Examples of 40 m.p.h. winds are called force 8 gales, giving 20 ms^{-1} equivalent. Force 5 are fresh winds of a speed of 21 m.p.h. while Force 10 are stormy winds with a speed of 59 m.p.h. (27 ms^{-1}). Typical values of velocities met in this type of measurements are:- wind speeds of gale force to the order of 20 ms^{-1} , wave speeds of the order of 5 ms^{-1} , and current speeds of the order of 1.5 ms^{-1} .

The "Wind Rose" is an appreciation of the velocity in a directional sense for the area. This is a plot of the number of durations along the major axes of the compass ± 22.5 degrees which results in a plot of the most probable prevailing wind. This representation is independent of the magnitude of velocity but is direction dependent with the frequency of occurrence being the deciding parameter (Fig. 2.18a). Calms of no significant velocity are identified by a circle of arbitrary radius at the centre.

A second version of the "Wind Rose" is obtained from pre-recorded data. (cf. RAF Chivenor, North Devon). Here the sorting out stage for each of the sampled data covered the number of durations along the major axes with each addition multiplied by a velocity factor. The velocity factor was calculated as a proportion of the maximum wind velocity measured. This additional factor assessed in the final plot associated higher wind velocities together with the prevailing wind direction (See Fig. 2.18b).

Strengths of winds are proportional to the isobar arrangement. These are obtained from weather charts which give an indication of direction and magnitude. The symbol used is in the form of an arrow with a number of indicators showing the intensity of the wind. Measurements of wind velocity are linked to the duration of the storm and the fetch length. The fetch is the distance over which the velocity of wind is maintained and can be as much as 100 Km for the site on Ilfracombe (See Fig. 2.1).

2.4.1 General Pattern of Winds

Southerly gales are due to a high pressure moving west across Europe, while low pressure centres move along the west coast of the British Isles. Westerly gales are a result of high pressure over the Atlantic moving south over the Azores. The gales so produced last several days at a time.

Wind generated waves with their subsequent growth are not only a result of strength of wind blowing over the water surface. They

are also limited by the fetch and duration of storm. The significance of this is that for a wind blowing at a certain velocity, the wave height increases until a limit is reached, beyond which no further increases are detected. The reason for this is that the wave velocity has reached or surpassed the wind velocity. Further increases are only viable with a wind speed that is larger than the current wave speed. The same holds for a fetch increase. The direction of the driving force and driven mass of water comes into play in this phenomenon of wind generated waves.

The waves generated in a limited fetch situation differ from those generated in the open ocean. The length of waves is limited once a given strength is reached, under these conditions of fetch. As long as conditions of wave generation are within a degree of saturation, atmospheric instability will only effect the severity of waves.

Wind duration, fetch, and velocity all contribute to the generation of waves. Short period waves and swell produce the more damaging effects. The effect is prone to be more severe in the flood of a storm tide. The reason is that a storm surge adds to the height of the actual tidal level.

In wind generated waves, energy is imparted by friction between air in motion and the water surface. The physical process is described as due to a passing wind. The action of the wind on the front face of the surface of the water imposes a pressure while the lee face is relieved of pressure. The resulting energy imparted takes the

form of a rise of the water level about the mean sea level. This gives the wave a velocity of progression. The secondary but equally important aspect of this type of wave generation is that the symmetry of the wavefront is not upheld. Therefore a condition of a steeper wavefront to the back, from the crest's view point, is set up. This degree of instability is further enhanced with the wave travelling over reduced water depths.

2.4.2 Wind Wave Field — Waves In A Generated Area

Wind generated waves reach a stationary state after a short while. Such a state is described by directional wave spectra. The wave field consists of swell and pure wind waves. The latter predominate with continual blowing over the surface. The distinction between the two types of waves is extracted in the frequency spectrum and also in a directional spectrum, as described elsewhere. The latter defines the spread of energy over a central definite direction of progression⁽⁶²⁾.

The spectral parameters are fetch related. Spectral parameters are identified with the type of wave generating them in the frequency spectra. Frequencies within the vicinity of the peak frequency, reflect waves that obey rules of linearity in terms of dispersion relations. Spectral components in the higher frequency range are due to waves of a non-linear nature⁽⁶³¹⁾. This type of wave is mainly of a capillary scale. The insignificance of this type of wave on the main waveform means that it may be eliminated from the spectrum. This is valid only in an open sea situation⁽⁶³²⁾.

In a case of shallow water investigation the spectral parameters due to the non-linear effects will produce the principal form of energy source in the wave train. Increases in the amount of fetch, decreases the non-linearity component of the generated waves.

The main distinction between frequencies of waves are long waves and short waves. Long waves are a measure of wave groupiness⁽⁶⁴⁾. They are associated with swells and sways or unsymmetrical low period waveforms. They also have a larger spread of energy over the main direction. The consequence is that detrimental effects are on mooring lines and the generation of resonance in harbours.

Short waves are elements in a local sea state. Their spread of energy is more limited. Their direct influence to structural problems is in the short period motions of moored vessels. Short waves are a cause of rolling, pitching and heaving on such offshore structures⁽⁶⁵⁾.

2.4.3 Applications of Wave Climates

An initial factor in design is that the direction of approach of waves has to be considered everywhere and with an equal probability of occurring. However, this assumption does not hold in a real situation as encountered by a structure in coastal waters. This was observed in the current chosen site for experimentation. This behaviour is explained by obstructions present in front of the structure (Plate II). Due to prevalence of winds, the obstruction has a capacity of inducing resultant wave patterns. These patterns offer a greater influence of the extreme values in predetermined directions.

Two typical types of forces to deal with are the drag and the inertia force. The drag force on offshore structures is a function of the projected area and the square of the flow velocity. The inertia force is the function of volume and the acceleration flow⁽⁶⁶⁾.

The wave climate for a location is applied conventionally by taking the train of waves with a constant period and significant wave height and evaluating the time dependent forces. For the maximum force on a structure and its components, the worst case is determined to which is applied the dynamic magnification factor. This loading is applied to the structure statically. The dynamic analysis is carried out if the natural frequency is less than 0.5 Hz (Fig. 2.19). From the wave spectrum, the load spectrum is produced by applying a linear transfer function.

A comprehensive dynamic and static analysis can be done by determining the acceleration and velocity of water particles around the structure. This involves the choice of the relevant theory. Having obtained this information the forces are worked out using Morison's equation. From this, the static response is worked out and so is the dynamic response.

2.4.4 The Effects of Wave Height And Energy of Waves on Leaving The Generated Area

As irregularities subside, the swell is the predominant resultant wave. More tangible properties of a progressive wave train include the dispersion of energy. This dispersion occurs laterally over

the source area. The storm termination causes a sudden initial decay reducing with time. However, with the propagation of waves, the longer periods and faster moving waves aggravate the extent of this dispersion.

A reduction of energy dispersion is noted when the air resistance is moving against the waves. The catching up of the progressive wave motion on the main directional currents is due to the prevailing wind direction. Opposing currents steepen wavefronts, induce breaking and the loss of energy via turbulence. Further energy loss by internal friction is due to the viscosity factor but is insignificant compared to the rest⁽⁵⁷⁾. The decay of wave height is measured empirically by the Admiralty. The rule of thumb is that waves lose a third of their height when they travel the distance in nautical miles (1 n mi = 6080 feet) equivalent to their wavelength in feet.

2.5 VARIATIONS OF RECORDED WAVES WHEN COMPARED TO DEEP WATER WAVES

The main factors affecting a wave as it propagates over a reducing depth are:-

- (i) the friction effects of the sea bed.
- (ii) the producing of a steeper wavefront ahead of the crest.
- (iii) the introducing of waves with energy transfer from longer periods to local seas with higher frequency components.
- (iv) wave attenuation due to reflection.
- (v) differential refraction experienced by the distribution of periods due to a reduction in depth. This factor produces a predominance of waveforms over others which are characterised by frequency and amplitude similarities.

Bottom friction is supplemented by percolation (a permeability criterion) and dissipation by internal turbulence (or viscous criterion)⁽⁶⁷⁾.

The phenomenon of shoaling acting on a set of waves requires the accurate determination of the direction of propagation and the magnitude of the transmitted waves. Additional considerations are deviations from hydrostatic pressures when the linear assumptions are not being upheld by the approaching waves.

The shoaling process encompasses effects due to wave attenuation, reflection, refraction and diffraction. The contributions may be seen through one dimensional investigation of wave propagation.

The waveform is traced by its variations in wave steepness up to the stage of breaking. The behaviour may be simulated by carrying out the tests individually and then expressing their combined effect.

2.5.1 Wave Refraction

As a main influence of wave reduction, the refraction of waves cannot be overlooked. A theoretical solution carried out with first order cnoidal surface gravity waves satisfies the shallow water conditions⁽⁶⁸⁾. The solution is based on gentle sloping gradients with straight and parallel contours.

The determining factors in refraction are that the changes are solely due to depth reduction and the energy flux is maintained with progression. The reduction in depth has the same effect as reducing the celerity and wave length. As the period of oscillation remains constant, the subsequent rise in wave height follows.

Two adjacent orthogonals to the wavefront, are governed by two non-linear equations dependent on water depth and the cnoidal parameter (modulus, m). The cnoidal aspect brings about the discontinuity in the wave height and continuity in the energy flux. The solution is adapted for the particular angle of attack on the obstruction and covers a range of periods of oscillation.

The consideration for refraction is the extent to which the gradient of the beach rises. The deviations resulting from flat beaches are that they provoke dispersion while steep beaches provoke reflection. The implication of this statement is that the energy contained in the wave is affected in its travel across the varying contours. Whether the waves' energy is dispersed or reflected, the assumption of constant energy is a limited one in a real situation.

However, this assumption forms a basis of assessing the behaviour of a pattern of waves travelling over a shoaling beach. The motion is considered two dimensional, and together with this assumption, the appropriate wave theory is applied locally. The deep water characteristics act as a means of non-dimensionalising the parameters.

For constant period T , the equivalent deep water wavelength is given by,

$$L_0 = \frac{T^2 g}{2\pi} \quad (2.14)$$

Once L_0 is determined, by specifying the depth, the new wave height is assessed (Fig. 2.20). For these modified characteristics, the new wave profile is determined using the modulus in the cnoidal theory. The modulus, m is related to the non-dimensional parameters of $T\sqrt{g/d}$ and H/d .

The wave shape is drawn to the scale of wave height, H . The difference in wave height establishes the upper and lower bounds. From this scaled drawing the value of the wavelength is determined. The profile of the wave itself gives the location of the mean water level.

It is the plan area of the wave at this level that is used for comparative purposes of the progressive wave. The basic dimension of this representation gives an indication of the development of the steepness of the wave as it approaches the shoreline. The major importance of the variations of steepness for practical purposes is to establish the stability of the wave. The measure of stability gives an indication at what water depth the breaking of the waves will be predicted.

A thorough investigation of wave patterns requires the contour variations profile of the seabed appertaining to the site concerned. For this purpose a detailed hydrographic survey in the form of depth soundings is to be carried out. A way of carrying out the survey is to use a stabilized narrow beam echo sounder which gives results to 1 m accuracy⁽⁶⁹⁾. Sound attenuation, sound velocity and bottom roughness are the main parameters that will interact with echos from the seabed. The reduced depths obtained from such a survey are supplemented and cross checked by those obtained from Admiralty charts for the area (See Figs. 2.4, 2.8, 2.9).

2.5.2 Diffraction

Another means of transposing the wave profile is by diffraction. The importance of this influence comes into effect in the study of wave patterns around breakwaters and into harbour entrances. This does not apply to the type of sea defences considered in this research. The process is described through the curving of waves around sharp corners. The consequence is that the wave pattern appears to propagate in the shadow of the obstruction⁽⁷⁰⁾.

2.5.3 Reflection And Transmission

Reflection of waves is an important consideration when dealing with the design of marine structures. Reflection is the cause of seabed scour. The design would incorporate the prediction of the amount of reflection present, and ways to reduce the amount of reflected

waves. Together with reflection of waves are associated aspects of dissipation and transmission of waves in the case of free standing marine structures. Their determination has been updated by Goda (1976),⁽⁷¹⁾ Mansard (1979),⁽⁷²⁾ and Ahrens (1980)⁽⁷³⁾.

Reflection, described in terms of wave energy is a process by which waves are given a second sense of direction on reaching an obstacle. The direction of reflection depends on the direction of the incident waves. The magnitude of the reflected wave energy is dependent on the inclination of the wall to the vertical. It also follows that the presence of a marked reduction in depth produces, in itself, a degree of reflection of the wave energy. The reduction in wave energy is represented by the coefficient of reflection K_r , which is a ratio of the reflected to the incident energy.

$$K_r = \frac{a_r}{a_i} \quad (2.15) \quad (74)$$

The coefficient bears a direct relationship to the respective amplitude (attenuation) for monochromatic waves.

The energy associated with dissipation and transmission is related to the reflected energy by their respective coefficients.

$$K_r = [1 - K_D^2 + K_T^2]^{\frac{1}{2}} \quad (2.16) \quad (74)$$

The significance of this expression is that increases in dissipation energy are associated with lower reflective energy components.

Also, the steeper the wave, the larger is the dissipation of energy.

This relationship is a form of design consideration for marine structures.

The objective is to increase the energy dissipated to produce lower reflective properties. This criterion is satisfied by the use of a curved return wall. The degree of dispersion on impact is not only produced in the horizontal but also more effectively in the vertical direction. The reflected wave therefore assumes a change of direction in the vertical sense. The resulting force contribution to the wall is significantly less than if an impact were to be directly reflected off the wall; as would appear in a parabolically shaped wall surface (reflector)⁽⁷⁵⁾. The justification of the reduction in energy is attributed to the energy lost in dispersion of the fluid. Typical values of energy reduction have been detected at 20% for incident frequencies 0.18 Hz. This is culminated in the uprise of the water jet after impact has taken place.

A further extension of this design parameter is its use in armoured blocks as a protective layer to a marine structure. In this case the dissipation energy is brought about effectively through the interstices around the blocks⁽⁷⁶⁾. [Note:- the determination of reflection coefficients bears a common similarity with the study of run up, and breaking wave occurrence on beaches of varying slope and roughness]. When reflection energy is measured from the superimposition of the incident and reflected wave, the accuracy is governed by the identifying of the positions of phase and out of phase addition of the two waves.

2.5.4 Currents. Type of Wave Breakers

Propagation of waves are affected by a current field. They have the effect of lengthening the waves when they occur in the same direction of propagation. Conversely the waves are shortened by opposing currents. The effect is additive vectorially. The effect of a change in current velocity produces the same effect as refraction would. This is signified by the wavelength change occurring in both cases. Consequently, wave height variations are recorded in current flows.

Notably, when current is flowing in the direction of propagation, the horizontal variation in velocity results in an upwelling of the wave profile. An opposing current results in a horizontal deformation, as is encountered in the steepening of the front of a wave profile. This is the beginning of the formation of breaking waves. The rate at which the steepening occurs distinguishes one type of breaker from another.

The categories of breaking waves fall under plunging at one end to collapsing at the other. The criterion of determination is the velocity of the crest relative to that of the body of water. When the former exceeds the latter, a plunger is formed, producing an overturning effect. At an intermediate level, a spilling breaker is one which has comparative velocities. This is characterised by a small amount of surf appearing at the crest. The collapsing wave is a spilling breaker where not enough wave height is maintained. The case shows a fair amount of surf present and occurs mostly in the

surf zone of a beach with a low gradient. A rough indication of a shallow beach is given by a slope of 1 in 20. A steep beach is given by a slope of greater than 1 in 5 tending towards a vertical wall obstruction in the limit. A more formal description of the different types of breaking wave is seen in 4.7.3.

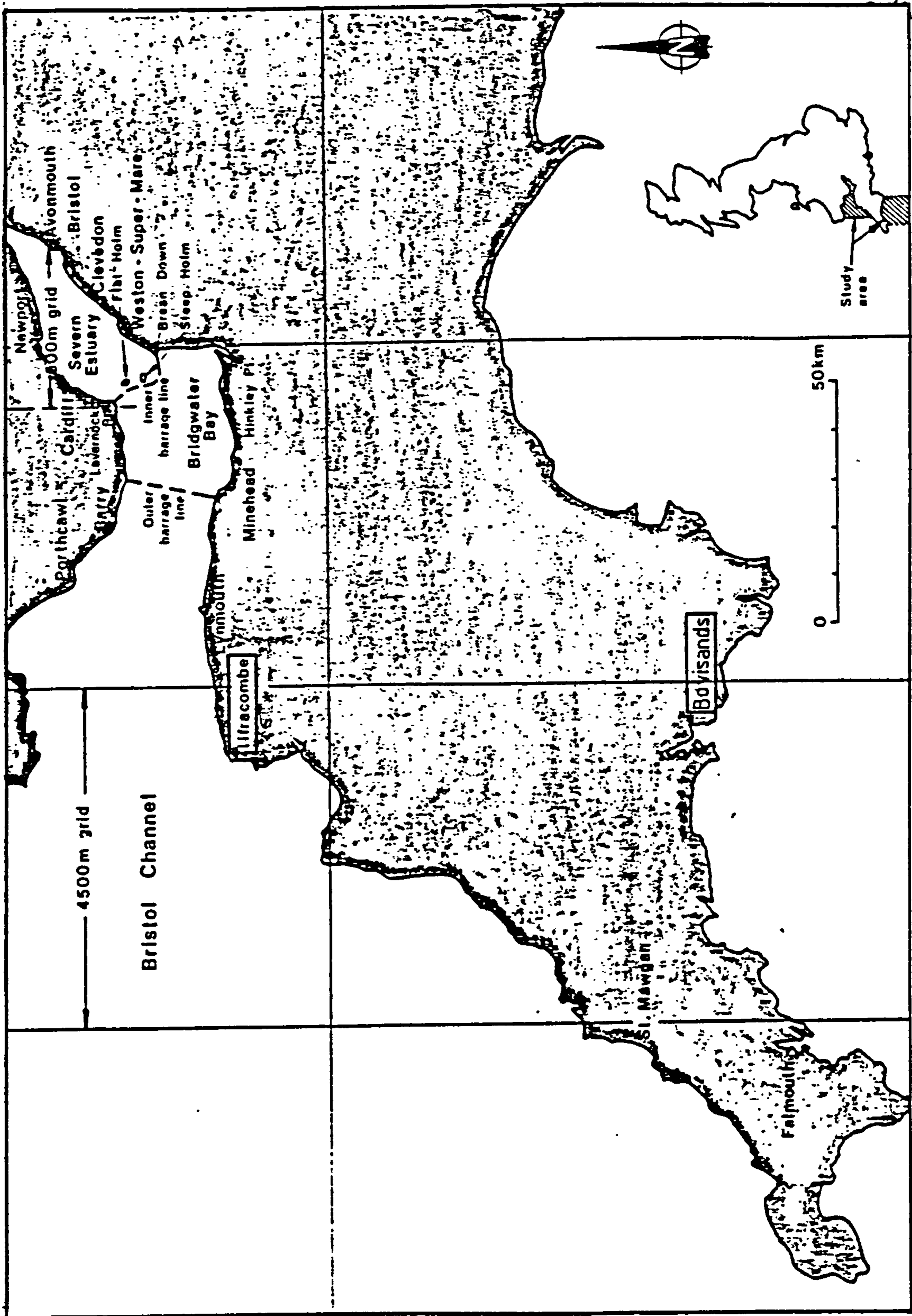


FIG 2.1 GENERAL LOCATION OF FIELD TESTING AT ILFRACOMBE AND BOVISANDS

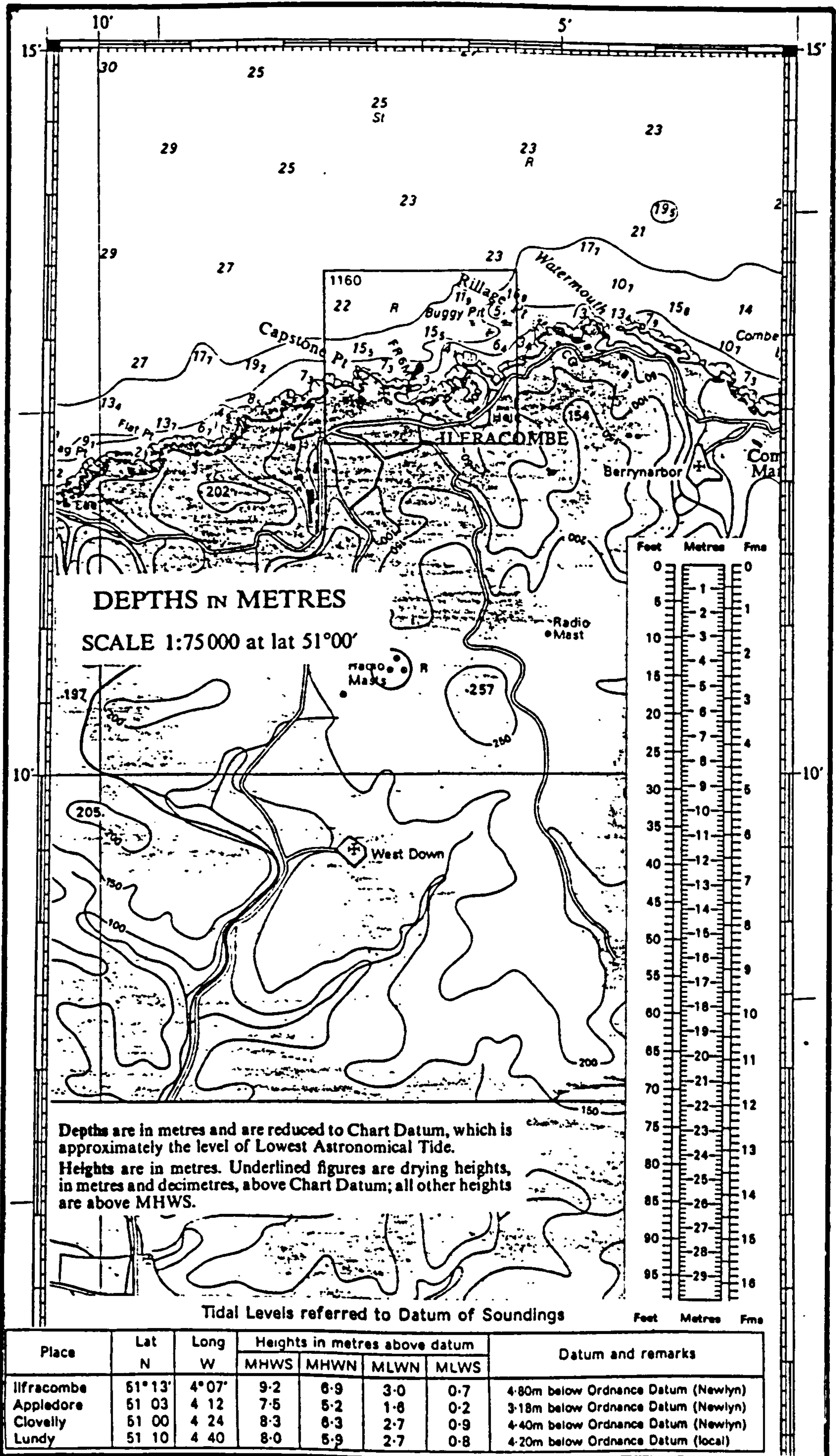


FIG 2.2 DETAILS OF TESTING SITE AT ILFRACOMBE

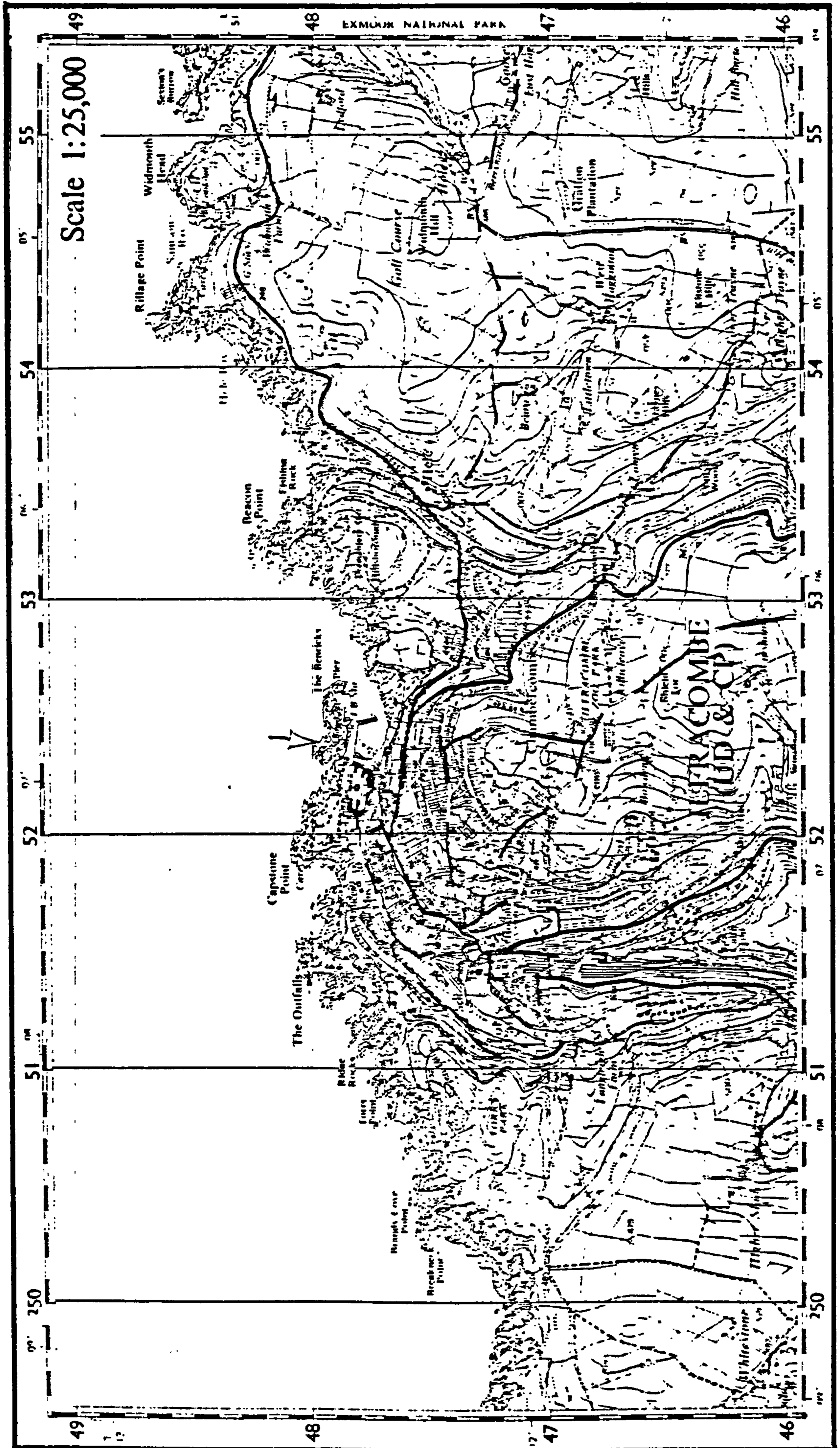
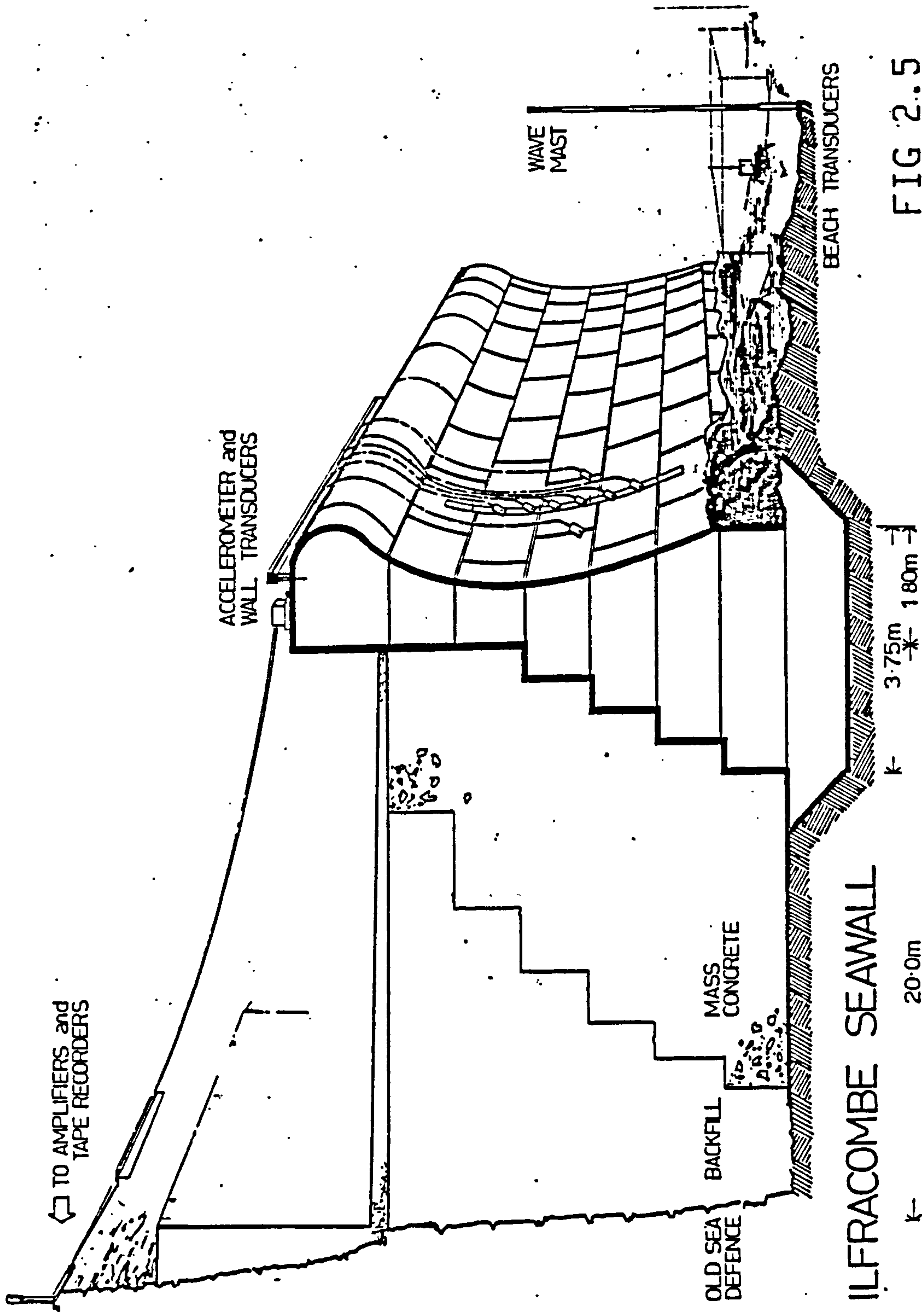


FIG 2.3 MAP SHOWING LOCATION OF ILFRACOMBE



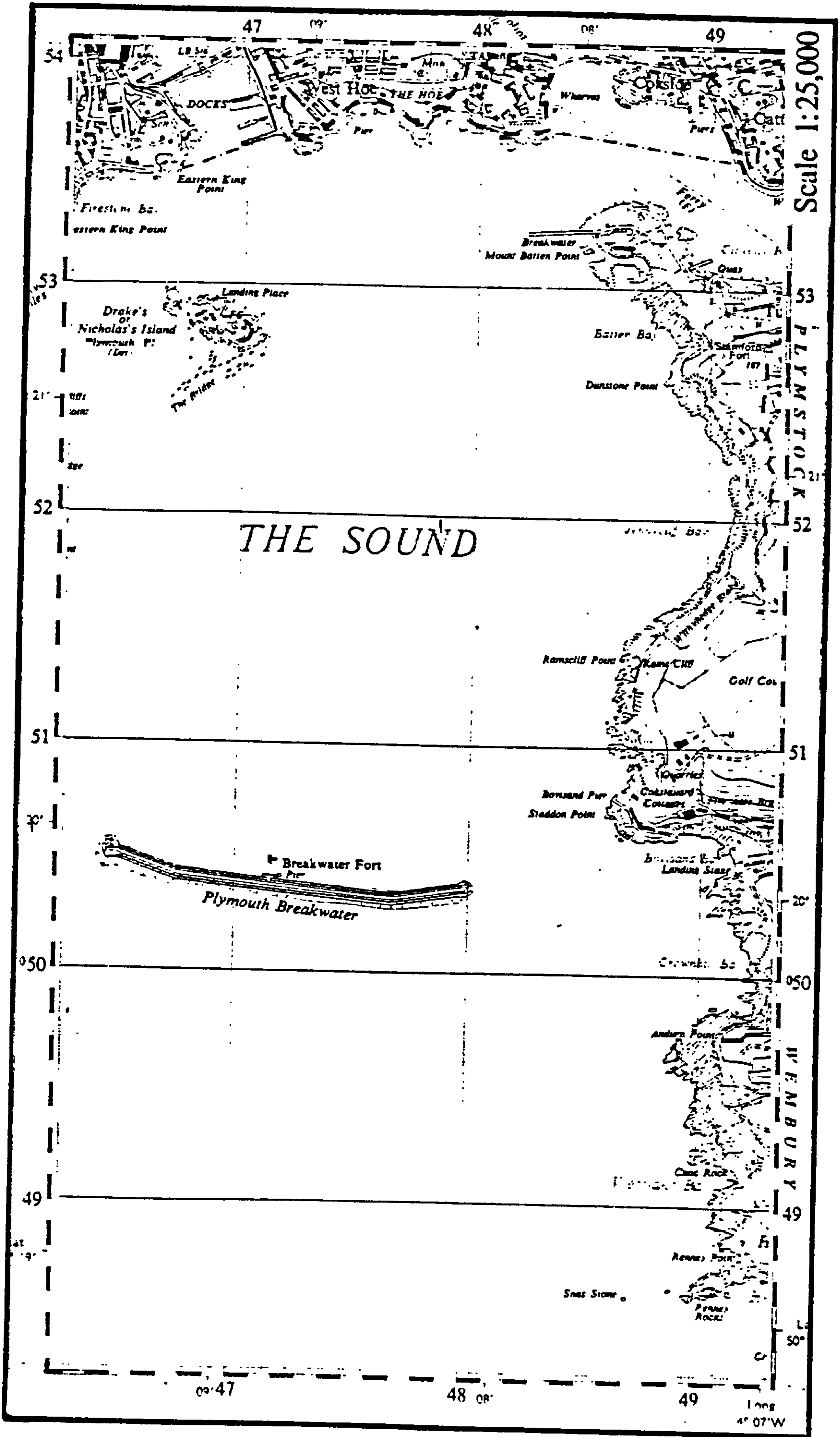


FIG 2.7 MAP SHOWING LOCATION OF BOVISANDS

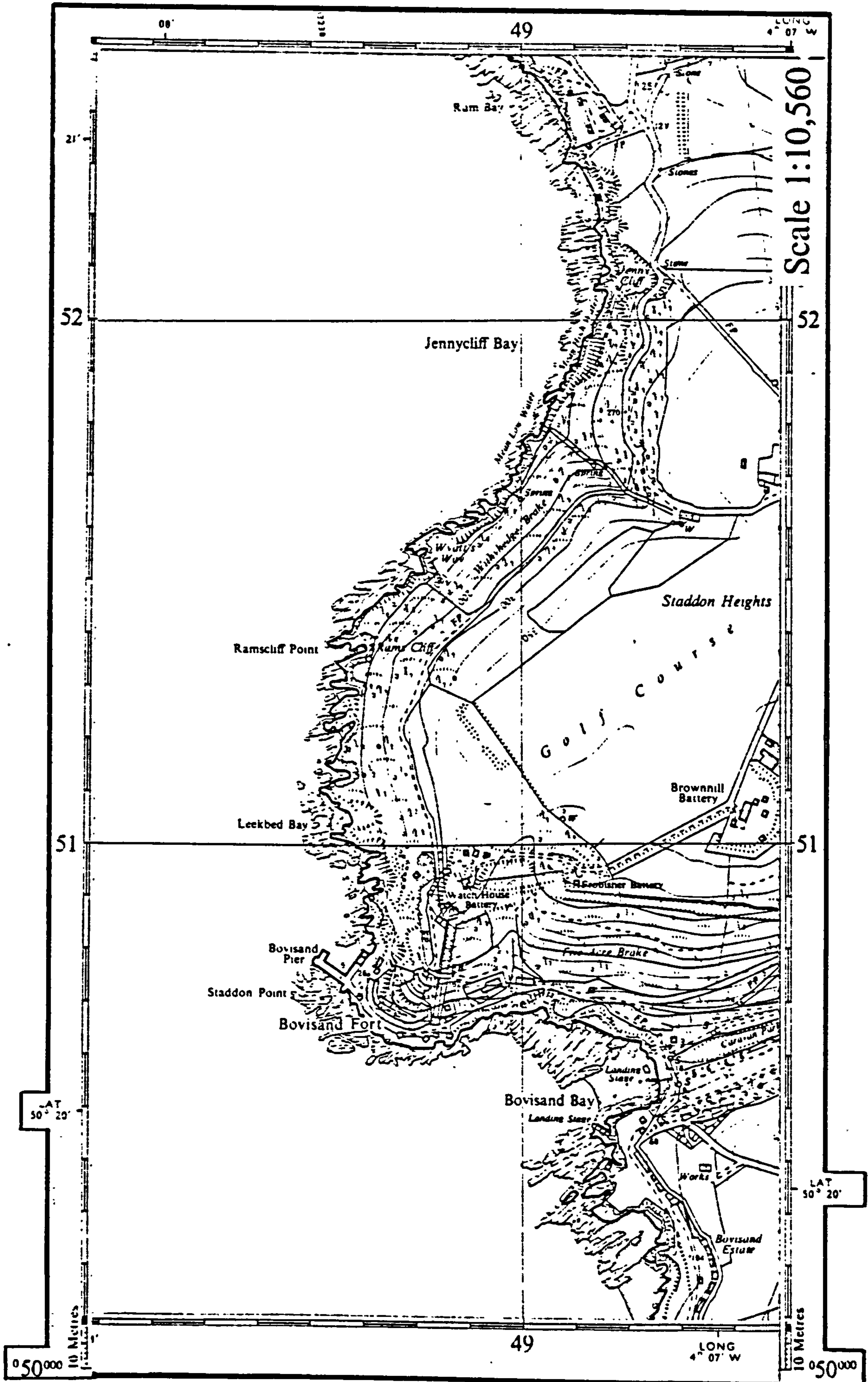


FIG 2.8 DETAIL OF AREA AROUND BOVISANDS

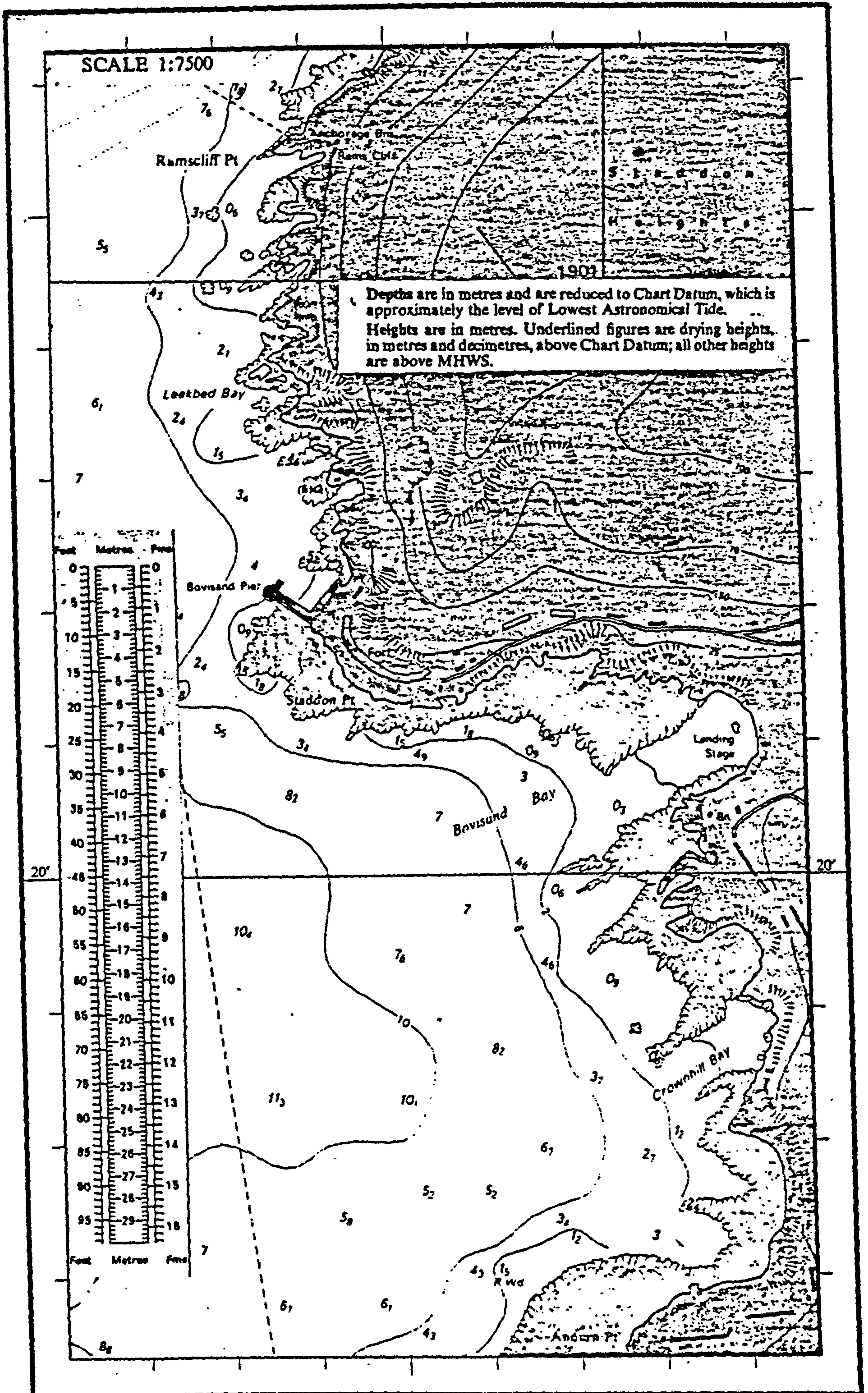


FIG 2.9 DETAIL OF SEA AROUND BOVISANDS

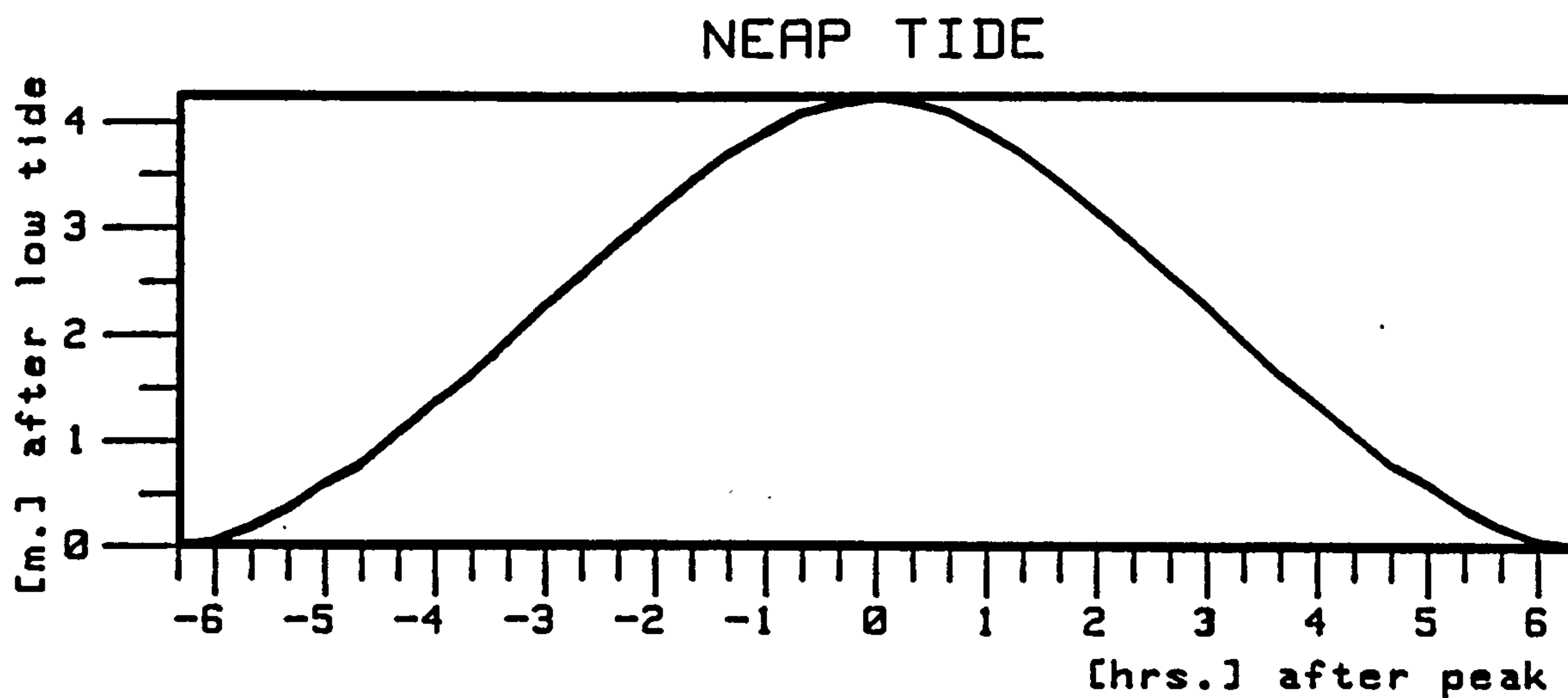
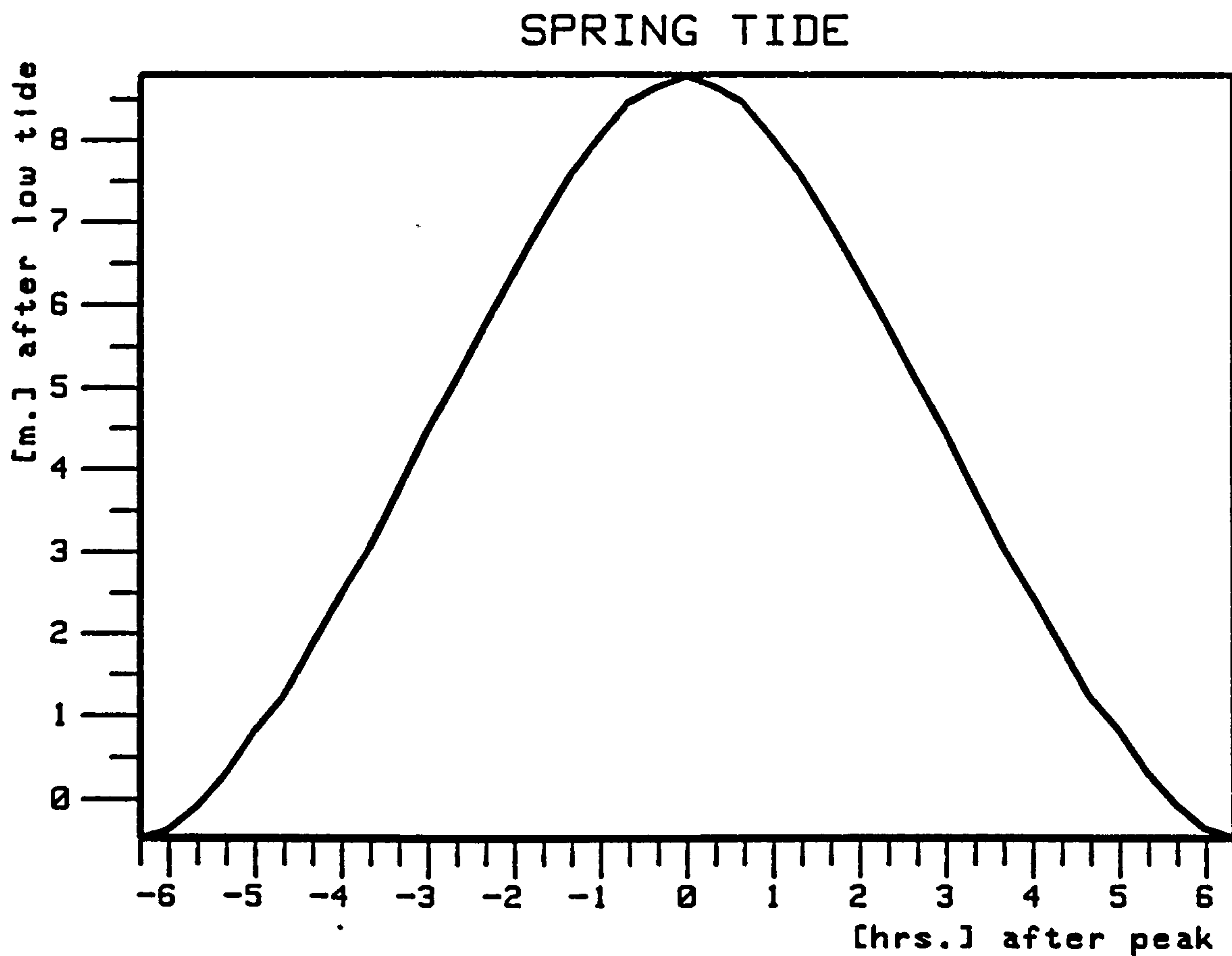


FIG 2.10 VARIATIONS OF SPRING AND NEAP TIDES FOR ILFRACOMBE

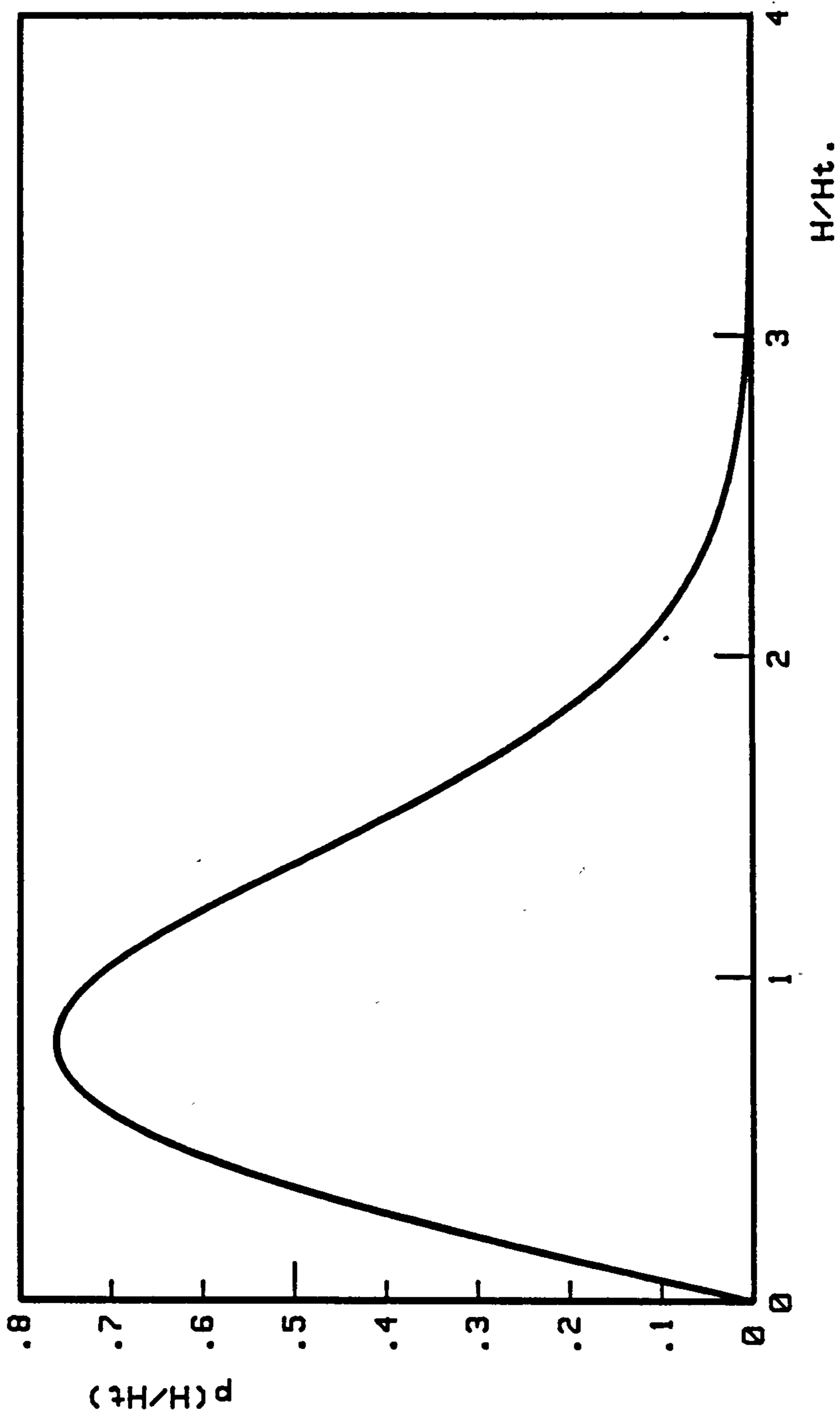


FIG 2.11 RAYLEIGH DISTRIBUTION FUNCTION
per unit mean wave height, H_t .

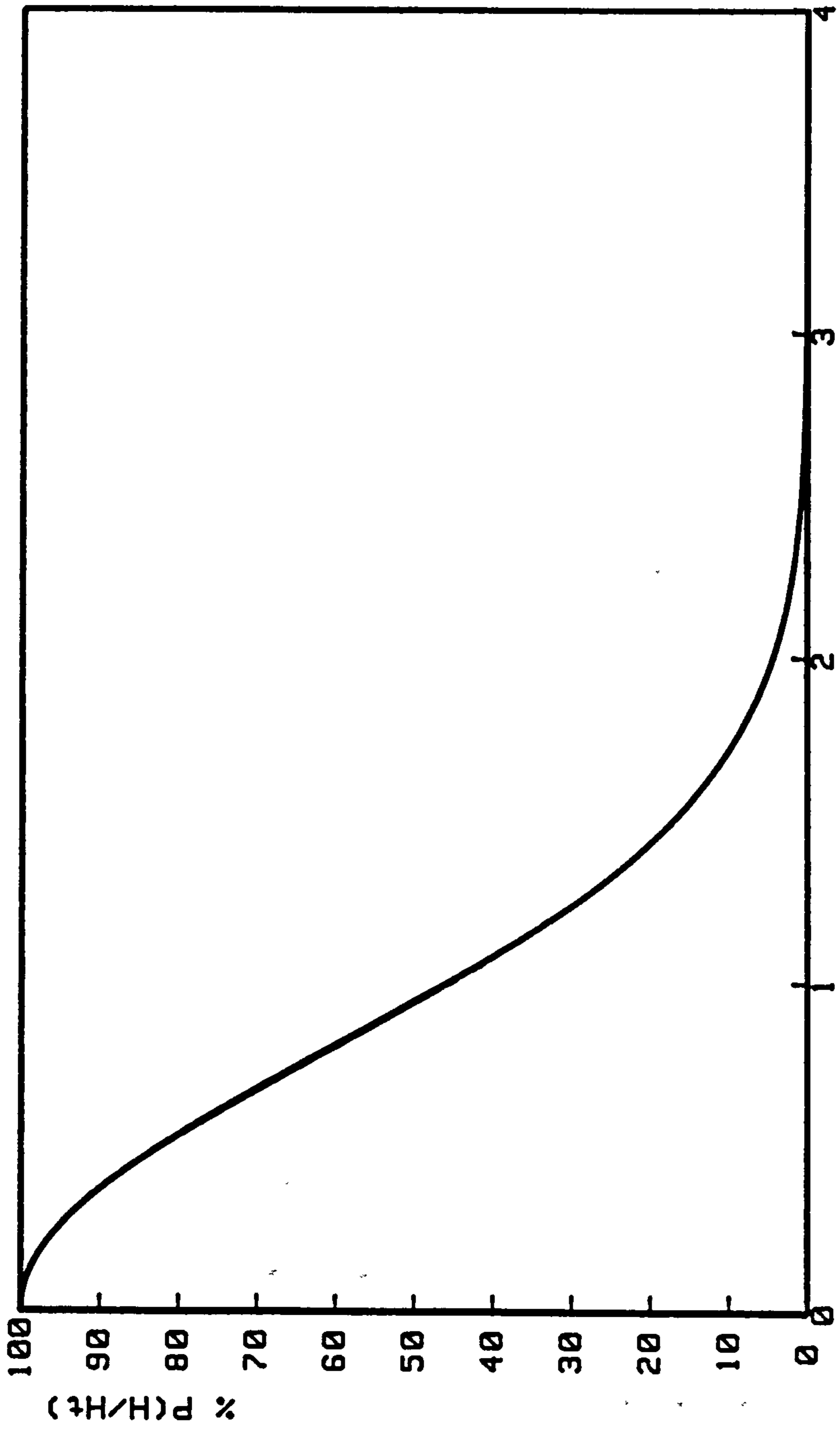
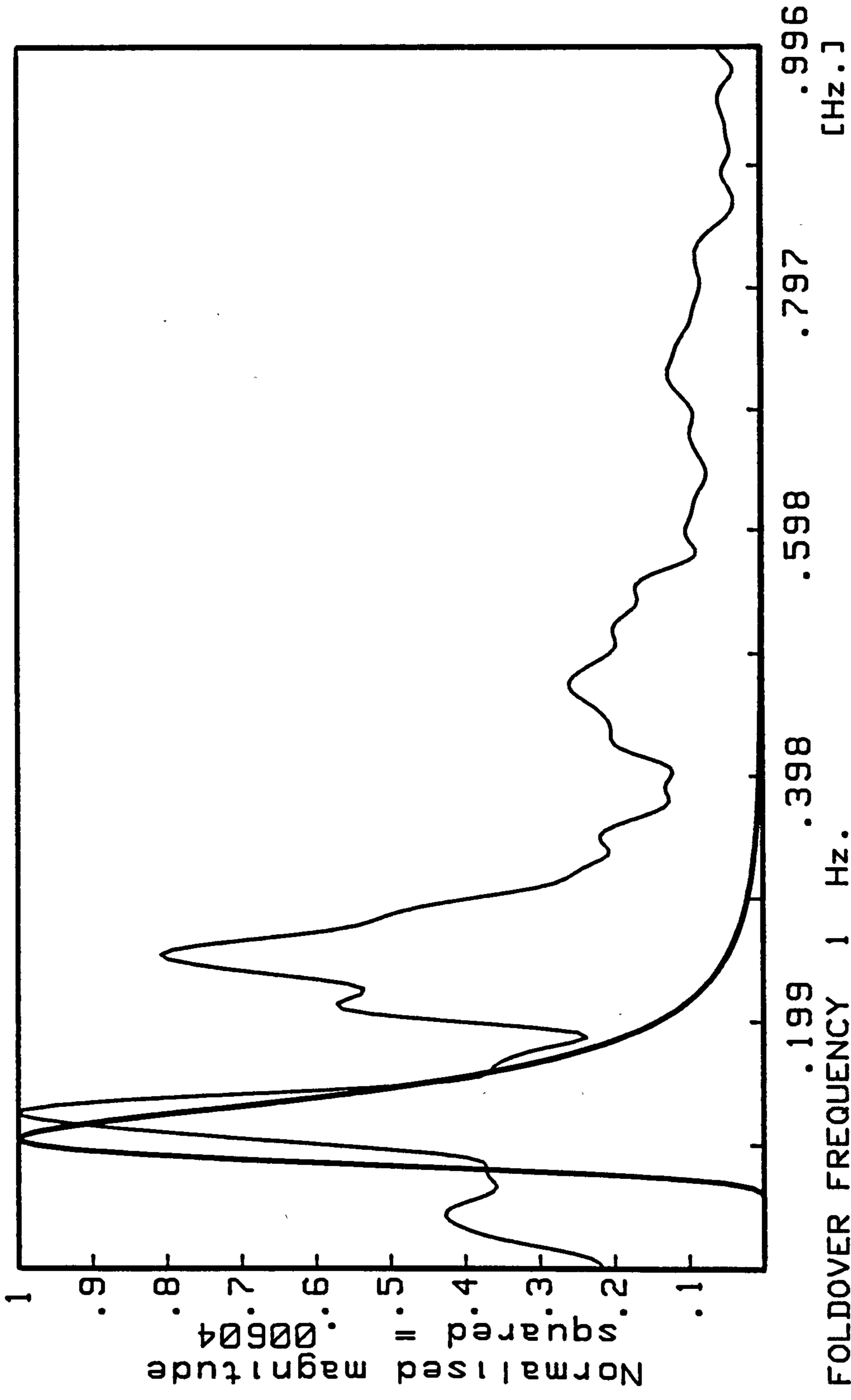


FIG 2.12 RAYLEIGH PROBABILITY DISTRIBUTION
per unit mean wave height, Ht.



FOLDOVER FREQUENCY 1 Hz.
 RESOLUTION FREQUENCY .00391 Hz.

FIG 2.13 THE BRETSCHNEIDER SPECTRUM (superimposed on FIG 3.12)

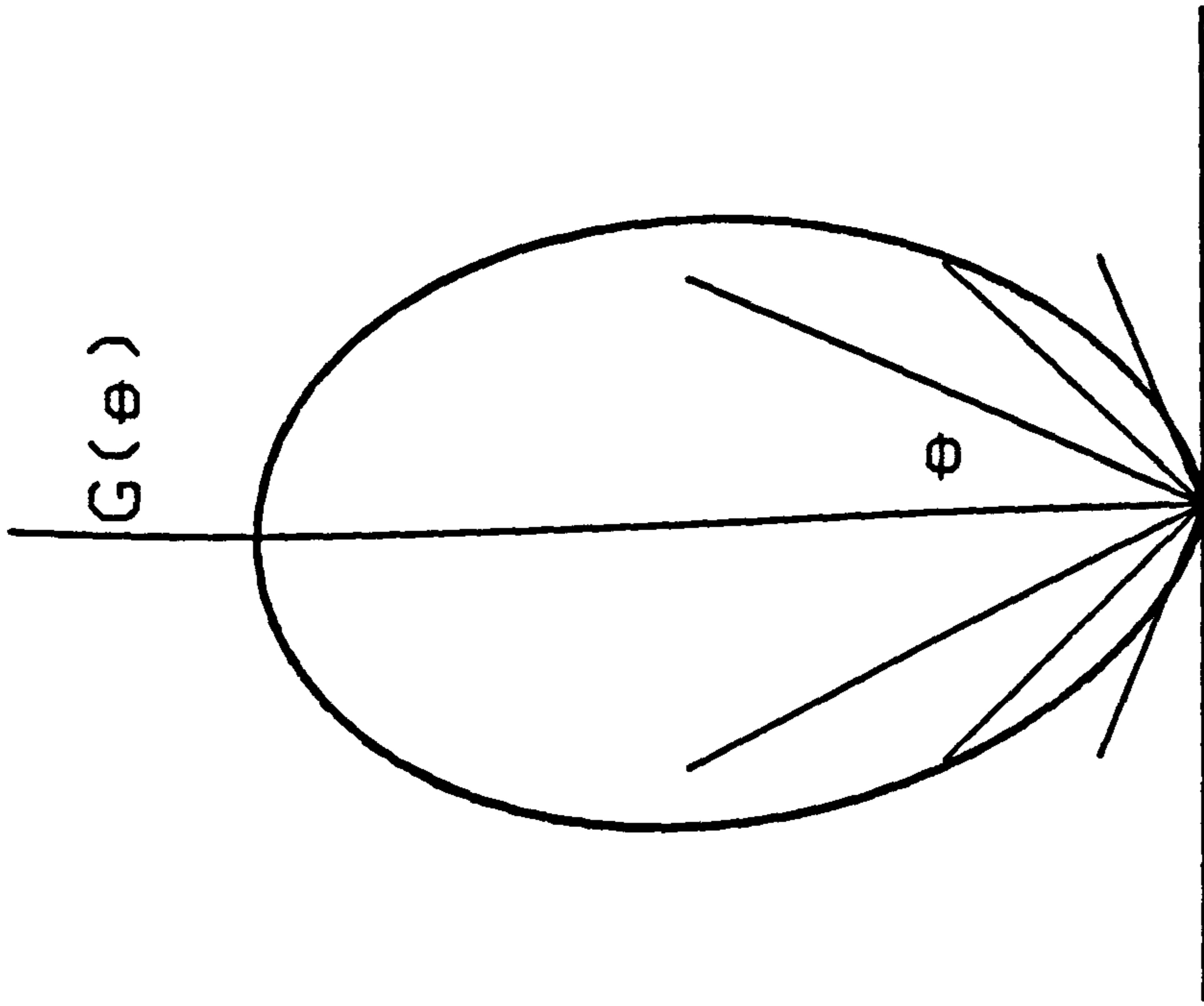


FIG 2.14(a) DIRECTIONAL SPREAD
COSINE SQUARED

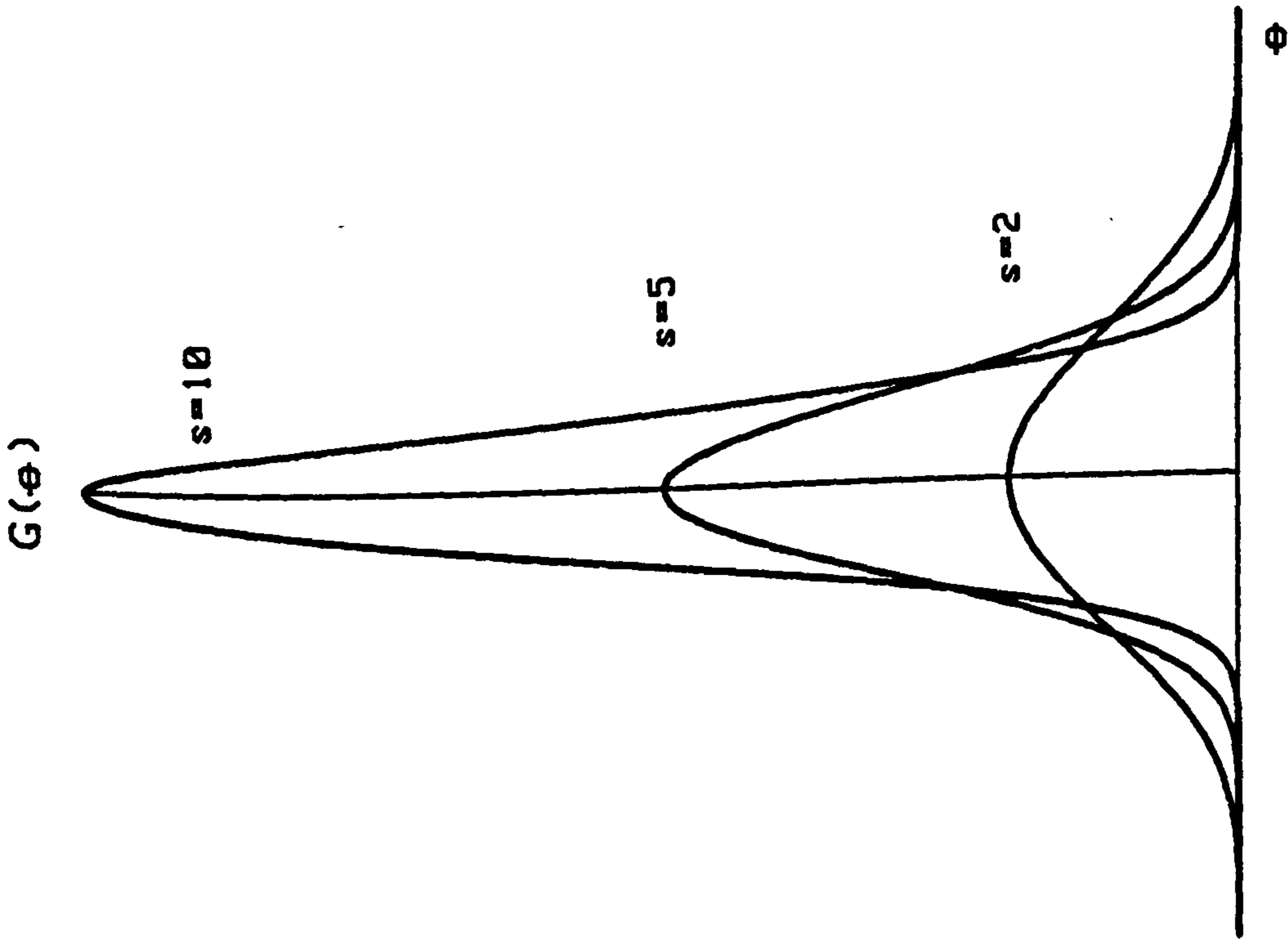


FIG 2.14(b) DIRECTIONAL SPREAD
COSINE POWER

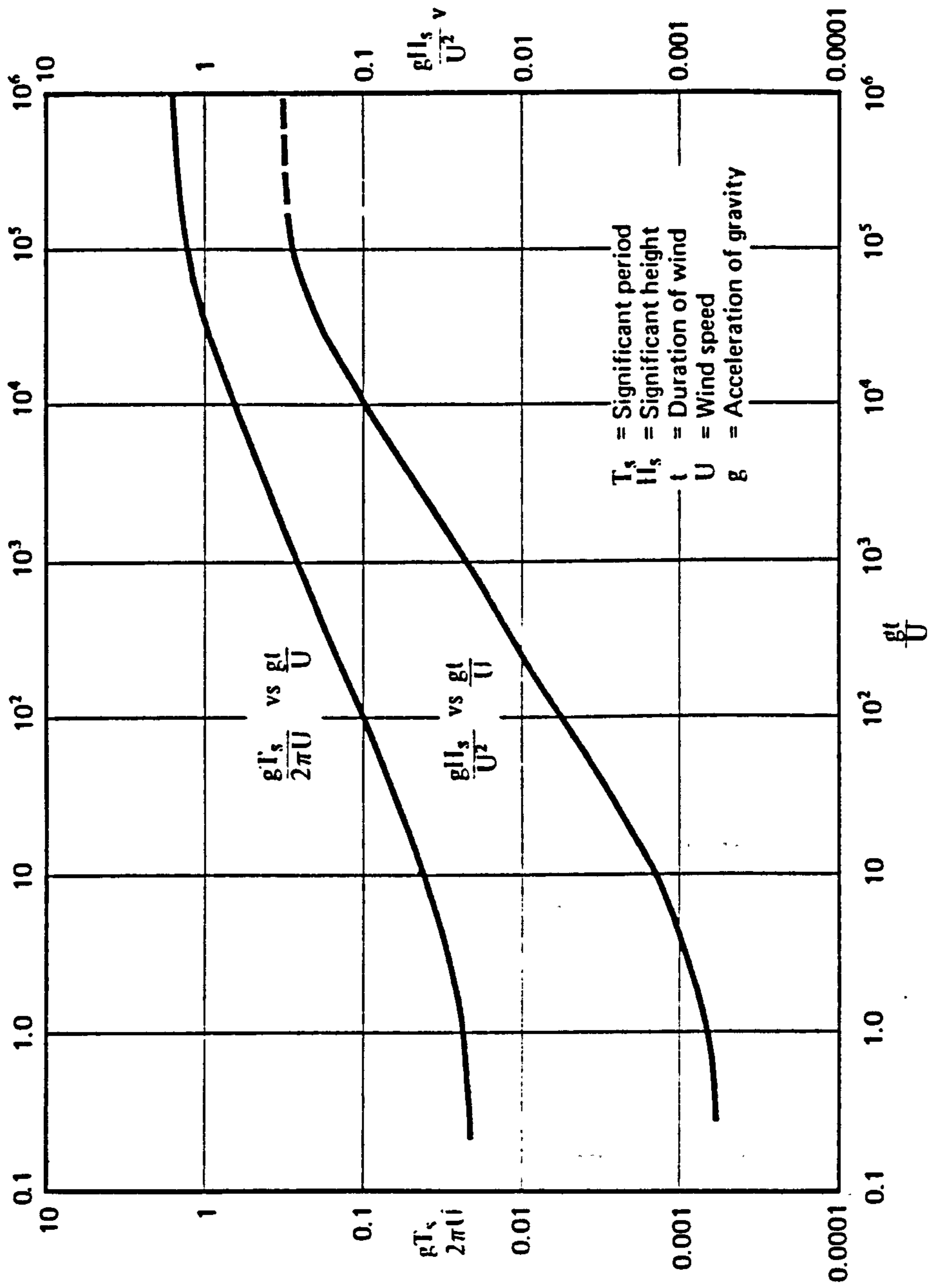


FIG 2.15 GRAPH OF WIND VELOCITY AND DURATION FOR SHORT FETCHES

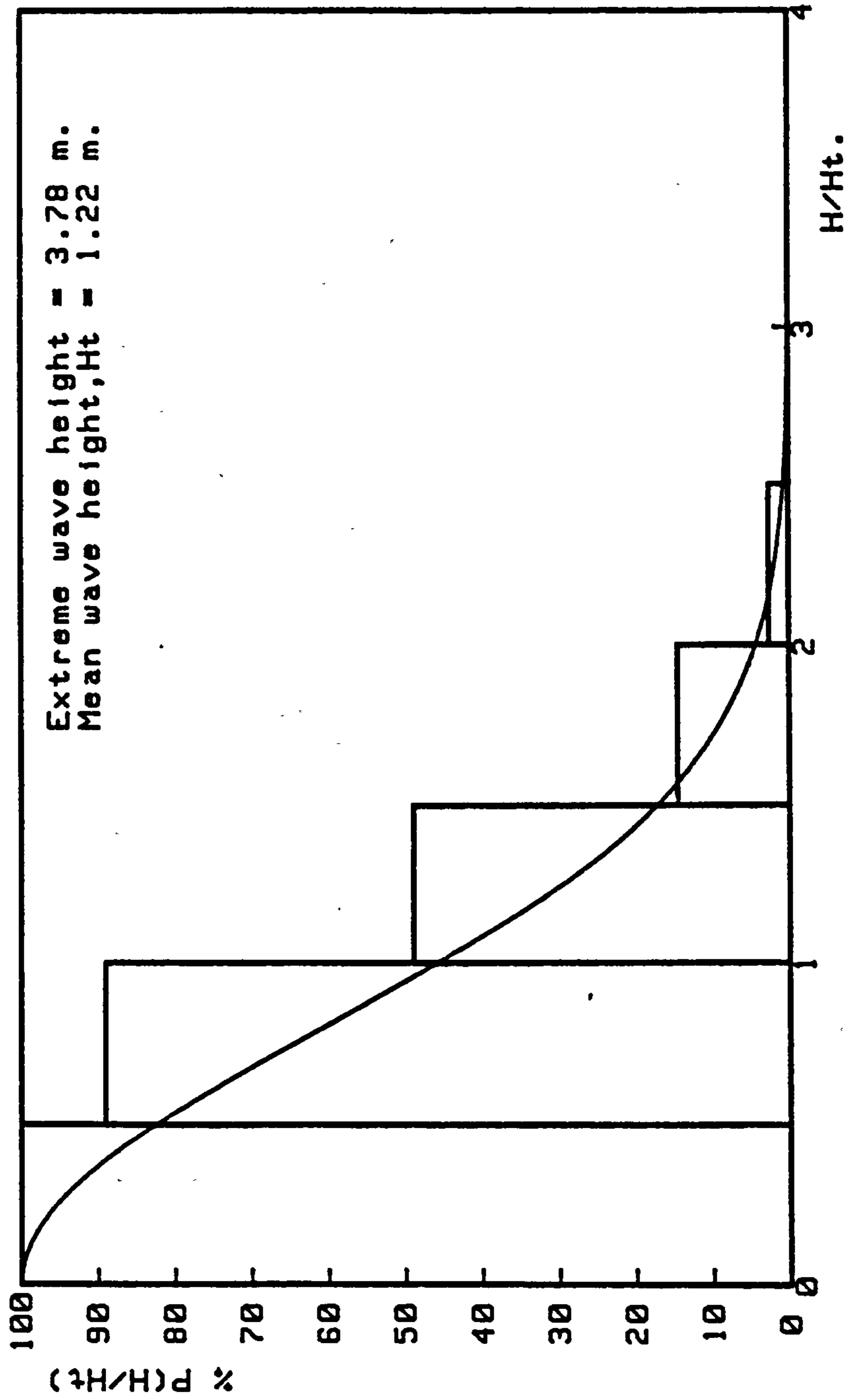
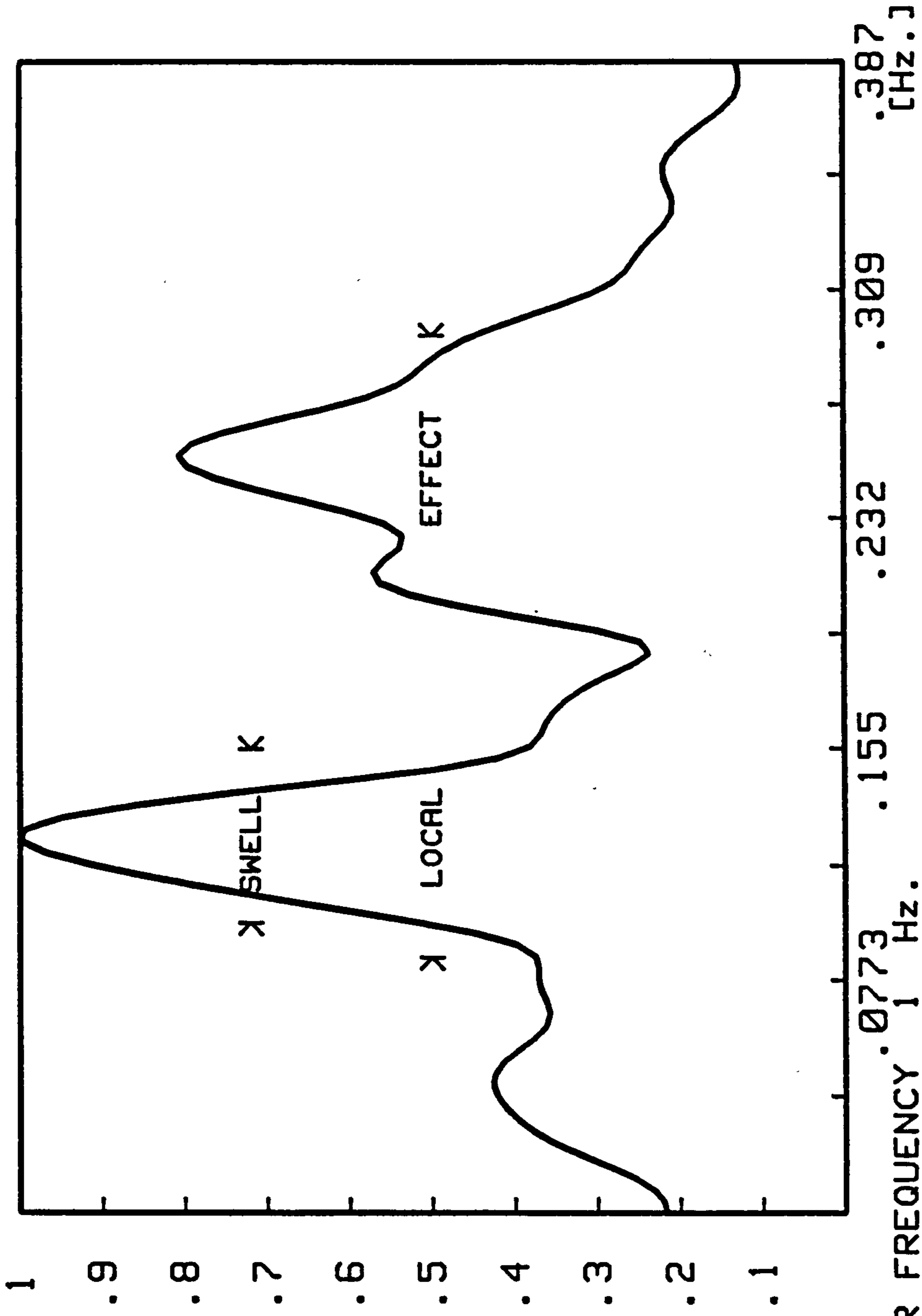


FIG 2.16 RAYLEIGH PROBABILITY DISTRIBUTION WITH EXTREME WAVE HEIGHT PREDICTED



Normalised magnitude squared = .00604

FOLDOVER FREQUENCY .0773 Hz.
 RESOLUTION FREQUENCY .00391 Hz.
 FIG 2.17 FREQUENCY DOMAIN. DIFFERENCE BETWEEN SWELL AND LOCAL SEA EFFECTS

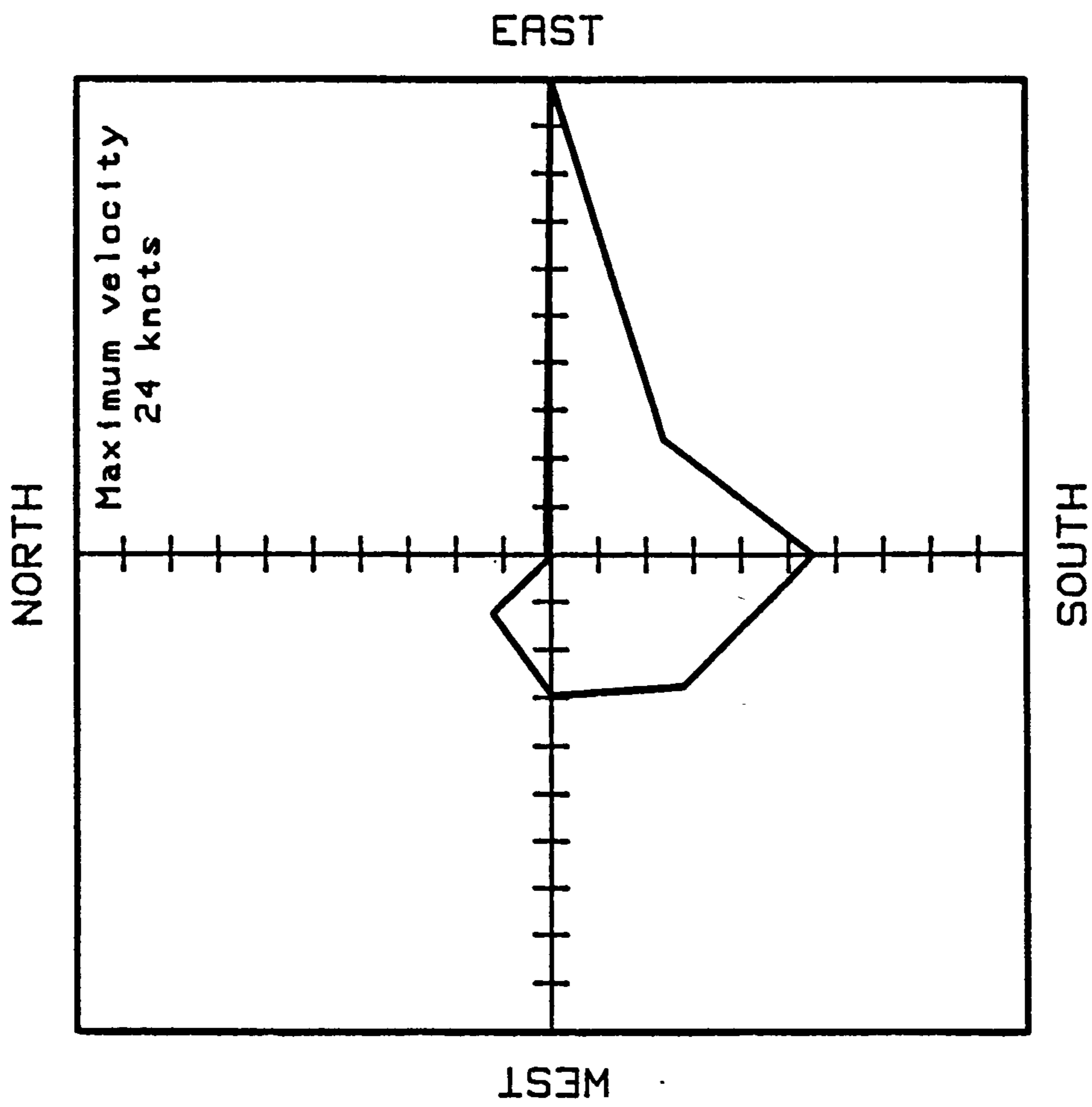


FIG 2.18(a) WIND VELOCITY 'ROSE' BY DIRECTION ONLY
TYPICAL DATA FROM R.A.F. CHIVENOR (17th - 31st October 1982)

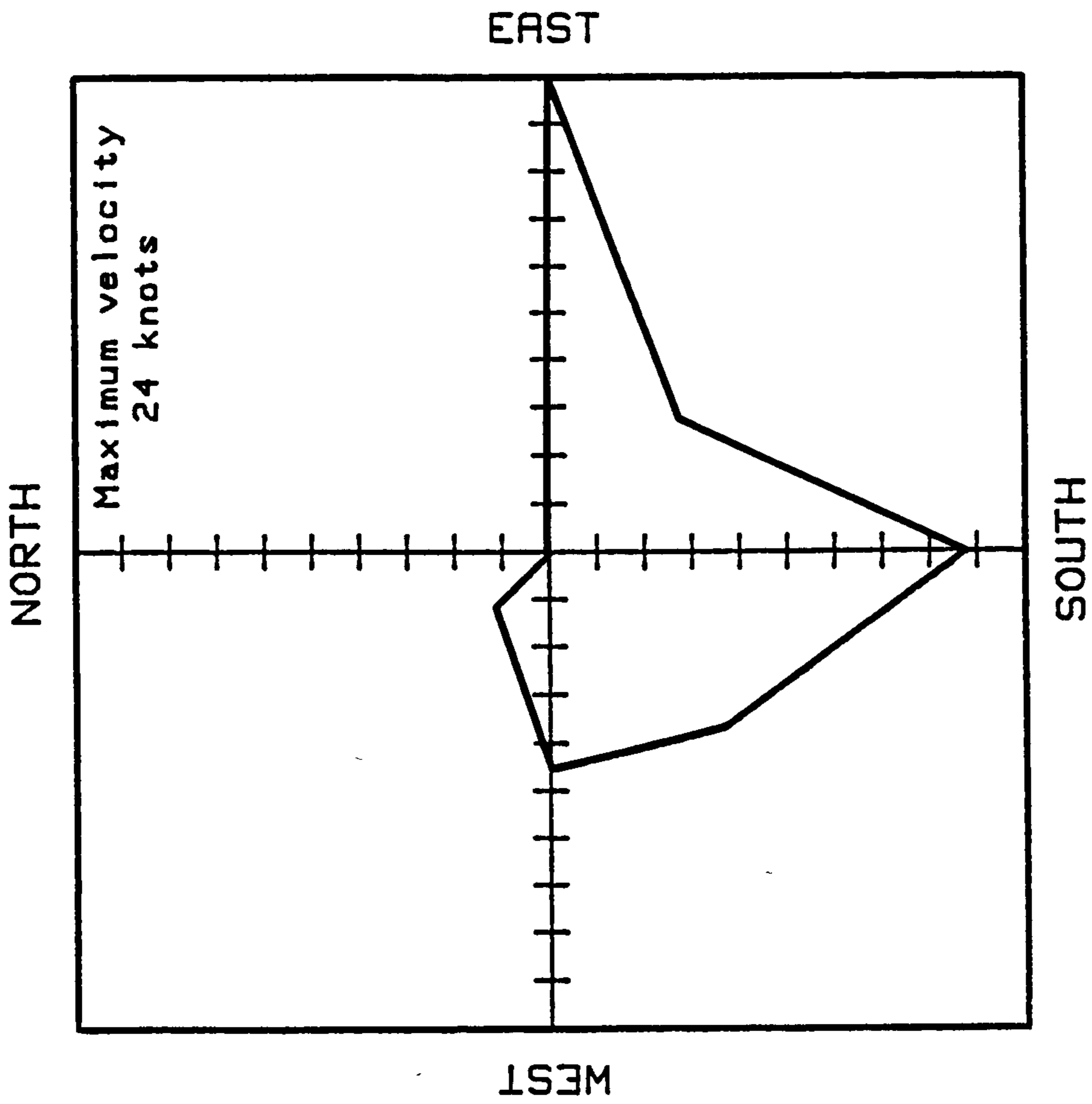
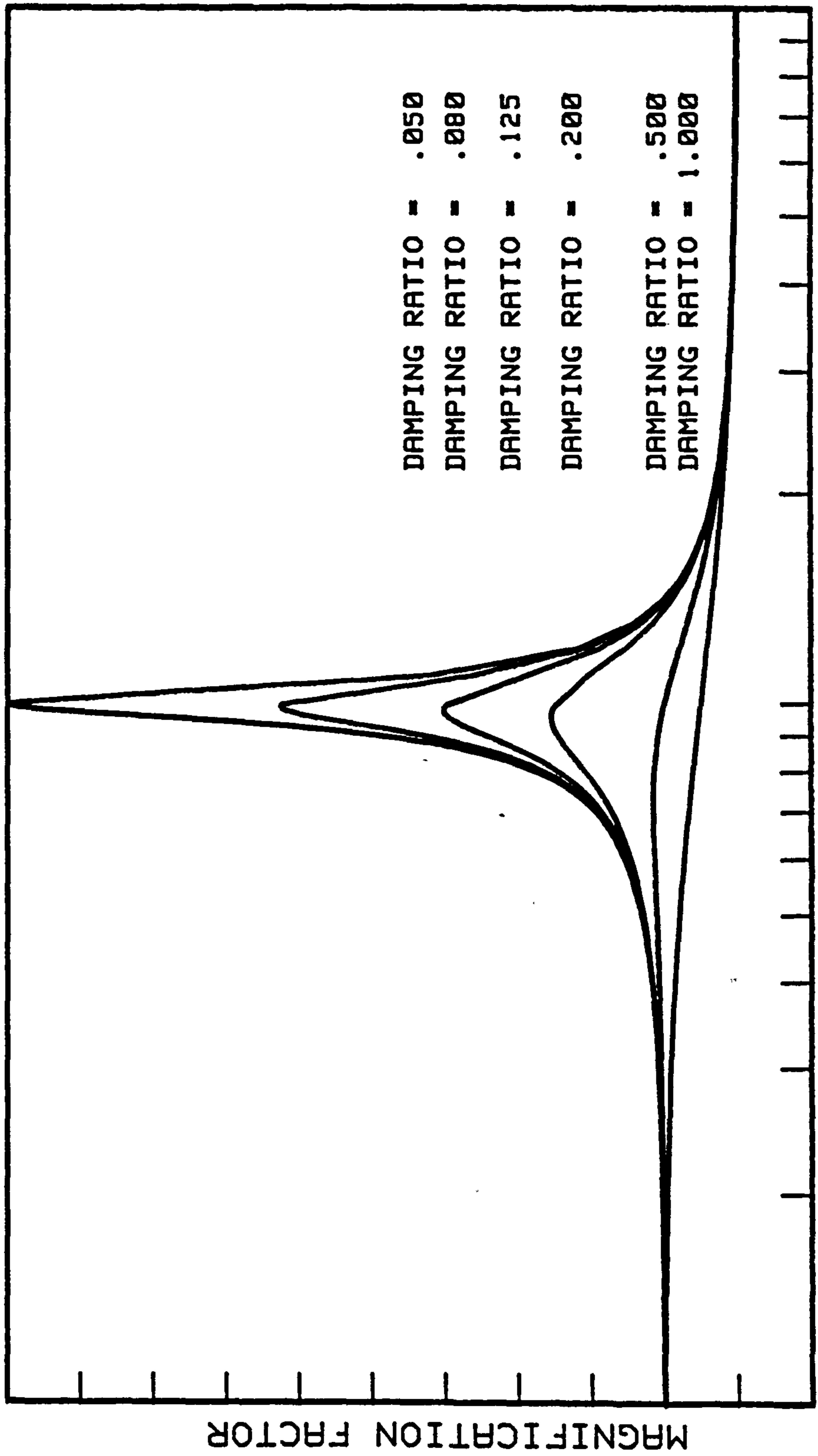


FIG 2.18(b) WIND VELOCITY 'ROSE' BY DIRECTION AND SPEED
 TYPICAL DATA FROM R.A.F. CHIVENOR (17th - 31st October 1982)



FREQUENCY RATIO

FIG 2.19 DYNAMIC RESPONSE

MAGNIFICATION FACTOR

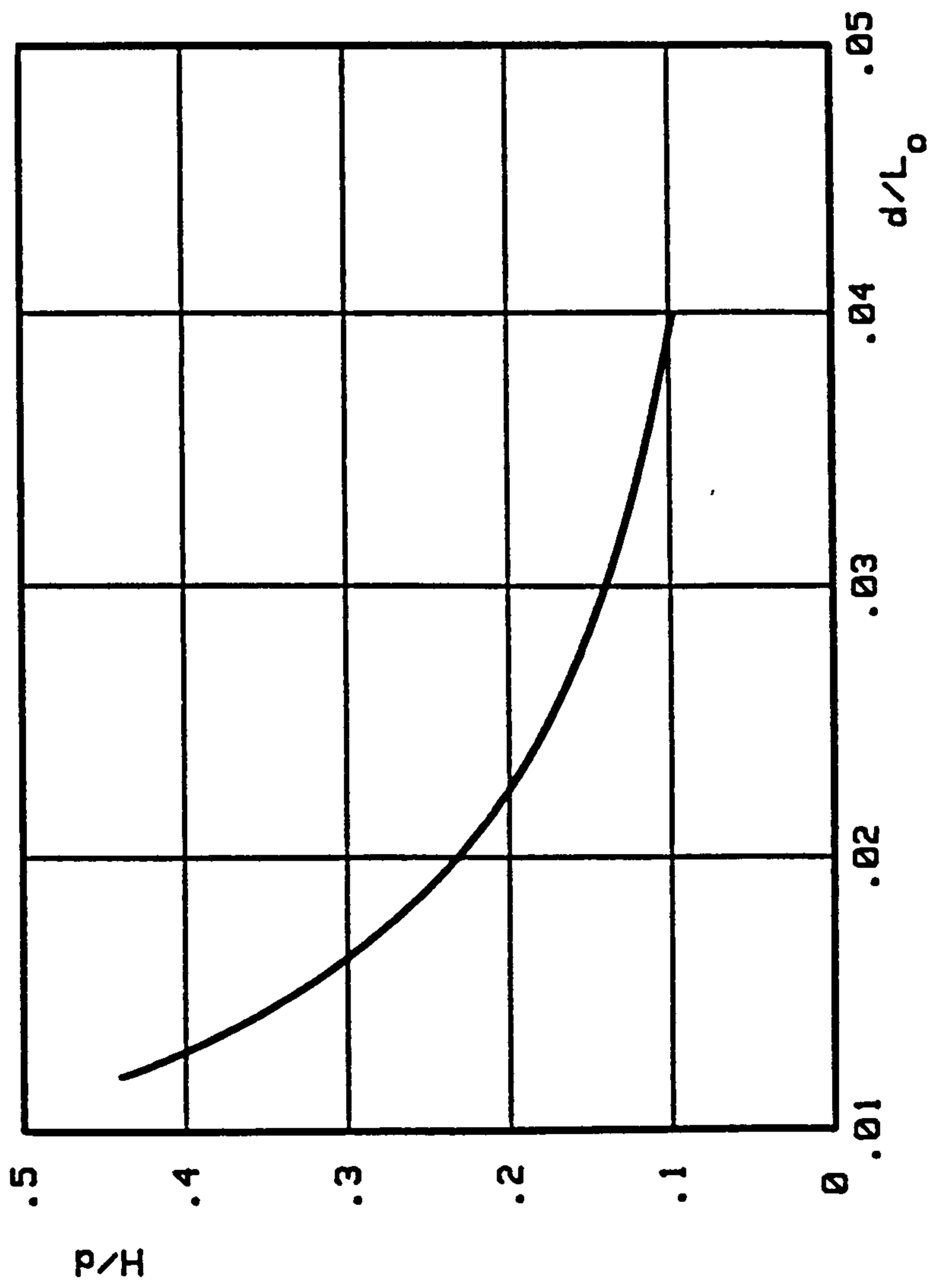


FIG 2.20 GRAPH OF WAVE HEIGHT AGAINST WATER DEPTH



PLATE I GENERAL VIEW OF ILFRACOMBE SEAWALL



PLATE II ROCK OUTCROPS SEAWARD OF ILFRACOMBE WALL

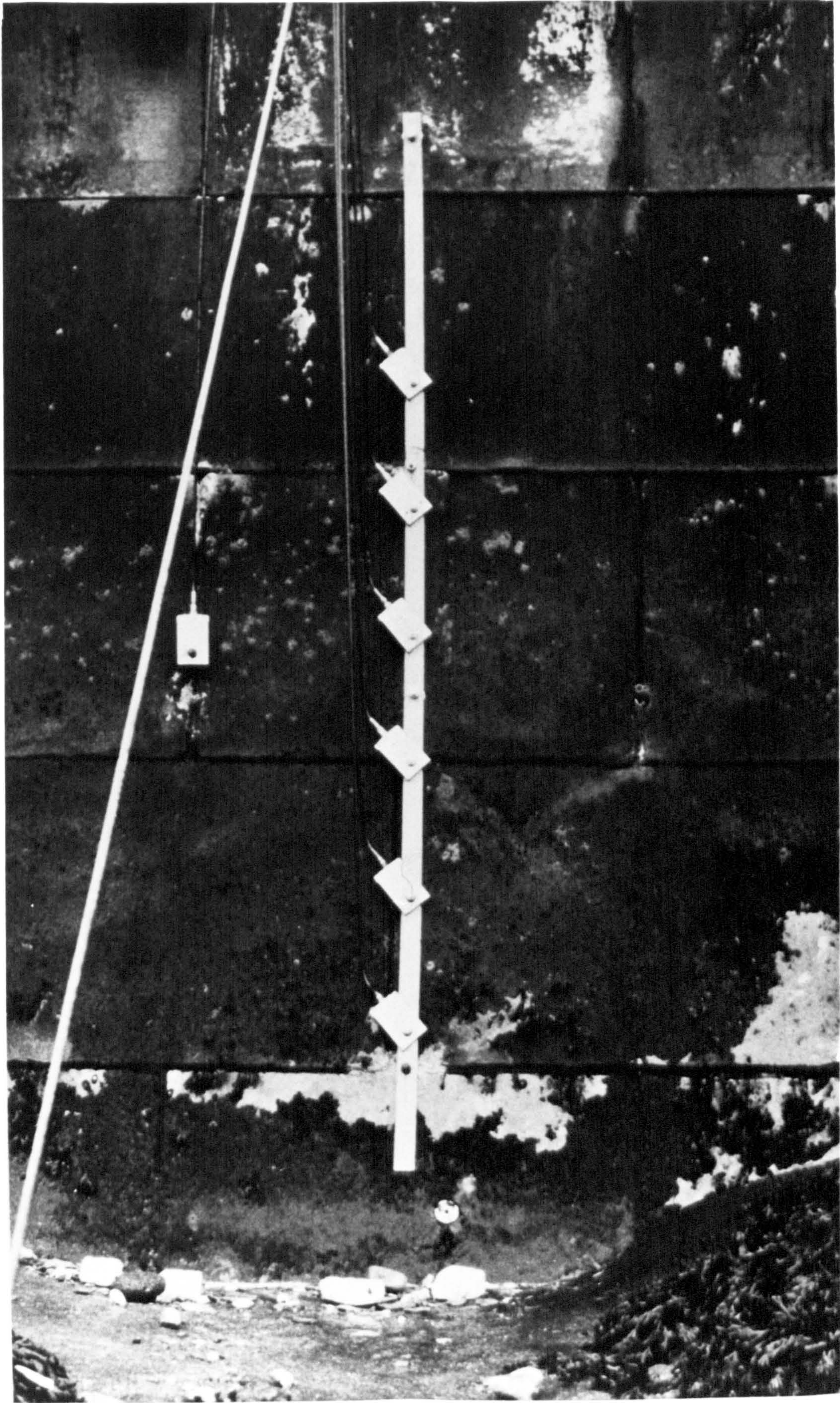


PLATE III VERTICAL ARRAY OF PRESSURE TRANSDUCERS

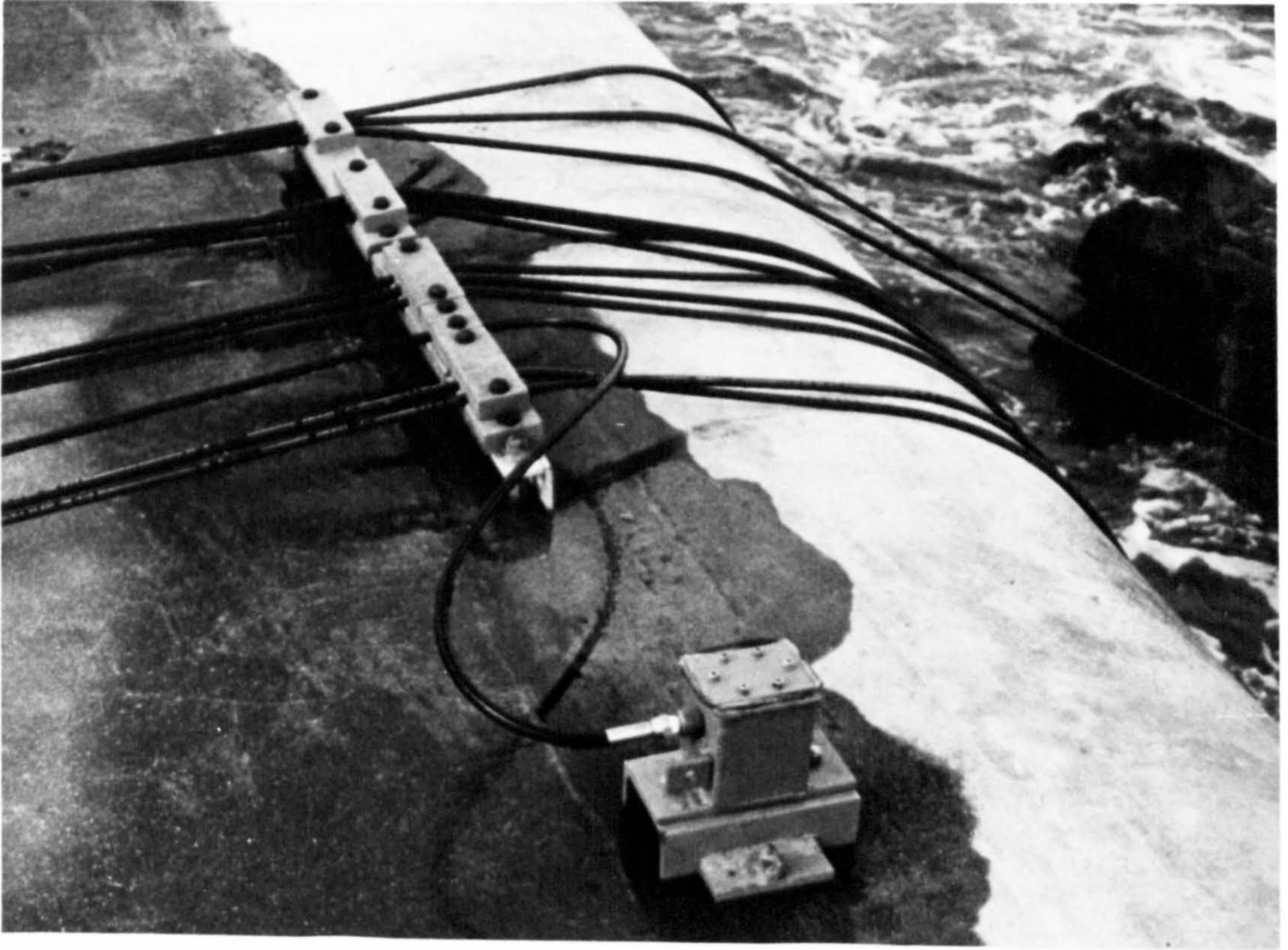


PLATE IV DETAIL OF CLAMPING OF CABLES ON TOP OF WALL

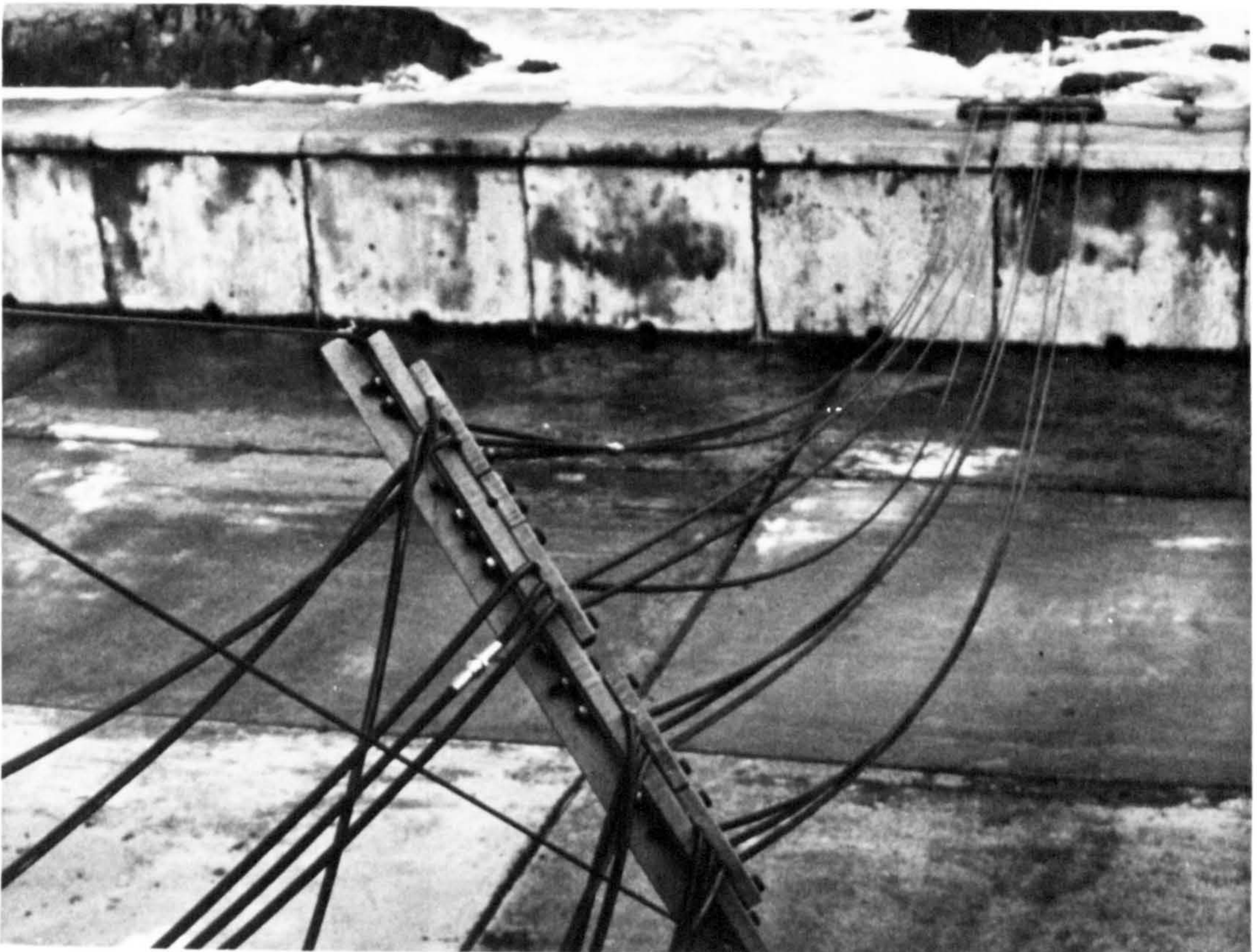


PLATE V VIEW OF CABLE FIXTURES

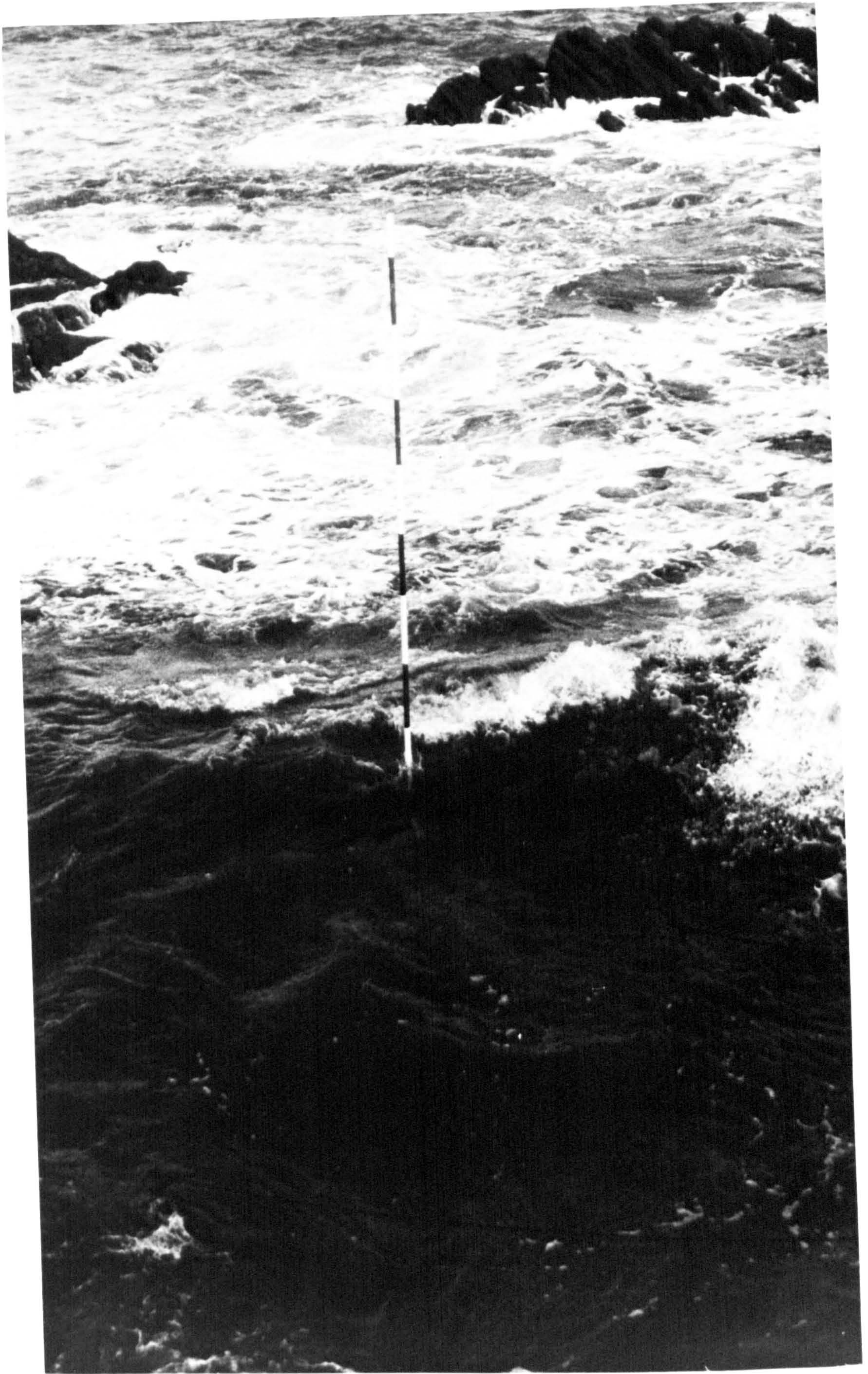


PLATE VI WAVE MAST



PLATE VII DETAIL OF FIXING FOR BEACH TRANSDUCER



PLATE VIII A FLOODING TIDE ACTING ON A TRANSDUCER



PLATE IX GENERAL VIEW OF BOVISANDS SEAWALL



PLATE X DETAIL OF FIXING FOR ALENCO HOSE



PLATE XI DETAIL OF PROFILE OF SEAWALL AT BOVISANDS

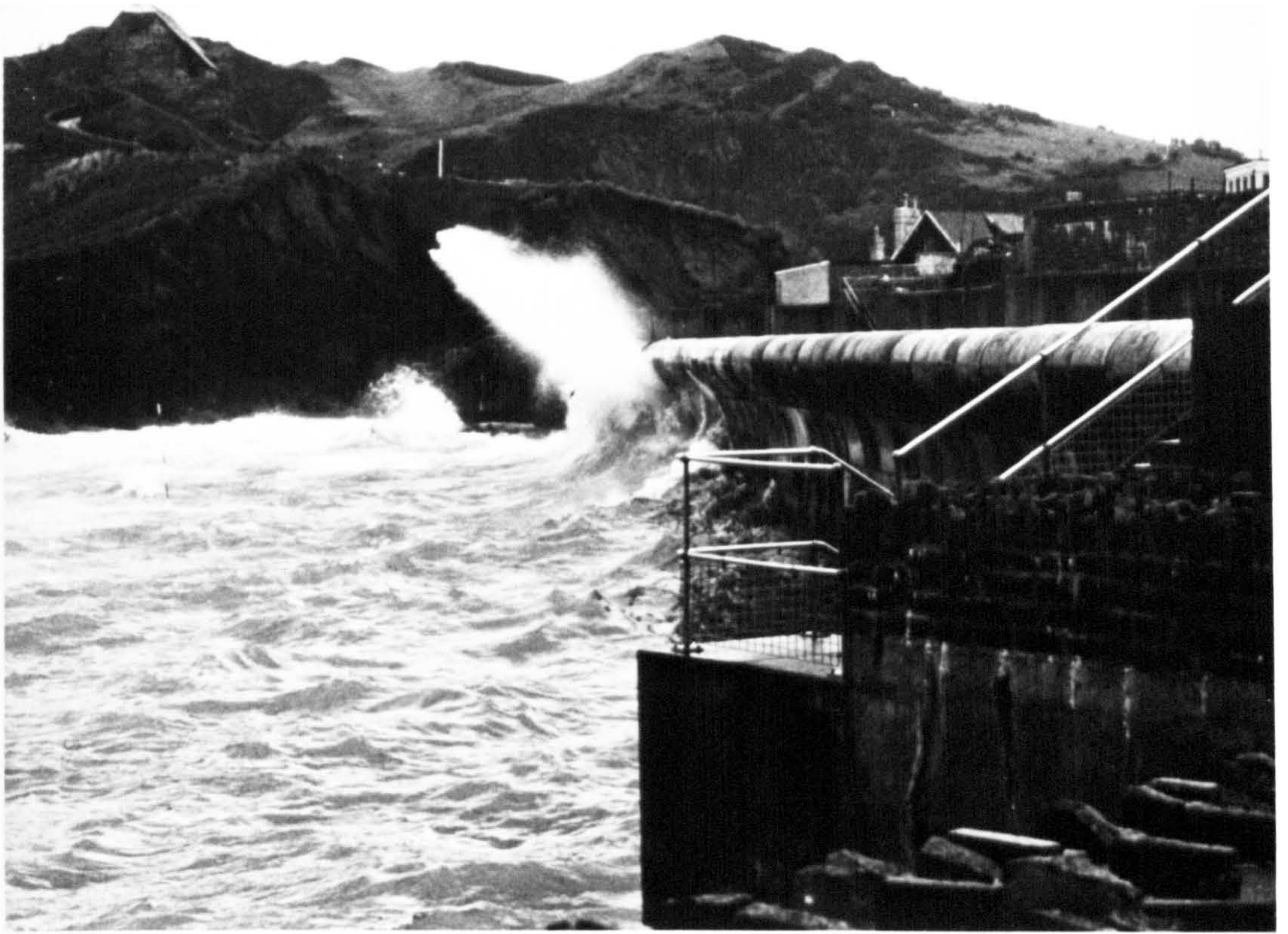


PLATE XII IMPACT PRESSURE MEASUREMENT AT ILFRACOMBE



PLATE XIII WAVE ACTION AT BOVISANDS



PLATE XIV IMPACT PRESSURE MEASUREMENT AT BOVISAND



PLATE XV EXAMPLE OF SPILLING BREAKERS



PLATE XVI FORMATION OF A PLUNGING BREAKER



PLATE XVII EXAMPLE OF A LONG CRESTED WAVE



PLATE XVIII IMPACTS AND AIR ENTRAINMENT

CHAPTER THREE

DATA ACQUISITION

3.1 RANDOM SIGNAL PROCESSING

The data, as recorded from the experimentation, took its form as a continuous analogue signal stored on magnetic tape. Although required for the determination of specific values of the properties of the waves and their actions, the data required a fair deal of work before this could be carried out.

The main concern at this stage was to isolate the extraneous parts of the recorded signal and to remove them as much as possible.

The extraneous nature was disguised in a number of ways, almost, in some cases, to the point of being deeply integrated in the main signal. The processing involved for the random signals required thought to be able to prepare the data in a standard way common to all samples.

The processing of the random data was necessary to compare the experimentally controlled data to the theoretical work. In the processing stage, speed of execution, because of impact pressures, took priority as a quality to be maintained throughout the methods opted for.

With an analogue input, the choice of digitisation helped to give a better control over the manipulation of the data. This control required the application of algorithms. The algorithms were either purpose made or modified to suit their application. The digital process was a facility to provide an indirect isolation of the frequency of interest. This digital option had an advantage over the analogue one in producing power spectra by a more straightforward

method. The ease of understanding digital methods stemmed from the fact that all the processes are treated numerically. By means of a computer and working interactively in the editing mode, the development of the processes involved could be taken to their final stage on a purely logical basis.

The main objective of the processing was reduced to the discarding of the unwanted part of the signal. Although signal components are additive, the combination proved to be more complicated than that of producing a simple arithmetic solution. The complexity of the processing was overcome by following an organised system of preliminaries to the final stages.

The system involved steps in preprocessing techniques, prequalification, qualification, analogue to digital conversion and digital filtering. Further detailing was also carried out on the resulting digitised signal for transient capture. For this overall system, a further explanation of why these steps had to be carried out, follows. This was necessary because each sample signal was treated on its own merits. Therefore, in order to proceed further, decisive action had to be taken throughout the processing. There had also been instances where the standard method did not apply, to which suitable modifications had to be designed.

Consider a sample record to be prepared for processing. The preprocessing stage was done to eliminate any spurious signals. It also detected any malfunctioning of the transducer, and excessive noise present on the recording. At any stage of the processing, reference to

a digital storage scope was used to view the updated product on which a decision for proceeding was taken. While still in the analogue state, preprocessing was carried out for error detection otherwise shown to be complex in digitised form. Other objectives included the identification of trends, the verification of familiar results and the preparation of non-dimensional variables used for the presentation. This stage involved the conversion of the acquired data by reformatting to real values having significant meaning to the rest of the research.

The prequalification stage was used to remove any high frequency additive components. Further to this, trends, shifts and distortion in the signal were detected, to which were applied the appropriate corrections. Any temperature changes in the splash zone generated a drift component in the signal which could also be detected at this stage. General preparation of the data was necessary to produce conclusive results in some of the later analytical processes. This included the cross correlation of two waveforms and the isolation of the individual parameters of the data ready for statistical calculations.

Qualification of the data ensured that the results were a true representation of the randomness of the data. It also provided a means of assessing by how much the data varied from the normal distribution. The probability density function was calculated to ascertain the difference between the randomness and the sinusoidal form for the data. This stage involved data acquired from different sources. Therefore a standardisation procedure had to be carried

out to apply uniformity to the results. Taking unbiased estimates helped to remove any overlying trends appearing out of order with the time domain signal.

At the analogue to digital conversion stage, the prime concern was to maximise the information while maintaining the structure of the waveform. A proficient use of Hewlett Packard (HP) hardware cards brought about their potential while defining the limitations to which the conversion was carried out. The computer software used from this stage onward employed algorithms devised for discrete data values. The objective at this stage was to detect and evaluate the character of the waves and their forces on the seawall.

In order to remove high frequency components from a recorded signal, a digitised filtering system was designed and utilised. Another use of the filtering was to remove residual DC components. The parts of the signal processing associated with this stage of the time series analysis included windowing, zero padding, segmenting and segmenting by overlapping.

The windowing was carried out to broaden the main lobe within the foldover frequency limiting range while reducing the side lobe leakage that lies outside the limit. This frequency domain characteristic also helped to improve the resolution and variability associated with the spectral response of the recorded data. Zero padding was used to complete a short time domain sample ready for performing the Fast Fourier Transform (FFT) on it. This was necessary because the FFT was carried out in fixed data sample lengths (lengths of 2^n

where $n = 1, 2, 3, \text{ etc.}$). An improved resolution on the power spectra was achieved through the option of segmenting, which effectively reduced the spectral length for FFT determination. By means of overlapping the individual segments, a smoother composition of the power spectrum resulted.

In the case of transient analysis, the procedure was required to represent the dynamic pressure experienced by the wall. Other factors included the measurement of the burst of momentum associated with the transient, plus a facility for reviewing a captured signal. Throughout the time series analysis the introduction of error was inevitable. The error was minimised to acceptable levels by applying aliasing and quantisation principles.

The data acquired from the field took the form of a random signal. The randomness was described to include time varying averages and had, in the first stage, contained either a useful signal or unwanted interference, or a combination of both. It was only through suitable application of linear systems that the relevant parts of a signal were highlighted while discarding the unwanted parts.

The method adopted throughout this experimentation was used mostly with the signal present in its digital format. By this format was understood a means of representing a continuous signal by a sequence of numbers. With the signal in this format, the processing was carried out by techniques that used digital methods. This enabled the basic characteristic parameters of the signal to be determined. In this form the algorithms based on interpolation, differentiation and integration could be applied directly.

Interference in the form of noise from a signal was to be removed to reduce the signal to a form more familiar to the reader. From its raw state, a form of preprocessing was essential to the preparation of the data for digital processing by computer methods. As an alternative, the simulation of a signal in its digital form was a means of its study in comparison to one obtained through an experimentally controlled environment. The deductions obtained by manipulating both either separately or together gave the economical and efficient solution before putting the system to a large scale test.

3.1.1 Introduction To The Concepts Involved In Digital Processing

The most important part of the processing is digital filtering which is used to operate on the analogue to digital converted signal. When reconverted to an analogue output in the form of plots or continuous waveform, the system simulates the analogue filter technique ⁽⁷⁷⁾ ⁽⁷⁸⁾. This means that the filter characteristic must be recognised in digital format. An all digital system requires the knowledge of the inverse Fourier Transform and the FFT as tools to obtaining the spectrum which determines the signal characteristics. The FFT utilises a process much faster than real time analysis. This is incorporated in the software package in the form of a practical algorithm. The signal is conceptually passed through a discrete time sampling process. The signal is therefore a true representation of the original signal and not an approximation to the analogue signal. This requires the sampling to be carried out at an appropriate rate to capture the range of frequencies under study. The increase

in importance of digital signal processing has necessitated the improvement and development of digital filtering in the form of software and even hardware. Digital signal processing emphasises that the system is linear shift invariant. This is analogous to a linear time invariant continuous signal as is present in recorded form. For representation of this type of system an important tool, similar to FFT in the frequency domain, is the convolution counterpart in the time domain. A difference is identified between analogue and digital processing theory carried out in the time domain. Of interest, the digital theory is based on numerical analysis methods.

3.1.2 Discrete Time System

A signal representation of the analogue version may be given as a function of the spatial or time independent variables. The likeness of these variables is such as to perpetrate interchangeability. The representative in digital format is to be true in its parameters but most of all in its structure and stepwise progression potentials. The digital software utilises time as a standard independent variable in a form consistent in all its processes.

Transformation of a signal by processing techniques is a means of separating two signals combined in some way. The objective is to enhance a component of the signal making it easier to estimate a specific parameter of the signal. The transformation process, may itself be analogue or discrete in time.

Analogue techniques may be modified to suit digital techniques if the sequence is treated as an impulse train. However, in discrete time processing, the discrete sampling is thought of as emanating from a digital system. Although most of the processes associated to a digitised signal may be simulated by analogue methods, this is of secondary importance when the signal is manipulated using directly related software.

3.1.3 The Sequence

The digitised signal is seen as a discrete sequence of amplitude variations in the time domain. While the interval length is arbitrary, the intermediate levels of amplitude are dismissed. Therefore, the nearness of the sampling period defines the extent to which a reconstructed signal from a digitised sample will look like the original one.

The discrete sequence is understood as a number of impulse values of unit magnitude multiplied by the respective amplitudes. The mathematical significance to these unit impulses is linked to the Dirac function. The more important consideration is that the energy of the waveform is assessed from these values. The sequence is said to have an energy representation equal to the sum of the squares of discrete amplitudes.

A direct application of the Dirac function is the coordination of the amplitude magnitude and the impulse response. This is the basic example of convolution and the result is a linear shift invariant

signal. The significance of this is that the Dirac function is considered as the basic transfer function in any signal processing. Two transfer functions acting in series over the same signal effectively act as a multiple of both. If parallel, the signal is mapped by the sum of each transfer function only.

3.2 PREPROCESSING TECHNIQUES

The data, as obtained in its raw state, requires a certain amount of preparation in the form of preprocessing techniques. The initial editing of the data is done with the aim of detection and, if possible, elimination of spurious signals, transducer malfunction and excessive noise. The spurious signals show up as high frequency oscillations with extremely high amplitudes reached. The singling out of these signals is carried out on the basis that they stand out in isolation in the signal continuum. Although few and far between, these sharp rises are a hindrance, especially in the determination of transient analysis. They are mainly identified by having a component in the negative potential following the large positive potential. They are known to occur during the switching on of electric power within the same circuit as the recording or even measuring instrument. Whereas the former forms part of the analogue signal, the latter are superimposed and are removed by simply repeating the detection process.

Instances of transducer malfunction are detected as drop outs of the recorded signal. The drop out could be of a no response output in the case of the incoming signal to be totally isolated from the recording equipment. The other sort of malfunction is represented by a continuous high voltage output. This occurs in the failure of the water proofing of the system. This problem then becomes a workshop problem to be tackled on return from a recording session.

Besides these hazards, the signal containing valuable information may occur in the presence of excessive noise interference. This renders the original signal ineffective for amplitude magnitudes of the same order as those being measured. The problem would be less troublesome if the extreme values were to appear intermittently. This helps to identify the signals' main characteristics which may later be used to isolate the rest of the signal from the noisy source.

3.2.1 Storing Data Temporarily

Although the data is stored on magnetic tape, the output is what matters with a view to its response as extracted from the data. Preliminary to all this, an instrument was required for the purpose of taking immediate decisions on instantly produced results. The fast results of viewing the data provided a quick method of adopting a visual vetting process. The visual nature did not produce quantitative results, which were not required at this stage, but it detected the extraneous features to be bypassed in the complete analysis. The appropriate instrument satisfying these functions is a digital storage oscilloscope. An OS 4200 Gould was used throughout the analysis especially at preprocessing level⁽⁷⁹⁾.

The digital storage oscilloscope is operational on dual channel mode. The monitoring was carried out by feeding the output direct from the backplaying of the recorder via B.N.C. connectors off the tape deck. The first impressions of a signal picked up the unwanted characteristics, so ways had to be devised to remove, or at any rate, reduce them. This is a means of temporarily storing the signal to show the extent of drift and strength of signal.

The extent of drift is related to the ground level of the trace. The ground base is obtained by removing the input signal from the scope's amplifier. The use of the GND switch activates this function. The trace involves the drift due to environmental changes and also to a DC offset. The offsets due to environmental changes are transitory and are adjusted by appropriate balance control during the data collection stage. The DC offset is due to submersion of the transducers when in operation. This produces a hydrostatic pressure on the measuring device with an equivalent voltage producing a stable DC offset over a short length of sample. This observation came in handy when looking for the effects of tidal level variations on the mean water level of the recorded signal.

The trace is generally viewed on a DC input coupling switch. This gives a representation of the signal variation along the y-axis, with time being represented in the x-axis scale. The option of scale for the y-axis is related to the amplitude of the input signal. The value is a measure of the sensitivity by which the signal may be read. The scope includes the usable range of 0.1 volt to 5 volt per cm. in a 1:2:5 proportional increase. The captured signal shows the amplitude variation over the DC offset. From this representation of the signal, the peak or maximum value for the amplitude is determined. The deciding factor at this stage is whether the peak value of the signal reaches the distortion level for the recording. The y shift is a facility for homing in the ground level and signal level in two stages for definite measurements.

Immediate modifications for the signal include the expansion of the y-channel by a factor of 2, 5 or 10. This function also operates in the stored mode. Other useful modifications especially in the preprocessing phase, are the inverse mode and the lowpass (LP) filtering facility. The LP filter attenuates frequencies in excess of 10 kHz which are not covered by virtue of the band width for the recording.

Although the distortion capacity is identified on the monitor of the recorder itself, the capacity for this purpose is limited. The limitations are obvious with the high frequency components present in an impact pressure recording. The quick rise times are captured by the triggering mode, also available on the scope. This mode of operation will be explained later (See 3.7.1) and in some detail, as it forms a basis for the observations of the transients.

The remedial action taken for this random observation of the recorded signal is to change the input attenuation level for the recording. An upgrading will allow the inclusion of a high peak value and a down grade will improve the amplitude to signal ratio.

3.2.2 Preparation For Preprocessing

Error detection applied to an original signal is more complex once a signal is digitised. This favours the analogue readout for the initial examining of the obtained data. With a signal still in its voltage format it represents the unconverted aspect of the data being measured.

The analogue voltage format is one that allows comparisons to be made without attaching the rigid marks of identification on the material. The importance of this phase can be seen when the quantitative analysis still has to be developed. The object of this phase is to carry out the procedure to verify familiar results with new sets of data. Also this approach helps to discover aspects and trends otherwise unknown before the research was carried out. Manipulating the data in this format gives it the non-dimensional aspect that is usually favoured for presentation purposes.

The preparation and manipulation of data helps to overcome any pitfalls likely to crop up during the presentation stage. It makes one aware of the discussions likely to be aroused for presenting the data in that way. It ensures that all related data be incorporated, in order to sum up all the dependent variables.

For this preconversion stage, a useful tool used on the analogue data is the condensation of the data. The significance of this is to capture a transient on the scope and, by means of a tape loop, repeat the recording over a number of times. The repeated signal is connected all together under one recording. The spectral analysis of such a signal gives the initial expectancy of the frequency range that predominates in one signal and not another.

3.2.3 Reformatting And Conversion

Having worked with qualitative values, the data, at some stage, must be converted to real values. One case arises when the data has been converted from analogue to digital. The digitised information is initially present in machine code requiring conversion to decimal code. The machine code may be binary or a language particular to the machine only. Although machine code proves to be a faster technique for the processing of data, the decimal code helps one to understand the results with a more realistic attitude.

This realistic attitude is further enhanced when the digital values are converted to physical values. In this case, the use of calibrated values becomes essential. The calibrated values are usually straightforward to apply with linear variations as is governed by this experimentation. What has to be included are the upper and lower bounds associated with any experimentally obtained value. This defines the accuracy to which a value may be quoted.

Unfortunately, the calibration values only form the basis of converting a measurement to its physical units. This is because a series of multipliers pertaining to the experimental technique used must also be applied. The most obvious one is for pressure measurements taken of a surface elevation with a sensor situated on the seabed. This arrangement generates a condition whereby pressures further away from the sensor are attenuated to those applied directly to the

sensor. Therefore, depending on the depth present at the time of the measurement, the appropriate attenuation multiplier is applied to the calibrated value. This shows that even for accurately calibrated instruments, the effects due to the immediate environment have to be taken into consideration ⁽⁵¹⁾.

3.3 PREQUALIFICATION

The prequalification of the data includes the detection of those unwanted elements that cannot be removed by applying highpass filtering techniques. The types covered include trends, unwanted shifts in the signal and isolated extraneous signals. The shifts are explicit as the DC component, or imposed at recording stage to avoid distortion of the signal.

Drift in the output response is the most likely sort of trend present in the signal. There are different forms which contribute to the drift component in some way. These are variations in temperature which are conditioned to changes between wet and dry measurements. The variations mostly occur in the splash zone due to substantial difference between the air and water temperatures.

Secondly, the drift may be a longer time variation component. This is due to large swells, of which the more likely being that of tidal action, contributing by its long period characteristic. A way of identification of a trend is to follow the temporal variation of the mean value of the signal. The longer the signal trace, the greater are the variations of the mean.

Removal of trends is necessary to uncover a significant signal that may be disguised by superposition. The larger variations in time also produce a degree of distortion in favour of the low frequencies when working in the frequency domain. This is of particular importance when evaluating the power spectrum of a waveform. The detection

of the trend is emphasised in cases where it is identified from known courses as is evident in signal drift present in the recorded signal. Another case where a trend is inhibiting is in the evaluation of the cross correlation of the two waveforms.

Other practical applications of an explicit trend in the main determining signal is in the evaluation of the probability density function. In this case, the trend would produce exaggerated results in the highest and lowest levels of the distribution. The consequence is that any statistical comparison to a theoretical distribution becomes indeterminate.

3.3.1 Trend Removal

When the trend is identified by the mean variation, the longer the record, the greater are the variations of the mean. Also, as these trends are non-linear the higher degree of polynomial shows up more in the shape of the trend for the long record. One solution is to subdivide into short discrete samples in the form of segments. This reduces the variation to that of a large curvature so that an assumption of linearity may then be taken for analysis purposes.

On this basis, the trend removal becomes a case for curve fitting, introducing low order polynomial curves to eliminate baseline trends. The method opted for is based on least squares determination. A polynomial of up to the second degree is common to take into account a change of slope present in the mean variation with time. The principle supporting this method is that for a sequence of dependent

variables at equal discrete time intervals, a polynomial of a predetermined degree is required to pass through it. The polynomial is characterised by one extra value of coefficient over the number of degrees decided upon (80).

The value of the polynomial is evaluated at each discrete level. The routine is such that the difference between the estimated and given value is squared and minimised. This is repeated for as many times as there are unknown coefficients. The minimisation is carried out by equating the differential to zero. The set of equations generated for the number of unknowns is solved by matrix inversion. The equation is then set up with the solved coefficient. This equation is again evaluated at the discrete points and subtracted from them to remove the trend depicted by the determined polynomial.

Further elaboration on this technique is to start with the mean values of a set of dependent variables for a range of independent variables. Then, the regression line is evaluated through these average values. The values of the coefficients of the straight line are then used to prepare a prediction model for the independent variable.

3.4 QUALIFICATION

After prequalification, the record will have to be classed as stationary and ergodic before it may be used to produce significant results as a representative of the random process. An ergodic sample is one taken from a random process. The ergodic nature is defined when the time average and standard deviation of each of the ensemble averages are of the same order. The individual samples are said to be stationary when these same sampling properties are maintained irrespective of where, off the record, the sample is taken. The follow up of this is that the verification of an ergodic and stationary sample will justify the same properties of the random process from which the sample is obtained.

The qualification of the data is to see whether the random data is stationary and ergodic. If not, the data may be modified before the rest of the processing is carried out. The test for stationarity is to carry out the normality test.

The number of these samples falling within a frequency range makes up the bar of a frequency histogram. This gives the observed frequency at each interval, f_o . These values are compared to the expected number of samples per frequency interval from a predetermined probability distribution, denoted by f_e . The probability distribution chosen for comparison is the normal Gaussian curve. The sum of the square of the difference is then evaluated to produce a statistic for comparison between one sample and another. This comparative value may be carried out for any random dependent variable. However,

in this exercise, the amplitude level was chosen for comparison. In the discrete format, a totalling of the samples, f_i , that occur within the incremental level of variables is carried out. This gives the observed frequencies for the various levels. By repeating for the standard curve, the values of f_e are obtained. The comparison was done by working out the χ value given as,

$$\chi^2 = \sum_1^k \frac{(f_i - f_e)^2}{f_e} \quad (3.1)$$

Here k denotes the class intervals which are chosen of equal width, that is, with the level of variable made up of incremental differences (See Fig. 3.1).

As this test gives an acceptance as to the normality of distribution of the random data, a measure of by how much the random data varies from the normal distribution is also required. The non parametric or distribution free procedure for this is called the runs test. The method in this case involves the counting of the number of times in which a random variable falls within one of two classes. In this case the random variable is again treated in discrete samples. The comparison to a distribution function is avoided by choosing the two classes to be values that fall above and below the mean value. The number of changes for a given set of observations gives the number of runs. The total number of runs determines whether the variable is dependent on the independent random observations or not. The hypothesis is tested against a table of values (See Table 3.1) which gives the number of runs in the lower and upper bound values for a given confidence limit⁽⁸⁰⁾.

3.4.1 Probability Density Function

In the above tests, reference to normal distributions shows the necessity of producing an algorithm that works out the probability density function for a given sample. The standard method is to apply the normalisation routine to the sample in the discrete sequence.

By defining ten counters, these are restricted to ten different levels of equal amplitude increments. These cover the range of between maximum negative to maximum positive values possible in a normalised arrangement. By looping through the discrete data points, the counters are augmented as the data point falls within each specific level. At the end, the confirmation of this routine is done by totalling the values of each counter which should read as the number of data points. The probability density function is represented by the sum of values making up each level. This is worked out as an area over each class interval and given in terms of the total number of data points. The resulting values are therefore real, non-negative and all together make up the probability density function (Fig. 3.1).

The combined effect of qualified data is required to proceed with the determination of sample properties and characteristics. Besides providing a comparison to the normal distribution, the probability density function ascertains the difference between randomness and sinusoidal form of acquired data.

3.4.2 Standardisation Of Variable (Dependent)

Once the data qualifies as being stationary and ergodic it is ready to be treated with the relevant digital processes. The condition of standardisation arises from the random data having been acquired from different sources. As already mentioned, it is preferred to present time domain data in its normalised form. However, as is the case, in its raw state the data also includes a shifted mean value (Fig. 3.2). This would deter from giving the data a full meaning of the time variations relative to its maximum positive or negative fluctuations.

The application of standardisation, therefore, gives a uniformity to the presentation of results. The procedure is to evaluate the mean value of the discrete samples. The mean is then subtracted from the discrete values. The standard deviation as the root of the variance by which the data fluctuates about the mean is then calculated. The division of the discrete samples by the standard deviation standardises the variance of time domain data Fig. 3.3).

The transformation of the data by this method also classifies it as being normal distributed with zero mean value and unit standard deviation. This stage is necessary to work out the probability density function and compare it to the standard distribution. This transformation generates a multiplier to be taken into consideration at the conversion stage. The multiplier is equivalent to the standard deviation, and without it the data is still processed under standard procedures. This is justified as long as the multiplier is included when giving absolute rather than relative results.

Unbiased estimates are used in straightforward presentation of data in the time domain. The meaning of this is that the data is free of overlying trends or sections that would appear out of order (Fig. 3.4, 3.5). The latter part signifies the deviation from the average value, in part of the data. This is rectified by weighing the section to bring it in line with the rest of the data. This discrepancy occurs with the presence of modulation of signals especially in the processing stage.

3.5 ANALOGUE TO DIGITAL CONVERSION

For this process, the standard independent variable relating to the amplitude is time. The conversion is done by sampling the analogue signal at a given rate by means of a microprocessor. The microprocessor is made up of a series of cards each acting according to the relevant software⁽⁸¹⁾.

When converting, the number of samples per signal is limited by the capacity of memory storage space. At any one go, the internal mass storage on any one disc is 8200 data points each occupying 8 bytes of information. Taking this into consideration, the minimum value of sampling rate to be opted for is governed by other limits. Sampling is carried out to obtain the maximum amount of information while at the same time maintaining the original structure of the waveform. The other limitation is defined by the largest sampling period that will reproduce the frequency of interest present in the overall signal.

3.5.1 Particulars Of Multiprogrammer For Conversion To Digital Output

The components making up the Hewlett Packard (HP) multiprogrammer are grouped in the form of I/O cards. These are the (69336 B) high speed scanner card⁽⁸²⁾, the timer/pacer card (69602 A)⁽⁸³⁾ and the high speed A/D conversion card (69422 A)⁽⁸⁴⁾. The intrinsic function is the scanning of up to 16 single ended channels of which a group of seven are connected to each of the 8 track Racal recorder via a multiplexer. The timing pace controls the scanning at a programmable

rate. The process involves the external trigger with a steady pace with which a sequential number of channels are read as discrete voltage outputs.

Other cards used in the system are compatible to the HP 9826 microcomputer. They include a ROM, read only memory which extends the basic 64K bytes by 256K bytes from the additional memory board. This combination improves the storage capacity of the random access memory, RAM required for both data storage and program execution.

A voltage regulator card also forms part of the integrated system. The requirement for the cable connections is 16 core, screened and gauged to physically fit the set up. The screening of the cable is also essential for the three conductor cable linking the I/O cards to the Data Common point.

Prevention of the A/D to be internally triggered is achieved by the replacement of one jumper connector to another. This change activates triggering to be carried out via the edge connector. For only one scanner card installed, the connection of two pins to the edge connector ensures proper use in the system.

When in operation, the jumper configuration of the A/D converter card enables the controller to be initiated via a gating system. The scanner card operates from a start at the highest channel number rotating in sequential order from all the analogue inputs connected. The last value in the overall channel outfit is zero.

The variable allocated to the scanning rate is called the sampling rate. This is a value of product of the range and period chosen to pick the maximum frequency the signal has to offer. The limit for this transfer rate without any further addition is 1000 readings per second. $\overline{\text{DTE}}$ (Data Transfer enable), $\overline{\text{ISL}}$ (Input select), SYE (System enable), TME (Timing mode), are control words used by HP enhanced basic language. They correspond to specific digital quantities which, when called in a given sequence activate part or all of the function of the hardware. The programming order for the scanning to take place is that the period is activated with DTE off so that no internal triggering could take place. This is followed by the range.

Input is passed to the A/D card via a control word. This is applied with commands $\overline{\text{ISL}}$, SYE, TME in basic software. The no gate facility of this card sets up external triggering to timer/pacer card. A conversion to digital mode is covered by passing the control via the A/D card.

3.5.2 Fundamentals Of Program Sequence

Full details of this sequence are given in HP Product Note, 6940 B - 1⁽⁸⁵⁾. What follows here is a brief summary.

The control word is based on a value of " -4096 ". The commands TME, SYE, $\overline{\text{DTE}}$ and $\overline{\text{ISL}}$ are given values in multiples of 16 with 1,2,4,8, respectively.

The program sequence for the timer/pacer card is done via the mode, range and period. The mode identifies whether the sequence is of single shot or of repeat mode. The range gives values in multiples of 10 raised to the power of I, where I is an integer value. The basic zero value is equivalent to one microsecond. However, when this value is multiplied by twice the period, the limiting value lies at 1000 samples per second. The other factor limiting the period is that it does not exceed 2047.

An image specifier of free format with control word is W. The output addressable to 12, is given by digital equivalent of the control word with the SYE command. The range value is then passed via the timer pacer card controlled by a multiple of 4096, according to its slot address with the numerical value of 3072. This utilises the recirculate mode.

The period data with the slot address in digital form is loaded on the timer/pacer card. The command to trigger the pacer card internally is the digital sum of the control word, data and SYE.

After triggering the data, the start channel has to be called up. This is done via the control word and the SYE command followed by the number of channels used and the slot address for the scanner card.

Finally, the A/D converter is programmed via the digital sum of the control word, \overline{ISL} , SYE and TME values. The remote control of the A/D is operated with the primary and secondary address operating

on the A/D slot address. This sequence is repeated for data collected in a loop around the number of channels. On termination of loop through the number of data values collected, the data is converted from a bipolar voltage reading to a decimal value, and stored on memory.

3.5.3 Other Uses For Computer Software

The simulation of a signal digitally is useful when comparing it to one obtained as random data in the experimentally controlled environment. The signals in digital form allow a number of algorithms to be performed on. The algorithms are purpose devised to incorporate the characteristics governing part of the research in question.

The digital approach shows its advantages when evaluation of the characteristics is carried out. The reason is because, in order to determine a characteristic like wave height accurately, say, a number of steps have to be accomplished beforehand. This example would require the establishing of the mean value, the position of the zero up crossing along the mean value and the positions of the zero slope along the profile of the wave. Only with the determination of the significant localities, can the physical sum of the maximum and minimum amplitude be achieved to give the wave height for that part of the signal. Now, as can be expected, these routines require a number of mathematical steps with accompanying memory allocation. Therefore, on this basis, and with the intention of carrying out the whole process repeatedly for lengths of recorded signal, the computer becomes indispensable (See Fig. 3.6).

Another combination of use between the digital signal and the associated computer software is connected to transient allocation. This is necessary to determine accurate readings of peak values and the rise time to reach this value. Together with these primary values are included the secondary values bearing equally important significance throughout this study (Fig. 3.7). The routines used for this exercise are performed on a suitably obtained record. The digital record for the purpose must account for the high frequencies associated with the rise time. This consideration is allowed for in the sampling rate of the digitised process. A rate of 0.02 sec. gives definite results for initial measurement purposes. The signal is then examined for the variations in slope along its length. Having established what the maximum slope is to be for the sample, a scan of the data is triggered when this slope is reached and is of a positive nature. The scan can be achieved so as to allow 25% of the data points displayed to precede the point of maximum slope. Accurate determination of the rise time is what is critical and is found by counting the discrete samples to reach the maximum point. The rest is purely a question of routine which involves values to which is applied suitable conversion relating to the calibration values. Transients captured in this way avoid the physical measurements to be taken off hard copies. The results are just as accurate and the need to set up arbitrary frames of reference from which perpendicular offsets may be taken, is done away with completely.

The added practicality of using computer software is that the displayed format is easily reproduced via the high level graphics output.

The 7470 A HP plotter provides excellent facility for this by ensuring a high resolution capability with multicolour pen options as a few of its features.

Although the language used is in Basic hardware, the modified HP basic gives that extra versatility for manipulation and execution. The extended basics in this range have the added advantage of increasing the language power of the routines. Speed to the system may then be introduced by the use of the machine coded languages (approaching the loading/compiling/running of the program) for example, Pascal. However, during the initial stages the program can only be ascertained as an overall process once its different levels of production have been verified. For this aspect, the basic language proves its worth for ease in editing and understanding.

3.6 DIGITAL FILTERING

Linear filters form a system implying a selective device or processor. The object of applying a filter is to transmit a predetermined range of frequencies while attenuating other frequencies. The terminology used in describing each of these two processes is band-passing and band-stopping respectively.

Qualification of the data makes it statistically representative of the characteristic parameters by which the signal is to be determined. At this stage, the time domain data will need to have its interference removed to a form more familiar to the reader. This procedure comes under the heading of filtering and is an essential part of the processing. The filtering has to be seen in conjunction with data conditioning. After editing and trimming, this involves the process of averaging and windowing of the time domain data in preparation for the analysis stage. Otherwise, the results obtained will not be a true representative of the measured signal but also due to the additional superimposed unwanted parts. The data conditioning is essential for the frequency response evaluation, like the power spectrum, to produce information exclusive to the frequency range under examination.

3.6.1 Filtering Design

The design of a filtering process consists of starting with a frequency response specification. An equivalent impulse response is obtained from the inverse Fourier transform (IFT) for the discrete values. The impulse response defines multipliers in the digital filter,

the values of poles and zeros which are obtained at this stage..

The filter is then defined by a gain constant, a polynomial in zeros divided by a polynomial in poles.

Filters with finite impulse responses have a representation in the time domain that is recursive and can be represented by the sum of a series of coefficients. The more practicable version is one, as seen above, that rearranges the series into a ratio of two polynomials multiplied by a gain constant. The degree of each of the polynomials may vary or be of the same order. The number is related to the amount of simultaneous bands of frequency the filter is to capture. Each polynomial is factorised to give roots from which the time domain of the filter may be obtained. The roots at the numerator are called zeros while those at the denominator are called poles. The poles appear in conjugate pairs represented by complex variables.

The physical value of this arrangement is to represent the filter by a set of roots which, when put in configuration in a certain way produce the required filter or filtered effects. The way in which the pole arrangement works is that each pole is supplemented by an equal one of the same magnitude but with a reflection in the phase angle. The arrangement is plotted diagrammatically by a unit circle. The poles and zeros are represented as vectors radiating from the centre. Their magnitude is given by the length of the vector and phase angle given from the zero positive line. The determining factor for the value of the poles and zeros is that their magnitude must be less than unity. Otherwise, a condition

of instability is reached, when the output of such a filtered signal deals with infinite values. This condition of instability is not used for signal processing purposes. A pole outside the unit circle plot is therefore to be avoided (See Fig. 3.8) ⁽⁸⁶⁾ ⁽⁸⁷⁾.

3.6.2 Removal Of The DC Component

The presence of a definite average for a signal implies that the frequency spectrum results in having zero frequency components. These zero frequencies or DC component value augment the lower frequencies producing considerable distortions in the power spectrum. This component in the spectrum stops the analysis from producing a realistic representation of the frequency components that matter. As mentioned earlier, this component may be removed by standardising the data. However, in some cases, after filtering has taken place, the resulting spectrum shows, to some extent, an indication, though not necessarily predominant, of the zero frequency components. This value is unwanted especially when dealing with low frequency identification as are frequencies associated with wave profiles.

The identification of this problem requires a more definite way of putting it right. One of the successful ways is by using a digital filter design especially for removing this type of frequency component.

The value of the filter coefficient to reject the DC component is to apply a zero of magnitude close to unity and phase angle of nought degrees. The resultant spectrum from the signal is one that

attenuates the zero frequency components. The profile of the transfer function of the filter is also reflected in the frequency domain (See Filter 0.3.0.) The code adopted for referring to the use of filters is made up of:-

transient number: filter type: part number

where transient number refers to the transient stored on Bdat file.

The filter type is chosen according to the cut off frequency. The part number is the secondary classification by which the stored transient may be divided according to the transducer number (Fig. 3.8).

3.6.3 Filter Types

In the following documentation, both centre and cut off frequency have been interchanged to mean the same function of frequency⁽⁸⁸⁾.

The three main types of filter that have been applied and approved in practice are the low-pass, the high-pass and the band-pass filters. These are classed according to the positioning of the centre frequency. The low-pass, described previously, is one that centres its cut off frequency at zero frequency and is therefore not of direct use for this analysis. The band-pass is one where the cut off frequency can be varied anywhere along the spectrum. The implication of this is that for a broad bandwidth of frequency response, the characteristic frequency can be enhanced. This improves the detailing of the response in the locality. The applied filter should therefore fit the predetermined frequency components of the centre frequency. In the case of the high-pass filter (0.3.0) the cut off frequency is limited to the higher frequencies.

The design of the filter in digital form is based on the positioning of poles and zeros to satisfy the predetermined centre frequencies. In the case of the digital output the sampling period is arbitrary throughout the analysis of the signal. The significance of the sampling period comes about in the range of frequencies to which the power spectrum is representing. This is called the Foldover Frequency and is half the value of the sampling frequency. The choice of the number of points to build the Fast Fourier Transform (FFT) in the development of the power spectrum gives the resolution or accuracy to which the frequency component may be quoted. This is worked on the ratio of the sampling frequency and the FFT size.

It will now be seen how the sampling period is used to determine the design value of poles and zeros in terms of their magnitude and direction. The predetermined frequency is given in terms of the angular measurement, that is,

$$\omega = 2\pi f \quad (3.2)$$

The product of this angular measurement to the sampling period gives the angle the filter component has to turn through from the zero phase angle. This value is the equivalent radian measurement, so a suitable conversion to degrees has to be carried out, that is,

$$\phi = \omega T \cdot \frac{180^\circ}{\pi} \quad (3.3)$$

For instance, in a particular example 11 Hz becomes the centre frequency for a band-pass filter where the sampling period was 0.03 sec. for two signals digitised at 0.015 sec. simultaneously. From this equation (3.3) the resulting angular measurement in phase angle is 2.08 radians or 120 degrees. This gives the angle at which the

pole is located along the radius of the unit circle. The conjugate of this value is fixed by reflection of the pole in the real axis.

3.6.4 Windowing

Difficulties arise when the impulse response of a filtered signal contains a large number of terms. Reduction in the trailing ends of a signal is carried out by truncation. Here, the use of windows as multipliers may be either of the rectangular type or of a varying distribution. The choice of window results in the extent by which a pass band distinguishes itself from the frequencies that are attenuated, or the stopband part of the filtered signal. In the case of sharp edges as in rectangular windows, the formation of Gibbs phenomenon comes into force. The unwanted condition is overcome by shaped filters that tail off, like the Hamming or Hann filter ⁽⁸⁶⁾.

The spectral distribution of this windowed impulse response produces a low-pass filter with a smoothing distribution effect over all the frequencies. A reducing degree of attenuation results with increased distance from the centre frequency which is zero frequency in this case. In the choice of windows, the Hamming depicts a cosine function in the time domain. This brings about the meaning of a transversal multiplier. This is a window acting as a filter function that would impose the product of its discrete values to the time response of the signal giving a filtered time response. The spectral response in the frequency domain is then represented as a result of the filtering on the input signal.

Other window functions exist with similar relationships to the one above. Their main purpose is to suppress frequencies in phase between band-pass and stop-pass. The trade off for this to happen while maintaining a smooth profile is the gradual attenuation of the frequencies in the band-pass region. The attenuation is least at the cut off frequency and increases with distance from the frequency. The variations between the amount of attenuation is particular to the various types of window functions available. Such types include Kaiser's and Hann's windows as featured in A.P. Oppenheim and R.W. Schaffer⁽⁸⁹⁾ (1975).

3.6.5 Mechanics Of Windowing Functions

So far, the mention of windows covers how they improve the spectral response as a form of filter. How they operate in the time domain becomes part of the mechanics of the digital program to produce the spectral analysis. The digital program used is FFT determined and is applied to a number of samples wholly divisible by numbers made up of powers raised to base 2. This requires that the data be either truncated or that zeros are added to it to fulfil this requirement.

Another feature is to "remove leakage" of a true spectral lobe spreading into negative sections⁽⁸⁰⁾. This is done because the spectrum is truncated at the foldover frequency to produce the resulting power spectrum with a minimum of leakage possible. The use of the appropriate window, other than rectangular or boxcar, suppresses the tail ends in the time domain. This action has the effect of broadening the

main lobe and reducing the side lobe leakage in the frequency domain. Choice of the FFT size, sampling period and the reproduction in linear, squared or log format all accentuate the spectral estimate to the adequate level of resolution and variability. The variability is an indication of the smoothness of the frequency response, a feature mostly attained by segmenting and overlapping.

Bingham, Godfrey and Tukey⁽⁹⁰⁾, suggest the cosine tapering function, (mentioned earlier in 3.6.4.) known as the Tukey window, for windowing purposes. Its improved qualities over the rectangular window is that up to a tenth of the ends of the original sample are suppressed. The application of this function introduces a modification to the variance of the tapered data. The variance reduction is given in terms of the frequency response with a broader main lobe and greatly reduced side and negative lobes. The compromise is in the magnitude of the frequency estimate components to which a scale multiplier can but put them right.

The characteristics of the windowing function are grouped together in its frequency response. The response shows a lower peak value for its main lobe, which does not reduce to zero at the sampling frequency. Also the negative lobes are reduced to insignificant values. The width of the main lobe for this function is such that at half power the value is equal to half the value at full power.

Original samples having less than the required number for the FFT routine are padded by additional zeros to the sequence. The consequence is that the estimates are given in terms of the augmented

length. Therefore, this forms a means of improvement to the frequency resolution. A power spectrum that consists of a number of discrete isolated values produces an undesired discontinuous picture. This is overcome by increasing the number of samples in the FFT size, thereby also improving the resolution of the response (See Fig. 3.9).

3.6.6 Further Averaging For Resolution And Smoothing Improvements. Segmentation.

Segmenting is effectively dividing the sample record, and the frequency response is applied to each segment. This acts as a means of averaging and produces a better resolution of the frequency response. The reason for this is that each segment having a lower sample length will provide a frequency response with a larger bandwidth over the same FFT size as was the larger sample. This implies that the same frequency range is covered by a larger bandwidth. The averaging of the spectral estimates obtained from each of the segments will therefore produce the improved resolved frequency components in the spectrum.

A further increase in the bandwidth is obtained by taking the isolated segments made up from the adjacent parts of the original signal, and to them include overlapping segments. Whereas previously, the averaging of the spectral estimates are calculated from individual bandwidths, the averages are now combined by the common segments. This clearly introduces a collective bandwidth made up of individual segments put together by the binding segments which bridge the contiguous ones. The final result takes into consideration both

the advantage from the improved resolution resulting from the averaging and the smoothing characteristic resulting from the combination of the segments in this way.

The process is summarised by dividing the whole sample into segments, performing the FFT on each segment, squaring the elements of the frequency components and averaging over the whole segments. The additional advantage in this ensemble averaging is that much less computing time is occupied by applying FFT to individual segments rather than to the combined signal.

The estimation of the spectral components from individual segments produces a degree of uncertainty in the values close to the sampling frequency. This problem arises by use of the shorter sample lengths. The estimation is reverted to a high level of confidence by applying the windowing properly to each segment, to taper off the tail ends of the spectral estimates. Overlapping ensures a further improvement on the values close to the sampling frequency, obtained from individual segments. Left over data from the formation of segments out of the original sample is ignored (Figs. 3.10, 3.11, 3.12).

The other use of segmentation is that it allows breaking up of non-stationary data into quasi-stationary segments. The idea of non-stationary data is that which presents itself with a time varying mean value. This type of data has come across in this experimentation. It is due to drift and physical effects of the lower frequency superimposed data. Previous methods have been described to remove this component in the main. However, the extent to which the trend

is removed is only relative to the samples and may still contain traces of it. This non detrimental, yet persistent extraneous component is further reduced with the use of segments during the analysis.

The method by which the use of windowing, zero padding and segmenting are used to average out the periodogram or power spectrum can first be attributed to Welch⁽⁹¹⁾.

3.7 TRANSIENT ANALYSIS

A transient is classified as a particular type of random data where its time history starts and ends at the zero value. Thus the response obtained from an impulse falls under the categories of transients. The data is considered non-stationary in that it has a time varying average.

A transient may be analysed as a periodic signal by condensing it by multiple playback. The repetition time of the transient playback is necessarily longer than its duration. This has the effect of changing a line spectrum to a continuous one. In terms of energy units the spectrum is converted by multiplying the power units by the repetition time. The power of the signal is determined in R.M.S. terms. This is possible as long as the averaging time interval T_a is much larger than the repetition interval by which fluctuations in the spectrum are evened out.

This method is applicable to both analogue and digital processing. The non-stationary aspect of the transient is overlooked when the same analysis techniques as those used for stationary signals are used. The effective length of the transient is characterised by the effective bandwidth, B_{eff} which is the reciprocal of the duration of the transient. Another factor to be defined is the filter bandwidth or reciprocal of the filter response time denoted by B .

The concept of bandwidth follows from band-pass filtering. Ideally this filter transmits the power contained between two specific

frequencies. Any power beyond these limits is attenuated. Hence the bandwidth is the difference of the two frequencies where the power is of importance.

A measured value is restricted by the resolution frequency in the degree of uncertainty in frequency terms. Its value is obtained from the product of the bandwidth (from the repeated period) and a weighting. The weighting is a measure of the type of windowing used — 1 is used for the rectangular window. The accuracy is given in terms of a bandwidth and is independent of the filter bandwidth especially with a digital filter. The determining factor is the length of the record, $T \cdot N_{FFT}$ where N_{FFT} is the number of samples used in the FFT size, which produces a bandwidth of an accuracy of the reciprocal of this product. By increasing the sample length in terms of the FFT size used to determine the frequency of the sinusoidal components of the waveform, the spectrum is given a more accurate representation in frequency terms. However, the signal may be transient of total duration of the sample where the bandwidth of uncertainty is given as a reciprocal of this length of time.

The filtering of a transient signal by a high-pass filter reduces it to an oscillating signal with a definite start and finish. This determines the duration of the transient in terms of time domain. A burst of energy level characterises this signal way above the neighbouring signal. The energy is determined by squaring the amplitude of the power spectrum and integrating its values in the frequency domain. The comparison of transients in this way highlights their

relative rise times and their maximum amplitude. The rise time is measured from the frequency or line spectrum within the duration of the oscillation.

When the transient length is less than 10% of the repetition time this method of analysis becomes inadequate. This is because the dynamic range is effectively reduced by a ratio of the repetition time to the transient length. Dynamic ranges are optimised when the averaging time is of the same order as the transient length. This involves a triggering process of the transients from which linear integration is performed to evaluate its power.

3.7.1 Triggering Mode

Quick reference of the captured signals may be necessary to reduce the digitised output to its calibration equivalent. The instrument used for this purpose is a digital storage oscilloscope (Gould OS 4200), as mentioned earlier in 3.2.1. However, the essential function for this scope is the use of its triggering mode used for both observation and study of the transients. The necessity arises to overcome the otherwise speedy continual updating of the screen at a chosen time base of 0.5 sec. per cm. The fast time base is used to capture the high frequency components present in the transient measurement, in particular its rise time. The time base sensitivity of the scope has limits of 1 μ sec. to 20 sec. per cm in a 1:2:5 increasing order ⁽⁷⁹⁾.

The transients present in an input signal are captured once the predescribed set parameters are reached. These parameters are given in terms of the level of triggering. The manual level controls a shift from the ground level of the channel. It also forms the mid-section of the window within which the signal may be triggered. The trigger window is operational with a positive or negative slope control. The slope controls either direction of the rapid change in signal amplitude over a discrete sampling period. The threshold for the internal trigger window is adjustable between 0.5 cm to 6.0 cm.

The combined effect of the operation initiates the time base sweep. The scope being armed either in single shot or normal mode, then triggers when receiving the impact signal. The signal is allowed .25% of the screen to be taken up by data preceeding the instant of triggering. This provides the same basis for measurements carried out on different impacts.

Together with these settings, the availability of AUTO TRIG overrides the triggering facility to continually update the screen picture. However, internal triggering of the type explained above, is activated by either of the two channels. The coupling mode in the DC position allows the triggering of the instrument at specific voltage levels. The AC coupling mode, acts as a high-pass filter. It attenuates frequencies below 1.5 Hz, including the zero frequency ones. This is useful when backplaying of signals that have a tidal variation superimposed on the direct signal. The LF reject is useful as it stops triggering due to the presence of a spurious signal in the alternating voltage range of 50/60 Hz (mains frequency).

The triggering of a signal is noted by the lighting of a red bulb to which the scope is reset for the next run. Once captured, in the signal mode, the signal is automatically stored on the screen. However, when in normal mode, the signal is stored via the HOLD button, to avoid a freshly triggered signal overwriting the previous one. It is noted that in the switching of the recorder, it sends a spurious signal large enough to rearm the triggering mode. This is to be considered even when the single shot operation is in action.

Modifications in the x-axis on the stored signal include a time base expansion for an increase in accuracy in the readout. The two options available may be operated independently or concurrently. The first alternative is a quadrant expansion where the screen of 4000 samples is segmented in 1000 samples in the time domain with an overlap of 500 samples. This magnifies the time base by a factor of 5. The other alternative is to rotate the adjusting knob completely to the right to give a corresponding magnification factor of 10.

3.7.2 Digital Storage

The obtaining of data in digital form requires the use of an efficient mass storage system. This is done on the HP peripheral device. It takes the form of 133 mm diameter discs which have a capacity of 32 tracks on each side. The discs are initialised when introduced for the first time. The initialisation clears the disc of damaged tracks by simply ignoring them. The magnetically coated surface of the disc allows data to be recorded by magnetic head provided by the RAM unit (Random Access Memory) as a peripheral on the internal system⁽⁹²⁾.

The data is stored in bytes with a restriction of 8 bytes for real variables and 2 bytes for integer variables⁽⁹³⁾. The creation mode of a Bdat file on which the data is stored takes the form of a number of records in the file and the number of bytes per record anticipated to occupy the data space. The Bdat file is a file devised for use in HP Basic Hardware. The use of records per file has been found useful to store information connected to the main data on file. The other need is for organisation of simultaneous input signals. These are either from the beach or as inputs in the form of transients from different channels on the wall. The organisation gives a good means of control when analysing the data especially at a comparative level. The main limitation per file is its size and this stands at 65 k bytes.

The commands associated with data storage are selective to write and read procedures. The use of the ASSIGN statement places the file at the beginning, even if previously found open, of any of its records ready for access. The variable has to be allocated its size next. Writing of data is carried out by an OUTPUT command, while reading is done by the ENTER command. At this stage any record within the file can be specified to contain the data. The data is stored in the efficient way of free format, a fact to bear in mind when assessing the information. Care must be taken when digitised information is collected in bulk and stored in that way. The use of routines that read the data and sort out by sequential accessing are mandatory for overcoming this situation.

The Bdat file store is defined in terms of random and serial access. The serial access makes it difficult to obtain information other than that at the beginning of each record. The random access, reading and writing to the file may be carried out from any record in the file. This disadvantage is overcome by the use of ASCII files for storage purposes. The ASCII file stores information compactly in serial access only. The ASCII or LIFASCII stands for logical interchange format adapted for HP Basic Hardware⁽⁹²⁾.

3.7.3 Sources Of Error In The Digitisation Process

A common source of error in the conversion of data from analogue to digital format is due to aliasing effects. This error gives misleading results in terms of frequency components present in the input signal. Assume the input signal has a predominant frequency, F and a choice has to be made on the sampling frequency for digitisation.

If sampling is carried out at 4 samples per wavelength, the joining of the sample points would show a more definite nature of the signal. This method is most commonly used in practice. Distortion from the original signal when present is a function of the sampling frequency. A reduction in the sampling frequency to half the original amount produces a degree of distortion large enough that the nature of the signal is lost. If the sampling is again reduced to one sample per wavelength, the waveform is maintained while the frequency detection is disrupted. This case explains aliasing as the frequency discrepancy between two signals of the measured and true characteristics.

The minimum sampling rate to be used for sample values is therefore related to form an adequate substitute for the original signal. The consequence of aliasing is that for frequency components greater than the foldover frequency, there is an overlap between the adjacent repetitions of the spectrum. This is repeated at twice the sampling frequency. With such an overlap, the spectrum will not represent the true frequency components. To overcome this possible error, the value chosen for the sampling rate should at least be twice the highest frequency of interest in the sample. This is called the Nyquist frequency (Fig. 3.13).

A second source of error is due to Quantisation, the accuracy associated with conversion from analogue to digital information⁽⁹⁴⁾. A range of input signal of V Volts, is converted in terms of a digital word made up of a number of bits, denoted by n. This implies that the range may be divided into 2^n equal intervals with an input at each interval represented by a different digital value.

For the finite interval difference, the error associated with the digital value varies from 0 to a maximum of $\frac{1}{2} 2^{-n}$ volts for a value stored at mid point of the interval. The error involved when using an 8-bit word works out at .2% of the full scale voltage used⁽⁸⁶⁾. The accuracy is improved by the use of a larger number of bits for the digital process (Fig. 3.14).

3.8 DEVIATION FROM NORMAL DISTRIBUTION

The normal distribution is given by the Gaussian form and is the character of random stationary data. The first parameters that can be derived from the random data are the average value and the standard deviation. The average value is the algebraic sum of the dependent variables divided by the number of observations. This value is also called the arithmetic mean. The relevance of the mean is first to reduce it to zero value by taking the mean value from the discrete values of the dependent variables. The equation used for the sequence set $\{x_n\}$ is,

$$\bar{x} = \frac{\sum_{n=1}^N x_n}{N} \quad (3.4)$$

where N = the number of observations.

The standard deviation is a measure of the spread of the dependent values to either side of the mean. This is calculated by taking the square of the difference between the discrete values and the mean and dividing by one less the number of observations. This first stage is called the variance while its root gives the standard deviation, s , that is,

$$s = \left[\frac{\sum_{n=1}^N (x_n - \bar{x})^2}{N-1} \right]^{\frac{1}{2}} \quad (3.5)$$

As mentioned earlier (in 3.4.2), the determination of these basic parameters is to standardise the input data. Any results obtained from the transformed data may be suitably reduced to the original values. Alternatively, knowing these parameters, the transformed

data may be referred to the original values. The statistical significance for the standardisation of these random discrete values is to compare them to the normal or Gaussian distribution. The Gaussian distribution expresses a definite shape of curve for zero mean and unit standard deviation. This is given by the expression,

$$p(x) = \frac{1}{s^2\sqrt{2\pi}} \exp \frac{-x^2}{2s^2} \quad (3.6)$$

where x is the dependent variable about the mean value μ_x . The standard value is a form of probability density function.

3.8.1 The Effect Of Amplitude Distribution By Linear Processing

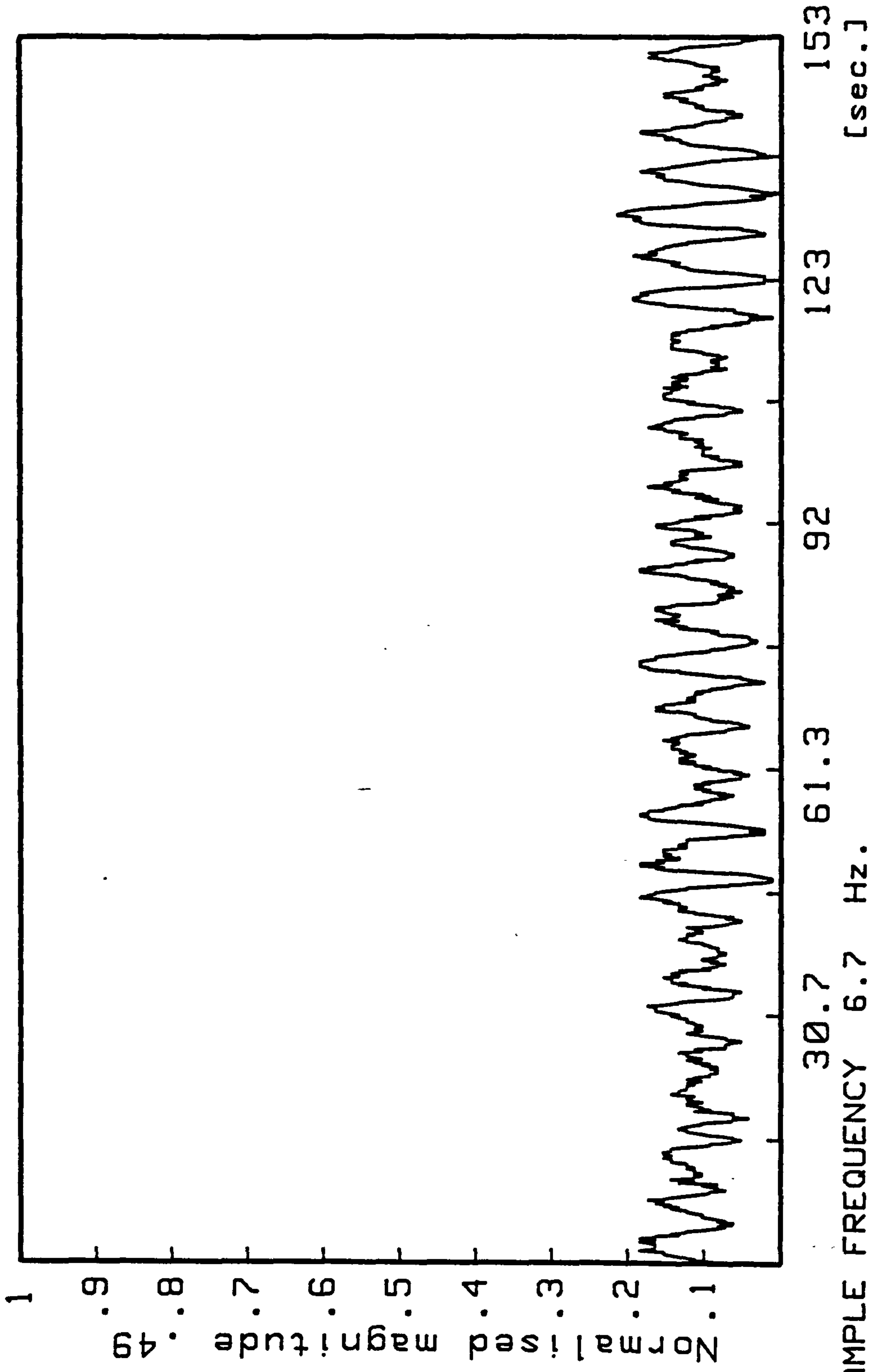
The conversion of an output from an input by a linear system such as a digital filter produces a change on the amplitude distribution. However, for original distributions from random signals that are Gaussian, their nature is maintained. This has been shown by the examples that the mean and standard deviation remain unchanged. The probability distribution of the amplitude is evaluated to represent the free surface elevation distribution.

The distribution also gives the value of the mean and standard deviation. By integrating the instantaneous values of the probability multiplied by the amplitude level, the first moment or mean is obtained. Similarly, by taking the square of the amplitude as the multiplier factor, the second moment or variance of the distribution is obtained.

These two values are related to the power functions of the waveform. While the mean is a measure of the average energy level of the signal, the standard deviation is a measure of the root mean square of the signal. Therefore the interpretation of the qualities and power inherent in a signal are given in terms of these tangible values. In the case of a random signal, the governing variable becomes the frequency component which may also be assimilated to the probability of a certain amplitude occurring.

The parallel of this argument in the generation of the random distribution for positive values only, lies in the definition of its characteristics. These characteristics may be reduced to the position of the peak value relative to the zero value and the skewness of the distribution.

Kurtosis is a form of ratio of the n^{th} order moments of the statistical distribution. The n^{th} moment is given as the difference of the sample values (events) from the mean value raised to the power of n . Kurtosis is given by the ratio of the fourth moment to the square of the variance. It measures the relative peakiness of the normal distribution. Skewness is defined as the third moment divided by the variance raised to the power of $3/2$. The skewness gives a measure of the asymmetry of the normal distribution curves representative of a number of events.(Fig. 3.15).



SAMPLE FREQUENCY 6.7 Hz.
 SAMPLE LENGTH 153.3 sec.

FIG 3.1(a) TYPICAL WAVEFORM DATA RECORDING
 DATA FROM BEACH TRANSDUCER Sch.
 23rd March 1983 (See SITE NOTES 4.7)

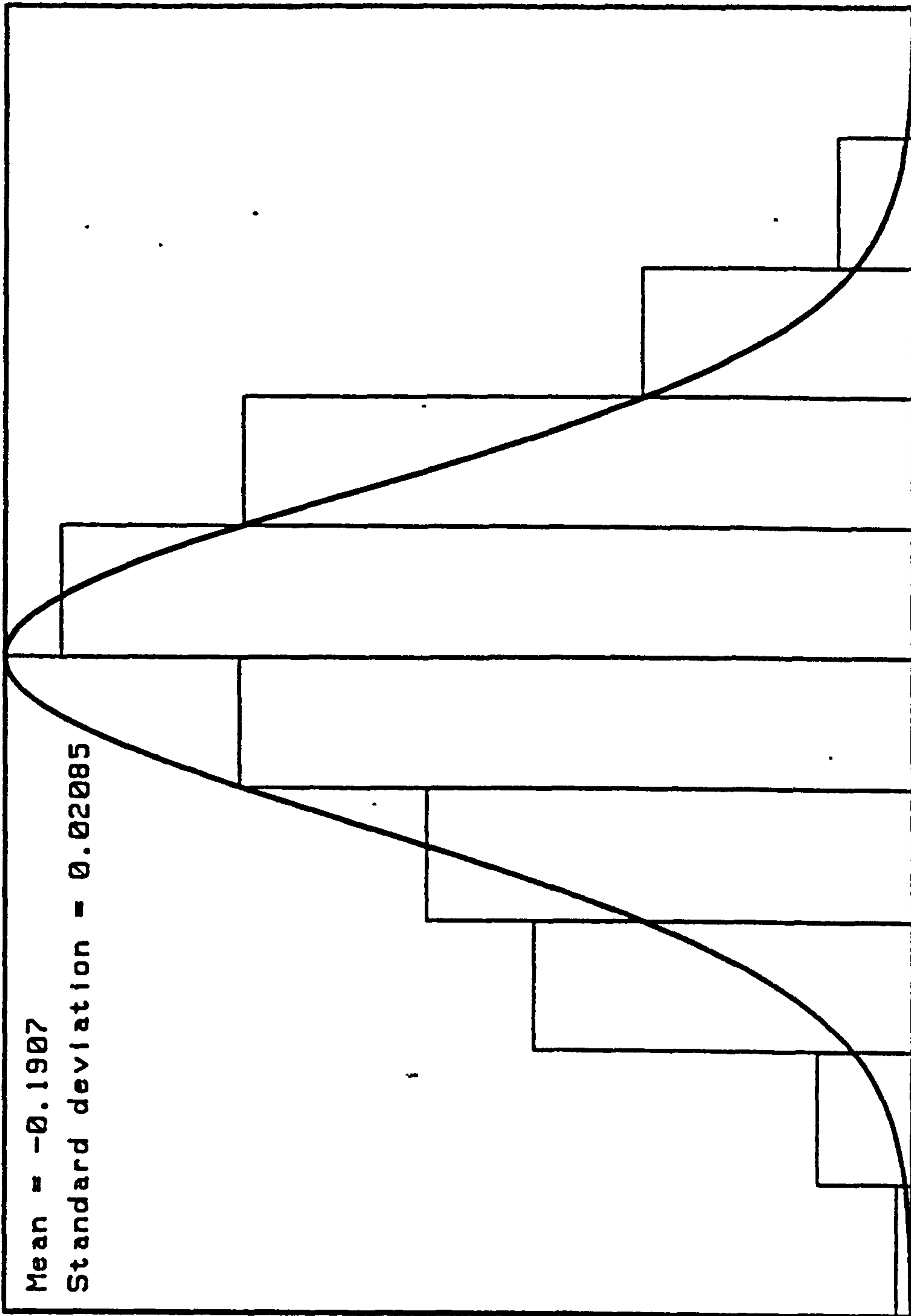


FIG 3.1(b) AMPLITUDE PROBABILITY DENSITY AGAINST
GAUSS'S NORMAL DISTRIBUTION
(DATA as shown in FIG 3.1(a).)

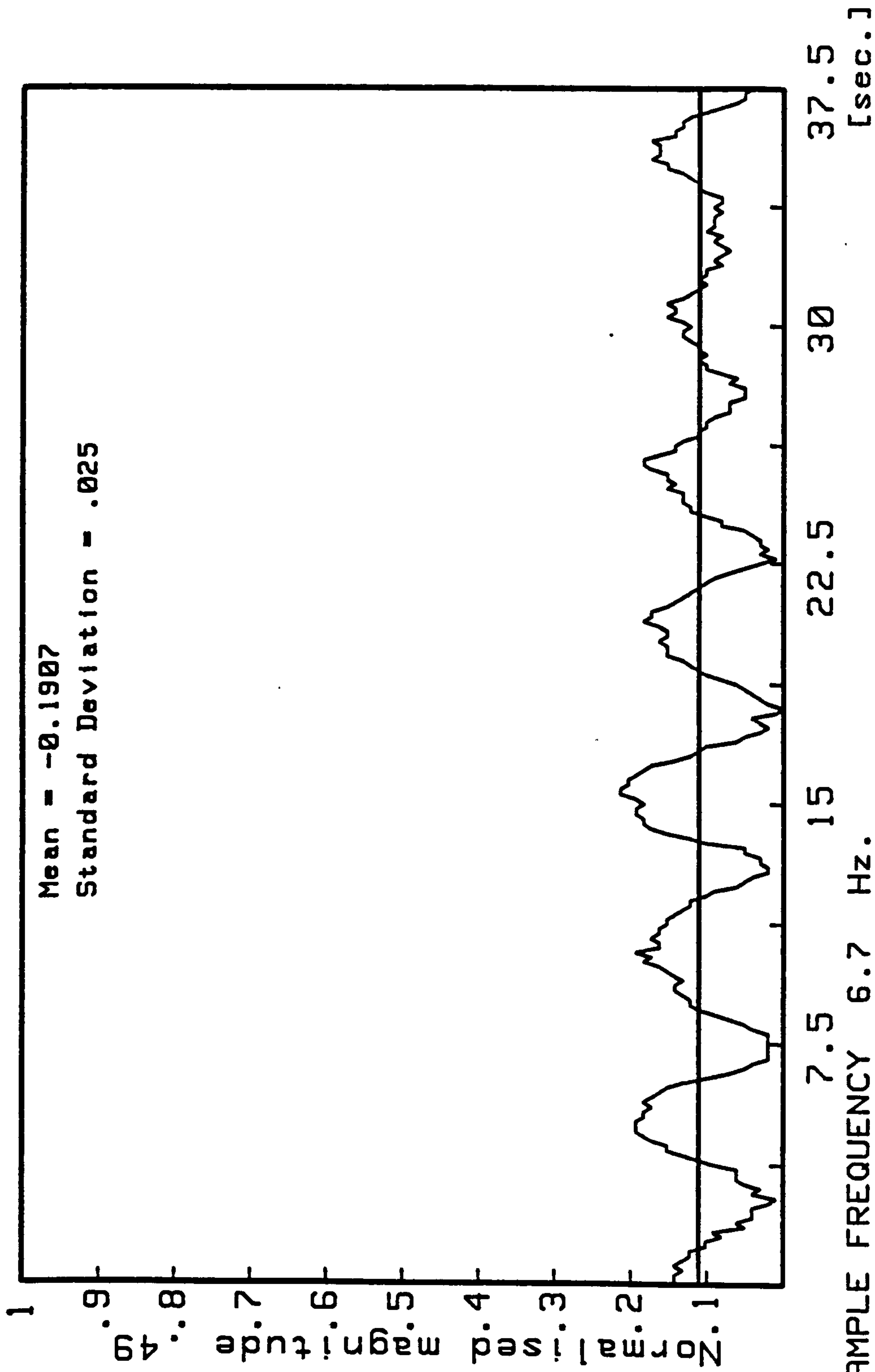


FIG 3.2 TIME DOMAIN SIGNAL WITH A SHIFTED MEAN
(SAMPLE FROM DATA shown in FIG 3.1(a).)

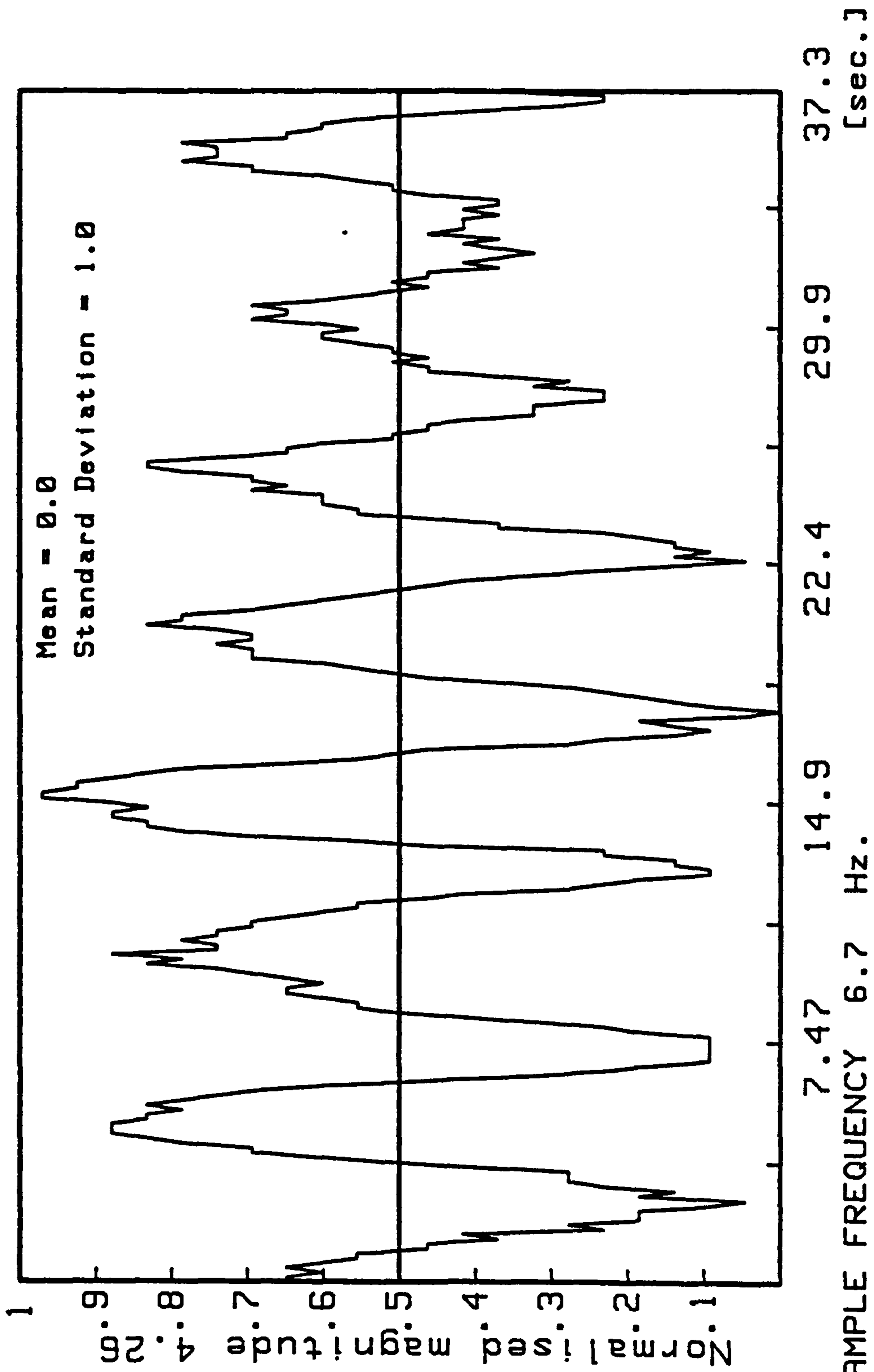


FIG 3.3 STANDARDISED TIME DOMAIN SIGNAL
(DATA shown in FIG 3.2)

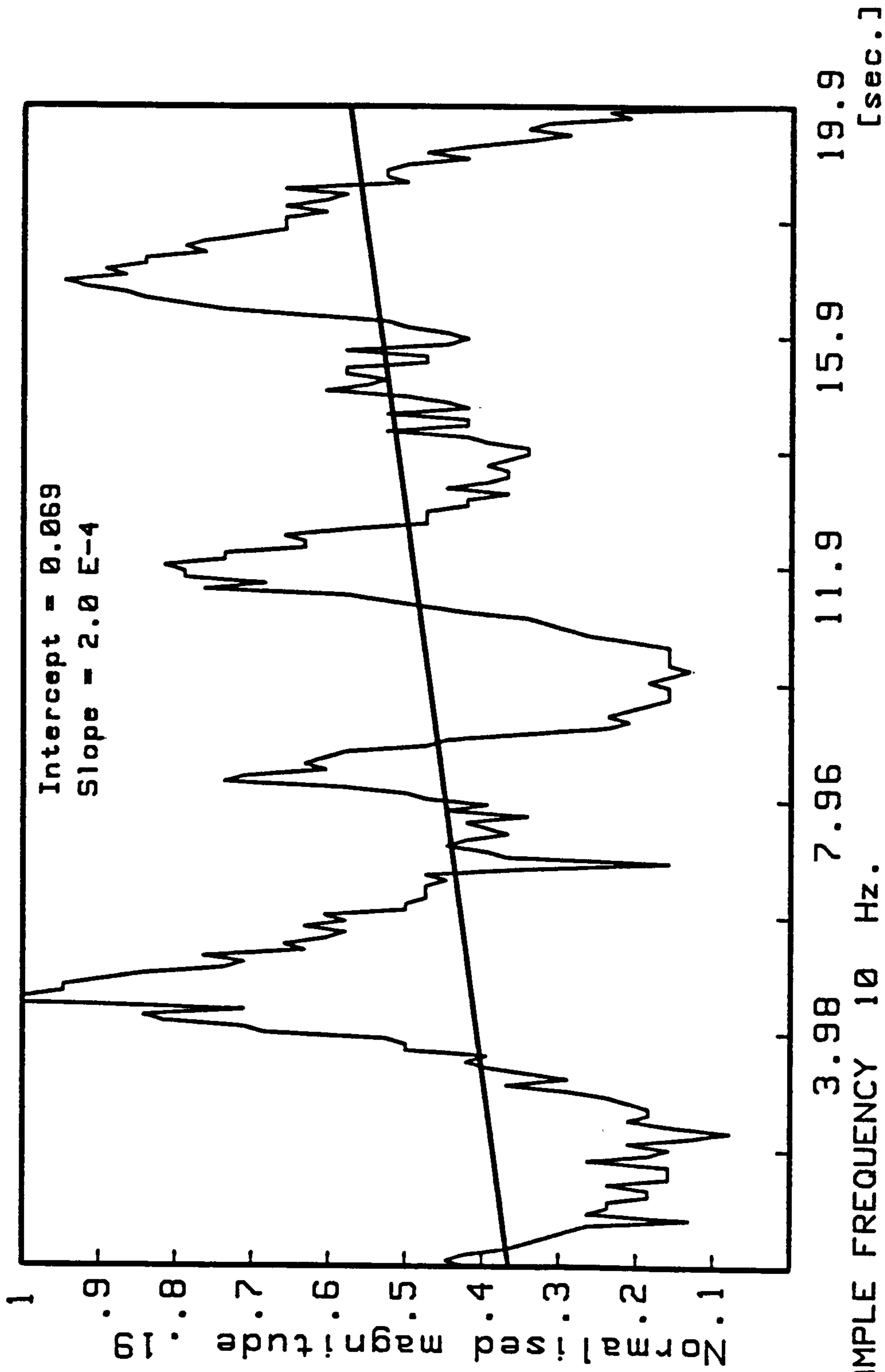
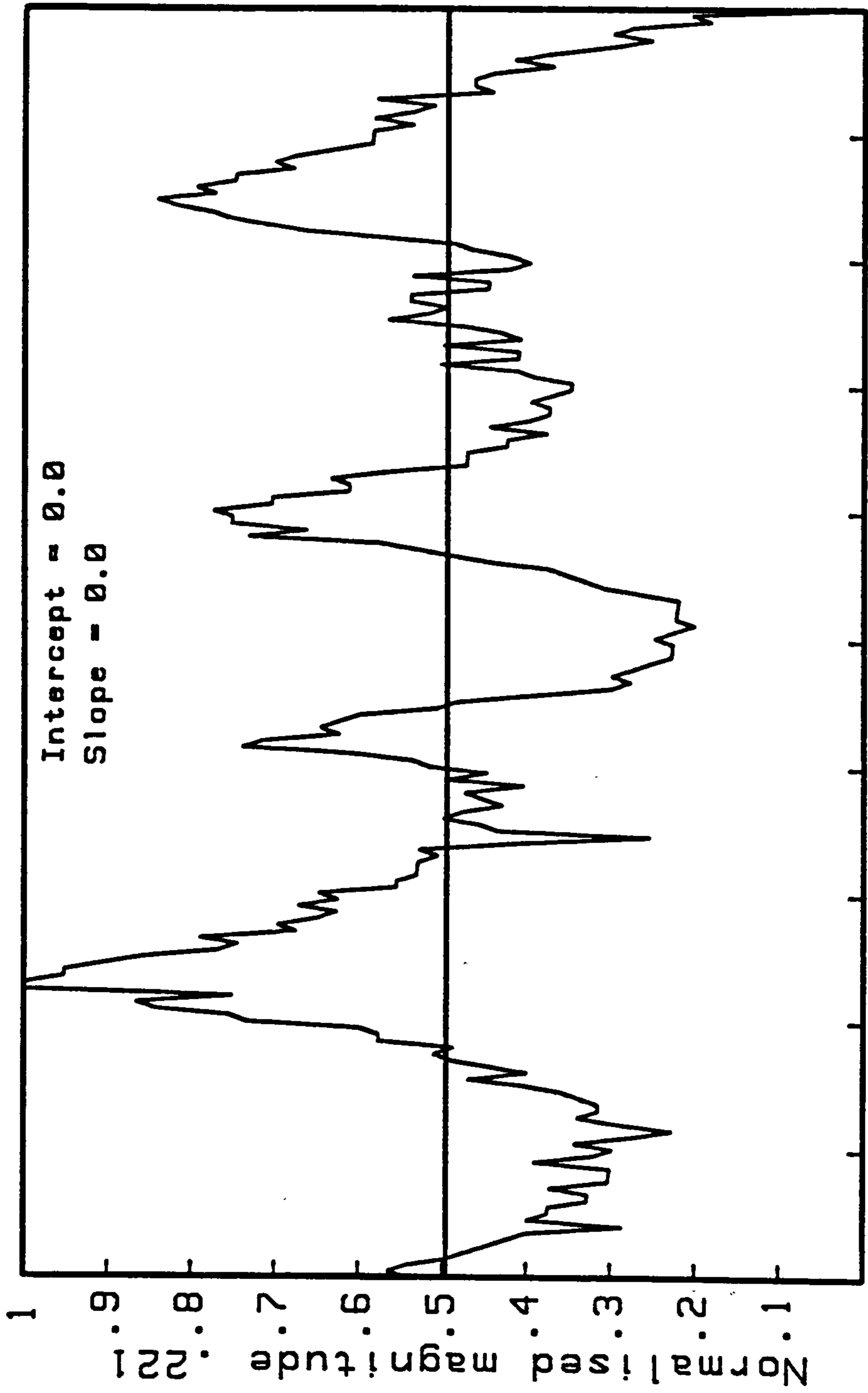
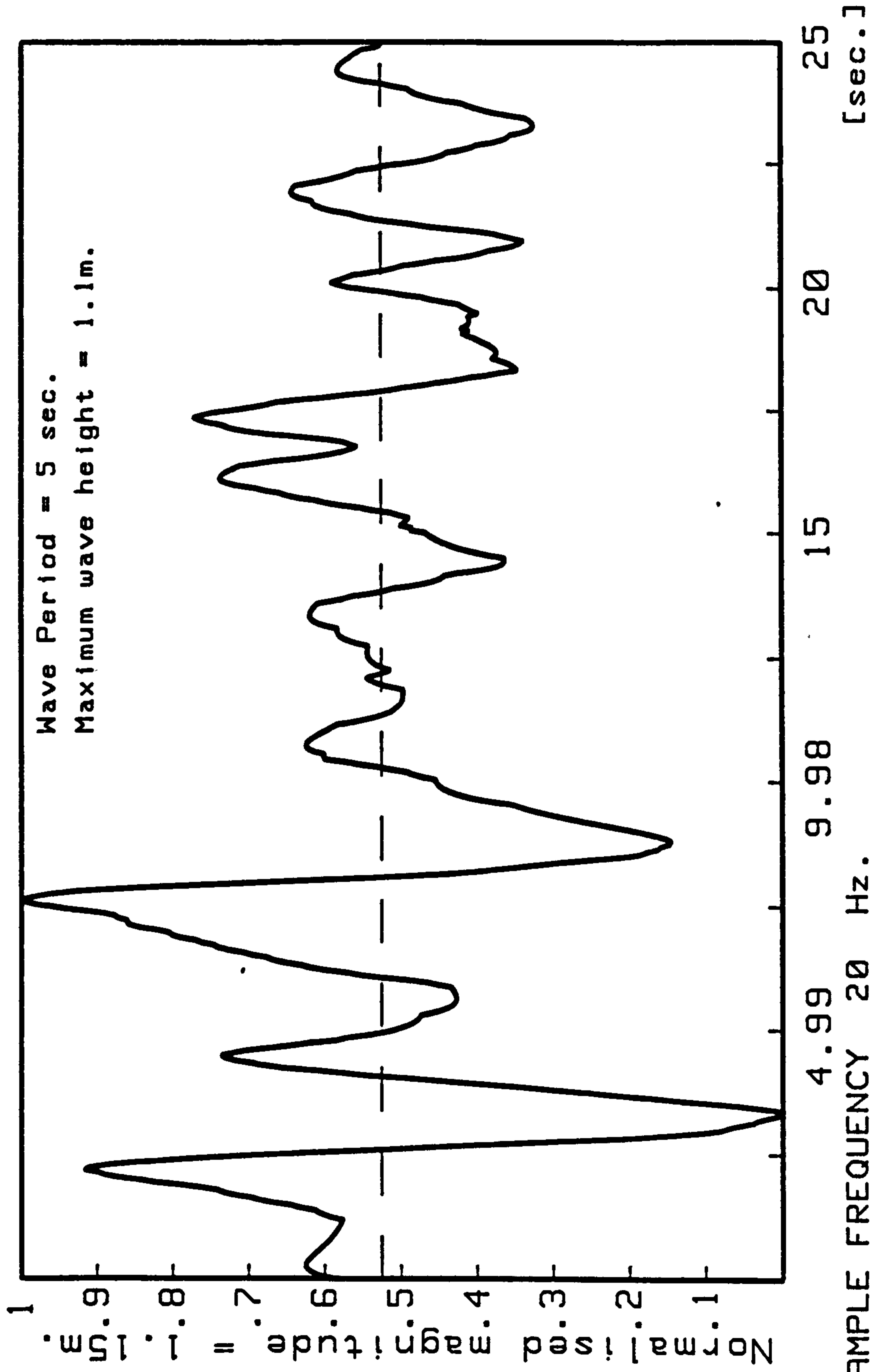


FIG 3.4 TIME DOMAIN SIGNAL WITH UNDERLYING TREND

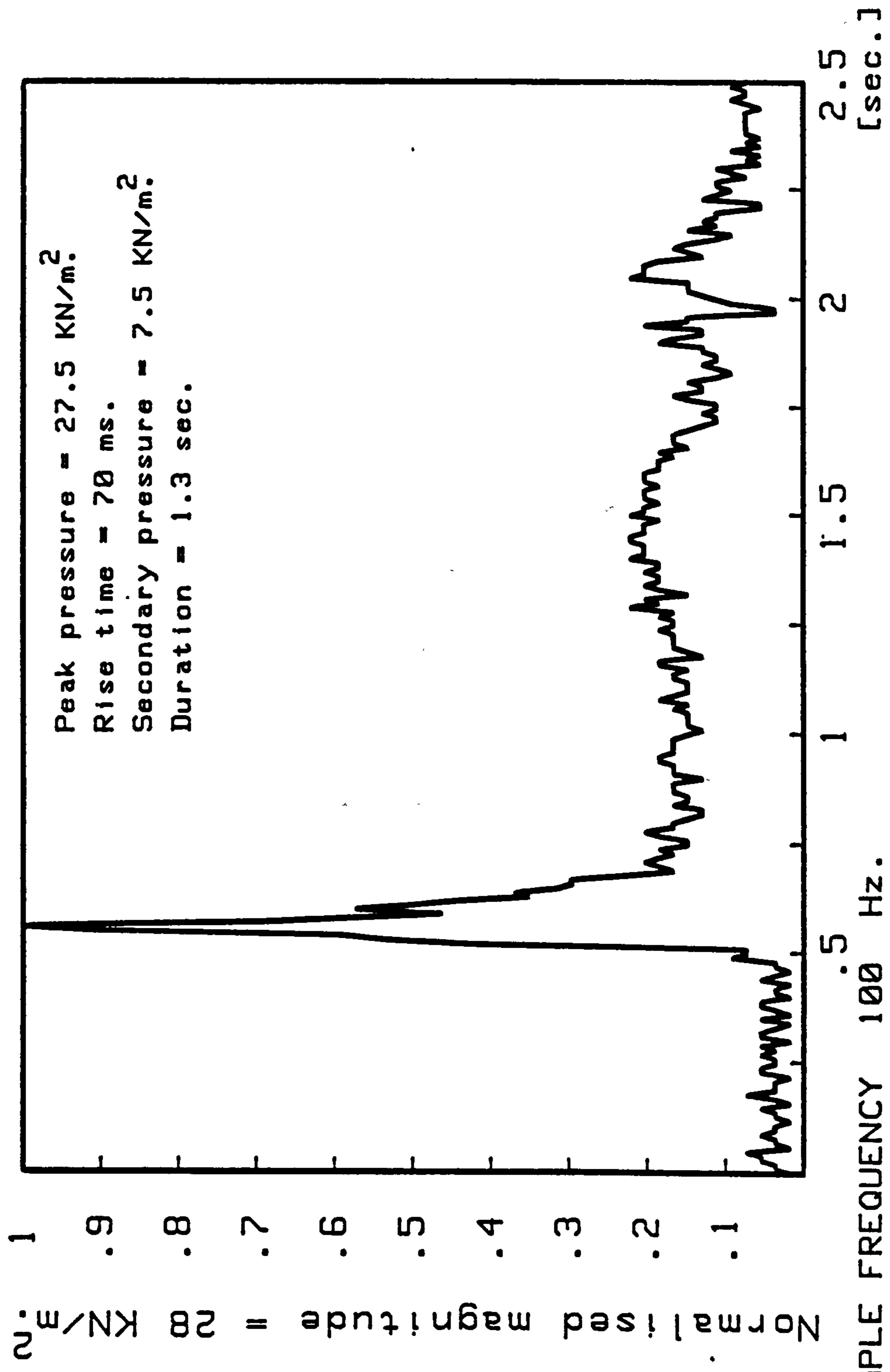


3.98 7.96 11.9 15.9 19.9
 [sec.]
 SAMPLE FREQUENCY 10 Hz.
 SAMPLE LENGTH 19.9 sec.

FIG 3.5 TIME DOMAIN SIGNAL WITH TREND (shown in FIG 3.4) REMOVED



SAMPLE FREQUENCY 20 Hz.
 SAMPLE LENGTH 24.95 sec.
 FIG 3.6 WAVEFORM SAMPLE FOR CHARACTERISTIC MEASUREMENT



SAMPLE FREQUENCY 100 Hz.
 SAMPLE LENGTH 2.5 sec.

FIG 3.7 IMPACT AND SECONDARY PRESSURE CHARACTERISTICS
 AS MEASURED ON SEAWALL

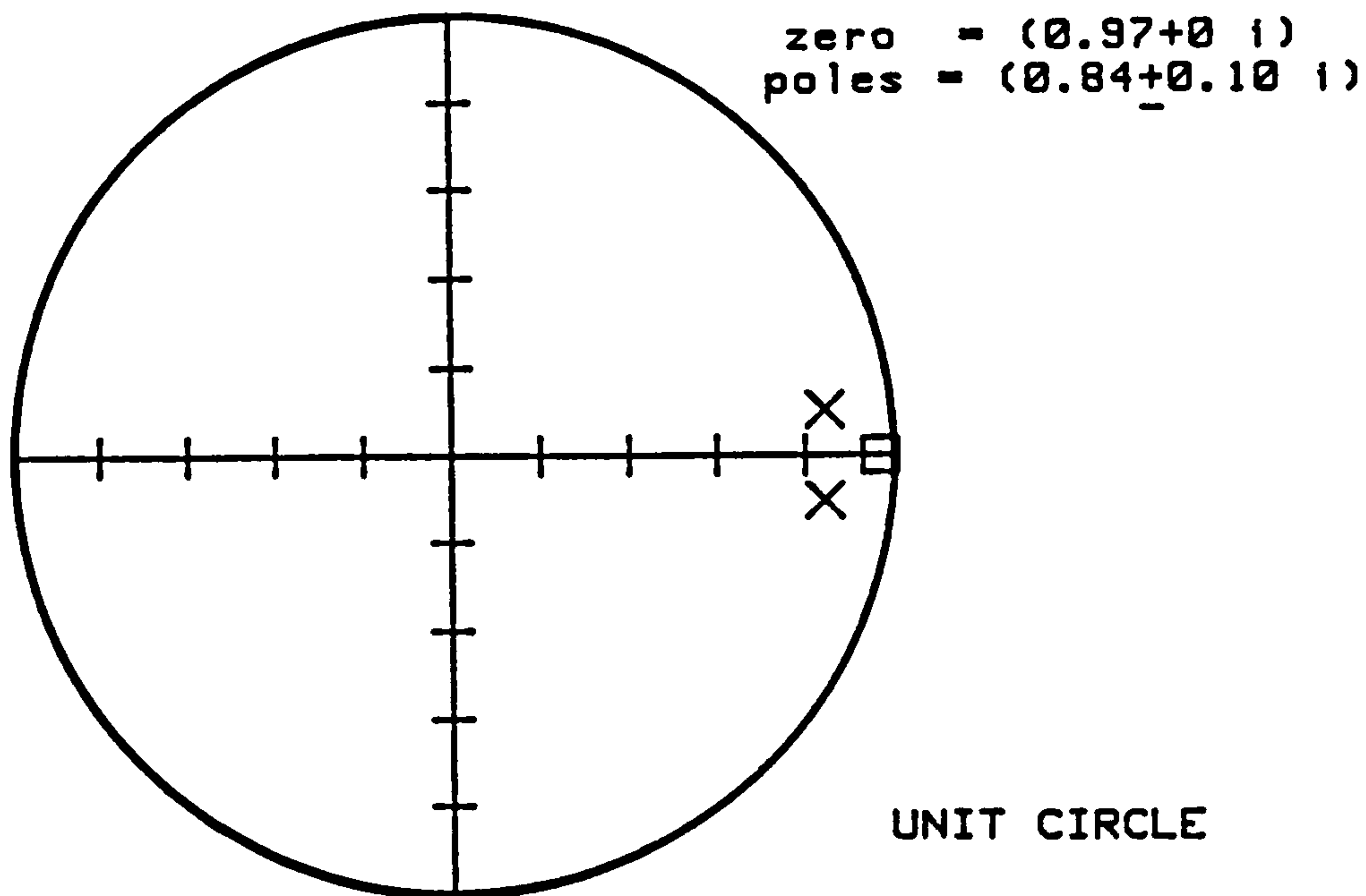
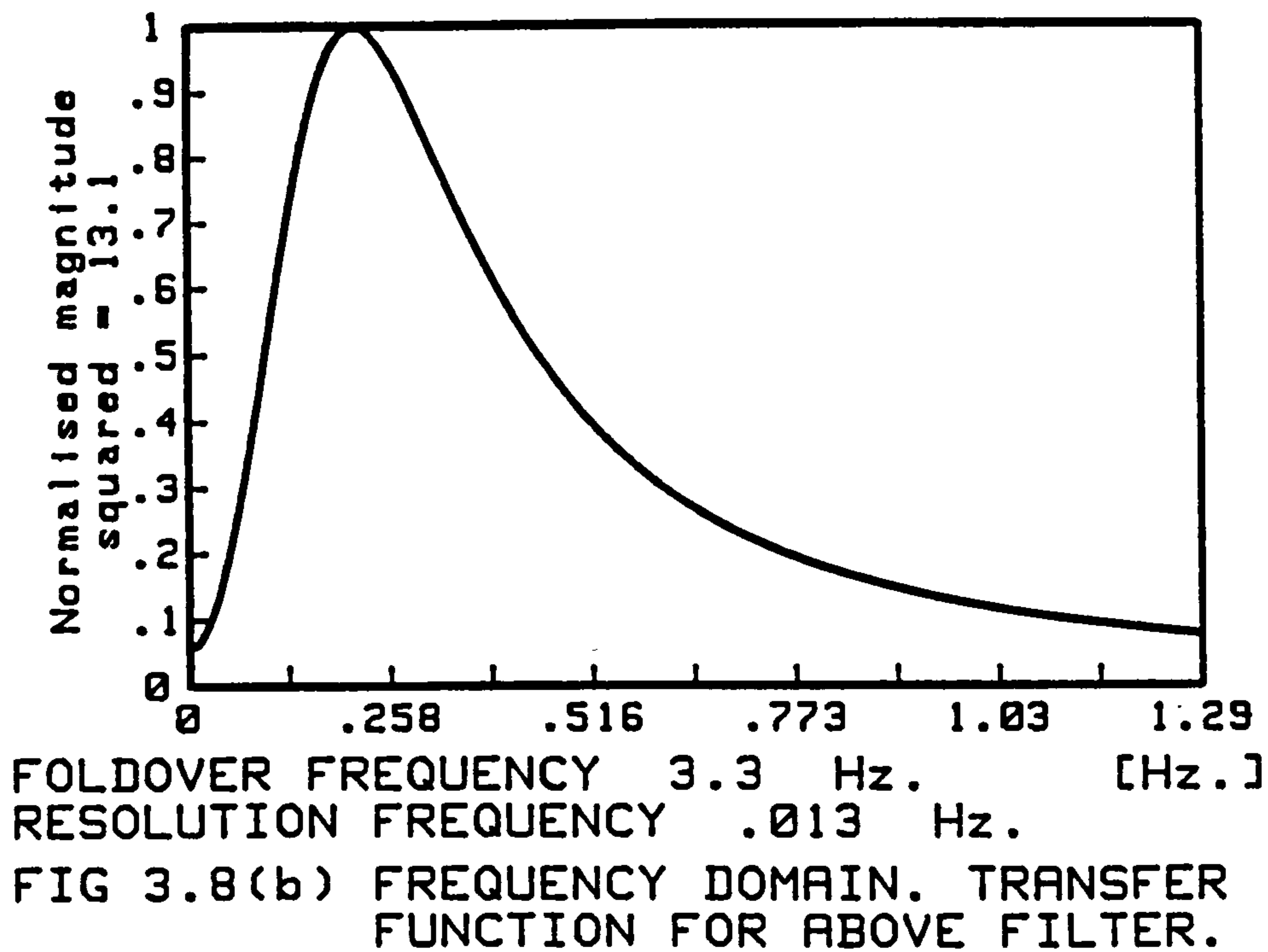


FIG 3.8(a) POLES AND ZEROS FOR FILTER A.1.0



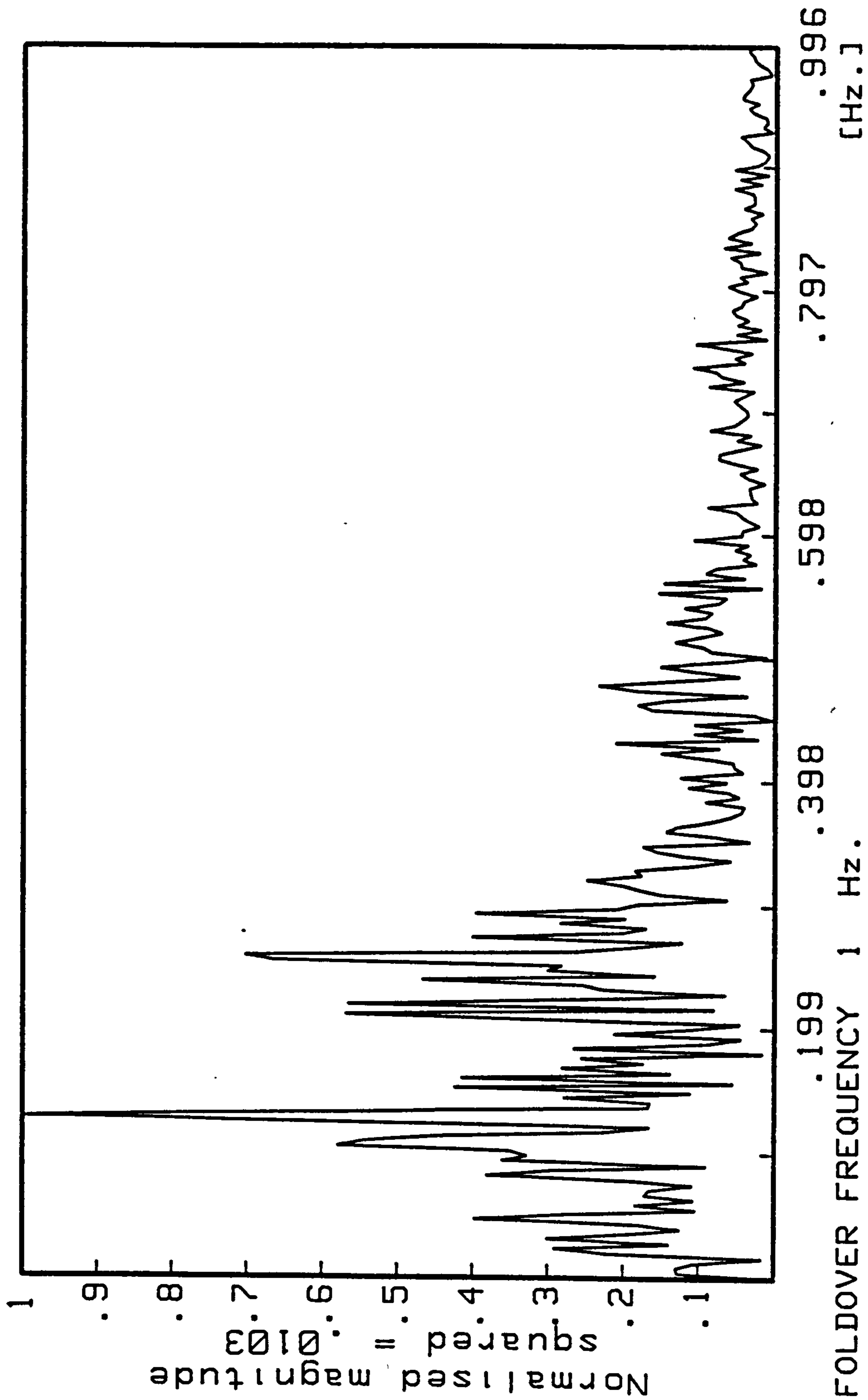
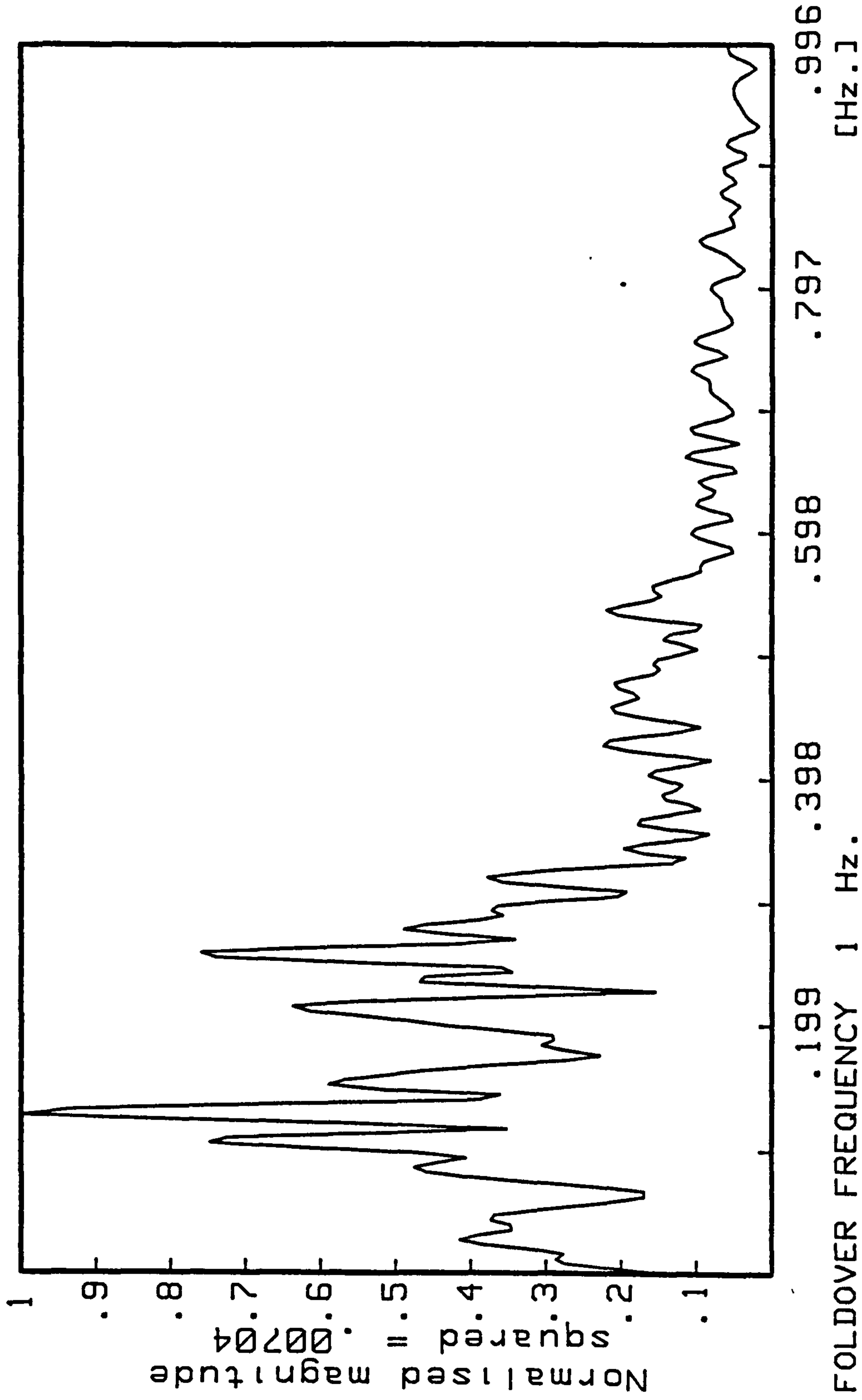


FIG 3.9 FREQUENCY DOMAIN. SINGLE SEGMENT WITH ZERO PADDING
 DATA FROM BEACH TRANSDUCER Sch.
 10th December 1982 (See SITE NOTES 4.4)



FOLDOVER FREQUENCY 1 Hz.
 RESOLUTION FREQUENCY .00391 Hz.

FIG 3.10 FREQUENCY DOMAIN. THREE SEGMENTS WITH NO OVERLAP
 DATA as in FIG 3.9

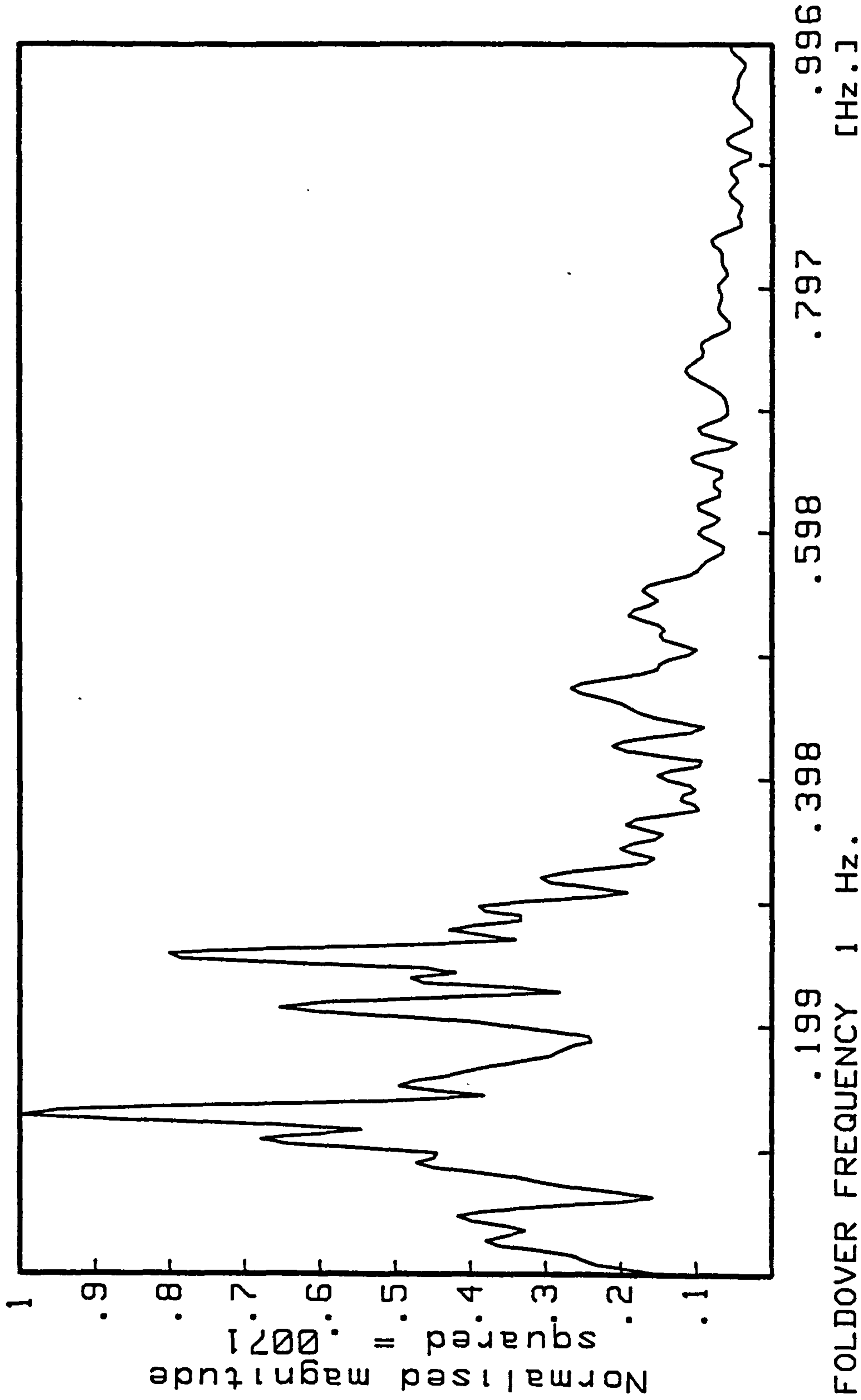
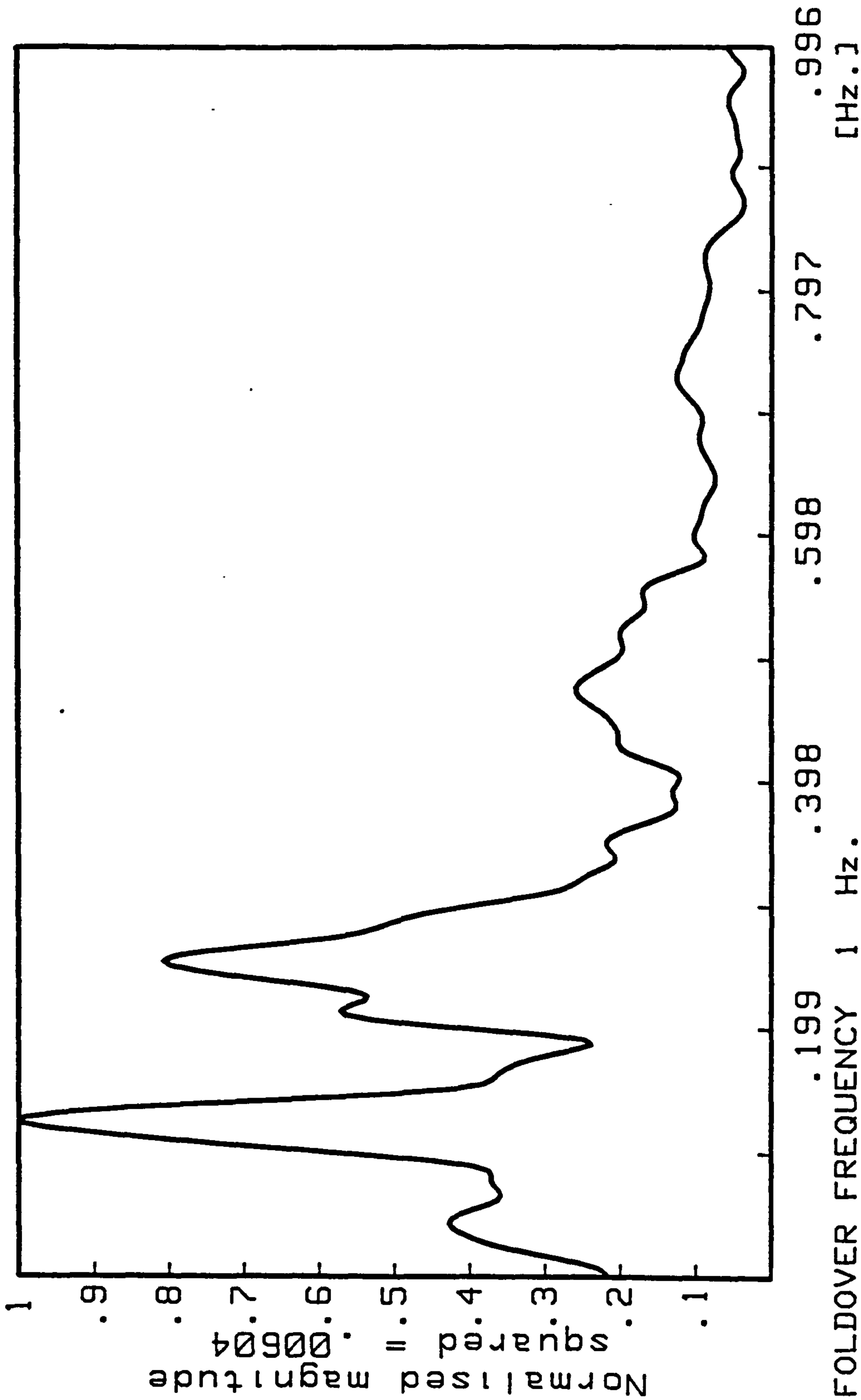


FIG 3.11 FREQUENCY DOMAIN. FIVE SEGMENTS WITH OVERLAP
DATA as in FIG 3.9



FOLDOVER FREQUENCY 1 Hz.
 RESOLUTION FREQUENCY .00391 Hz.

FIG 3.12 FREQUENCY DOMAIN SPECTRUM. SEGMENTING AND WINDOWING
 DATA as in FIG 3.9

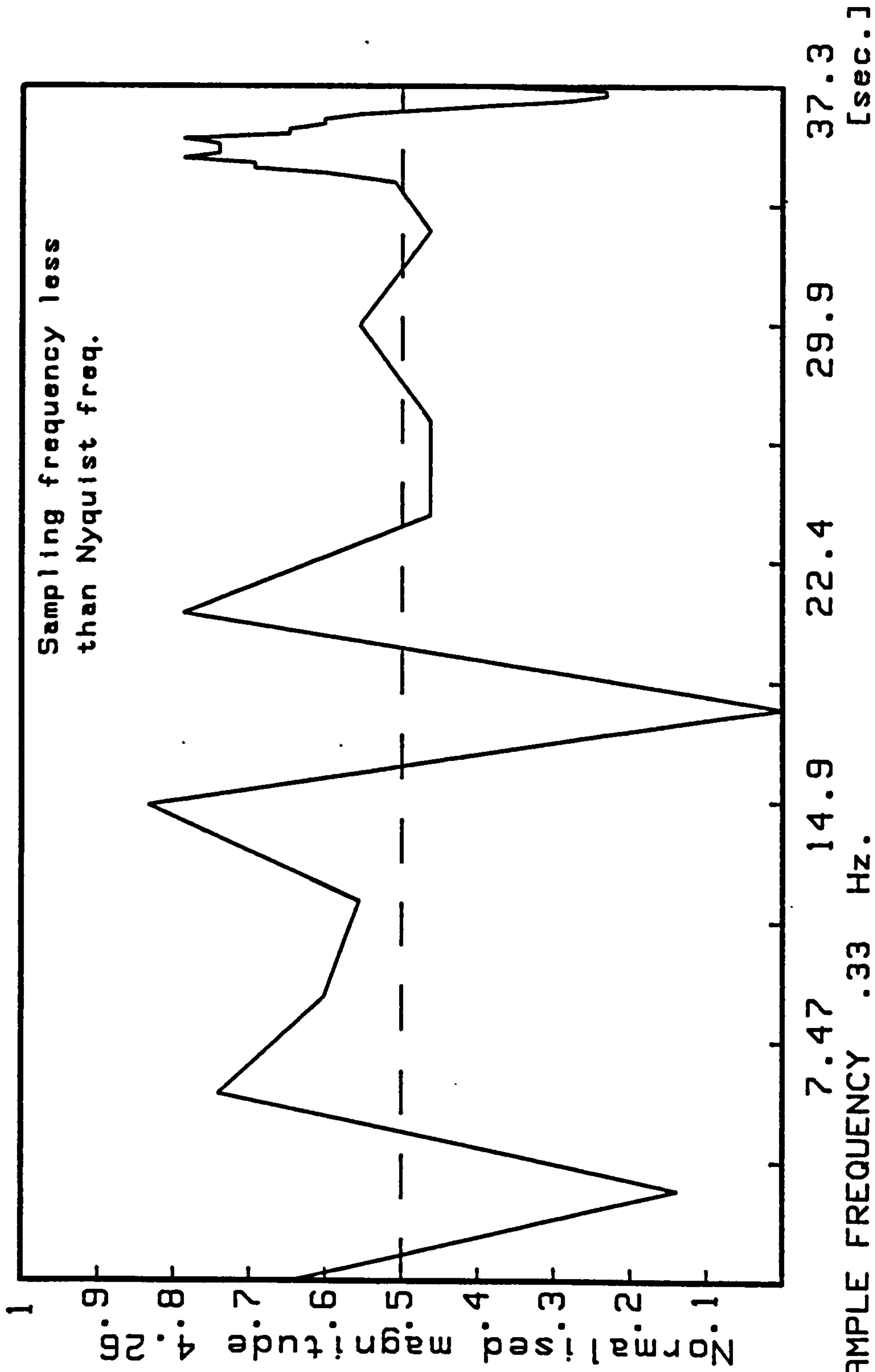
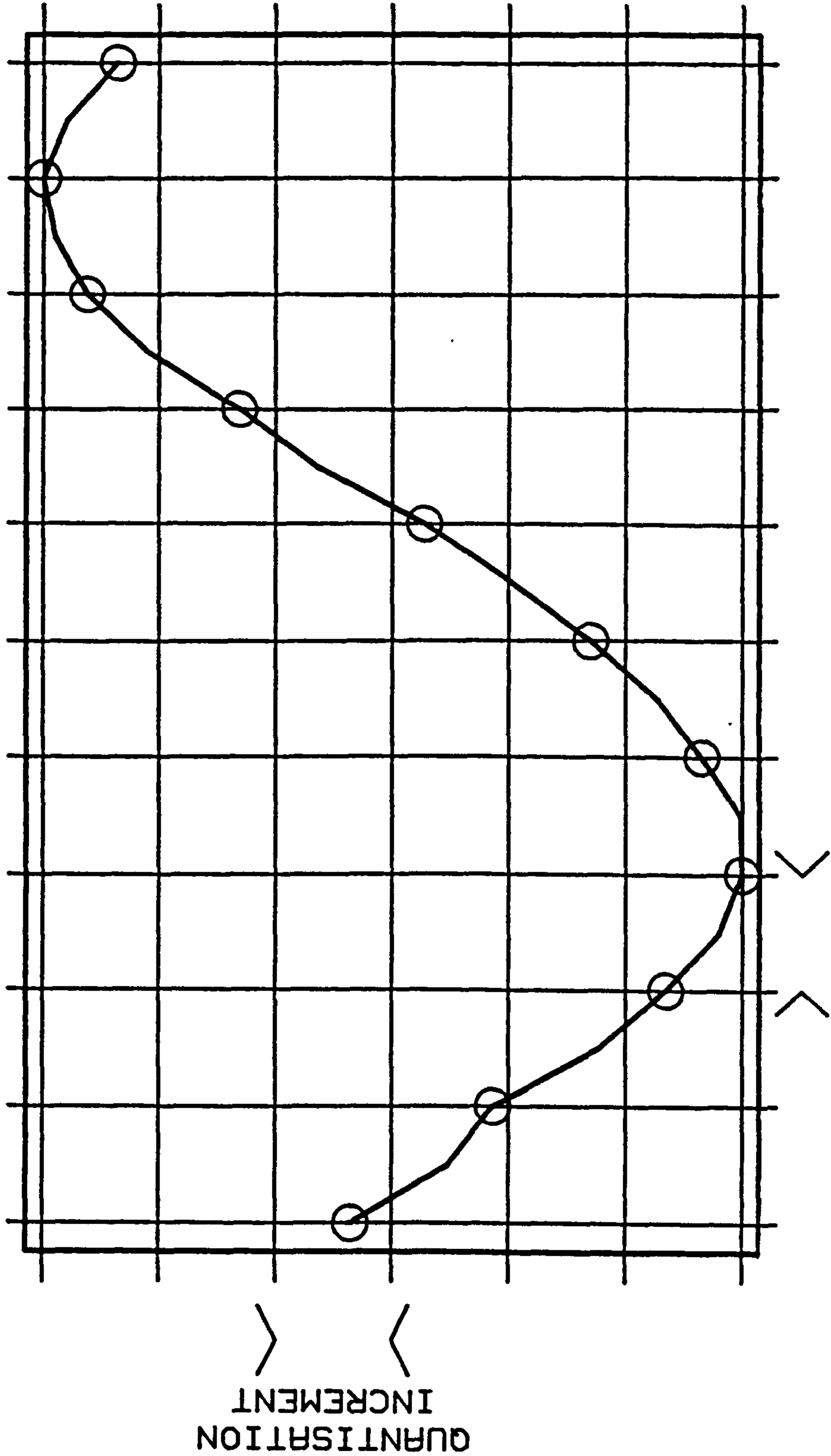


FIG 3.13 ERRORS DUE TO ALIASING (as in FIG 3.3)



TIME INCREMENT
 FIG 3.14 ERROR DUE TO QUANTISATION

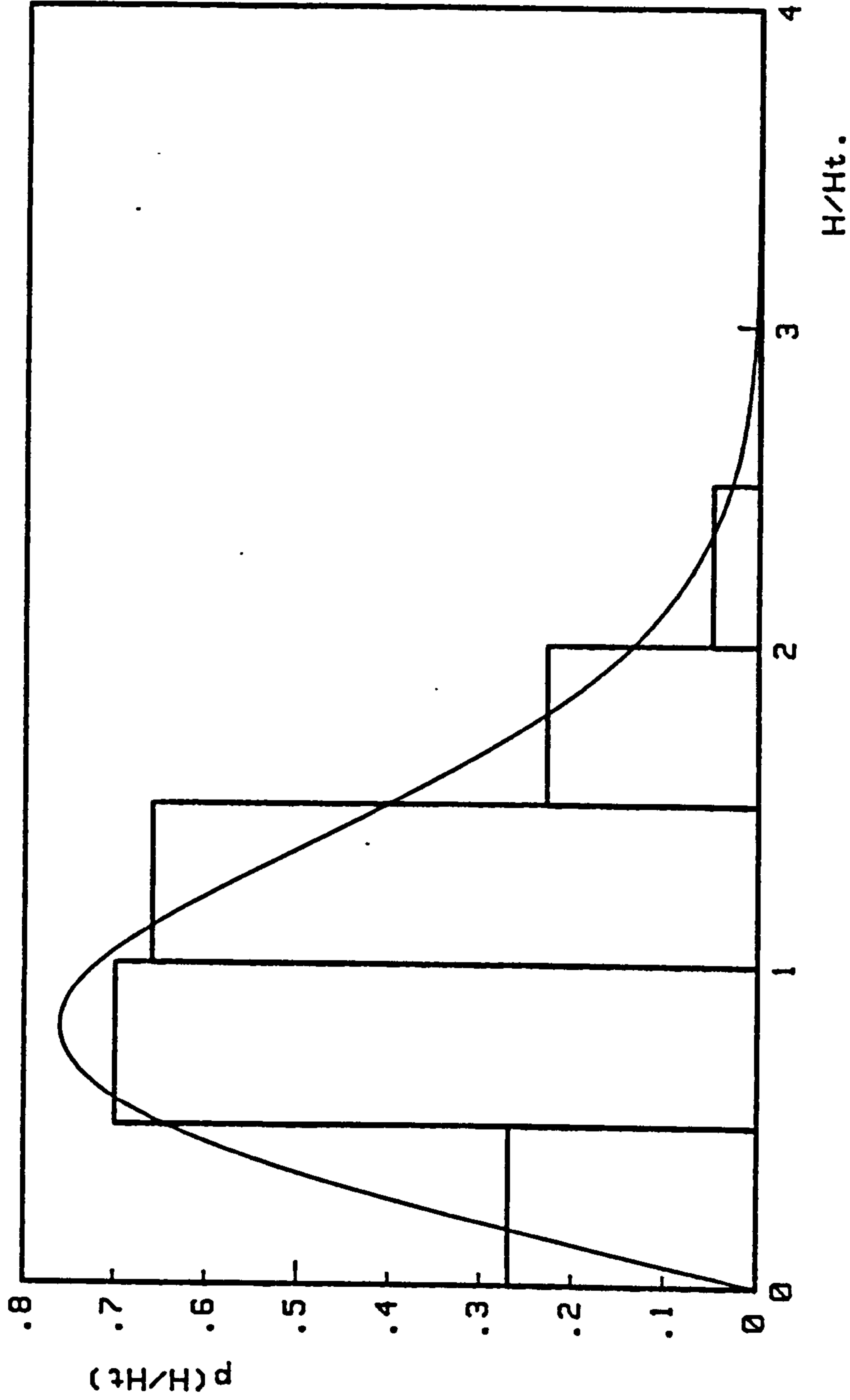


FIG 3.15 AN EXAMPLE OF KURTOSIS AND SKEWNESS FOR AN AMPLITUDE DISTRIBUTION OF WAVEHEIGHT

No. of Observations	No. of Runs for the given Confidence Limits			
	1	5	95	99
N				
5	9	8	3	2
6	11	10	3	2
7	12	11	4	3
8	13	12	5	4
9	15	13	6	4
10	16	15	6	5
11	17	16	7	6
12	18	17	8	7
13	20	18	9	7
14	21	19	10	8
15	22	20	11	9
16	23	22	11	10
18	26	24	13	11
20	28	26	15	13
25	34	32	19	17
30	40	37	24	21
35	46	43	28	25
40	51	48	33	30
50	63	59	42	38
60	74	70	51	47
70	85	81	60	56
80	96	91	70	65
90	107	102	79	74
100	117	113	88	84

TABLE 3.1 LOWER AND UPPER BOUND VALUES IN RUNS TEST

CHAPTER FOUR

WAVE THEORIES. TIME SERIES ANALYSIS

4.1 INTRODUCTION

In the study of fixed structures, the information from experimental data is measured and processed. The type of data sought after covers information from the sea and information from the wall. The data input is of a random nature which requires close examination of selected parts. The emphasis lies in obtaining a general representation in terms of distribution and also in accentuating peak values. The object of the work is to use the significant values obtained to overcome empirical processes used in the design of sea defences. The detailed information obtained out of the numerical data has shown the presence of contributing factors to the quantitative data required for design purposes. For data collection being based on analogue techniques, transferring of data on paper chart recorders was terminated due to the extensive use of paper involved.

The standardisation of the data reduction was applied in a number of stages. In the first case, the wave recordings from an array of measuring devices were processed to detect the velocity distribution and varying direction of the wave. These values are to be used in assessing the forces normal to the seawall. The condition of the recording for reaching these results is to be of a minimum noise quality, or suitably reduced. In the next stage, the record was examined for the number of waves per sample and also for the detection of the highest crest and lowest trough. Information like the significant wave height was evaluated from physical data. The listing of consecutive measurements from trough to crest elevations, and later rearranging them in ascending order was avoided. This

process was tried and found to be more tedious than by applying the method known as Rayleigh's method.

The assessment of significant wave height and period form an overall description of the random sea. Further information of interest includes the establishment of a mean water level as an indication of the tidal level variations at the time of the recording. Details of the surface elevation are also obtained, and from this a direct relationship with the relevant theory can be established. The approach to this section is to specify as accurately as possible the parameters connected to the measured profile used to describe the theoretical equivalent.

The types of waves of greatest interest are those waves which are approaching the breaking phase. This appears at different times of the development of the breaking wave. The related parameters become the prime objective of identifying with these waves. The extent of breaking restricted by the limiting height values becomes the main measurement required to relate directly to all pressure measurements on the wall. Therefore, after describing the actual state of the sea, the more intricate breaking wave situation becomes the main focal point of this research.

The importance given to breaking waves follows from their contribution to the forces on the seawall. The formation of a jet at the tip of the crest gives rise to that high velocity region. This high speed particle movement, together with high acceleration rates generates sharp high pressures when they impinge a fixed vertical

boundary. These pressures cause the impact, assuming that the approach momentum is reduced to zero values. The priority given to this impact pressure measurement is evened out by the secondary pressure detection. This pressure is a result of the mass of water approaching the wall after impact. The result indicates a hydrostatic type of pressure that acts over a prolonged time interval. This pressure constitutes an important aspect of loading to be considered in the design of the wall.

Of the inherent parameters detected in an irregular sea state, is the presence of local waves together with longer period waves. The interaction of these different wave types cause a wave grouping effect. From this wave grouping, the group velocity is detected as a basis of energy measurement found in the waves.

4.2 WAVE THEORIES

In the measurement of surface waves, an understanding of their hydrodynamics cannot be appreciated without a review of the relevant theories. It is not intended to reproduce these theories in detail but to reinstate their assumptions, terms of reference and results.

4.2.1 Assumptions And Frame Of Reference

For the development of wave theories, the accent on simplicity is achieved by assuming a two dimensional field. The justification of this assumption is carried through the study of waves with long crested dimensions (See Plate XVII). This means that in the plane normal to the cross-section of the wave profile the variations of the parameters are assumed constant.

In this field, the fluid motion is described by the velocity potential ϕ , and stream function ψ . They are functions of spatial components and of time. The spatial components represent fluid particles (namely water) in Cartesian coordinates within defined boundaries. The basic term associated to the wave motion and equations of motion are built on a specific reference frame.

The reference frame is based on a field coordinate system (x,y,z) of which the direction of z into the longitudinal section of the wave is reduced to a unit value. The standard origin is taken at the mean water level just below a crest. The main positive directions are for x along the direction of propagation of the

waves and for y away from the level of the seabed. The free surface deviation is a function of position x and time t , and is representative of the fluid particles relative to this system (See Fig. 4.1).

The simplified approach extends the fluid assumptions to being homogenous, irrotational and incompressible. As an irrotational fluid, the vorticity and eddy currents generated through turbulence are ignored. The incompressibility of the fluid is maintained with a phase velocity that lies well within the limit of 300 ms^{-1} (the speed of sound in clear water is 1450 ms^{-1}). One further practical assumption is to eliminate the temporal variations as an independent function and restrict variations in the spatial sense only. This is done by modifying the reference frame to move with the phase velocity or celerity, c in the positive x -direction. The effect of this transformation is to modify the parameters dependent on x to their equivalent based on the celerity. For example x becomes x' such that,

$$x' = x - ct \tag{4.1}$$

also,

$$\phi' = \phi - xc \tag{4.2}$$

4.2.2 Equations Of Motion

The velocity potential and stream function satisfy Laplace's equation independently. The simple solution excludes the analysis of complex variables, thus reducing the equations of motion to be dependent

on velocity potential only. Laplace's equation is given as,

$$\frac{\delta^2\phi}{\delta x^2} + \frac{\delta^2\phi}{\delta y^2} = 0 \quad (4.3)$$

The body of water enclosed in a region is also governed by its boundary conditions. The boundary conditions fall in the category of either kinematic or dynamic. They are primarily expressed at the free surface boundary and the fixed boundary of the seabed. Other boundary limitations to contain the region in a closed area will be discussed in a later chapter on numerical analysis (See Chapter 5).

The kinematic condition states that the velocity of the particles normal to the free surface is equivalent to the velocity of the surface in that direction. This implies that the surface moves in the same regime as the particles making it up. The condition is represented by the equation,

$$\frac{\delta\eta}{\delta t} + \frac{\delta\phi}{\delta x} \cdot \frac{\delta\eta}{\delta x} - \frac{\delta\phi}{\delta y} = 0 \quad \text{at } y = \eta \quad (4.4)$$

The dynamic condition at the free surface is pressure related. For an uncontaminated surface, the pressure at the free surface is due to the variations in the free surface profile and the velocity components of the particles. The pressure at this level is equal to the pressure at the interface of the air to the water layers in a form of Bernouilli's equation. The dynamic boundary condition states that,

$$\frac{\delta\phi}{\delta t} + \frac{1}{2} \left[\left(\frac{\delta\phi}{\delta x} \right)^2 + \left(\frac{\delta\phi}{\delta y} \right)^2 \right] + g\eta = \frac{p_s}{\rho} \quad \text{at } y = -d \quad (4.5)$$

where ρ is the density of the fluid

d is the water depth of the still water level

The dynamic boundary condition at the fixed boundary states that the velocity normal to the boundary is zero,

$$\frac{\delta\phi}{\delta y} = 0 \quad \text{at } y = -d \quad (4.6)$$

The combination of these relationships subject to their respective limitations resolve into the various theories that waves are likely to follow. The theory development covers aspects of application such as the generation of waveform from linear to non-linear phases. The boundary conditions provide the limitations on the simplified theories, which in turn produce unacceptable deviations between theory and real physical observation. This results in the introduction of more involved theories – which necessitates a complexity factor on the mathematical evaluation of the parameters. This observation is made more complex by the requisite of periodicity present from the outset. The trade off for accuracy is therefore, complexity. This determining parallel comes into force when assessing the degree of accuracy required in the estimation of the design parameters. This depends on the stage in which the designed project is in force, from an initial to a final completion stage. The theory which qualifies for use, depends on the conditions the wave motion is subjected to in the area under investigation.

4.2.3 Airy Theory

This is the theory of small amplitude waves and its linearity is maintained with a wave height, H that is of a smaller order to the wavelength, L and water depth, d . Consequently, the free surface

variations with position along the x-axis are negligible. The boundary conditions at the free surface are therefore reduced to relationships at $y = 0$ of :-

$$\frac{\delta\eta}{\delta t} - \frac{\delta\phi}{\delta y} = 0 \quad (4.7)$$

$$g\eta + \frac{\delta\phi}{\delta t} = 0 \quad (4.8)$$

Equations (4.7) and (4.8) combine to give the independent equations:-

$$\frac{1}{g} \frac{\delta^2\phi}{\delta t^2} + \frac{\delta\phi}{\delta y} = 0 \quad (4.9)$$

$$\eta = - \frac{1}{g} \frac{\delta\phi}{\delta t} \quad \text{evaluated at } y = 0 \quad (4.10)$$

What is left, now, is to consider the periodic nature of the waves and deduce the relationship governing ϕ in terms of its known components of wave characteristics. This technique was attributed to Airy and involves the separation of ϕ into two independent variables together with the use of the moving reference frame mentioned earlier.

$$\text{Let } \phi' = Y(y) \cdot X(x) \quad (4.11)$$

Thus, Laplace's equation becomes,

$$X^2 \cdot \frac{\delta^2\phi}{\delta y^2} (Y) + Y^2 \cdot \frac{\delta^2\phi}{\delta x'^2} (X) = 0 \quad (4.12)$$

But, as Y is independent of X , equation (4.12) implies,

$$\frac{1}{Y^2} \cdot \frac{\delta^2 Y}{\delta y^2} = \frac{-1}{X^2} \cdot \frac{\delta^2 X}{\delta x'^2} = k^2, \text{ a constant} \quad (4.13)$$

forming two independent differential equations:-

$$\frac{\delta^2 Y}{\delta y^2} - k^2 Y = 0 \quad (4.14)$$

$$\frac{\delta^2 X}{\delta x^2} + k^2 X = 0 \quad (4.15)$$

Mathematically, the general solution to the equation (4.15) is periodic while that to equation (4.14) is of a hyperbolic nature. Thus:-

$$Y = A \cosh ky + B \sinh ky \quad (4.16)$$

$$X = C \cos k(x-ct) + D \sin k(x-ct) \quad (4.17)$$

By applying the boundary conditions and the origin at $t = 0$ above a crest, then the four constants of integration in equation (4.16) and equation (4.17) are solved.

For equation (4.10),

$$\begin{aligned} \frac{\delta \phi}{\delta t} &= X \frac{\delta Y}{\delta t} + Y \frac{\delta X}{\delta t} \\ &= Y \frac{\delta X}{\delta t} \end{aligned} \quad (4.18)$$

as Y is independent of the time variable therefore equation (4.10) becomes,

$$\eta = -\frac{Y}{g} \cdot \frac{\delta X}{\delta t} \quad \text{at } y = 0 \quad (4.19)$$

by substituting for X, Y from equations (4.16) and (4.17) we get,

$$\eta = -A [Ckc \sin k(x-ct) - Dkc \cos k(x-ct)] \quad (4.20)$$

However, η is represented as a function of cosine when considering the origin of the waveform. This implies that $C = 0$. By the

fixed boundary condition given by equation (4.6),

$$Ak \sinh kd - Bk \cosh kd = 0 \quad (4.21)$$

Then,

$$B = A \tanh kd \quad (4.22)$$

Substituting $\eta = H/2$ at $x = 0$ and $t = 0$ in equation (4.20) gives,

$$A \cdot D = \frac{gH}{2kc}$$

$$\text{or, } D = \frac{gH}{2Akc} \quad (4.23)$$

Substituting equations (4.22) and (4.23) into equation (4.11) gives,

$$\begin{aligned} \phi &= Y(y) \cdot X(x-ct) \\ &= \frac{gH}{2kc} [\cosh ky + \sinh ky \tanh kd] \sin k(x-ct) \end{aligned}$$

$$\text{or, } \phi = \frac{Hg}{2kc} \frac{\cosh k(y+d)}{\cosh kd} \sin k(x-ct) \quad (4.24)$$

Since ϕ is periodic in the x -direction, it repeats itself after every wavelength, that is, $L = 2\pi/k$, and every wave period $T = 2\pi/kc$. From this statement, two other terms associated with wave motion are k , the wave number and ω , the wave angular frequency, where, $\omega = kc$.

By substitution of equation (4.24) in the identity (4.9) and applying the appropriate reduction, we get,

$$c^2 = \frac{g}{k} \tanh kd \quad (4.25)$$

This is known as the linear dispersion relationship which effectively relates the celerity to the wavelength and depth of water.

Now let,

$$\begin{aligned}\theta &= k(x-ct) \\ &= kx - \omega t\end{aligned}$$

where θ is the phase angle, (4.26)

equation (4.24) reduces to,

$$\phi = \frac{H\pi}{Tk} \frac{\cosh k(y+d)}{\sinh kd} \sin \theta \quad (4.27)$$

By performing the appropriate partial differentiation, the velocity components of the water particles reduce to:-

$$u = \frac{\delta\phi}{\delta x} = \frac{\pi H}{T} \frac{\cosh k(y+d)}{\sinh kd} \cos \theta \quad (4.28)$$

$$v = \frac{\delta\phi}{\delta y} = \frac{\pi H}{T} \frac{\sinh k(y+d)}{\cosh kd} \sin \theta \quad (4.29)$$

While the acceleration components for the particles are:-

$$\dot{u} = \frac{\delta u}{\delta t} = \frac{2\pi^2 H}{T^2} \frac{\cosh k(y+d)}{\sinh kd} \sin \theta \quad (4.30)$$

$$\dot{v} = \frac{\delta v}{\delta t} = \frac{-2\pi^2 H}{T^2} \frac{\sinh k(y+d)}{\sinh kd} \cos \theta \quad (4.31)$$

The horizontal particle displacement, ξ is given as,

$$\xi = \int_0^t u \, dt = \frac{-H}{2} \frac{\cosh k(y+d)}{\sinh kd} \sin \theta \quad (4.32)$$

while the vertical particle displacement, ζ is given as,

$$\zeta = \int_0^t v dt = \frac{H}{2} \frac{\sinh k(y+d)}{\sinh kd} \cos \theta \quad (4.33)$$

The solution of equation (4.33) follows from the initial conditions:-

$$\zeta = H/2 \text{ at } y = 0 \text{ and } \zeta = 0 \text{ at } y = -d, \text{ all at } x = 0 \text{ and } t = 0.$$

The pressure variation in the body of water is derived from Bernouilli's equation (4.5) by neglecting all the second order terms to satisfy the linear approximation set by this theory. For values above atmospheric pressure, P_s becomes,

$$P_s = -\rho gy - \rho \cdot \frac{\delta\phi}{\delta t} \quad (4.34)$$

Substituting for ϕ from equation (4.27), we get,

$$P_s = -\rho gy + \frac{\rho g H}{2} \frac{\cosh k(y+d)}{\cosh kd} \cos \theta \quad (4.35)$$

The set of equations from (4.27) to (4.35) make up the linear theory of waves. Further particulars of the theory are from the different categories of waves encountered in deep and shallow waters. If the hyperbolic functions are approximated at the limits of $kd < \pi/10$ and $kd > \pi$ then, governed by these corresponding limits are wave conditions of:-

SHALLOW WATER	with	$\sinh kd = \tanh kd = kd$
$(kd < \pi/10)$		$\cosh kd = 1$

DEEP WATER	with	$\sinh kd = \cosh kd = 0.5e^{kd}$
$(kd > \pi)$		$\tanh kd = 1$

With these approximations further simplifications may be made to the derived equations, in particular to the shape of the water particle orbits. It has been seen that the orbits vary from circular for deep water to elliptical for shallow water waves.

The range in between these two sets of waves is called the intermediate range which does not have hard definite limits.

Deep water waves express an equation of interest to a comparative study in,

$$L_o = \frac{gT^2}{2\pi} \quad (4.36)$$

by taking the approximate value of large kd . For this range of waves, the particle velocities are reduced to exponential curves decreasing in value with depth. In the limit, as the depth tends to half the wavelength, the particle velocities tend to negligible quantities.

The linear equation for total energy per unit crest width is,

$$E = \frac{\rho g H^2 L}{8} \quad (4.37)$$

This is made up of kinetic energy and potential energy.

Consider the region bounded by wave profile and the seabed over one wavelength. The value of kinetic energy is given by,

$$\int_0^L \int_{-d}^{\eta} \frac{\frac{1}{2}\rho(u^2+v^2)}{L} dy dx \quad (4.38)$$

where the value of dy is reduced to a unit quantity along the x -axis.

As the potential energy for the undisturbed fluid is not equal to zero, for a unit horizontal area, the potential energy is given as,

$$\begin{aligned}
 P &= \int_0^L \int_{-d}^{\eta} \frac{\rho g y \, dy}{L} - \int_{-d}^0 \rho g y \, dy \\
 &= \int_0^L \int_0^{\eta} \frac{\rho g y \, dy}{L} = \frac{1}{2} \rho g \bar{\eta}^2 \quad (4.39)
 \end{aligned}$$

While the kinetic energy gives the value of the dynamic pressure, the potential energy is a measure of the mean square of the amplitude.

The mean power transmitted per unit crest of wave is given in terms of the group velocity, C_G , that is,

$$P = C_G \frac{\rho g H^2}{8} \quad (4.40)$$

4.2.4 Stokes Theory

When the linearity assumption ceases to exist, Airy's theory has to be substituted by more advanced theories. Non-linearity in wave theory resulting in the setting up of Stokes theory was first applied by Stokes⁽⁸⁾ (1847, 1880) himself. Further contributions were by De⁽⁹⁾ (1955), Borgman and Chappellear⁽⁹⁵⁾ (1958) and Tsuchiya and Yamaguchi⁽⁹⁶⁾ (1972). More recent trends into computational analysis have been tackled by Schwartz⁽¹¹⁾ alone in 1974, and later together with Vanden Broek⁽⁹⁷⁾ in 1979.

Stoke's theory covers waves with finite wave steepness or wave height to wavelength ratio. However, there is still a constraint on the steepness to be low in magnitude. This condition was pointed out by Peregrine ⁽⁹⁸⁾(1972), who says that the Stokes wave expansion method is valid in the limits of $d/L < 0.16$ and $H/L \ll 1$.

The theory involves the expansion of the velocity potential at the free surface about the still water level. The expansion is in the form of an infinite series of non-linear terms. The theory is limited by the water depth reaching the shallow limit. In this case, the wave profile in equation form is rendered valid by including more terms in the expansion. This would necessitate a higher order of Stokes theory to be considered.

When it comes to select the appropriate theory for the shallow water waves, the Cnoidal theory proves superior to the Stokes theory as noted in a comparison of the two by De ⁽⁹⁾(1955).

4.2.4.1 The Expansion Method

The theory is subjected to the same basic assumptions, reference frame and boundary conditions as given in section 4.1.1. The velocity potential and all related surface properties are expanded by an infinite series,

$$\phi = e\phi_1 + e^2\phi_2 + e^3\phi_3 + \dots \quad (4.41)$$

where e is called the perturbation parameter. The perturbation parameter is dependent on the wave height. This statement satisfies

a condition that, for low wave heights, higher orders of e are ignored, thus reverting to a linear theory. The subscripts in (4.41) determine the order to which the power series may be developed to produce a Stokian theory with an increasing degree of accuracy. This is done by grouping like powers of e after applying the series to Laplace's equation and the boundary conditions.

Thus Laplace's equation (4.3) becomes,

$$\frac{\delta^2 \phi_n}{\delta x^2} + \frac{\delta^2 \phi_n}{\delta y^2} = 0 \quad \text{for } n = 1, 2, 3 \dots \quad (4.42)$$

The boundary condition, (4.6) at $y = -d$ becomes,

$$\frac{\delta \phi_n}{\delta y} = 0 \quad \text{for } n = 1, 2, 3 \dots \quad (4.43)$$

A simplification of the other dynamic and kinematic boundary conditions is to express them as two independent differential equations as suggested by Phillips⁽⁹⁹⁾(1977). This avoids the problem of tackling the product of non-linear terms in ϕ and η both expressed in terms of e . The changes of the boundary conditions at $y = \eta$ are as follows and are written in more compact tensor or vector notation.

Equation (4.5) becomes, as a dynamic equation,

$$\eta = - \frac{1}{g} \frac{\delta \phi}{\delta t} - \frac{1}{2g} \underline{u} \cdot \underline{u} \quad \text{where } \underline{u} = \frac{\delta \phi}{\delta x} + i \frac{\delta \phi}{\delta y} \quad (100) \quad (4.44)$$

Now, by partial differentiation of equation (4.44) with respect to time and space dimension x , we get,

$$\frac{\delta \eta}{\delta t} = - \frac{1}{g} \frac{\delta^2 \phi}{\delta t^2} = - \frac{1}{2g} \frac{\delta u^2}{\delta t} \quad (4.45)$$

$$\frac{\delta\eta}{\delta x} = -\frac{1}{g} \frac{\delta}{\delta x} \left[\frac{\delta\phi}{\delta t} \right] - \frac{1}{2g} \frac{\delta \underline{u}^2}{\delta x} \quad (4.46)$$

Substitution of equations (4.45) and (4.46) into the equation (4.4) gives,

$$\frac{\delta^2\phi}{\delta t^2} + g \frac{\delta\phi}{\delta y} + \frac{1}{2} \frac{\delta \underline{u}^2}{\delta t} + \underline{u} \cdot \nabla \left[\frac{\delta\phi}{\delta t} \right] + \frac{1}{2} \underline{u} \cdot \nabla (\underline{u}^2) = 0 \quad (4.47)$$

where $\nabla () = \frac{\delta}{\delta x} () + \frac{\delta}{\delta y} ()$

$$\text{but } \underline{u} \cdot \nabla \frac{\delta\phi}{\delta t} = \underline{u} \cdot \frac{\delta \underline{u}}{\delta t} = \frac{1}{2} \frac{\delta \underline{u}^2}{\delta t}$$

so, equation (4.47) becomes,

$$\frac{\delta\phi^2}{\delta t^2} + g \frac{\delta\phi}{\delta y} + \frac{\delta \underline{u}^2}{\delta t} + \frac{1}{2} \underline{u} \cdot \nabla (\underline{u}^2) = 0 \quad (4.48)$$

as a kinematic boundary condition.

The two boundary conditions are evaluated at $y = \eta$. A means of reducing them to expressions of $f(y) = 0$ at $y = 0$ is by applying the Taylor series which is given in the form,

$$f(y) + \eta \frac{\delta f}{\delta y} + \frac{\eta^2}{2} \frac{\delta^2 f}{\delta y^2} + \dots = 0 \quad \text{for } y = 0 \quad (4.49)$$

Analysis may proceed to produce solutions for ϕ and η to varying orders of approximations. Summarising the series at $y = 0$ with R to be substituted by any function found in either Laplace's equation or in the boundary conditions is given as,

$$R = R + \eta \frac{\delta\phi}{\delta y} + \dots \quad (4.50)$$

where $\phi = e\phi_1 + e^2\phi_2 + \dots$

$\eta = e\eta_1 + e^2\eta_2 + \dots$

Thus, the first order solution is obtained by comparing single powers of e , giving,

$$\frac{\delta^2\phi_1}{\delta t^2} + g \frac{\delta\phi_1}{\delta y} = 0 \quad (4.51)$$

$$\eta_1 = -\frac{1}{g} \frac{\delta\phi_1}{\delta y} \quad \text{evaluated at } y = 0 \quad (4.52)$$

These solutions bear a direct resemblance to the boundary conditions obtained in Airy's linear solution, and need to be evaluated to work out the second order solution.

The second order solution is then obtained by comparing second powers of e , giving,

$$\frac{\delta^2\phi_2}{\delta t^2} + \eta_1 \frac{\delta^2}{\delta t^2} \frac{\delta\phi_1}{\delta y} + g \frac{\delta\phi_2}{\delta y} + g\eta_1 \frac{\delta^2\phi_1}{\delta y^2} + \frac{\delta}{\delta t} \frac{\delta\phi_1^2}{\delta x} + \frac{\delta}{\delta t} \frac{\delta\phi_1^2}{\delta y} = 0 \quad (4.53)$$

$$\eta_2 g = -\frac{\delta\phi_2}{\delta t} - \eta_1 \frac{\delta^2\phi_1}{\delta t \delta y} - \frac{1}{2} \frac{\delta\phi_1^2}{\delta x} - \frac{1}{2} \frac{\delta\phi_1^2}{\delta y} \quad \text{evaluated at } y = 0 \quad (4.54)$$

Therefore, for,

$$\phi_1 = \frac{\pi H}{kT} \frac{\cosh k(y+d)}{\cosh kd} \sin \theta \quad \text{from equation (4.27)}$$

$$\eta_1 = \frac{H}{2} \cos \theta \quad \text{evaluated at } y = 0 \quad (4.55)$$

These two equations (4.27), (4.55) lead to the solution for the second order Stokes wave theory as:-

$$\phi_2 = \frac{\pi H \cosh k(y+d)}{kT \sinh kd} \sin \theta + \frac{3 \pi H \pi H \cosh 2k(y+d)}{8 kT L \sinh^4 kd} \sin 2\theta \quad (4.56)$$

$$\eta_2 = \frac{H}{2} \cos \theta + \frac{H \pi H \cosh kd}{8 L \sinh^3 kd} [2 + \cosh 2kd \cos 2\theta] \quad (4.57)$$

On the basis of the equation (4.56) for the velocity potential, the velocity and acceleration components of the water particles and their displacements may be derived in equation form. The pressure at any point in the fluid may also be determined. The main point of interest in the equations is that to the terms given by the linear theory, a second term is added. What this second term has in common throughout the equations is that it represents a periodic function with twice the frequency shown in the first term. This has the effect of modifying the sinusoidal waveform found in the linear theory to one with sharper crests and flatter troughs. As a result the mean level of the waveform drops below the half way mark of the Airy theory. Another means of interpreting this change in level is by assessing the area under the curve above the mean level. In this case, the mean level is treated as a variable. The level is adjusted until the area under the curve below the mean is made equal to the previous one. This approach is a form of balancing out the energies in the crest and trough area respectively. The value obtained from this theory is accentuated by the fact that its profile is of a closer representation of the waves as observed by the random sea state.

The limitation of this theory includes fairly shallow water $d/L_0 < 0.07$. Then the solution to Stokes theory of orders higher than 5 is complex⁽¹⁰¹⁾. When a secondary crest appears in some solutions of the Stokian theory, this gives an unrealistic location of a crest in the centre of a trough. More accurate solutions to higher order Stokes' equations have been implemented by Cokelet⁽²⁰⁾ (1977). In cases of low values of depth to wavelength ratio, a non-linear shallow wave theory is more appropriate to fit with experimental results.

A further point of interest is that the linear dispersion relationship for the celerity still holds. However, the particles' orbits are no longer closed. As a result of this behaviour, the second order theory introduces a mass transport or drift velocity component on the particles in the horizontal sense.

4.2.5 Cnoidal Theory

In the shallow water range, when Stokes finite amplitude wave theory begins to become unsatisfactory, other theories with the pre-requisites of a finite height and water depth have to be developed. Following an intuitive theory by Korteweg and de Vries⁽¹⁴⁾ (1895), the Cnoidal theory has since been developed. In this theory, the wave profile is covered in a range from one with an infinite wavelength at one end and the sinusoidal waveform at the other. The first of these is called a solitary wave. Although the theory may be expanded to any number of degrees, it is within its first approximation that it covers quite adequately direct applications to the engineering field.

The development of this theory was introduced by Friedrichs⁽¹⁶⁾(1948) and later outlined by Stoker⁽¹⁰²⁾(1957). When waves propagate in shallow water, a distortion of the surface profile has the effect of concentrating the velocities and accelerations to high values around the crest area. The suggested formulation in the Cnoidal theory accounts for this factor. A comprehensive table of values has been listed by Wiegel and Masch⁽¹⁰³⁾(1961).

The variables associated with the wave profile are non-dimensionalised on the basis that the vertical components are of a smaller magnitude than the horizontal ones. The ratio of these proportions is dependent on the wave depth to wavelength ratio. As a result, the non-dimensionalising is carried out accordingly. Thus Laplace's equations and boundary conditions are weighted by the relevant parameters, such as,

$$\begin{aligned}
 \text{Linear relations} \quad X &= \frac{x'}{l} & S &= \frac{s}{d} & N &= \frac{\eta}{d} \\
 \\
 \text{Velocity relations} \quad U &= \frac{u}{\sqrt{gd}} & V &= \frac{v}{\sqrt{gd}} \cdot \frac{d}{l} \\
 \\
 \text{Pressure relations} \quad P_s &= \frac{\Delta P}{\rho g d} & & & & (4.58)
 \end{aligned}$$

for a fixed reference frame of (x', s) where,

$$\begin{aligned}
 x' &= x - ct & (\text{as in equation 4.1}) \\
 s &= y + d & (4.59)
 \end{aligned}$$

The origin has been shifted to the seabed and is still located below the crest of the wave.

Introducing m as the square of the depth to the wavelength ratio, then Laplace's equation (4.3) is written in its dimensionless form as,

$$m \frac{\delta^2 \phi}{\delta X^2} + \frac{\delta^2 \phi}{\delta S^2} = 0 \quad (4.60)$$

where $m = \left(\frac{d}{1} \right)^2$ and is much lower than unity in value.

The equation which satisfies this relation and the dynamic boundary condition at the seabed is given as,

$$\phi = \cos (m \cdot SD) f(X) \quad (4.61)$$

where D is the differential operator d/dx and f is a function of X determined by the free surface boundary conditions.

This equation when expanded by a lower series, as shown by Fenton⁽¹⁷⁾ (1979), indicates how the velocity potential varies with depth, such that,

$$\phi = \left[1 + m \frac{S^2 D^2}{2} + m^2 \frac{S^4 D^4}{4} + \dots \right] \cdot f(x) \quad (4.62)$$

When dealing with the lowest order of approximations, this governing equation and its boundary conditions reduces to an ordinary differential equation. This is shown by Laitone⁽¹⁵⁾ (1960) and is given as,

$$\frac{\delta^3 F}{\delta X^3} + aF \frac{\delta F}{\delta X} - b \frac{\delta F}{\delta X} = 0 \quad (4.63)$$

Where F is a function of X and a, b are constants.

The solution to this equation is periodic and is given in terms of the Jacobian elliptical function denoted by cn , hence the name

Cnoidal. This function has an argument q and modulus κ . The real period of the function is $4K(\kappa)$, where $K(\kappa)$ is known as the complete elliptical integral of the first kind.

The modulus κ is the basis for the determination of the wave profiles from its design characteristics. Its value ranges from 0 to 1 and those nearer to 1 show greatest interest as they represent shallow water waves. Besides $K(\kappa)$ other dependent functions of κ are highlighted by Abramowitz and Stegun⁽¹⁰⁴⁾(1965) with related tables and graphs. These include $E(\kappa)$ as the complete elliptical integral of the second kind, γ is the ratio of $E(\kappa)$ to $K(\kappa)$ and κ' is represented as,

$$\kappa'^2 = 1 - \kappa^2 \quad (4.64)$$

In turn, the value of κ or κ' is related to the wave characteristics in the form of Ursell's number in either tabular or graphical form.

Ursell's number, at a first approximation is governed by the relationship

$$U = \frac{L^2 H}{d^3} \quad \text{or} \quad \frac{H}{L} \cdot \frac{L^3}{d^3} \quad (4.65)$$

Given the value of the wave height, wavelength or period and water depth, the value of κ^2 and other dependent functions may be estimated from their appropriate table or graph (See Figs. 4.2, 4.3, 4.4).

Once known, the values are used to produce the theoretical wave profile to the first approximation, given by,

$$\eta = cn^2 q - \frac{(\gamma - \kappa'^2)}{\kappa^2} \quad (4.66)$$

where $cn q$ is given in terms of a series or in graphical form,

(See Fig. 4.5), as a function of κ and the phase angle θ which is a function of $K(\kappa)$ in the relation,

$$\theta = K(\kappa)^2 (2x/L - 2t/T) \quad (4.67)$$

4.2.6 Solitary Wave Characteristics

As a limiting case of the Cnoidal theory, the solitary wave is defined as that having an infinite wavelength. It is a wave of translation, by water particle velocity moving only in the direction of propagation. The profile lies above the still water level with a constant waveform maintained during its period of propagation. The profile of the free water surface is given by,

$$\eta = H \operatorname{sech}^2 \sqrt{\frac{3H}{4d}} (x - ct) \quad (4.68)$$

The total wave energy per unit crest width is given as a function of the water depth and wave height⁽¹⁰⁵⁾. The relationship is given as,

$$E = \frac{8}{3\sqrt{3}} \rho g H^{3/2} d^{3/2} \quad (4.69)$$

The pressure distribution is assumed hydrostatic for this wave profile.

Other theories that apply to water waves in their representation of a free flow motion are presented by Dean⁽¹⁰⁶⁾ (1955), as the Stream function, and Schwartz⁽¹¹⁾ (1963) in the extended Stokes form. The latter theory is used for the study of the behaviour of water waves with large steepness values.

4.3 REAL TIME WAVE ANALYSIS

What now follows are direct applications of parts of mentioned theories as used in the analysis of the experimental results.

In the study of fixed structures, information from experimental data is measured and processed. The significant values obtained are used to overcome empirical processes used in the design of sea defences. Emphasis on detail extracted out of the numerical data has shown the presence of contributing factors to the quantitative data required for design purposes. As data collection was based on analogue techniques, the transferring of data on paper chart recorders was terminated due to the extensive use of paper involved.

The standardisation of the data reduction was applied in two stages. In the first stage the record was examined for the number of waves per sample and also for detection of the highest crest and the lowest trough. In the second stage, information like the significant wave height was to be evaluated from the physical data. The listing of consecutive measurements from trough to crest heights and rearranging them in ascending order was avoided. This process was tried and found to be more tedious than by applying Rayleigh's method.

4.3.1 Pressure Attenuation With Depth

For measurements that have been taken by a pressure measuring instrument, values that are pressure dependent had to be amended in accordance with the attenuation experienced. The attenuation correction is dependent on the wave frequency and depth of immersion.

Pressure attenuation varies with depth and depends on the d/L ratio, or water depth to wavelength ratio. Any one wave has a given wavelength. For a value of kd less than $\pi/10$ the pressure attenuation is zero. For values of kd greater than $\pi/10$, the pressure attenuation increases as d/L increases, or effectively, as depth increases. The working limit is taken as $d/L = 0.5$ or $kd = \pi$ (deep water conditions). An attenuation of up to 90% occurs at this limit if measurements are taken from the seabed. Therefore, the decision of placing the measuring device, in the form of a pressure transducer, in the most responsive place has to be carried out. From an initial survey of the water depth, it is found that in the case of deep waters, the transducer is best located at an intermediate level. It is supported by buoy arrangement or by use of a metal spar attached to the seabed. The choice is dependent on the attenuation factor not being greater than say, 50%, to detect the variational differences of the surface elevation. The corresponding kd limit to place the transducer on the seabed is $4\pi/10^{(107)}$ (Fig. 4.6).

The governing equation for determining the pressure attenuation factor is given by,

$$\frac{\cosh k(y+d)}{\cosh kd} \quad (4.70)$$

4.3.2 Significant Wave Period And Wave Height

The amendment of the field measurements in the form of pressure readings is followed by the determination of the significant wave height and wave period. Vetting of the data at this stage was carried

out to ensure that the results do not appear to be inconsistent with the expected theoretical results. This aspect has shown up in samples that contained too many waves to give a realistic wave period. The problem of too many waves arises when the measured sea state is of a random nature. This condition generates, together with reflected waves, a spectrum which is less definite than one with a regular wave pattern. Besides this problem, the inclusion of noise components in the signal, adds uncertainty to the zero crossing determination.

The problem of accepting the measured data shows up when comparing the experimental to the theoretical data. This type of comparison shows up at local level barring any asymmetry differences. Quantities of the mean water depth and wavelength have to match for a common period and normalised wave height to within accepted tolerances. The program flow for the determination of the significant values is as follows. The input data is converted from analogue to discrete measurements. The next stage is to calibrate the conversion and to trim away any spurious signals. By scanning the data and reiterating with the numerical filtering technique, the frequencies of the data inhibiting the normal band of the frequencies of the wave data is removed. Then, a least square fit is applied to straighten the mean. The record can then be examined for determining the extent and position of all zero-up crossings and zero slope positions.

The systemising of records is carried out by obtaining the environmental data and recording simultaneously on the internal memory capacity of the microcomputer aided by additional memory boards. The objective

of the cataloguing of the data is to produce meaningful sea wave data as it is measured. This up to date monitoring is important in the control of offshore structures.

The analogue records of real wave data were used to examine the resulting program. The limitations for discarding wave heights at less than 30 cms were expressed, as these show inconclusive values to be part of the representative record. Also, with this limitation not being imposed, a group of waves that forms part of the record expressed a discrepancy between calculations by hand and computer results. The ambiguity extended to the location of zero crossing points for low amplitude variations. As energy is assumed to be related to the square of the amplitude, a 10% amplitude wave only produces 1% of the total energy of the normalised wave height. The implication of this observation is that these low waves add negligibly to the force measured on the wall.

This processing system as explained, can be formulated in a computer program. The applications of this method is the direct reading of data output from input signals obtained by wave data buoys, (such as Datawell) and the use of telemetry methods. Details of program flow for detecting and listing of significant data are shown on the flow chart in Fig. 4.7.

The following are the notes taken on site for the identification of the recorded data. This information is necessary for the matching of the transducer location and the corresponding recording track used throughout the analysis stage. Tape speeds and calibration details are also used at the recording stage. The notes isolate the beach recording from the wall recording. The constant use of this data requires that the site notes are accurately written and easy to read (See SITE NOTES 4.1 - 4.8)

4.4 WAVE VELOCITY AND DIRECTION OF APPROACH

The wave velocity and direction are obtained from three simultaneous traces from three separate pressure recordings. As the measurements are solely time dependent, the pressure attenuation factor is not included in the results. The accuracy of the measurements depends highly on determining the time difference between two recordings while identifying the same frequencies of the wave profile. The other factor to consider is the accuracy to which the plan distances between the source points have been surveyed.

The method opted for consisted of software programming to work out the correlation function between a pair of sampled digitised data. Initial correlation of the two different tape decks was achieved by the use of a digital oscilloscope.

Each tape deck contains an identical recording off the same signal output. A means of obtaining simultaneous signals between the two recorders is required. The problem is identified from the fact that from one recorder to another, there exists a discrepancy in speed control. As the signals are heavily time dependent, this effects them both at recording and at back playing of the signals. The other physical necessity arises from the fact that the system is liable to carry more than the seven channels allotted per recorder.

One projected approach to this problem is the use of a digital oscilloscope. The location of the signals on the tape is approximately known. In any event, this may be found by running a portion of the tape as a hard copy on a multicorder.

The digital scope operates on two channels. The facility applicable to this purpose is that it stores at a time base large enough, say 10 sec/cm. This covered a large portion of the recording at one go off the screen. The value of this facility is that a random sample quite often covers a range of significant periods of the order of 10 secs. As this implies, a train of eight consecutive wavefronts are easily visible at one go.

The other main facility used in this exercise is the Split Trace facility. A portion of the signal of one channel stored on one tape deck is back played, digitised and stored on the scope. The output of the signal is fed through the channel 2 of the scope. It is this channel that is frozen once the Split Trace is held. This implies that the corresponding signal from the other tape deck may be back played on channel 1 of the scope without interfering with the prestored signal. The direct comparison of the two signals is therefore present on the screen. An accurate measurement is then taken of the time delay due to a shift of origin between the two signals. The measurement is read out off the scale, with the added advantage of using the expansion facility in the time domain. The accuracy is related to the similarities in the stored signals and the sensitivity of the time base scale. This is of the order of $\pm 0.5\%$ (1 in 200) of the time base chosen. The value for the expanded version is given as 1 in 50.

4.4.1 Cross Correlation

As an extension on the principles of the auto correlation function, the cross correlation involves two signals in the time domain.

As a simplified example, when two signals differ only by their time difference, the cross correlation is given in terms of its evaluation as a cross correlation function. The function is continuous and is due to an imposed time shift τ . When two identical time signals are given an imposed delay of τ , the result of the cross correlation function is most definitely pronounced at this value. This is the consequence of the similarities between two signals in terms of their frequency, amplitude and structure (Fig. 4.8).

A formal investigation of the cross correlation function is achieved when the two mono-frequencies are separated by a phase shift θ . The resulting cross correlation gives a function with half the product of their amplitude, at their common frequency and phase (or time) shift.

The application of the cross-correlation is suitable for comparing random signals to give an average measure of the common frequency components in terms of their time delays.

4.4.2 Cross Correlation of 2 Random Signals

Difficulties in the use of cross correlation arose when the two time domain signals were obtained from two different sources. The direct comparison of the two signals by displaced superimposition

will, at times, not give a definite determination of the time difference. The reason is that, as a rule, the signals are structured differently. Whereas some components of frequency may be repeated in both cases, they will appear to be attenuated differently.

The main difference between the structure was brought about by the image to which the two signals were representing. The progression of the wave profile from one detector to another suffered distortion, to the extent of producing two different images of the same wave frozen in time. In spite of this, the significance of the cross correlation function was that, primarily, the differences in structure were overcome. This matching process could only come about after the time interval, still to be determined, has been eliminated from the pair of them.

The term used to displace the second signal from the first until a degree of correlation is found, is a lag. The number of lags in the digital approach of producing a correlogram is independent of the sampling period chosen for representing the two signals. A conversion to real time value is obtained by simply multiplying the number of lags by the sampling period.

The interpretation of a correlogram becomes that of an experienced person. Although the maximum value is what is aimed for, some cases have shown ambiguities, only cleared after the comparison of similar cases have been studied. The main problem lies in that the largest value is at zero lag, and a maximum is not evident at this point. This shows that the slope is simply reducing in value but has not

reached the zero value associated with a maximum. The implication of this observation is that the first signal, to which the second has been chosen to correlate to, has in fact been in advance of it at the moment of comparison. Knowing this, the adjustment of the order of the two signals is easily rectified. Another aspect is that the maximum falls in the negative half of the correlation function. The case when this happened is when a signal does not show a positive amplitude component at the correlation point. This occurrence has been verified by adjusting the mean value of the signal to incorporate positive signals in both cases⁽¹⁰⁸⁾.

Correlation may occur more than once at various intervals for a random signal. This shows up a subsequent volley of maxima in the correlogram. However, when the wave is specifically to be traced from one point to another, the corresponding time lag is to be identified. The way this was done was by comparing segmental portions of the signals to narrow down the influence of other parts of the signal. The method just described establishes an accurate means of time difference for a waveform to travel between two points, with an error of $\pm T$, the sampling period. The next step is to determine the direction of approach of the waves. This is done by assuming an arbitrary direction. The main decision is to establish which of the pair of the time differences is the longer. Then, the arbitrary direction is related to a rough indication of the origin of travel. The equations are set up to incorporate ratios of distances to time intervals per pair of data values. These ratios represent the celerity or phase velocity of the propagating wave —

the celerity is assumed constant in its travel over both sets of points. The solution of this single equation gives the direction of wave approach. Substitution of this angle in the velocity equation gives a value for the velocity.

The range of velocities (3 and over to 6 and over) and the direction of approach, reduced to a full scale bearing, are represented in "wind rose" formation, that is, vectorially on a unit circle. By dividing the rose into equal sectors, $\delta\theta$, the maximum sector area gives the main direction of approach. The power spectrum across this direction, from the sample of the wave that incorporates this direction gives a unidirectional power spectrum. The proportional values of the adjoining sectors gives the percentage dispersion of the energy of the waves. This is the 3-D effect, or the directional spread (Fig. 4.9).

In the recording of the continuous wave data on three instances, a full record of wave form over three beach transducers is also given in terms of impact pressures on the wall. The analysis following the acquired data identifies the velocity and direction measurements. These values are first presented as separate cases in the form of velocity roses. These examples bring up the more emphasised direction of the waves on approaching the wall. The graphical representation also gives the spread over which the wave formation covers. The direction of the wind generated waves is also compared to the site investigation of the main wind force and direction.

The other aspect of this obtained data is to compare the relationship of the pressure measured on the wall with the velocity of the oncoming wave. For this aspect the full set of complete data points were displayed together in graphical form. The analysis carried out involved the identifying of major trends, their reduction to best line fit curves, evaluating the likely errors involved in the grouping of the data points to this linear regression and the amount of scatter involved per batch of data points.

With the complete set of data values are included a full breakdown of the wave characteristics. Segments of the recorded data are used to compare the wave profile obtained experimentally to one which is determined theoretically, from the known values of the wave's characteristics. On verification of the experimental data, the extension of the theory covers the evaluation of particle velocities and accelerations and their pressure components as they appear throughout the water volume. (See TABLES 4.7.1 - 4.7.2, 4.8.1 - 4.8.2, 4.9.1 - 4.9.3).

4.5 SURFACE ELEVATION POWER SPECTRA

Consider a short crested waveform to be made up of a number of waves obeying linear behaviour and travelling from all directions, therefore having different phases. The wave component amplitudes⁽¹⁰⁹⁾ are related to the spectrum for a single main directional propagation, by the relation,

$$a_{mn} = \sqrt{2S_{\eta\eta}(\omega_m) \Delta\omega} \quad (4.71)$$

where a_{mn} is the amplitude magnitude of the wave components travelling in θ_n direction, and is a function of $D(\omega, \theta)$
 ω is the frequency component with resolution, $\Delta\omega$
 $S_{\eta\eta}$ is the directional spread density function
 $D(\omega, \theta)$ is the spreading function.

For spectral bandwidths of e less than 0.8, the random data is considered of narrow band. Most sea states have the value of e less than 0.8 which also defines the distribution of wave height as being Rayleigh distributed (See also 2.3.6).

The wave spectrum is used to apply a refraction solution of a deep water spectrum to predict near shore directional spectra. This is possible due to the assumption of linear superimposition of the number of wave components making up the random sea. This approach is used when determining the dynamic response of the structure at design level (Fig. 4.10).

4.6 MEAN WATER LEVELS ASSOCIATED WITH TIDAL CHANGE

The subdivision of a real time recording of the wave fluctuations is to reduce the discrete time intervals. The digitisation was carried out to extract the distribution of the free surface elevation of the random sea. The surface elevation is identified as the variation of the wave height in the time domain measured about the mean water level.

The mean level separates the crests from the troughs. The inclusion of the double peaked crests in the record provided the difficulty of identifying the significance of the wave height. The usual way of classifying the wave height is the difference between the maximum and minimum values of the surface elevation within a measurement given by the period of oscillation⁽¹¹⁰⁾. The period is, in turn, standardised as the time interval between two adjacent zero-up crossings of the surface elevation relative to a common datum⁽¹¹⁰⁾. These expressions are related to the irregular random information as measured from the sea. The common datum has been established as the mean value of the discrete values making up the continuous signal.

The determination of the mean water level becomes necessary for the expression of wave profile related parameters. For this reason it is given priority in presenting the tidal level as the key value in a set of readings. As the water level fluctuates it is doing so about a mean value. Unfortunately, the mean value is not stationary and effectively varies with the time of the recording.

This is due to the tidal movements of the sea which themselves vary from day to day. Other reasons for mean water movements of the sea are due to drops in atmospheric pressures. Fluctuations of a larger time interval are due to local water mass. A rise in the water level implies that waves travel in deeper water thus losing less energy in their contact to the sea bed. The consequence is that waves break nearer the shore.

The above shows the importance of obtaining the mean water level. The method considered was one that assumed the mean water level to be constant over discrete samples of time. Under this consideration, the time intervals are of a size to divide the sample in a number of complete cycles of the waveform. This is covered by the sampling at a rate compatible to the Nyquist Frequency⁽⁸⁰⁾ (see also 3.7.3).

The segmentation used covered a frequency attenuation of greater than 3 Hz. The initial spectral analysis gave a predominant frequency response in 0.13 Hz of a narrow bandwidth. The sampling of 1024 data points were chosen to cover 153 secs of recording. The digitised raw data has a definite displaced mean value relative to ground zero values. This quantity is particular to the individual sample and is distinct from the rate of change over a long time interval.

The determination of the mean level of the sample gives its position along the recording and therefore along the point in time measurement. The values of the mean levels were evaluated for consecutive segments. The location of a sample to actual time therefore fixes the whole

of the recording to real time analysis. The sample chosen to obtain a direct superimposition of the experimental to the theoretical values (which are obtained from tide tables) was obtained when the peak value of the subsequent averages was reached.

The samples so obtained, therefore provide a sequence of discrete mean values. The work proceeds in statistical determination and graphical representation. The mean values are tested for medians, maximum values and range, and from this a regression test is carried out. The best fit polynomial (the simpler being a quadratic for the duration of the record in question) is then obtained. Both the discrete values and the continuous curve obtained from the regression analysis are then plotted to the same axes. The maximum value of the curve gives the peak value associated to the high tide.

The values obtained are evened out for experimental error by introducing the regression analysis. Although the actual values are given as theoretical values they are based on predicted peaks and distribution pertaining to the day and time of the recording. The distribution is therefore reproduced in a scaled form covered by the restrictions of the range and rate of flooding and ebbing of the spring or neap tide. The essential factor is to relate the peak values from the two graphs obtained theoretically and experimentally. The comparisons then lie in the rate of change of slope. The approach does not involve the scaling difficulties arising out of the calibration conversion. The relative values are sufficient to express the respective curves under a common factor of overall length of recording and total rise in mean water level.

4.7 WAVE PRESSURES ON A SEAWALL

When dealing with a wall seaward of the shoreline, the dynamic pressures are depth dependent and velocity dependent. The components are related to the breaking wave characteristics. The crest height is assumed at 0.75 of the wave height relative to the S.W.L. This value of the wave height imparts a pressure equivalent to the static pressure. Any value above this pressure is considered dynamic. The dynamic pressure is equivalent to the square of the velocity and a factor. The factor K is determined experimentally from the results obtained from field testing. The breaker height is measured at the point of a plunging breaker. This is a result of the shoaling transformation effect that occurs due to the significant sloping bed of a beach. However, in the case of a negligible slope, the reduction in depth associated with shoaling is upheld by the approximate depth of the mean water level being tide dependent. This is the situation of the experimental set up (Fig. 4.12).

Such a situation is to be considered on a wall inward of the shoreline. The dynamic pressure, in this case, is related to the run up which is beach permeability and slope dependent. The dynamic pressure is given in terms of the pressure measured at the wall if it were located on the shoreline. The other determining factor is given by the equation,

$$P_m' = P_m \left[1 - \frac{x^2 \tan^2 \beta}{R^2} \right] \quad (4.72)$$

where P_m is the dynamic pressure if determined at a seawall located on the shoreline.

$\tan \beta$ is the slope of the beach

R is the amount of twice the breaking height

x is the distance of the wall from the shoreline

The value of R is found to represent the vertical projection of the water run up on the beach if the wall were not present. Experimental work in this field has produced given values for varying slopes and permeabilities⁽⁵⁹⁾ and are measured at times of neap tides.

4.7.1 Escalating Strengths Of Pressure On A Wall

The maximum value of pressure measured on a seawall is due to an impact which is generated by a breaking wave. This is height dependent under the same conditions of still water levels and velocity of approach. At the lower end of the pressure magnitude range are pressures due to standing waves. The pressure provides a condition to which other pressures, other than hydrostatic, may be compared. The increase in pressure in a standing wave is generated by the interaction of the incident wave with the reflected wave. The value of the equivalent wave height in pressure is as much as twice the significant wave height measured at the wall.

The larger pressures, more susceptible to cause large pressures on the wall, are due to the breaking wave. When the wave height reaches a limiting steepness of,

$$\frac{H_b}{L_b} = 0.142 \tanh 2\pi \frac{d_b}{L_b} \quad (4.73)$$

deformation of the crest by forming an asymmetrical profile begins to generate into a breaking wave profile⁽¹¹¹⁾ (See Fig. 4.13).

The transitional changes between the standing wave and the breaking wave are also significant when considering the pressure on the wall. This range of waves was frequently encountered in the experimentation of this research. The identity of this range has been established by the double peak per wave crest. The double peak is known to be due to the reflected mass of the seawall acting interactively with the incident wave (See Fig. 4.14).

The extent to which this type of wave occurs in a trace is obtained from the spectral bandwidth. This is identified in terms of the larger number of crests than zero-up crossings in a particular trace⁽¹⁾⁽²⁾. The part of the wave that forms the dynamic loading of this category is due to a large peak showing up first in the profile of the time domain. The explanation of the profile is due to the breaking of the wave before reaching the wall. This condition is detected in waves with higher wave heights that break and produce the uneven shape about the mean water level.

This implies that the momentum released on reaching the wall is not uniform. A larger pressure is detected due to the heavier wavefront, and a subsequent lower pressure is due to the rest of the wave. These measurements describe the characteristics of the wave that is made up of a steep wavefront. This condition is met with waves that have not reached their limiting stability. This is used to explain when the stage before breaking in a wave occurs (hence a study of velocity profiles from surface distribution in the time domain leads to important work in this field).

At the critical wave condition of total instability, the breaking wave produces the largest pressures. These are the impact pressures, so called because they produce a distinctive high pressure over a short period of time. The time difference is called the rise time and is of the order of 10 ms or lower. The application of this pressure on the wall is not all, the broken wave then hits the wall to produce a slower time varying pressure. This is of secondary magnitude to the previous one. However, the longer duration of the application of this pressure on the wall, has a more direct significance in the design of the wall structure to withstand the imposed loading. This will be shown later as direct loading in the seawall design.

4.7.2 Pressure Due To Standing Waves

The criterion for breaking waves on a plane smooth beach are the beach slope and wave steepness. With the propagation of the wave motion, breaking occurs with an increase in beach slope and wave height. The wave height increase is fixed by a threshold. Irribarren and Nogales⁽¹¹²⁾ (1949) gave the dimensionless parameter which depends on wave steepness related to deep water wavelength and the slope.

In the critical state, they say that as waves break so the reflection coefficient falls below unity. Therefore breaking waves reduce the tendency of reflection to take place on the inclined seabed. The consequence of this statement is that the energy contained in the wave profile decreases in a form of internal energy, by turbulence. Munk and Wimbush⁽¹¹³⁾ (1969) describe the breaking wave in fluid

motion terms. They say that the fluid acceleration downward along the slope cannot exceed the acceleration of a free falling particle $g \sin \alpha$, without causing breaking, where α is the angle of slope. The non-linear criterion of a breaking wave is that the free surface is vertical ⁽¹¹⁴⁾.

4.7.3 Types Of Breakers

After Galvin ⁽²²⁾(1968), the breaking wave is grouped into various categories. These include the collapsing, plunging and spilling. The collapsing wave is one which is associated with only a small amount of breaking at the shoreline. It occurs on shallow slopes with long stretches of a flat seabed.

The plunging breaker is one mostly associated with a large amount of energy loss by turbulence. It occurs with larger gradients and is due to a steady rise in wave height as it travels over the shoaling area. The trough ahead of a plunging breaker is noted to be undisturbed. The activity, in fact mostly occurs at the tip of the crest, where an overcurling effect of the wave at this point generates this high velocity region (See Plate XVI).

The example of the spilling breaker is one in which the front of the wave does not reach steep limits. Due to velocity differences, the crest of the wave moves faster than the body of water producing the white foam at the top. This breaker is again associated with moderate slopes and deep water (See Plate XV).

The results so obtained have shown a close degree of compatibility. The deviations are emphasised at increasing distance from the peak values. The reason is partially due to the interpretation of results when comparing the two curves, and also that variations in the predicted tidal levels are inevitable when considering the meteorological circumstances as well. In spite of this, the values obtained experimentally show that a high degree of confidence can be taken in the real water levels required for the design stages of the waveform analysis (Fig. 4.11).

4.7.4 The Limiting Wave Height

The character of a wave is such that, with a given wavelength, and placed in uniform water at a given depth, the wave height is limited to the point of maximum stability. This research is concerned with the generation of a breaking wave, so the interest in maximum wave heights cannot be overlooked. The basic criterion is determined by the phase velocity of the wave. If the particle velocity in the crest exceeds this velocity, a condition of instability sets in⁽⁸⁾.

By this criterion, the preliminary definition covered by Miche⁽¹¹¹⁾(1944) is that the maximum included angle at the peak is given by a maximum steepness of $H_b/L_b = 0.142$. This theory was extended to solitary wave comparisons. In solitary waves, the wavelength tends towards infinite values, so the criterion of maximum steepness is depth dependent. The ratio of maximum wave height to water depth is given by Chappellear⁽¹⁰⁾(1959) as 0.87. Longuet-Higgins and Fenton⁽¹¹⁵⁾(1974) obtained a value for this ratio of 0.827 for the solitary wave. They also gave a corresponding phase velocity of,

$$c/\sqrt{gd} = 1.286 \quad (4.74)$$

The breaking wave celerity is 20% faster than that of a linear deep water wave. This solution is also obtained from a simple application of Bernouilli's equation with a limiting wave height given by,

$$\frac{c^2}{gd} = \frac{2H_b}{d_b} \quad (4.75)$$

This value supplements Miche's results given by equation (4.73). The overestimated values for shallow water were given by Schwartz⁽¹¹⁾(1974).

The study developed into further theoretical work by Longuet-Higgins and Fox⁽¹¹⁶⁾(1978) on steep non-breaking waves. The theory differs from real examples in that the asymmetrical wave profiles are formed with a steepening wave. The result is that breaking occurs before maximum wave height is reached. This explains why, for the maximum impact pressures detected on the wall, the wave height had not reached its maximum steepness. With a recorded signal, the random sea presents variations in the wave period. As these variations also include close values of zero-up crossings they have to be ignored in determining the limits of a full wavelength. This definition of wavelength in a record is required to determine the phase velocity. The values of wavelength and velocity are then used to determine the values of steepness for a given depth.

4.7.5 Engineering Aspects Of Breaking Waves

In the design of a coastal structure, a solution cannot be found without taking into account the wave climate with particular reference to the breaking wave. The pre-breaking stage is extended to the breaking profile of a wave to apply the worse conditions to the design. Other indirect aspects that affect the wave to reach the ultimate state of instability are also considered. The key influences are energy losses, directional effects, wind contributions and transformation factors.

The main characteristics of a breaking wave come under the height, H_b and depth d_b at breaking. These are associated with deep water wave characteristics H_o/L_o and beach slope, m . The value of d_b/H_b

has not shown a definite pattern for experimental data⁽²⁵⁾⁽²⁶⁾(Fig. 4.15).

The attained magnitude in terms of height to depth ratio of a breaker depends on the:-

- i) steepness
- ii) slope
- iii) type of breaker

These three factors therefore formulate a parameter, β such that,

$$\beta = \frac{H_o}{L_o m^2} \quad \begin{matrix} (22) \\ (4.76) \end{matrix}$$

which in turn is used to define the limits of the breaker type.

The values range from > 5 for spilling, up to 0.1 for plunging breakers and lower than 0.1 for collapsing breakers⁽²⁶⁾. Although specific, these limits are not distinct. This is given by Peregrine⁽²¹⁾ (1979) when a spilling breaker can generate before a plunging breaker has broken. Longuet-Higgins and Cokelet⁽³⁷⁾ (1976) have analysed numerically the behaviour of a breaker in its travel after it has passed the vertical stage. They provide the variations of pressure and velocity of a propagating wave up to its stage of breaking and to its formation of a jet in the form of a plunging crest. Further to the detection of an existing fully developed breaker type, the understanding and utilising of the steps of the wave to reach this level provides a greater impetus to the engineer. This work was initiated by Longuet-Higgins and Cokelet⁽³⁷⁾ (1976) and expresses the surface flow as being periodic in its location in space, that is, it repeats itself in similar boundary conditions. However, once reaching the stage of instability, the wave will not revert to a breaking situation again, that is, it denies periodicity in time. The analysis takes place from initial conditions. However,

as the time stepping procedure is carried out, the values of the profiles at later time stages are used to determine velocity gradients.

This study is not complete without referring to values obtained from past experiments. Specific values for breaking waves for shallow water are depth limited with an average ratio of H_b/d_b of 0.89. The limiting range of the non-dimensional ratio is 0.7 to 1.2. This value follows from the shallow water simplification of limiting steepness,

$$\frac{H_b}{L_b} = 0.142 \tanh kd_b = 0.142 \frac{d_b}{L_b} \cdot 2\pi$$

(117)

$$\frac{H_b}{d_b} = 0.89$$

(4.77)

The engineering aspect of this criterion is to be used in the design of coastal structures. The mean water level at the structure fixes the height of the wave breaker that can be generated. This limiting value gives a corresponding value of forces applied to the wall.

The forces are identified as dynamic, together with static forces and are expressed in terms of forces due to breaking waves, described in a later section (4.8.2).

The energy dissipation is a measure of the flow fields of a quasi steady breaking wave involved with turbulence characteristics.

Phase speed measurements are based on corresponding points between adjacent wavefronts, that is, time separated examples of free flow.

Directional spectra of a general nature are used to express the loading history⁽¹¹⁸⁾. The spectra define the main energy in a prevailing direction of approach by emphasising the amplitude of propagation in a frequency component range.

The parametric values for the unidirectional spectrum are reduced to peak frequency, f_m and the area under the curve, E . These values are interchanged for the significant period and wave height respectively. Relationships between two pairs are given by I.S.S.C.⁽¹¹⁹⁾(1979).

$$H_s \approx 2.8\sqrt{E} \quad (4.78)$$

$$T_s \approx 0.95 f_m^{-1} \quad (4.79)$$

Raw data acquisition requires thorough research programs with the value of the information obtained seen in cutting the large costs involved in both the under-design and over-design of coastal structures.

The reference to wind velocities to produce wind generated waves is a specific value on the Beaufort scale. The quoted values are corrected for overestimated high wind velocities and underestimated low values. The new version is worked under the World Meteorological Organisation (W.M.O.)⁽¹²⁰⁾1976.

Statistical values are used in presenting data in a form which is representative of a specific number of parameters. This is valuable for wind or wave data collected over long periods of time. The simultaneous acquisition of data provides a working means of relating

a set of results to the equivalent values causing them. This identifies the relationship between wind and wave data within the field testing carried out. The same arrangement can be used to predict the unknown wave data from a set of recorded wind data. Wind data from other locations has been used to work on the required data. Wind sea spectra are compared to the JONSWAP.

As a basis for design, the statistical parameter for climatic data is such that the structure is allowed to suffer extreme conditions by accepting significant damage to a cumulative level. This climatic condition gives values of extreme storm states and their durations. The environmental parameters as worked on a diagnosis procedure (hindcasting) also work on a prognostic (forecasting) procedure.

Shallow water terms of reference include:-

- i) Depth induced energy redistribution (for example, refraction, shoaling and dispersion).
- ii) Dissipation in bottom friction, percolation, currents, etc.

The parametric aspect of shallow water models is covered by Gunther and Rosenthal⁽¹⁵⁷⁾ (1982).

The design of seawalls cannot be adequately carried out without studying existing examples in an environment that is liable to generate intensive wave conditions. For this purpose a continuous time sample is restricted to three hours data values. The optimisation design procedure includes a steady accumulation of data as well as characteristic extreme values — giving a joint probability density function. For seawall study, the determination of a mean water level gives the behaviour of wave formation and incident wave influence.

4.7.6 Wave Measuring Investigation Of Breakers

The water-air interaction shows its limitations when the level of instability reached is to be reproduced by mathematical model simulation or under laboratory controlled conditions. The natural occurrence in stormy conditions, makes the investigation of this aspect of wave mechanics worthwhile to be carried out as field measurements. Difficulties pertaining to data collection on a site situation require a sea state conducive to breaking wave formation. These restrictions and the numerous methods by which analysis has to be carried out justifies the full use of recording the data simultaneously from different measuring devices on magnetic tape. The measurements covered for this investigation include a detailed sequence of coordinates making up the wave profile.

The method of presentation of results was reduced to ten minute real time segments. The statistical parameters worked out for each of these segments are then used to give the overall stochastic picture of the investigation to a satisfactory degree of accuracy. Numerous correlations of data right across the whole set of measurements was carried out via Fourier series analysis. This included the producing of spectra of the data sets in the frequency domain.

The pressure transducer array is used in the direct measurement, within a wave field, of the wave characteristics. The array signifies the measurement of similar quantities from horizontally separated

points. The directional spectra are obtained by analysing the discrete wave trains from separate sources. The significance of a directional spectrum is that it gives an energy picture in terms of frequency and direction.

Arrays are used to yield the spatial distribution of the identical wave elevation as a parameter. Interrelationships between the array members provide wave directional information. In this experimentation, the tripartite arrangement is used, after suggestions by Snodgrass⁽⁶⁾ (1952), to obtain the wave bearing. Barber⁽¹²¹⁾ (1954) suggests the use of a linear array which is identified as being of one dimension rather than the two dimensions.

The one dimensional arrangement expresses ambiguity, however, in situations where wave direction is incident in more than one general direction. Also, it performs at its best when the waves are travelling normal to the line.

Panicker⁽¹²²⁾ (1971) suggests how the deviation of Fourier coefficients may be obtained from two dimensional arrays. Choice of spacing between array members should lie at a value close to one half the wavelength that contains the maximum energy, after Mobarek⁽¹²³⁾ (1965). Fan⁽¹²⁴⁾ (1968) adds, that spacing smaller than one half the wavelength gives better results than spacing greater than the wavelength.

[Munk⁽¹²⁵⁾ (1963) used a two-dimensional array for long period ocean swell measurements made of the vertices of an equilateral triangle 300m in deep water conditions of 100m].

The analysis of arrays to give velocity and bearing also provide important information on the energy magnitude and direction, after Mobarek⁽¹²³⁾ (1965). Discrete energy values are weighted to yield cross-spectral characteristics of pairs of wave gauges. This is done relative to the spacing and orientation of the gauge pair.

The use of directional spectrum is more complete than significant wave height, period and direction in design and prediction at an engineering level. The directional spectrum was used by Karlsson⁽¹²⁶⁾ to express the transformation of waves by refraction. He gave a governing equation of the distribution of spectra of waves of any depth. Breeding⁽¹²⁷⁾ (1969) shows how the group velocity rather than the phase velocity should be used for refraction considerations.

4.7.7 The Breaking Sea

What is now described is the breaking sea from its generation to its conversion to a smoothed waveform. The wave generation process to breaking stage basically involves the input of energy from the atmosphere. The subsequent dissipation of this energy takes place via friction of the water mass both internally and due to external contact with the seabed boundary. The high consumption of energy is the main factor when considering the cause of generating the white capped situation of an open sea⁽¹²⁸⁾. The simulation of these conditions theoretically forms a difficult task to have any significant response. However, the direct measurements of the sea that incorporate this ready made process produce more feasible and realistic results.

One suggested approach is of carrying out the investigation theoretically or by model analysis (Froude's Law and Reynold's Law). This however does not prove fruitful. The model testing makes use of the same liquid with a 1:1 proportion of density and requires the dramatic reduction of the model waves to correspond to nature's similarities. The problems associated with simulating the condition favours the theoretical approach. In any case, the objective is to accommodate the results from these two methods to those experienced by nature, and not vice versa.

An understanding of the mechanism of the breaking wave situation may explain the complexity involved in carrying out such an investigation. It is understood that energy is converted by an air-water mixture due to surface forces to bring about energy transformations in a surf zone. Bretschneider⁽¹²⁹⁾(1965) mentions this behaviour in the formation of a hydraulic jump of stationary flow. The bottom friction becomes an unlikely parameter when the transformations occur over short intervals⁽¹³⁰⁾. This explanation does in no way exclude the other possibilities of wave breaking due to shoaling water conditions. In this case the gradual reduction of water depth, becomes the prime cause of energy conversion by bottom friction.

4.7.8 Breaking Wave Heights

As a direct application to limiting wave height described in 4.7.4, the breaking wave height now follows. The engineering significance in design based on probability distribution of breaking wave height gives reliability, stability and probability of survival or life

span of a structure. The effect of a breaking wave is seen when a floating structure overturns under its influence. The alternative way to describe wave steepness is to divide the wave height by the square of the period. This definition is used due to the lack of adequate information to produce the wavelength.

The instability condition associated with a set of individual wave heights and period in succession is also determined from the direction. Additional causes of wave breaking are wind effects on crests of waves and short steep waves riding over longer waves.

An arbitrary definition of a breaking condition for a wave just reaching the point of breaking is given by,

$$H_b = \nu T_b^2 \quad (4.80)$$

where ν depends on the wave theory. Dean's Stream function⁽¹⁰⁶⁾ gives a value of ν for 0.267 ms^{-2} , for deep water waves. The value of ν is therefore ready to be changed according to the empirical data acquired.

Rayleigh's distributions are assumed for both wave height⁽¹³¹⁾ and the square of the period⁽¹³²⁾ ⁽¹³³⁾. The other relationship between root mean wave height and wave period as being directly proportional to one another is also assumed. This supplements the Rayleigh distribution of the wave height. The assumption of independence between two variables means that the percentage of waves that are breaking will be an overestimate over one where an assumed relation is maintained. The result of breaking wave height is therefore

conservative, and errors of such unknown relationships are favoured in this sense, when the data is to be applied directly to a design problem. The occurrence of a breaking sea state is only brought about by conditions created by extreme storms. These conditions are established by fetch and velocity of the wind which also relate interactively to an extreme value of one parameter matching the moderate parameter of the other. This relationship is independent of the storm duration.

4.8 WAVE FORCES ON RIGID VERTICAL WALLS

Reflection plays an important role with the interaction of incident waves reaching a vertical by the lack of action on breaking waves. However, the forces set up by reflection are unimportant when considering the extreme forces generated by impacts. In any case, waves reaching a wall without breaking interact with the reflected wave to form a standing wave. This type of wave, although it does not set up intense forces, contributes to the force on the wall. This is given in a magnitude of around twice the value of a regular wave reaching the wall, as is shown in the next section, 4.8.1.

4.8.1 Pressures From Non-Breaking Waves

The pressure beneath the standing waves is given by the linear wave theory as,

$$p = \rho g \left| \eta_s \frac{\cosh k(d+y)}{\cosh kd} - y \right| \quad (4.81)$$

where η_s is the elevation of the water surface of the combined incident to the reflected wave⁽¹³⁴⁾.

Assuming perfect reflection, the resultant elevation of the water surface is equal to twice the incident wave. This implies that when a wave reaches the wall, the value of water in contact to the wall is at a maximum of H_i , the incident wave height. The difference is that when the crest reaches the wall, the water contact area lies above the still water level, and when the trough reaches

the wall, this area lies below the still water level (Fig. 4.16a). In both cases, an excess pressure is detected above the water surface.

The force generated by this pressure has to be considered for an assumed wetted area. For a unit length of wall, let the force over the wetted area be F_{cs} such that,

$$F_{cs} = \int_{-d}^{\pm H_i} p \, dy$$

$$= \rho g \left[\frac{1}{2} (d^2 - H_i^2) \pm \frac{H_i}{k} \frac{\sinh k(d+H_i)}{\cosh kd} \right] \quad (4.82)$$

These values are given by linear theory with either the crest or trough reaching the wall, that is the \pm in equation (4.82).

With finite amplitude waves reaching the wall, the value of the force exerted on the wall is in excess to that given by small amplitude values above. The run up on the wall R_s , measured in terms of H_i is given by,

$$R_s = H_i + \frac{\pi H_i^2}{L} \coth(kd) \quad (4.83)$$

As the maximum level reached by the water is given by $R_s - 2H_i$, the maximum water level above the mean water level is larger than the minimum water level, that is,

$$H_i < H_i + \frac{\pi H_i^2}{L} \coth kd \quad (4.84)$$

and the rise of the mean water level is given by,

$$\frac{\pi H_i^2}{L} \coth kd \quad (\text{Fig. 4.16b})$$

The point of interest in the wall design is in the case of the wall height above the mean water level being less than the assumed run up. The amount of water in excess is measured as an overtopping quantity. It is the accommodation of this overtopping that is conclusive to the wall design. This decision reduces the maximum height of wall for an adequate factor of safety. The reductions are reflected in a reduction of cost of materials and labour, and in the reduction on the bearing capacity for foundation design. The trade off to these improvements to a wall design is overcome by a rapid draining facility of the excess water without undue inconvenience to the ambient area inwards of the wall.

The design of the wall under conditions of overtopping is to work out the moment and forces for pressure distribution less the excess passing over the top face of the wall. The inclusion of soil and backfill pressures are also to be considered to overcome these wall forces in the opposite direction. The condition of uplift from water through a permeable base has to be considered for the total stability of the structure.

4.8.2 Pressures From Breaking Waves

This research is involved with the extreme values of pressures likely to be encountered in the design of a seawall structure. Therefore, with this objective, the emphasis lies in the investigation

of that type of loading that generates these pressures. The research is therefore dealing with the pressure resulting from an impact hitting the wall. The nature of the waves causing this impact is known to be of a breaking plunging type⁽¹³⁴⁾. The magnitudes involved are obtained from the time pressure histories measured from breaking waves on the wall. The collection of data of this nature has been with the aim of furnishing statistically, the maximum impulse experienced by the wall. This aspect is treated, in this research, with a general aim of evaluating forces and moments on similar examples of wall. Alternatively, similar results are obtained by suitable modifications in cases of two walls with different profiles.

The pressure time history is characterised by the two major components:-

- i) impact pressures
- ii) secondary pressures (Fig. 4.17)

Impact pressures have two features, the maximum pressure reached and the time taken to reach it. The impact pressure is followed by the equally important characteristic of secondary pressure which should be included in the design of seawalls. This secondary pressure results from the mass of water reaching the wall, immediately after impact occurring and over a longer time interval than the impact rise time previously mentioned in 3.7. The time between successive impacts gives an indication of the fatigue experienced by the composite properties of the material in the construction of the seawall.

This is measured by the sudden loading and release of dynamic forces through a series of cycles related by the frequency of occurrence.

The impulse generated by the impact pressure P , with rise time t , is given by,

$$F = \frac{d(\mu)}{dt} \quad (4.85)$$

as the rate of change of momentum.

This implies, for an assumed area of contact,

$$d(\mu) = p A dt \quad (4.86)$$

Assuming triangular distribution,

$$\rho l_b A du = \frac{1}{2} p A t_m \quad (4.87)$$

and,

$$2\rho l_b u_b = p_m t_m \quad (4.88)$$

where u_b , l_b are phase velocity and virtual length of the breaking wave, p_m is the maximum pressure while t_m is the rise time. Equation (4.88) covers the relationship between the virtual length and the breaking wave characteristics.

The main factor to consider in this relationship is the proportionality between p_m and t_m . Hyperbolic in nature, the increase in pressure, p_m is counteracted by a corresponding decrease in rise time. Also a relation between rise time and the frequency of occurrence of the impacts is given by,

$$\frac{t_m}{T} = 0.001 \quad \begin{matrix} (134) \\ (4.89) \end{matrix}$$

where T is duration of secondary pressure.

The value of force from an impact on a wall can be compared with the hydrodynamic force of a jet impinging a plate normal to its surface. The value given is $\frac{1}{2}\rho v^2$. As the flow from the jet of a crest of a breaking wave is neither uniform nor steady, the value of the force of the wall is given by,

$$p = k\rho u_b^2 \quad (4.90)$$

The value of k depends on height, period of breaking waves, slope of seabed in front of the wall and the elevation of a non-vertical wall. Having found k by experiment, it can be used to determine the value of l_b the virtual length of the breaking wave.

These values are used for the prediction of p_{max} in the vertical distribution. For slopes of 1 in 25, 1 in 15 and 1 in 11, values of pressure have been measured to 15 times those predicted by the steady flow measurement. The higher magnitudes of pressure detected are a result of steeper beach slopes⁽¹³⁵⁾. In theory, Von Karman⁽¹³⁶⁾ in 1929 gave the limiting value of k as,

$$k_{lim} = \frac{c_w}{u_b} \quad (4.91)$$

where c_w is the speed of sound in water, 1450 ms^{-1} . However, this speed depends on air entrainment.

Gibson⁽¹³⁷⁾(1970) carried out experiments to determine the drop in speed of sound in water due to the air entrained, which was found to drop considerably for low percentages of air present in the water. The air entrained in the water is found in the upper layers of the water surface with a large distribution in the crest area of a breaking

wave (See Plate XVIII). The pressure of this air in the wave on impact explains the variation of coefficients obtained when relating the measured impact pressure to the phase velocity of the wave. The limiting value of the impact pressure is due to the limiting value of the speed of sound, giving, on substitution,

$$P_m \text{ lim} = \rho c_w u_b \quad (4.92)$$

This is known as the water hammer pressure.

For 10% air entrained, a speed of sound is reduced to 50 ms^{-1} .

The corresponding value of maximum pressure is given as 250 KN/m^2 for typical breaking wave velocity measurements.

Maximum pressures detected near the mean water level are compatible to the statement for pressure distribution. In the presence of a base that is made up of a rubble mound, the composite structure has an influence on the peak pressure location⁽¹³⁸⁾. The peak pressure distribution has a rapid decrease in value from the peak pressure.

Parabolic relationships are suggested by previous work as,

$$P_m = P_{\text{max}} \left(1 - \left| \frac{2y}{H_b} \right|^2 \right) \quad (4.93) \quad (138)$$

The total dynamic force acting on a unit length of wall F_m is given by,

$$F_m = \int_{-\frac{H_b}{2}}^{\frac{H_b}{2}} P_m \, dy \quad (4.94)$$

$$= 2 \int_0^{\frac{H_b}{2}} p_{\max} \left(1 - \left| \frac{2y}{H_b} \right|^2 \right) dy \quad (4.95)$$

$$= \frac{p_{\max} H_b}{3} \quad (4.96)$$

Nagai⁽¹³⁹⁾(1973) describes how to obtain predictions for p_{\max} .

The hydrostatic pressure distribution is also present with a volume of water in contact with the wall. An assumption of $H_b/2$ of water head above the mean water level gives an acceptable estimate for hydrostatic pressure. The hydrostatic pressure equivalent for design purposes is given as,

$$\frac{p_m H_b}{3} \quad (\text{Fig. 4.18})$$

4.8.3 Pressures From Waves Following Impacts

An important characteristic of pressure detected on the wall is the following up of the wave after the impact on the wall (secondary pressures). Field measurements have shown results for this type of pressure measurement to be compatible to pressure expected from standing waves. Assumed pressure distributions have been devised as linear from the still water level based on maximum p_m of $2.5 \rho u_b^2$, five times the expected pressure from a jet impinging a flat plate⁽¹⁴¹⁾. The influence of surf on these values leaves a single aspect in this field to be studied as a separate entity⁽¹⁴⁰⁾.

The data in this section is given experimentally by the data values of pressure measurements expressed in terms of impact and secondary pressures with corresponding time components (See TABLES 4.1.1 - 4.1.3; 4.2.1 - 4.2.11; 4.3.1 - 4.3.27; 4.4.1 - 4.4.9; 4.5.1 - 4.5.10; 4.6.1 - 4.6.6). These values are used to evaluate the impulse generated on the wall to form a basis for the collection of data values under definite limitations. The data values plotted in this form of grouping produces graphs with increasing order of significance when compared to previous work. The figure reached at on this comparison improves this present work by up to three times previous field results. (See Figs. 4.20a - 4.20e, 4.21, 4.22).

The values of pressure in the form of time histories are used to determine their vertical distribution. This work required that the results be grouped by the number of transducers used for recording the pressure-time variations. Analysis of the data then produced distributions represented in diagrammatic form relating to the object of identifying how both the peak pressures and slower second peak pressures vary with depth.

Note: Fig. 4.20e is the set of results previously obtained by P. Blackmore⁽³⁶⁾ in 1981. They are included as a comparative basis for the acquired data, with particular reference to the group expressed in Fig. 4.20a.

4.9 MEASUREMENTS OF WAVE PROFILES

Waves are described by the range their characteristic period covers; these are gravity waves (1 to 30 sec) and long period waves (swells and tidal variations). Gravity waves are wind generated waves, and are recorded as a water surface variation. Pressure sensors placed between seabed and water surface on other occasions, act as low-pass filters but also have an effect of attenuating the signal. This effect was minimised by placing the pressure sensors on the seabed. Band-pass filtering a recorded signal highlights the more prominent frequencies.

Proper filtering ensures a determining of an accurately placed mean water level. A waveform with symmetry in area about the mean water level is detected after filtering has taken place. The band-pass filter used has an arrangement of conjugate poles. As previously explained in 4.8.3, the determination of the still water level is fundamental to fixing the maximum pressures in the vertical distribution.

High crests and low troughs are established according to the fixing of the still water level (S.W.L.). The symmetry in area is brought about by adjustment of the S.W.L. until the area in the upper zone equals that in the lower zone. The waveform does not appear as a simple sine wave. The amplitude measurement in the crest area does not repeat itself in the trough area. The amplitude measurement difference means that the wave profiles detected show an amount of non-linearity. This is expected in the region of shallow water at which the experimentation is carried out. It is from this

non-linear result that a wave profile may be gauged as to the extent of its development to a breaking stage, as described previously in 4.7.1. From this information, the wave profile may be used to determine the pressure distribution acting on the wall.

The root mean square of the water surface is evaluated at an arbitrary level without affecting the results for comparative purposes. It has the significance of relating in value, to the energy of waves at a measuring point E, such that,

$$\text{r.m.s.} = \sqrt{E/2} \text{ or } \sqrt{2/2} \cdot \sqrt{E} \quad (4.97)$$

This is the root mean square derived from amplitude measurements.

In case of higher measurements, the root mean square value is given as,

$$H_{\text{r.m.s.}} = \sqrt{2E} \quad (4.98)$$

The average r.m.s. value of the waveform is independent of the waves' randomness for a small discrete number of points⁽¹⁴²⁾.

The waveform is said to have a wave period which is representative of the record, as a means of assessing the signal for analysis. It does not say that the wave is repeated periodically, but the averaging out of the periods in the record gives a characteristic about which the frequency of the bandwidth is centered. In determining the wave period, the number of zero up crossings of the record N_z , are used to divide it into the length of the record. This number is compared to the number of crests present in the record, N_c , to give the spectral bandwidth e , such that,

$$e = \left[1 - \left(\frac{N_z}{N_c} \right)^2 \right]^{\frac{1}{2}} \quad (4.99)$$

The bandwidth mentioned here gives an indication of the cross-section of wave types present in the record. The variations cover long waves and short waves. The significance of this is that short waves are superimposed on the long waves and the result is one of double crested waves. This type of wave profile was detected from the records by the increase in N_c over N_z , implying that e tends towards one. The performance of long waves acting as a swell results in the values of N_c comparing to N_z . The bandwidth e therefore tends to zero. These two limits are not reached in reality. However, as the record lies in between it gives a correct indication of whether the type of waves encountered are of a bias towards a localised size or towards a swell. This means that the distinction of the measured sea state can be identified along the scale of $e = 0$ to 1. The importance of this description lies in terms of the energy to be received by the seawall obstruction. The identification of the wideband process is seen through the detection of many more positive peaks than zero crossings. The other alternative is narrow band processes in which the threshold crossings correspond to a positive peak resulting in narrow banded spectra⁽¹⁴³⁾.

4.9.1 Wave Grouping

A group of waves is identified by its maximum height, H_g and the average period T_g of the component waves. Significant height, $H_{\frac{1}{3}}$ is used as a basis for correlation. Representative height parameters are obtained from Rayleigh distribution of wave heights. The average of the T_g values of a record is related to the maximum energy component of a frequency analysis⁽¹⁴⁴⁾.

"Every Seventh Wave Is The Highest" - Anon.

The description of sequences, beats (predominant accentuated signal), and groups of waves is characteristic of a swell. The study of the nature of wave groups comes into force under extreme wave height predictions. This arises out of wave height maxima occurring in a group of waves. Their importance as design factors is evident in the fact that they generate forcing functions, to produce a resonant response in the maritime structures of the non-massive type. The resonant response indicates that the tuning to the period of oscillation matches the structure's natural frequency. Wave groups produce long waves along shore-lines. This is known as a surf beat with its greatest importance given by the generation of resonance within harbour confines. The unordered sequence of wave heights⁽¹⁴⁵⁾ is standardised by the use of Rayleigh's distribution⁽⁵⁰⁾. Ewing⁽¹⁴⁶⁾ (1973) related adjacent heights in runs of high waves. Definition of group and intergroup parameters of wave records have been given by Smith⁽¹⁴⁷⁾ (1974).

The generic term for a group of waves generated under one low pressure storm is a swell train. Grouping of waves is predominant in swells of moderate steepness propagating over appreciable distances (in the ocean). This brings about the low frequency component (long period variation) of a wave record other than the local wave action. (Fig.4.19)

Sets of wave groups are identified with frequency measurements corresponding to their period variations. The significance is due to a different swell train originating at different areas. The isolating of the wave periods gives an actual significance of the

combination of energy content in the sea state. Wave grouping in the form of beats is a result of combination of waves with similar frequency and amplitude.

The largest wave occurs in the middle of a group of secondary wave trains superimposed on the main wave train. The theoretical deduction refers to actual measurements of groups of waves which lie within the middle third. This depends on the ratio of the phase speed to the group velocity. The principle of superposition applies to wave motion with higher frequency waves easier to identify when compared to lower frequency ones.

4.9.2 Parameters Of A Wave Group

The average period of waves in a group is denoted by T_g . The variability of period in a wave train is not high. Therefore not all the waves have to be taken into consideration to compute the average T_g . The limitation defining the boundaries of a wave group are the discontinuities in the wave train. These are identified as having an apparent period that is greater than half but less than twice T_g . The significance of a discontinuity of a wave group is the place where a change in phase is detected between one phase and another. Another reason is where the wave heights diminish in size, usually a third of the significant wave height. This is due to the combination of waves of similar frequencies and amplitudes at non-matching phases.

The maximum wave height, H_g is chosen to characterise the wave groups' variation in amplitude. This is because it is easily identifiable and can be measured if dominance of wave heights is found in the group. The groups examined from records of this experimentation show the wave height maximum is restricted to one wave. It is seen that this value is independent of the defined ends of the group. Other measured characteristics include the number of waves in a group and duration of the wave group, related to the limits of the group.

The phase difference between two wave trains of varying frequency that marks the ends of a group, is numerically, about 180° . The explanation follows from the variations of period of waves that is present in irregular wave formations. However, owing to difficulty in extracting this information from records alternative methods for establishing the wave group, terms of reference have been devised. These methods include energy criteria, where waves having less than 10% of energy of the significant waves define a wave height decrease due to a phase change. This method, not being totally adequate in all cases reverts to the discontinuity method by period determination for fixing the ends of the group. The minimum number of waves forming a group is two, but it is not common to find this arrangement in isolation.

4.9.3 Irregular Waveforms In Wave Groups

Symmetry in waveform is not always maintained. The irregularities take the form of skewed, square or peaked at the crest area .

Wave groups define a wave height, H_g for wave groups in a fixed time recording. The maximum H_g and minimum H_g vary with recorded time. They average at less than the significant wave height. With time as an independent function, the same gradient for the significant wave height and the mean group height \bar{H}_g are noted. These values are related to the significant wave height. The above deductions have also been verified for the data obtained experimentally.

This latter criterion signifies wave grouping to be related to the Rayleigh distribution. Pierson, Neumann and James⁽¹⁴⁸⁾ (1966) related height parameters to other statistical parameters other than the significant wave height. For extreme values, the maximum predicted height in a record is related to within 10% larger than the maximum group wave height. This depends on the number of waves.

4.9.4 Group Velocity

Dispersive waves propagate under a common velocity known as the group velocity. This concept extends to the local effect of the sequence of waves acting together. The effect is expressed as a slowly modulated wave train advancing with group velocity C_G . This velocity is related to the individual wave velocity for constant depth conditions by,

$$C_G = \frac{C}{2} \left(1 + \frac{2kd}{\sinh 2kd} \right) \quad (4.100)$$

The simplification to deep water conditions gives,

$$C_G \approx \frac{C}{2} \quad \text{for } kd \gg 1 \quad (4.101)$$

$$C_G \approx C \quad \text{for } kd \ll 1, \text{ with shallow water conditions} \quad (4.102)$$

The group velocity is exceeded by the phase velocity for general depths. This permits the wave crests travelling from the tail end towards the front of the group. The dynamical meaning of a group velocity is its velocity by which the energy of the waves is moved forward. This description contrasts with the phase velocity which is a concept associated with the movement within the bounded area of a local wave, that is, the kinematic qualities of the wave.

The time interval between two successive breakers can be expressed in terms of a group velocity. From the velocity of the group travelling at half the phase velocity it follows that two crests reach the peak after a time interval of two periods. If the steepness at the peak is large enough to cause instability, the breakers occur every two periods. This produces the white crests of breakers ⁽¹⁴⁹⁾.

4.10 DESCRIPTION OF WATER BEHAVIOUR ON IMPACT

Consider a mass of water of wave height H_b at mean water level d_b . The crest of a wave breaking on the wall causes an impact judged by the slamming on the wall. This is the part of the study when the high impact pressures are reached. These impact pressures act over a relatively short period of time.

On impact the momentum of the water mass is reduced to zero and the physical volume of water is limited to moving vertically up the wall. After the maximum point of its trajectory, the water mass then descends to generate a secondary pressure acting over a longer period of time. This pressure acts, together with the remaining mass of water of the broken wave, to make up the secondary pressure acting over a wider area than the impact pressure.

The pressure-time history is a measure of loading on the structure. The quick rising high pressure produces a certain degree of damage. It is the longer duration of the secondary pressure, which lasts for an appreciable portion of the wave period, that has detrimental effects and needs to be designed for.

In an earlier section (see section 4.8.2), it has been shown that the breaking of a wave on the seawall is a basis of all large impact pressures. The secondary pressure mentioned above can also occur when no breaking occurs and is comparable, in magnitude, to a standing wave set up at the wall. The vertical distribution of this pressure compares to the hydrostatic pressure but is larger in magnitude.

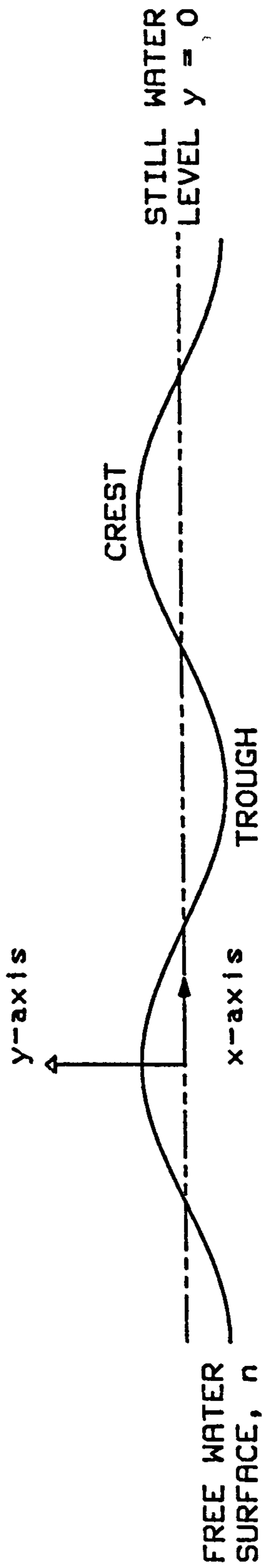
This is because of the falling mass of water after impact. The location of the centre of pressure lies above the S.W.L. for steep waves and falls below in case of low waves. The description of a secondary pressure in the absence of impact pressure shows that this type of pressure is more general to varied sea states (occurring during the life span of the structure).

The duration of the secondary pressure relates to the period of wave of approach ($0.1T$ to $0.5T$). This significant value of time together with the pressure measured, show that secondary pressures need more consideration in the design of maritime structures. These values are related to the design wave characteristics by a linear variation about the still water level, y . The steepness of the wave H_o/L_o is a measure of the breaking height of the wave, h_b for a given water depth.

Experimental results have shown a 300% increase over the hydrostatic pressure due to the mass of water (See 4.8.3). This occurs at the still water level. Also the distribution of the pressure is verified as being linear. The extension of the dynamic pressure above the still water pressure runs at six times the assumed wave height of the wave measured before reaching the wall.

WAVE HEIGHT, H is the vertical distance between a crest and a trough

λ WAVELENGTH, L



\Rightarrow WAVE VELOCITY, $c = \frac{L}{T}$



PERIOD, T is the time taken between successive crests or troughs

FIG. 4.1 REFERENCE FRAME AND DEFINITION OF TERMS

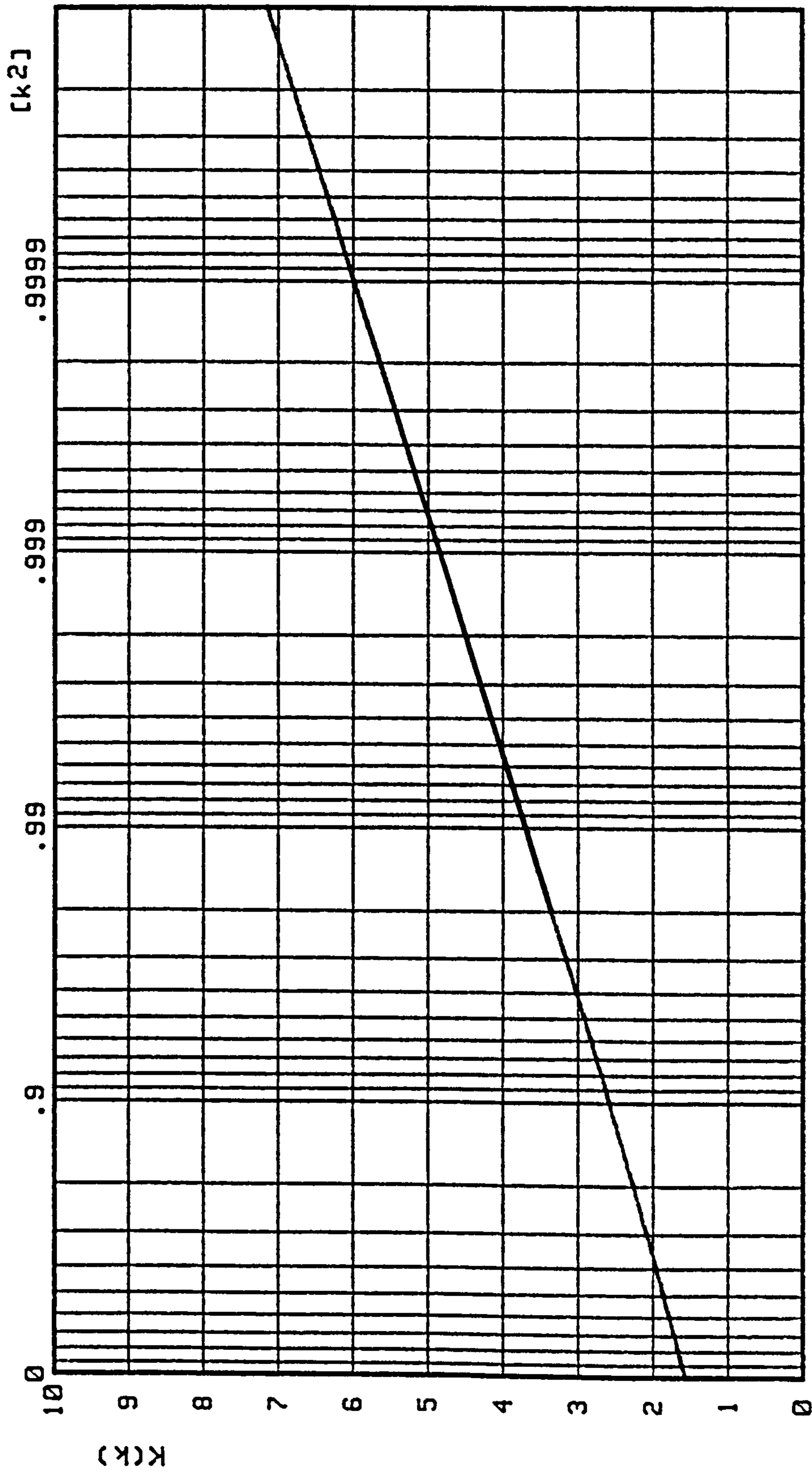


FIG 4.2

GRAPH of $K(k)$ vs. k^2

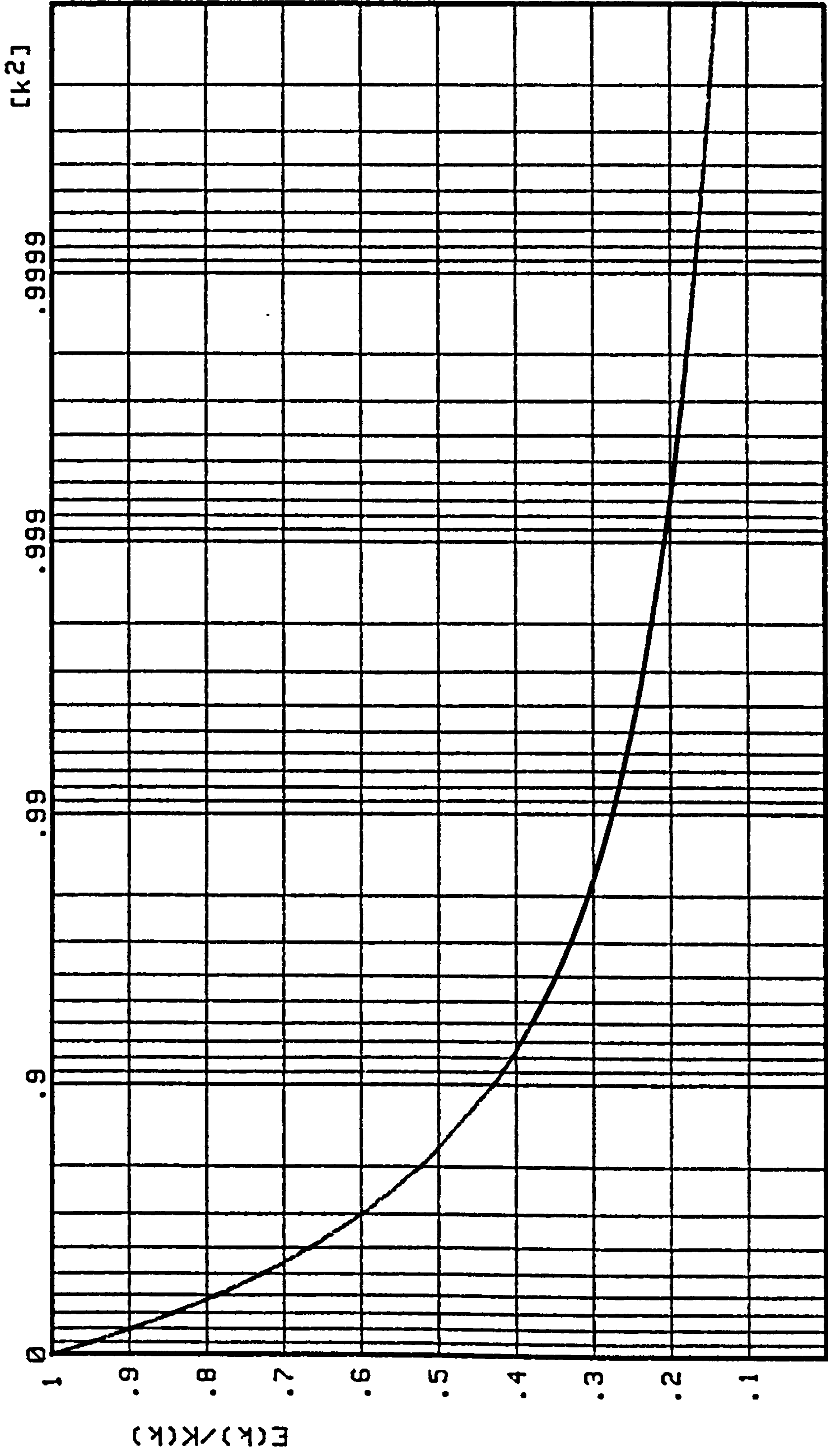


FIG 4.3

GRAPH of $E(k)/K(k)$ vs. k^2

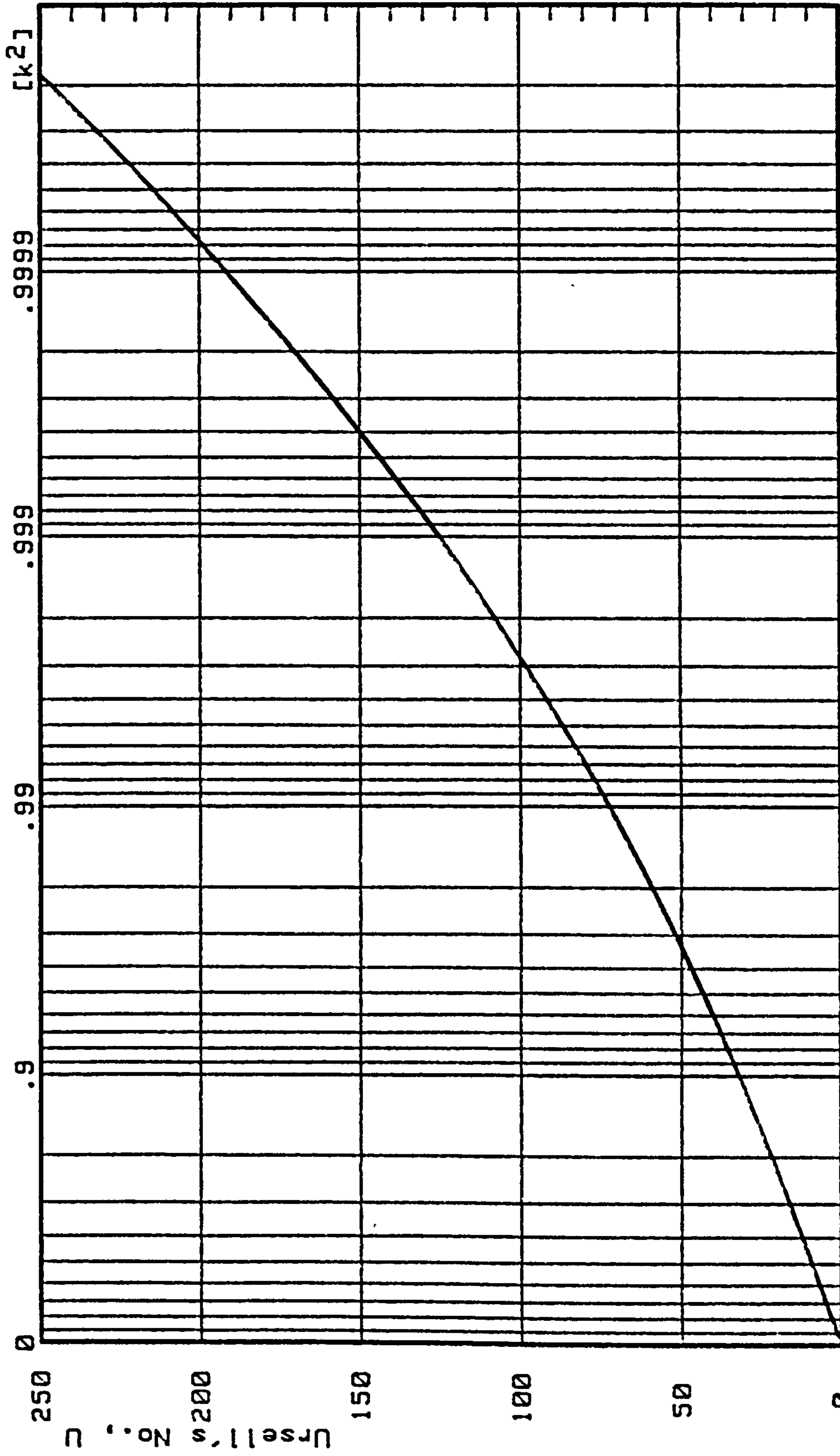


FIG 4.4

GRAPH of U vs. k²

FIG 4.5
 CNOIDAL FREE SURFACE ELEVATION WITH WAVELENGTH

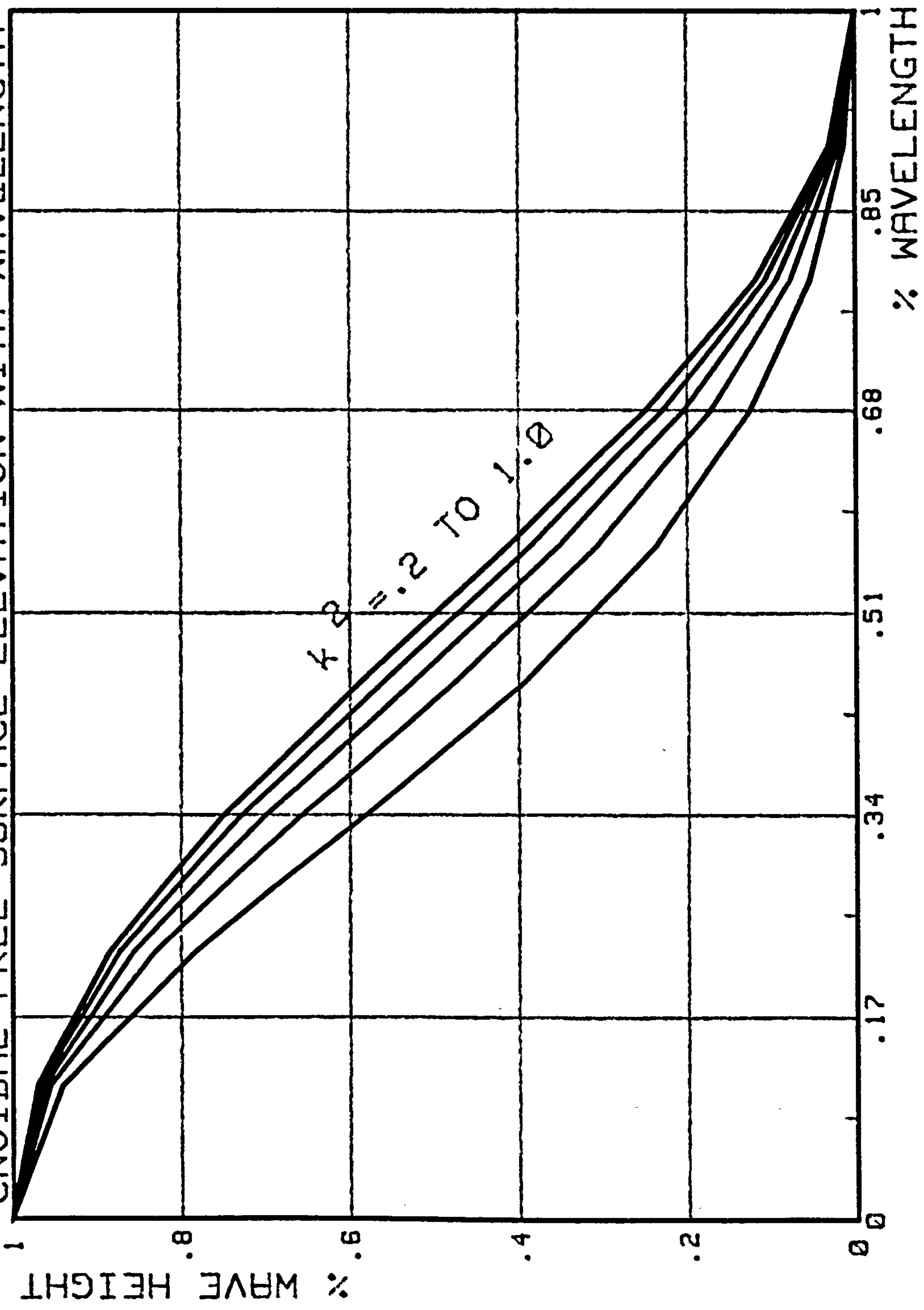


FIG 4.6

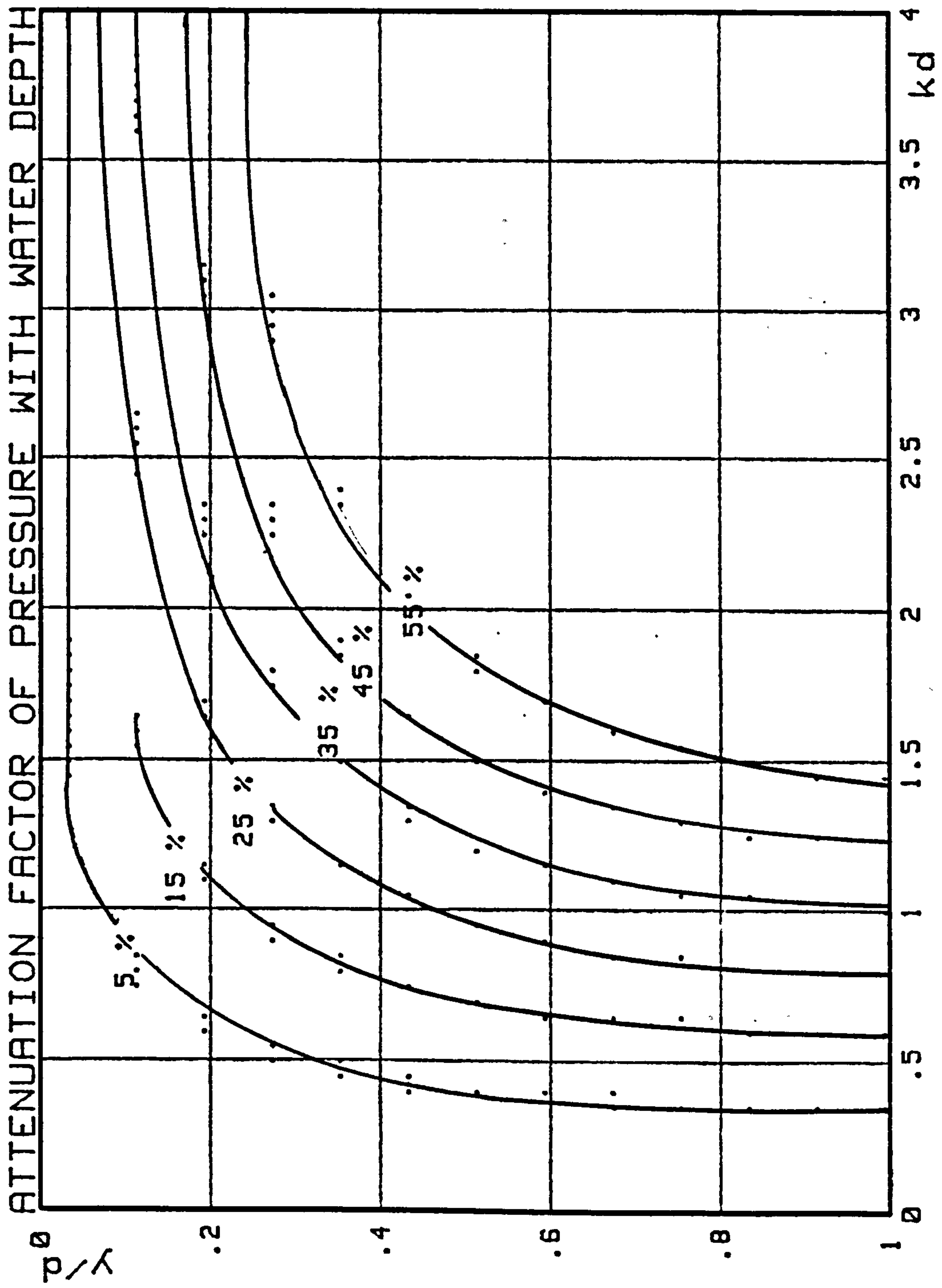
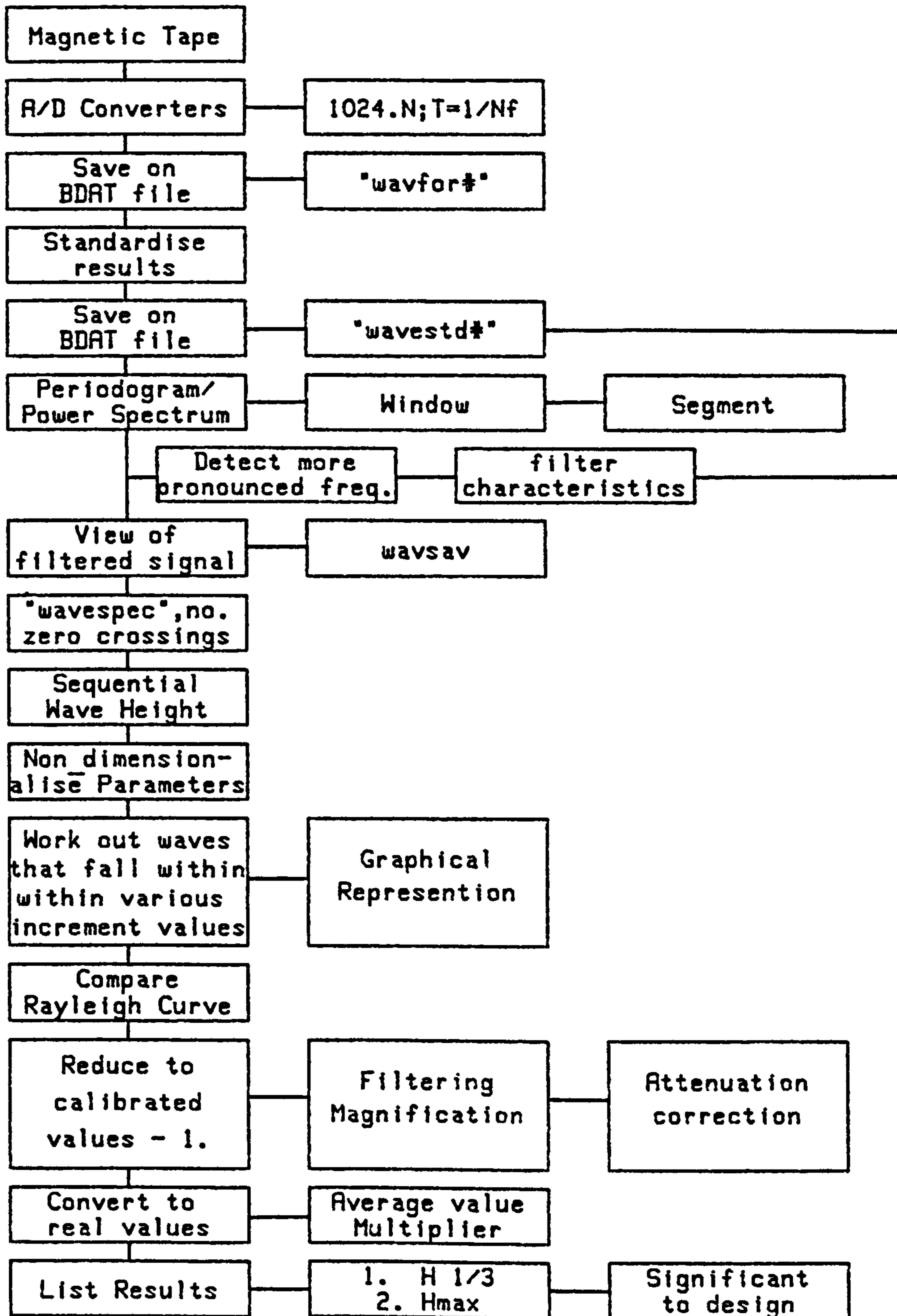
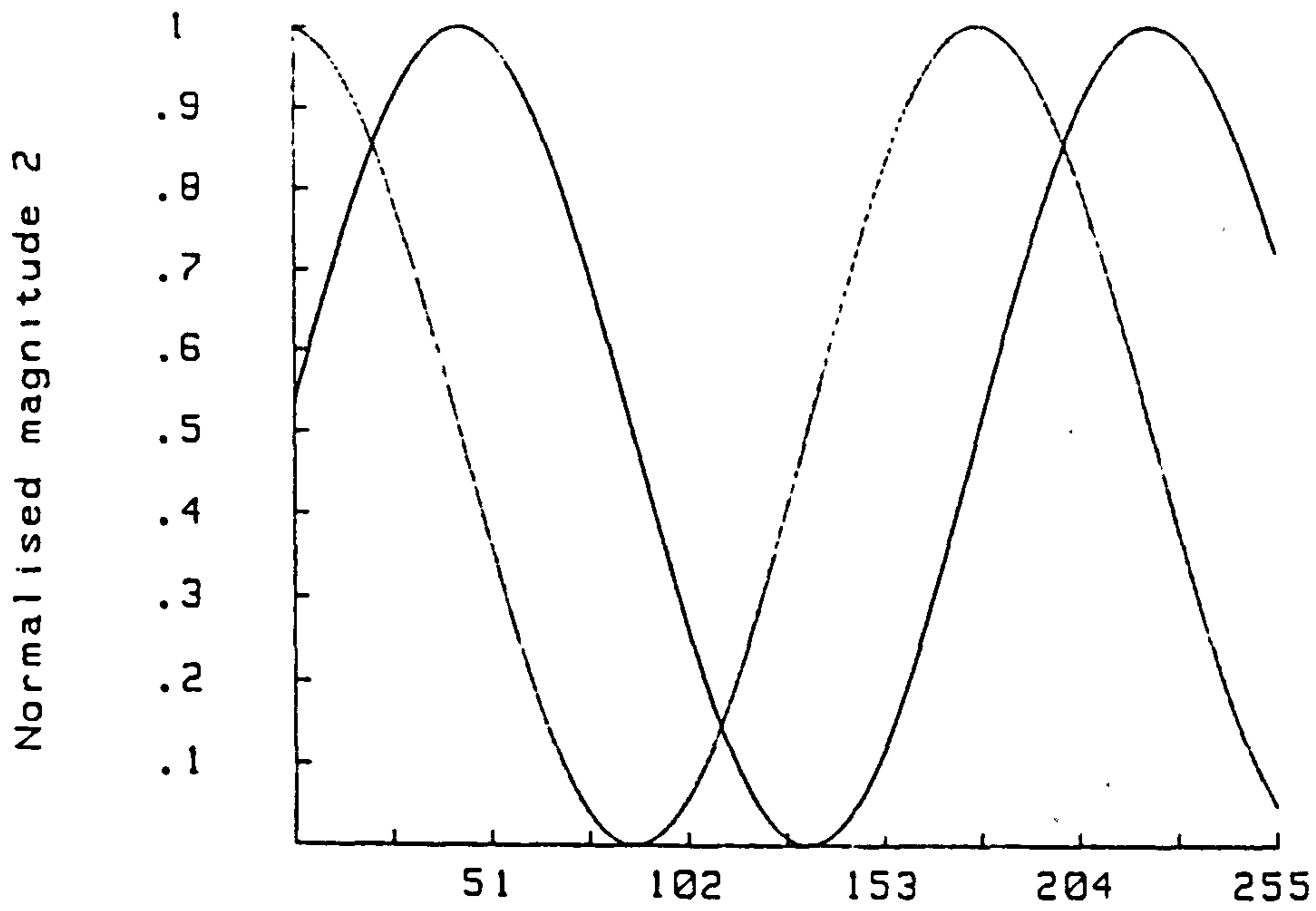


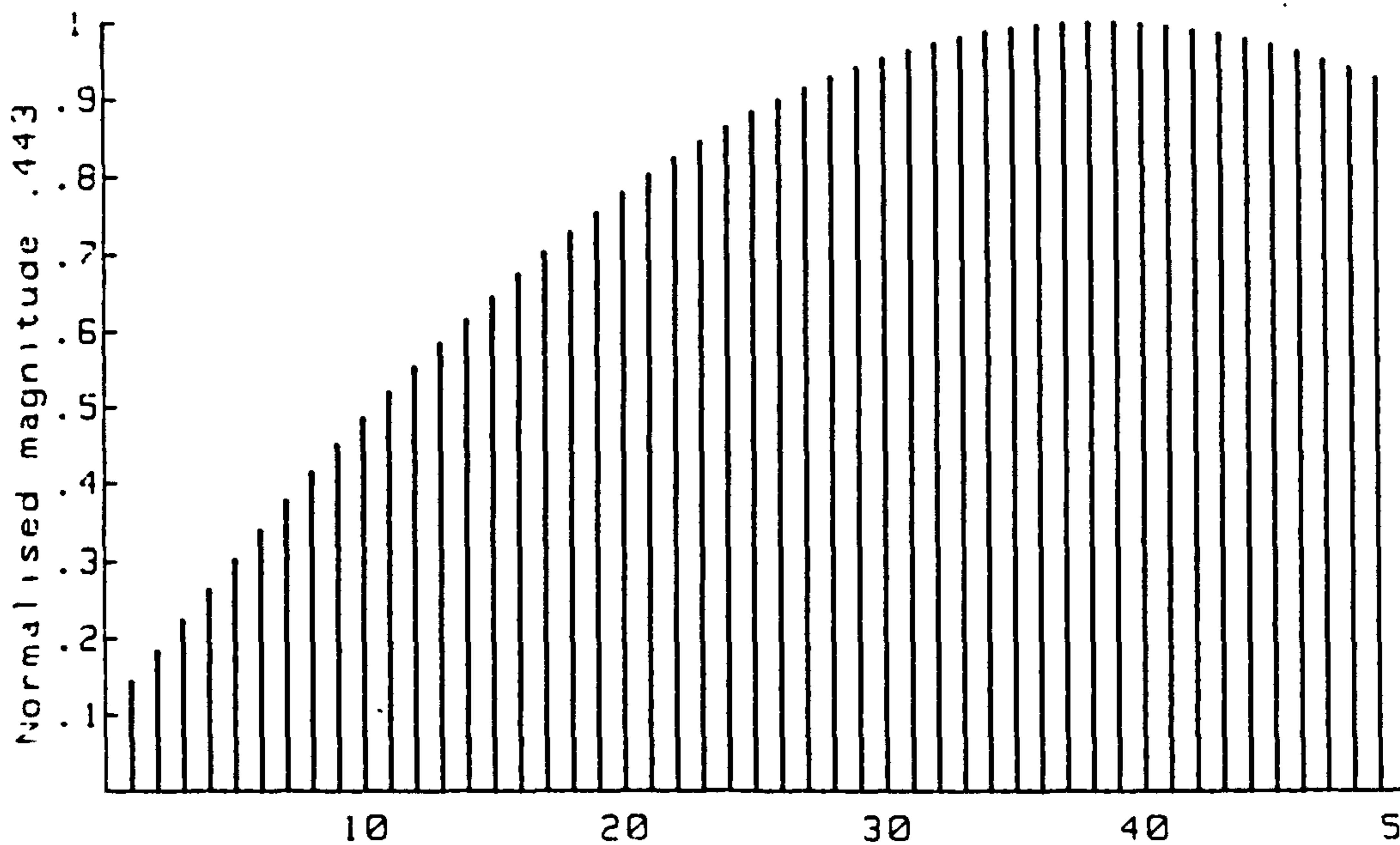
FIG 4.7 FLOW DIAGRAM FOR THE DETERMINATION OF WAVE CHARACTERISTICS, (H_s, T_s)





SAMPLE FREQUENCY 1 Hz.
 SAMPLE LENGTH 255 sec.

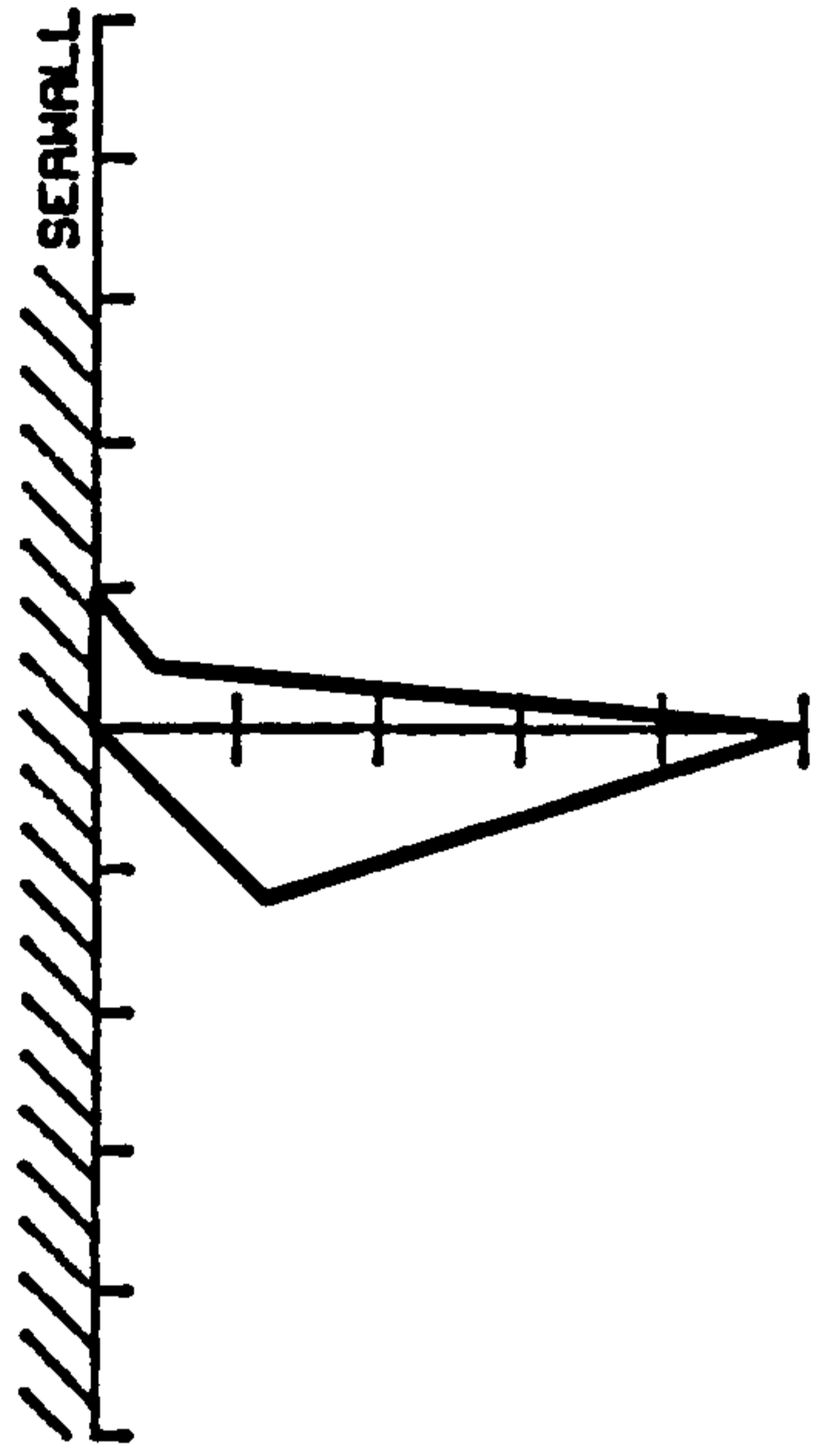
[sec.]



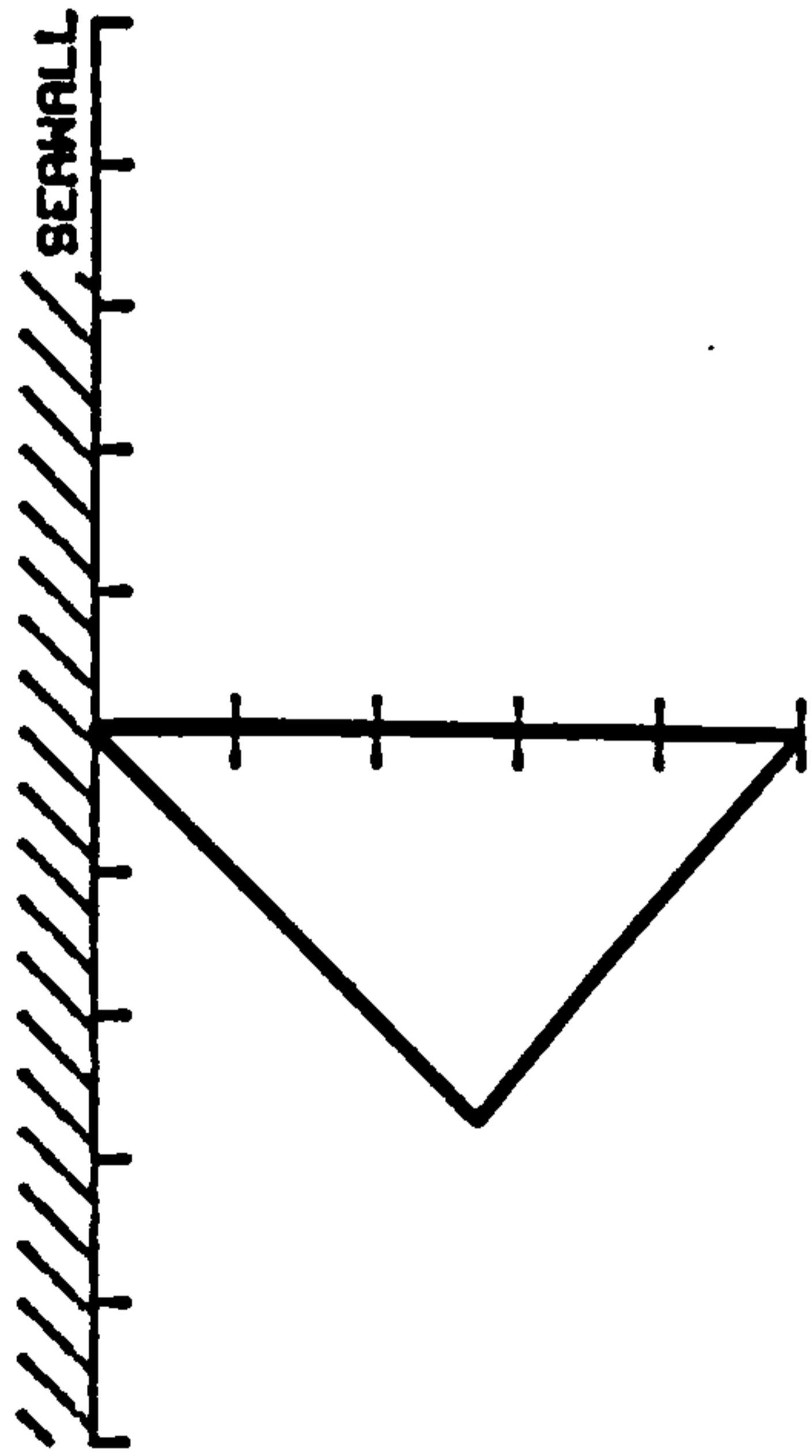
SAMPLE FREQUENCY 1 Hz.
 SAMPLE LENGTH 50 sec.

[sec.]

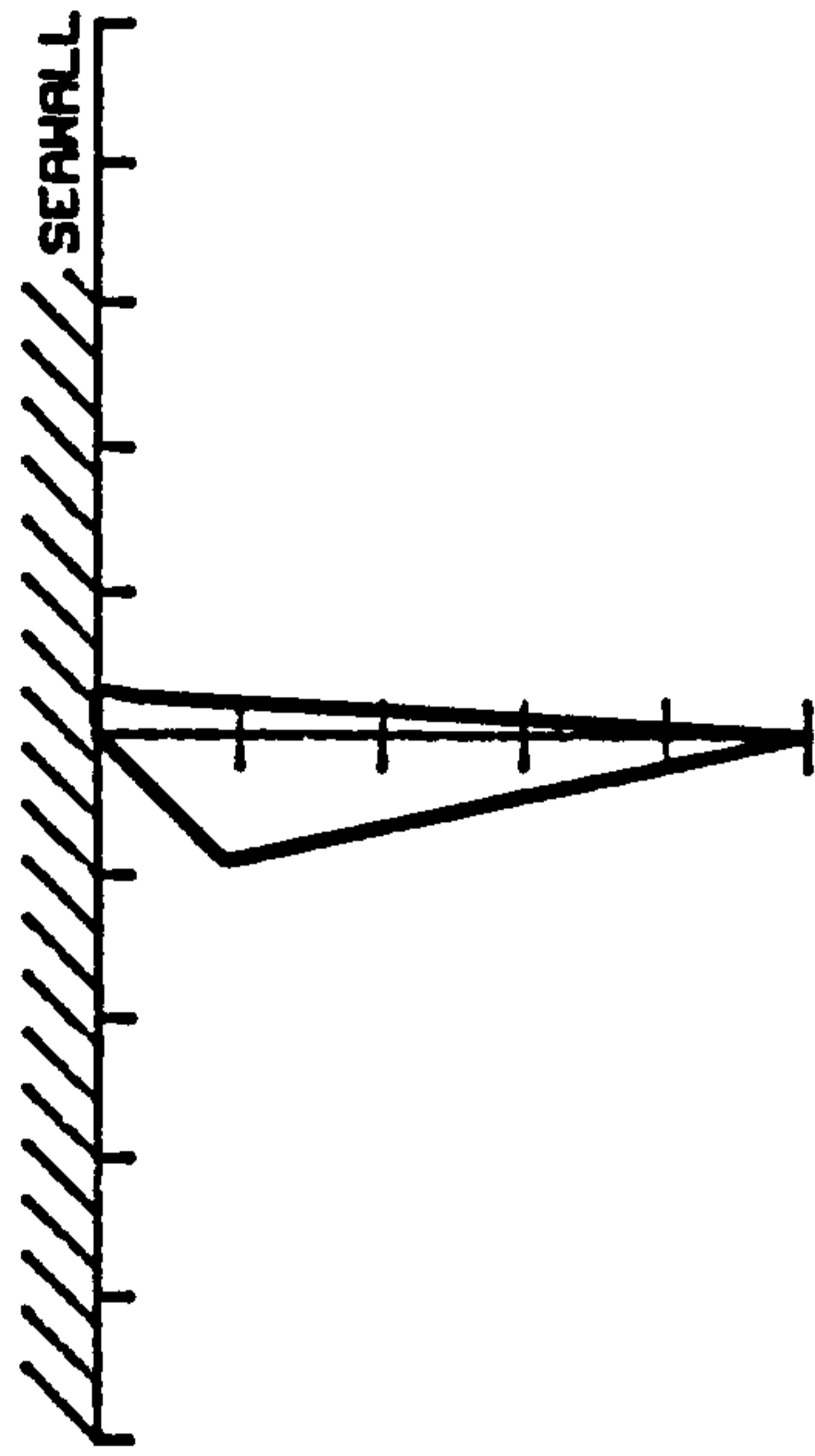
FIG 4.8 CROSS CORRELATION OF TWO SIGNALS
 DELAYED BY AN UNKNOWN TIME DIFFERENCE



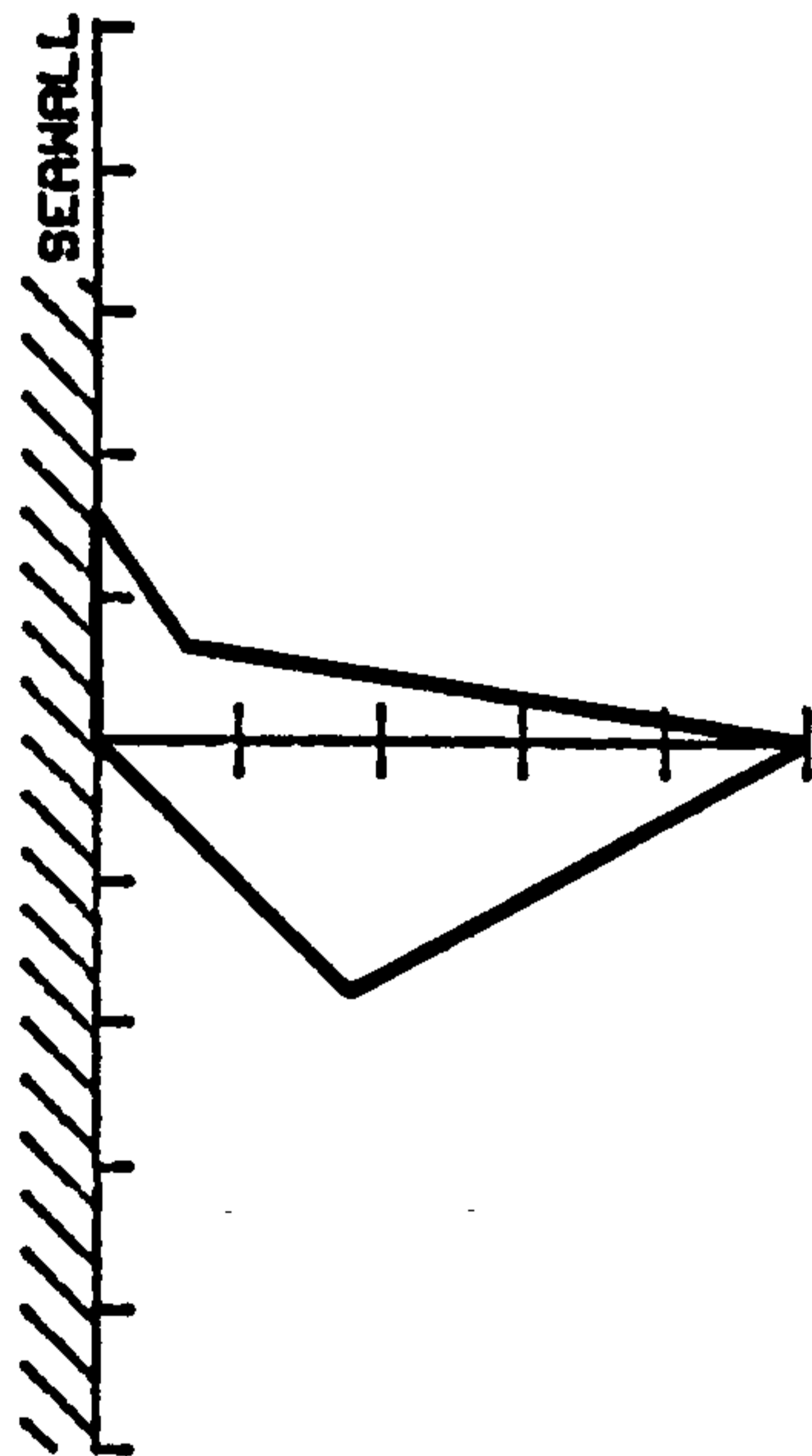
normalised celerity 7.42 m/s.



normalised celerity 9.8 m/s.



normalised celerity 10 m/s.



normalised celerity 9.74 m/s.

FIG 4.9 VELOCITY AND DIRECTION OF WAVE ACTION RELATIVE TO SEAWALL

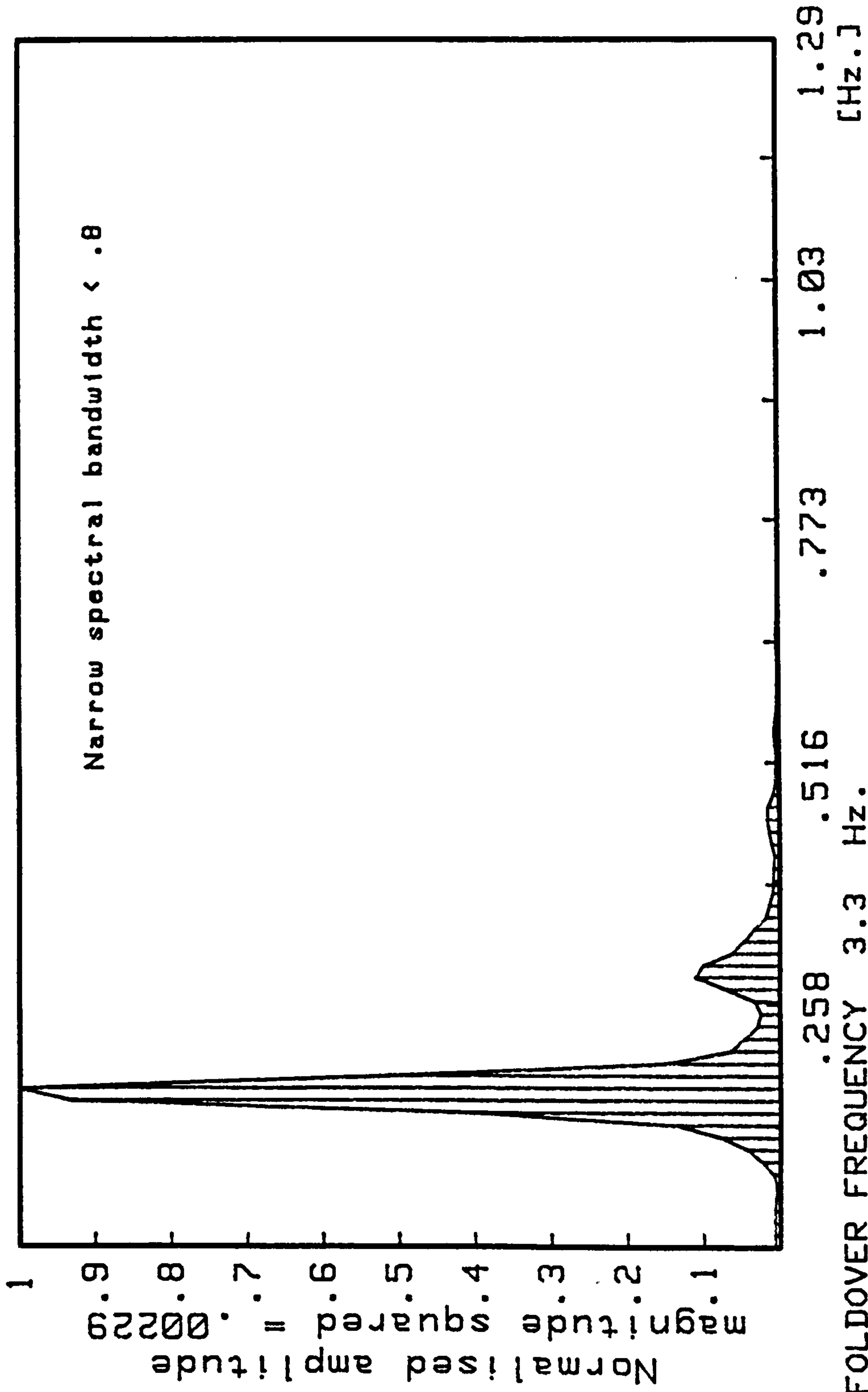
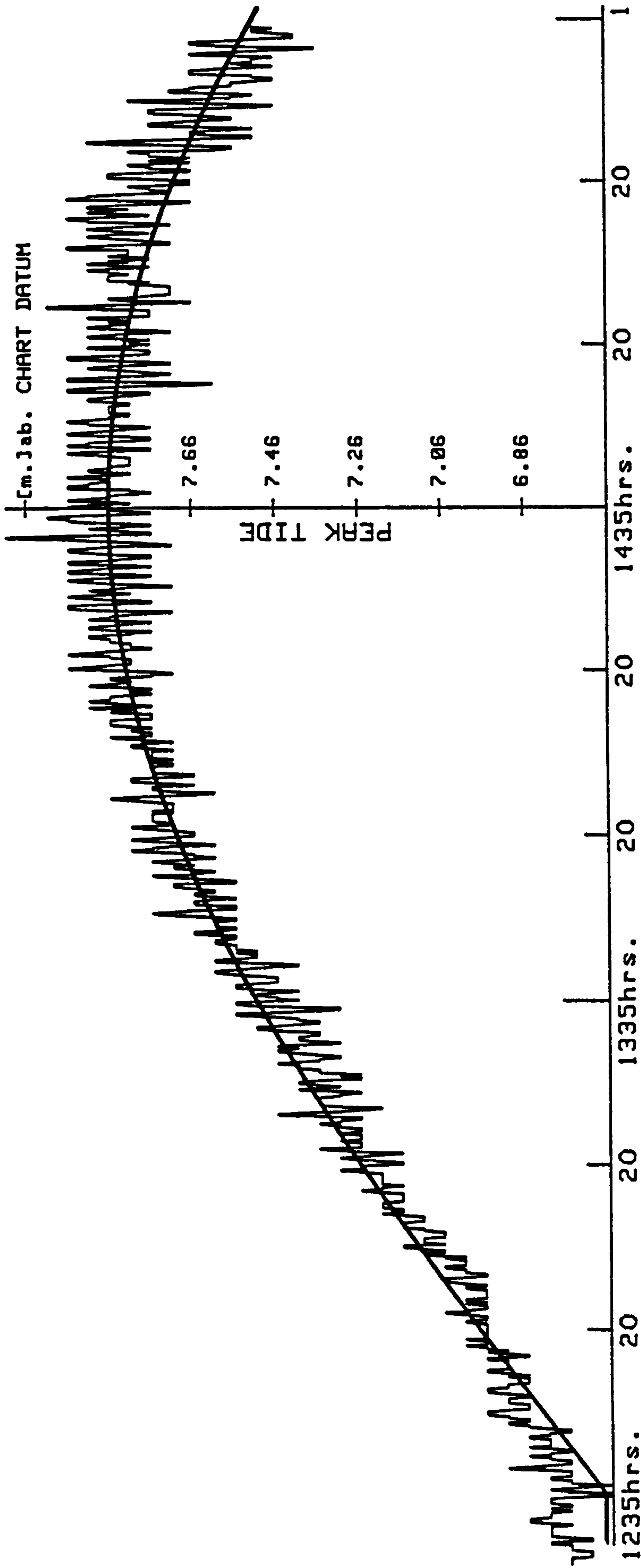


FIG 4.10 POWER SPECTRUM OF WAVE PROFILE (as seen in FIG 4.14)



Time of Sample = 44 secs. at a speed of 32 times real time

FIG. 4.11 GRAPH OF THEORETICAL TIDAL CURVE vs. EXPERIMENTAL CURVE

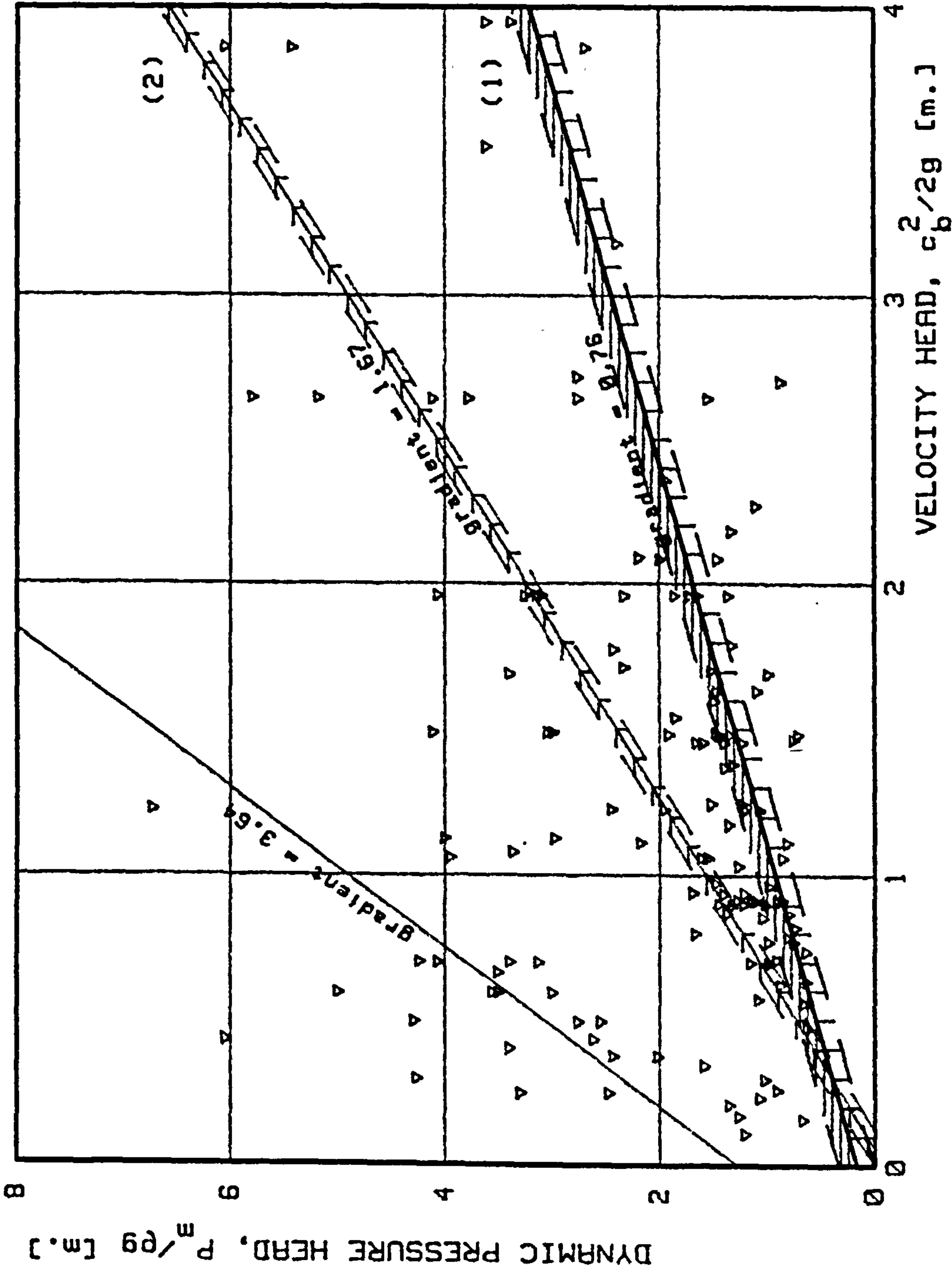


FIG 4.12 DYNAMIC PRESSURE MEASURED ON SEAWALL AGAINST WAVE VELOCITY
 (1) $P = 1/2 \rho v^2$ (2) $P = \rho v^2$

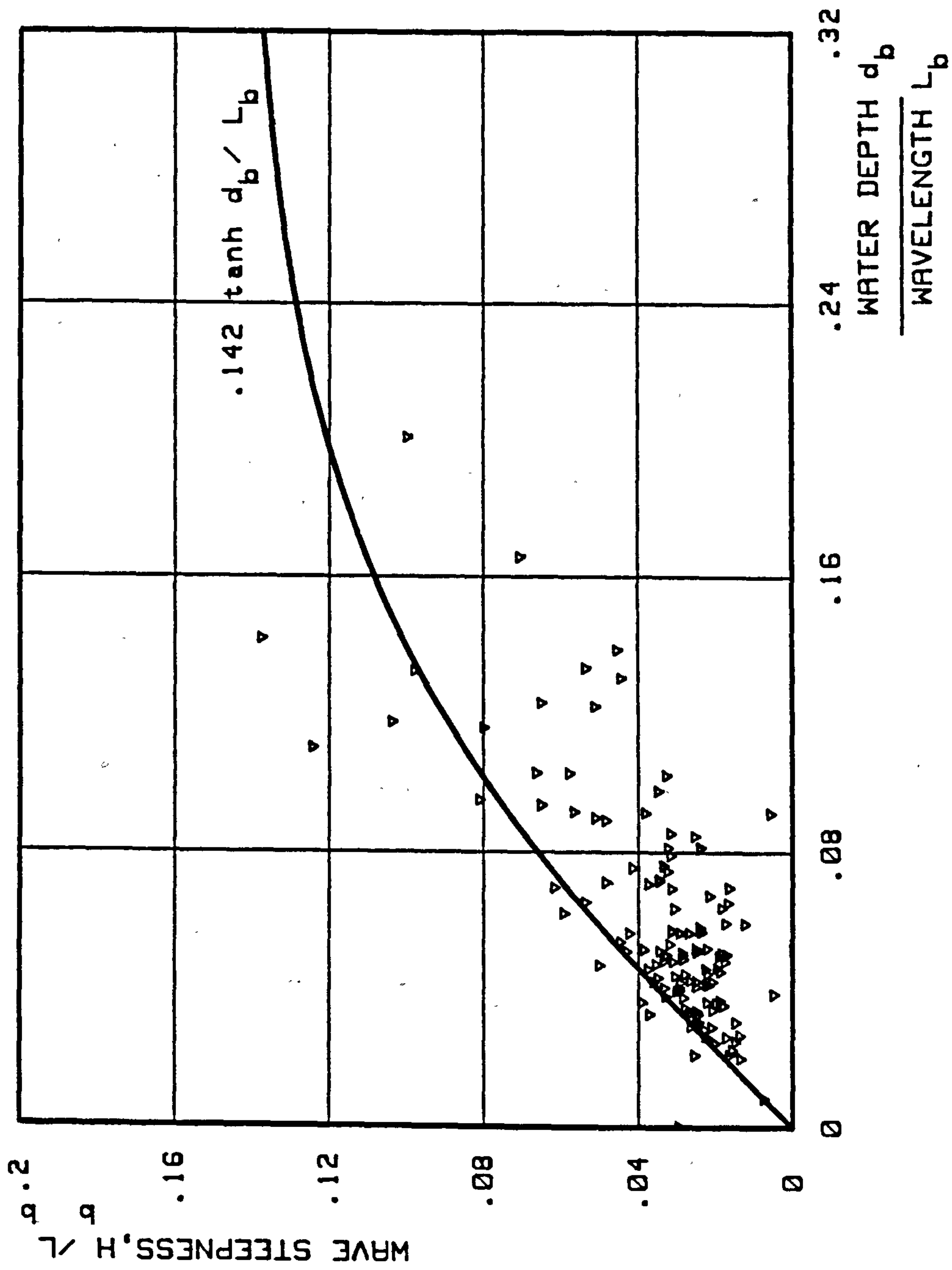


FIG 4.13 THE LIMITING STEEPNESS OF EXPERIMENTAL AGAINST THEORETICAL WAVES

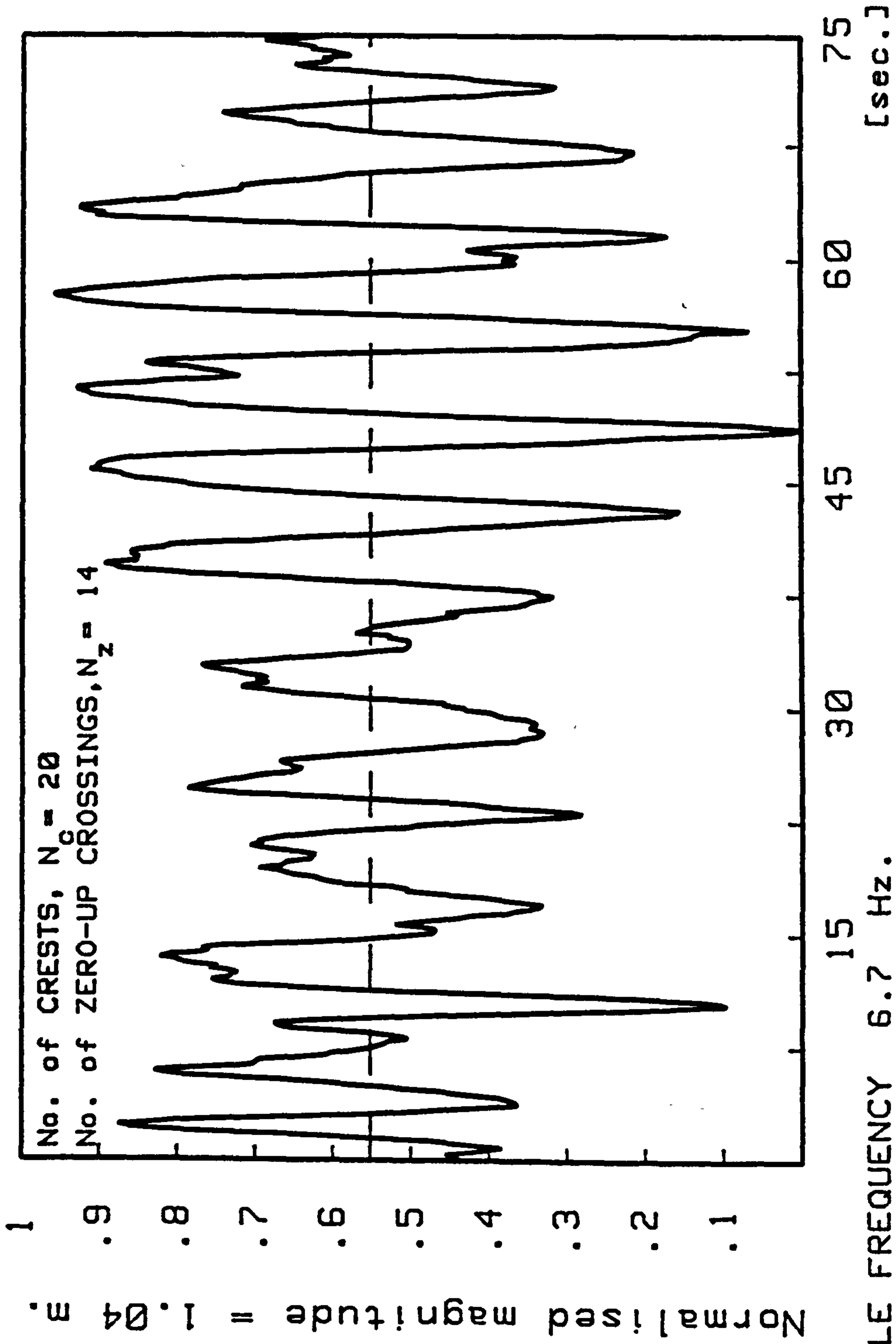


FIG 4.14 WAVE PROFILE SHOWING DOUBLE PEAKS AT WAVE CREST.

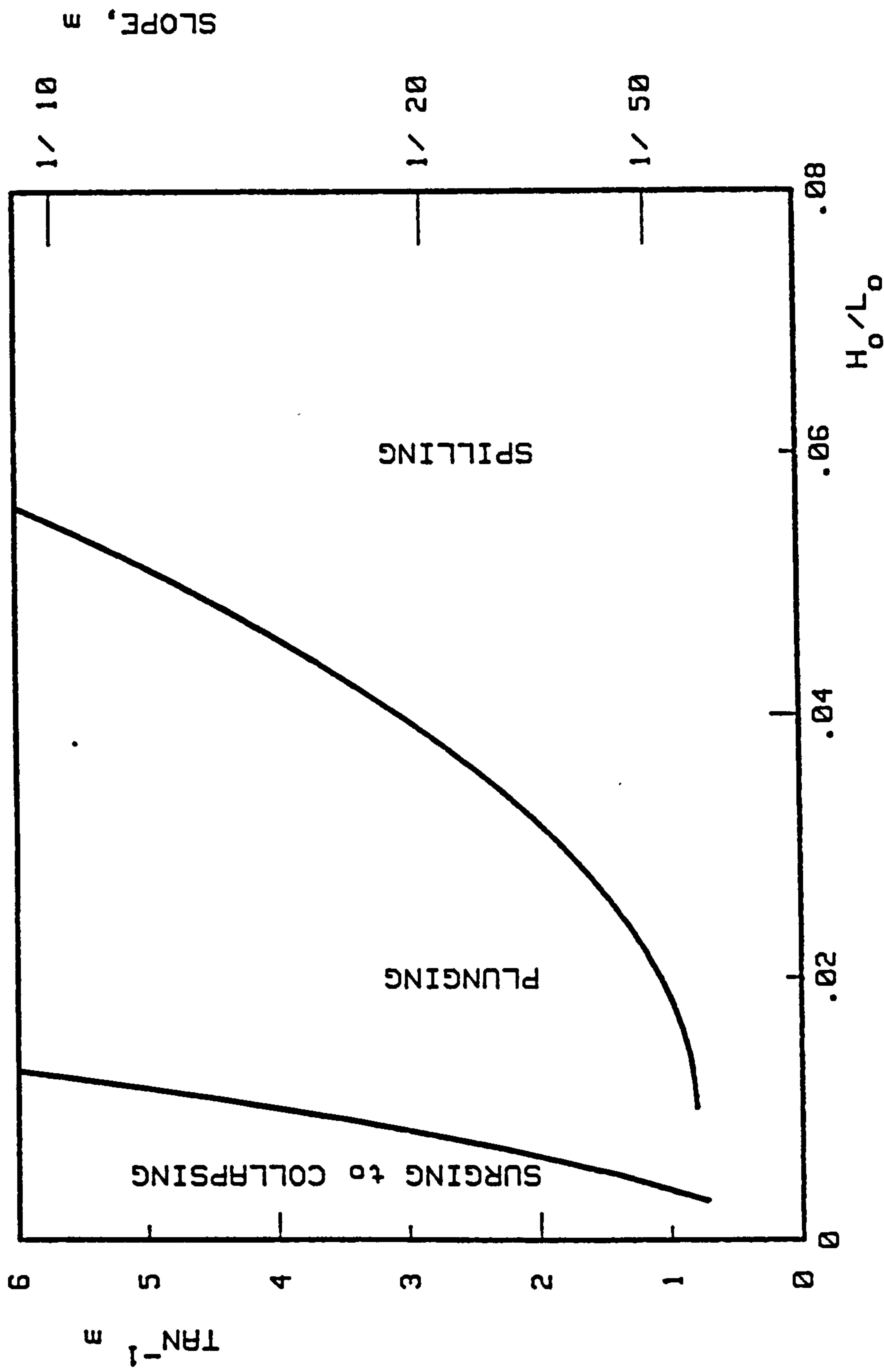


FIG 4.15 WAVE STEEPNESS AGAINST BEACH SLOPE WITH TYPE OF BREAKER FORMATION

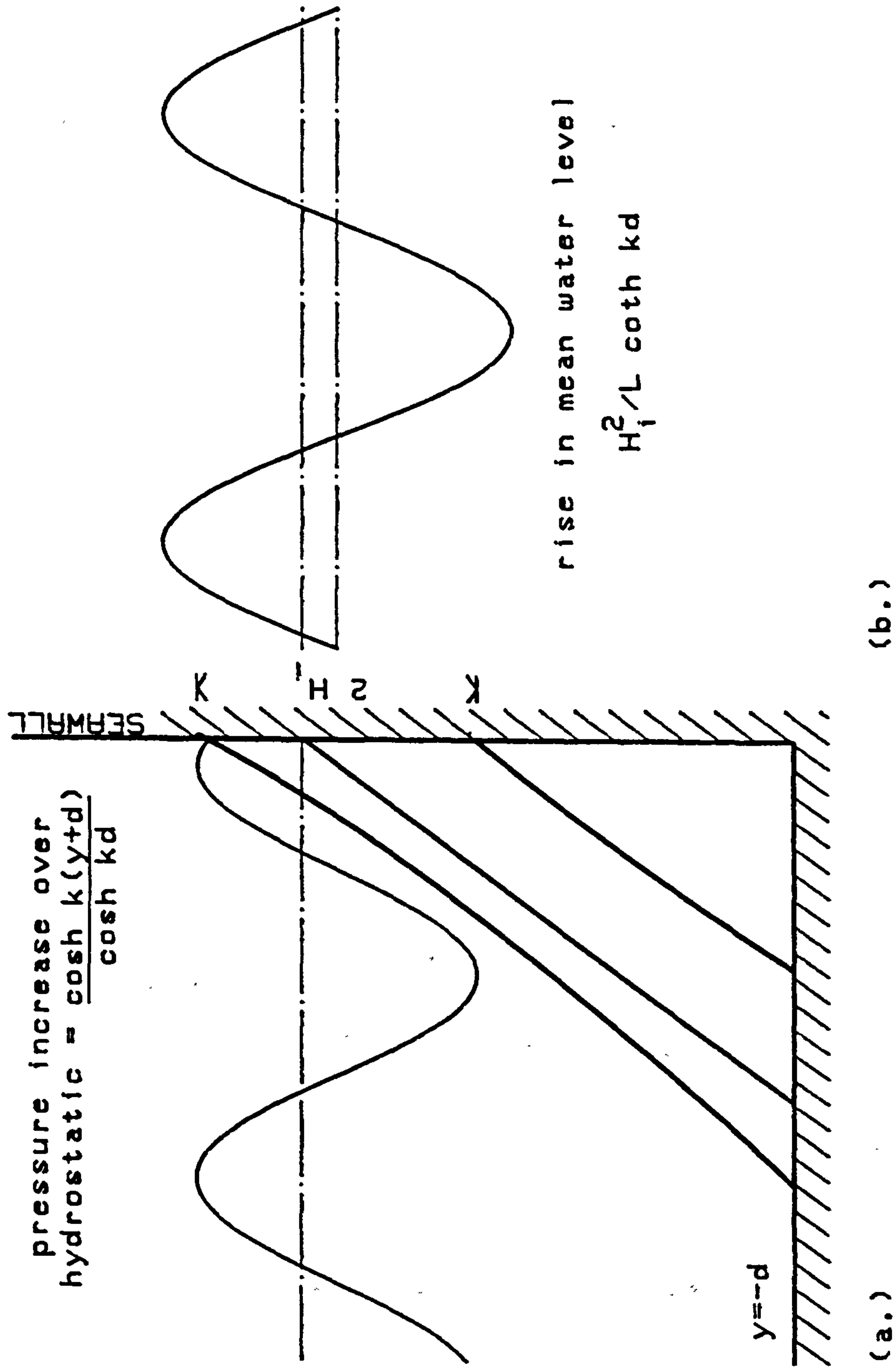
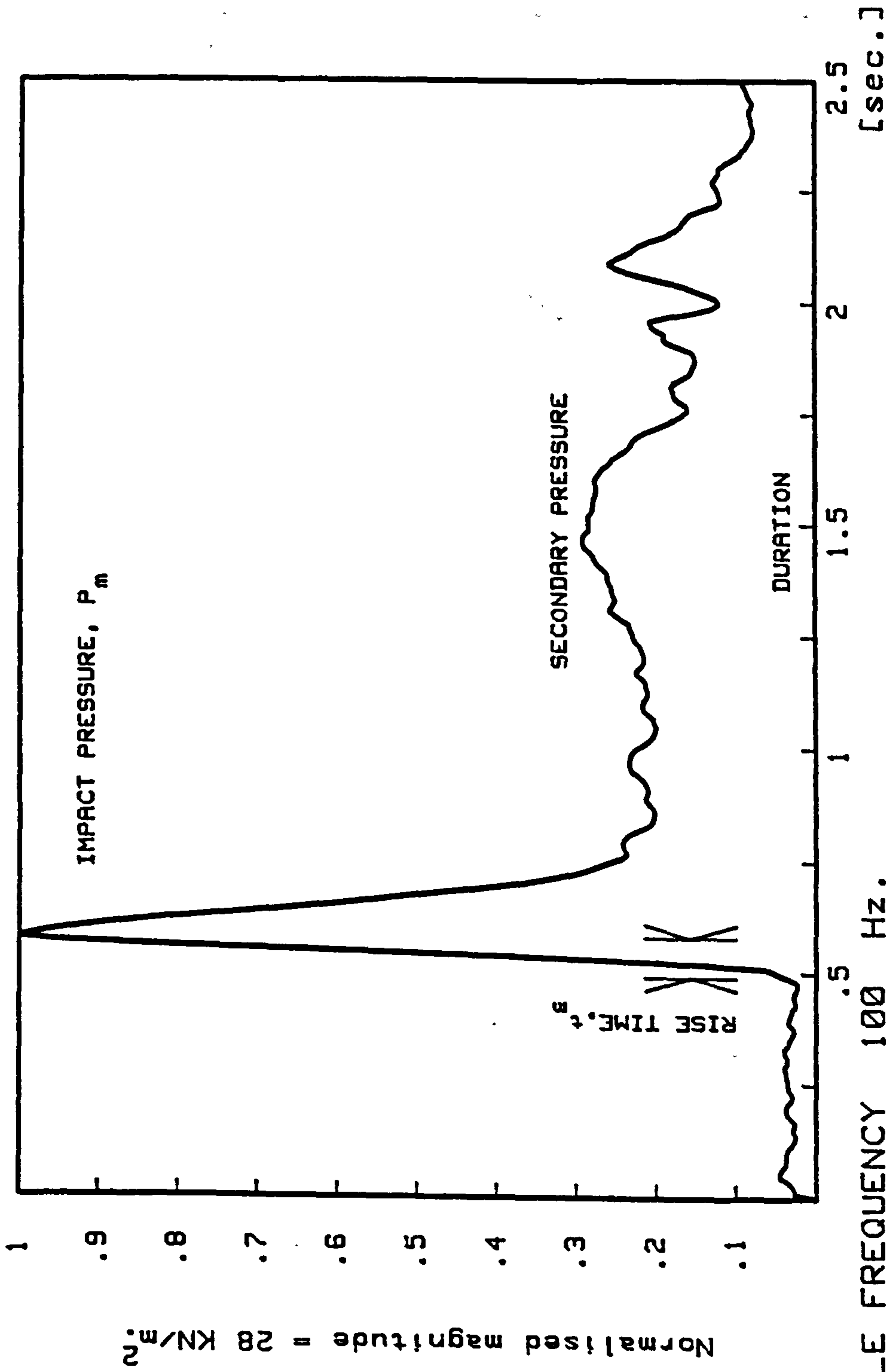


FIG 4.16 STANDING WAVE PRESSURE DISTRIBUTION AT SEAWALL



SAMPLE FREQUENCY 100 Hz.

SAMPLE LENGTH 2.5 sec.

FIG 4.17 IMPACT AND SECONDARY PRESSURE CHARACTERISTICS
AS MEASURED ON SEAWALL

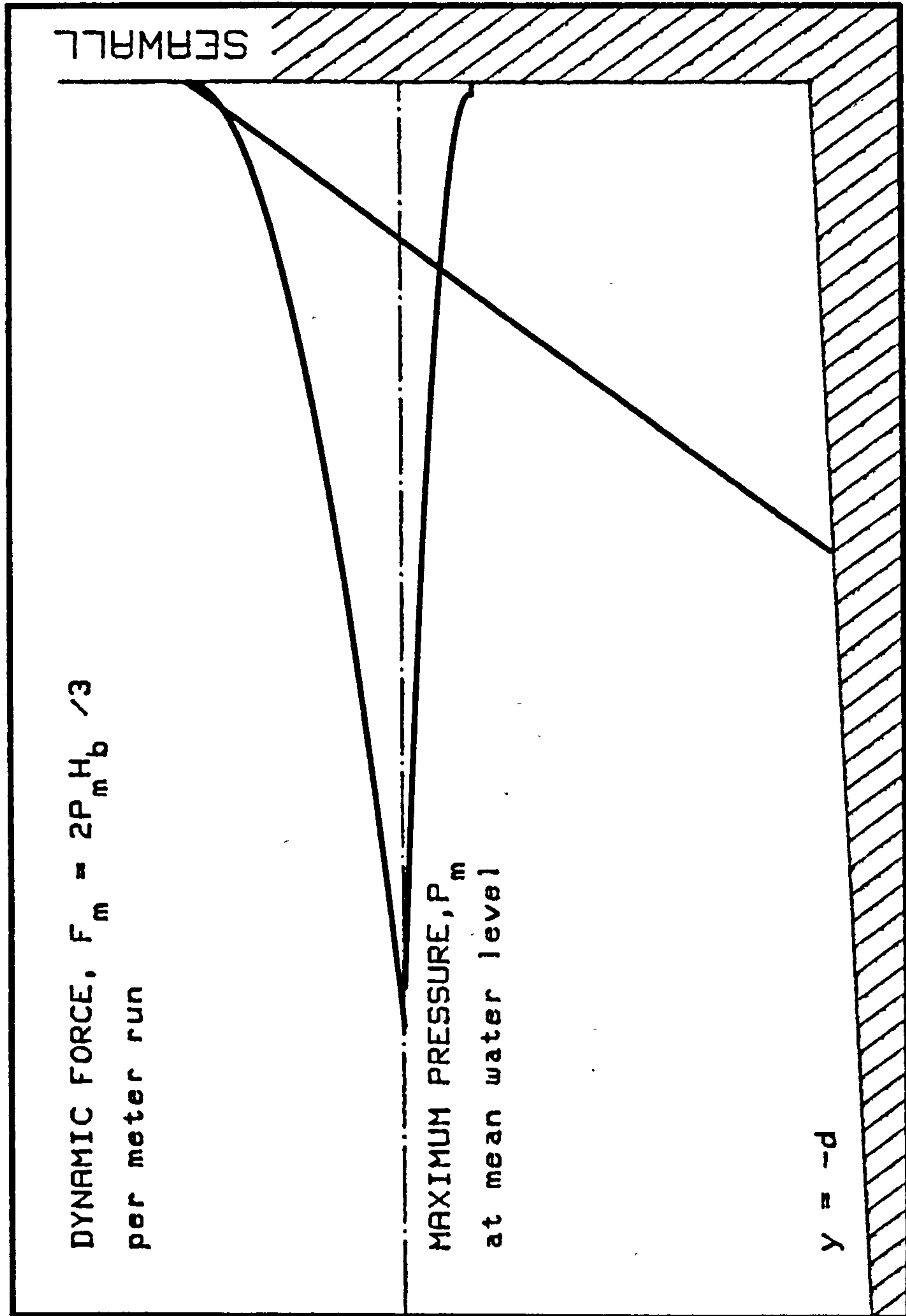
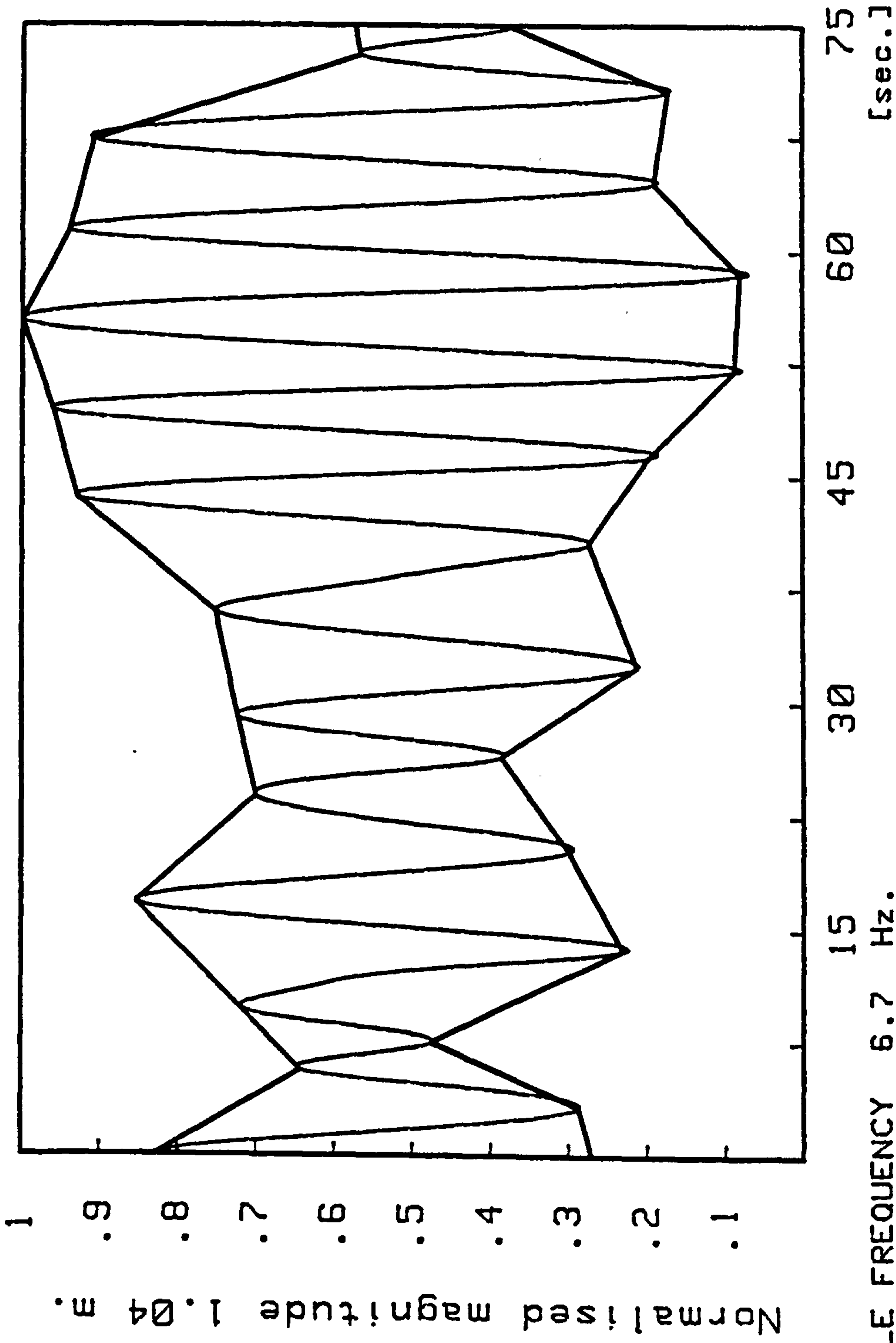


FIG 4.18 PRESSURE DISTRIBUTION OF A WAVE IMPACT ON THE SEAWALL



SAMPLE FREQUENCY 6.7 Hz.

SAMPLE LENGTH 75 sec.

FIG 4.19 WAVE GROUPING WITH AN UNDERLYING LOW FREQUENCY COMPONENT

Pt= 10

Pt= 1

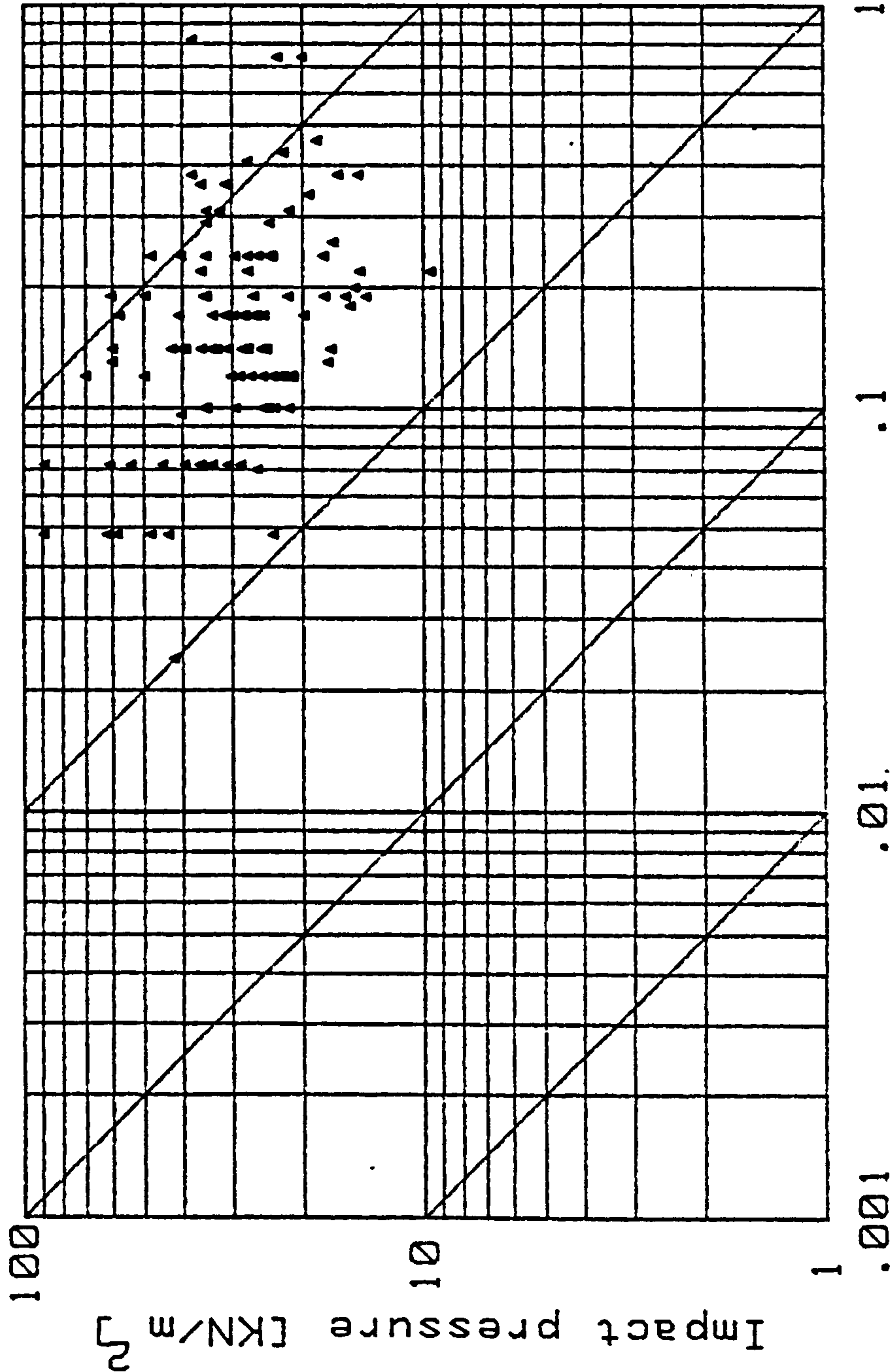


FIG 4.20(a) IMPACT PRESSURE WITH RISE TIMES
MEASURED ON SEAWALL
DATA FROM ILFRACOMBE AND BOVISANDS.
(See Tables 4.1.1 to 4.6.6)

Pt= 1 Pt= 10

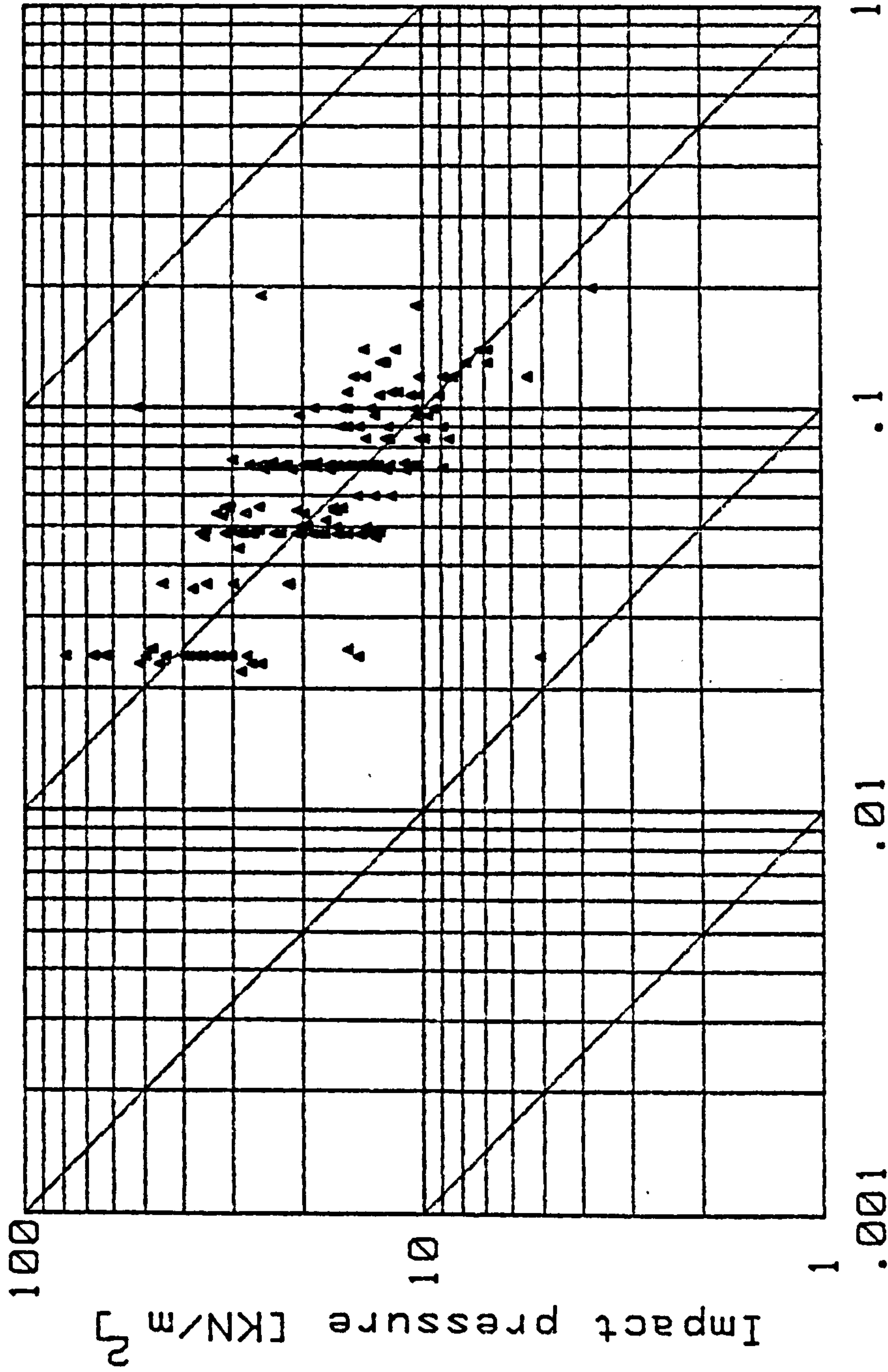


FIG 4.20(b) IMPACT PRESSURE WITH RISE TIMES
MEASURED ON SEAWALL
DATA FROM ILFRACOMBE AND BOVISANDS.
(See Tables 4.1.1 to 4.6.6)

Pt= 1 Pt= 10

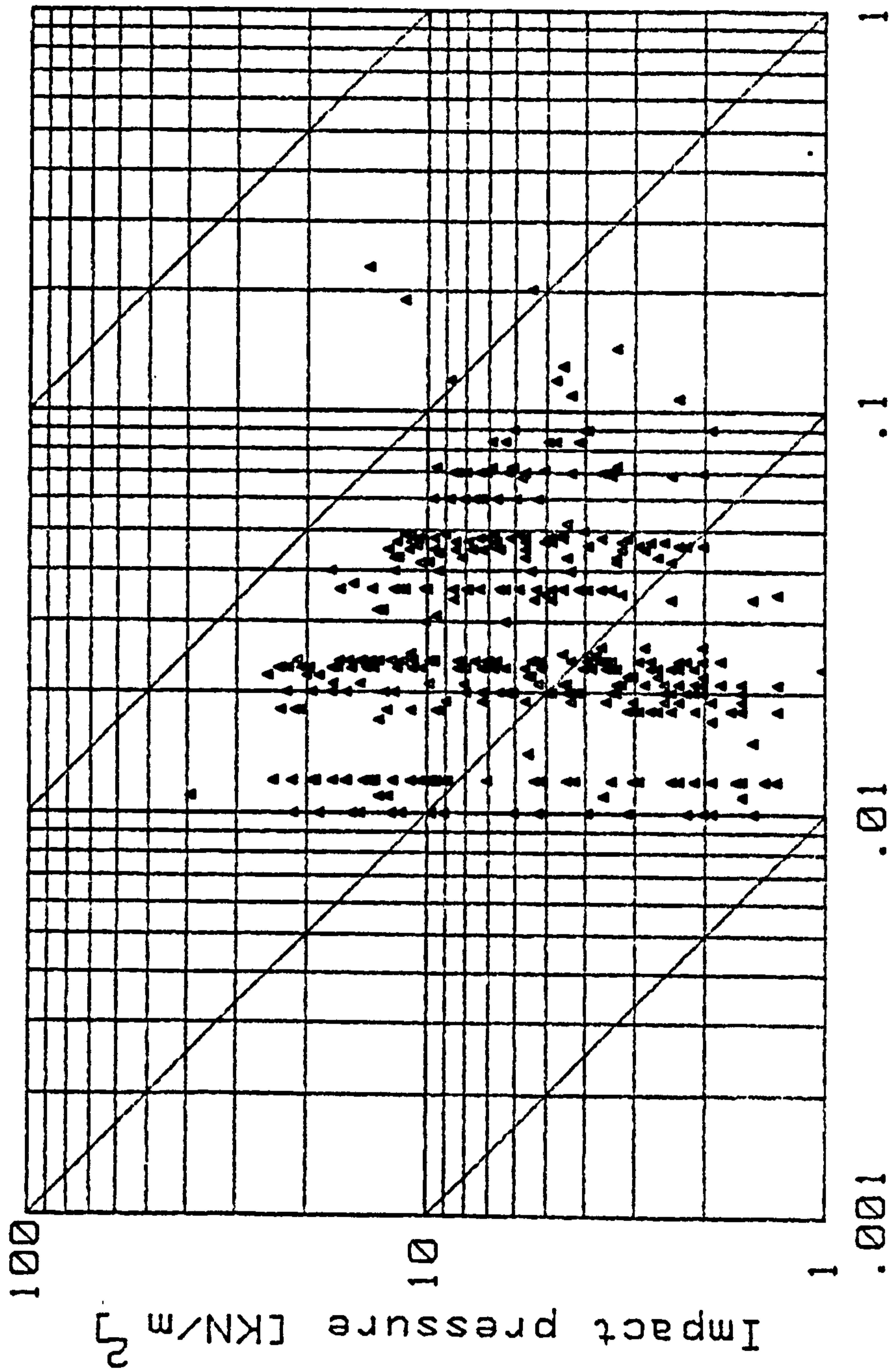


FIG 4.20(c) IMPACT PRESSURE WITH RISE TIMES
MEASURED ON SEAWALL
DATA FROM ILFRACOMBE AND BOVISANDS.
(See Tables 4.1.1 to 4.6.6)

Pt = 1 Pt = 10

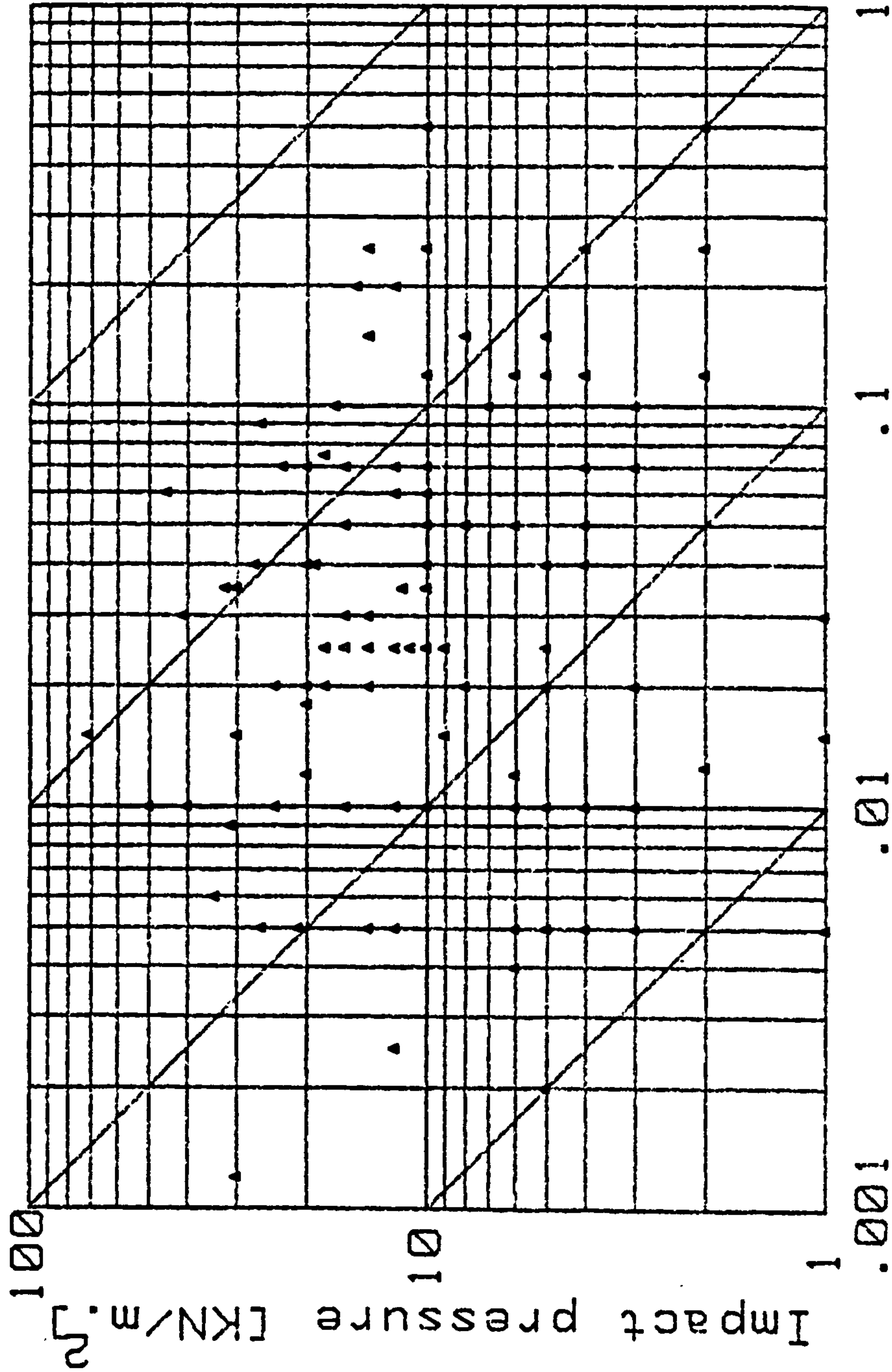


FIG 4.20(d) IMPACT PRESSURE WITH RISE TIMES
MEASURED ON SEAWALL
DATA FROM ILFRACOMBE AND BOVISANDS.
(See Tables 4.1.1 to 4.6.6)

Pt = 1 Pt = 10

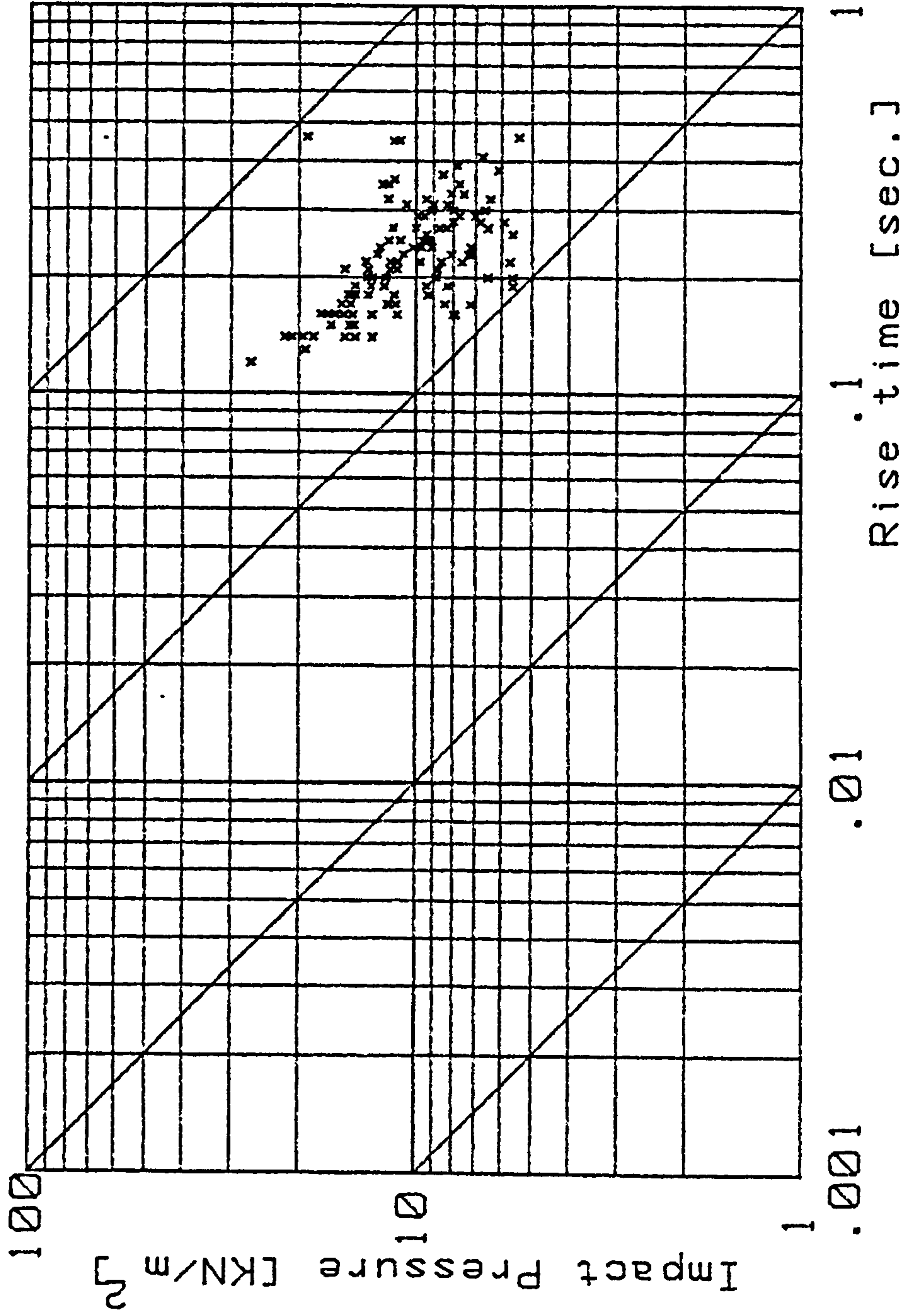


FIG 4.20(e) IMPACT PRESSURE WITH RISE TIMES
MEASURED ON SEAWALL
DATA FROM ILFRACOMBE by P. Blackmore (1982).

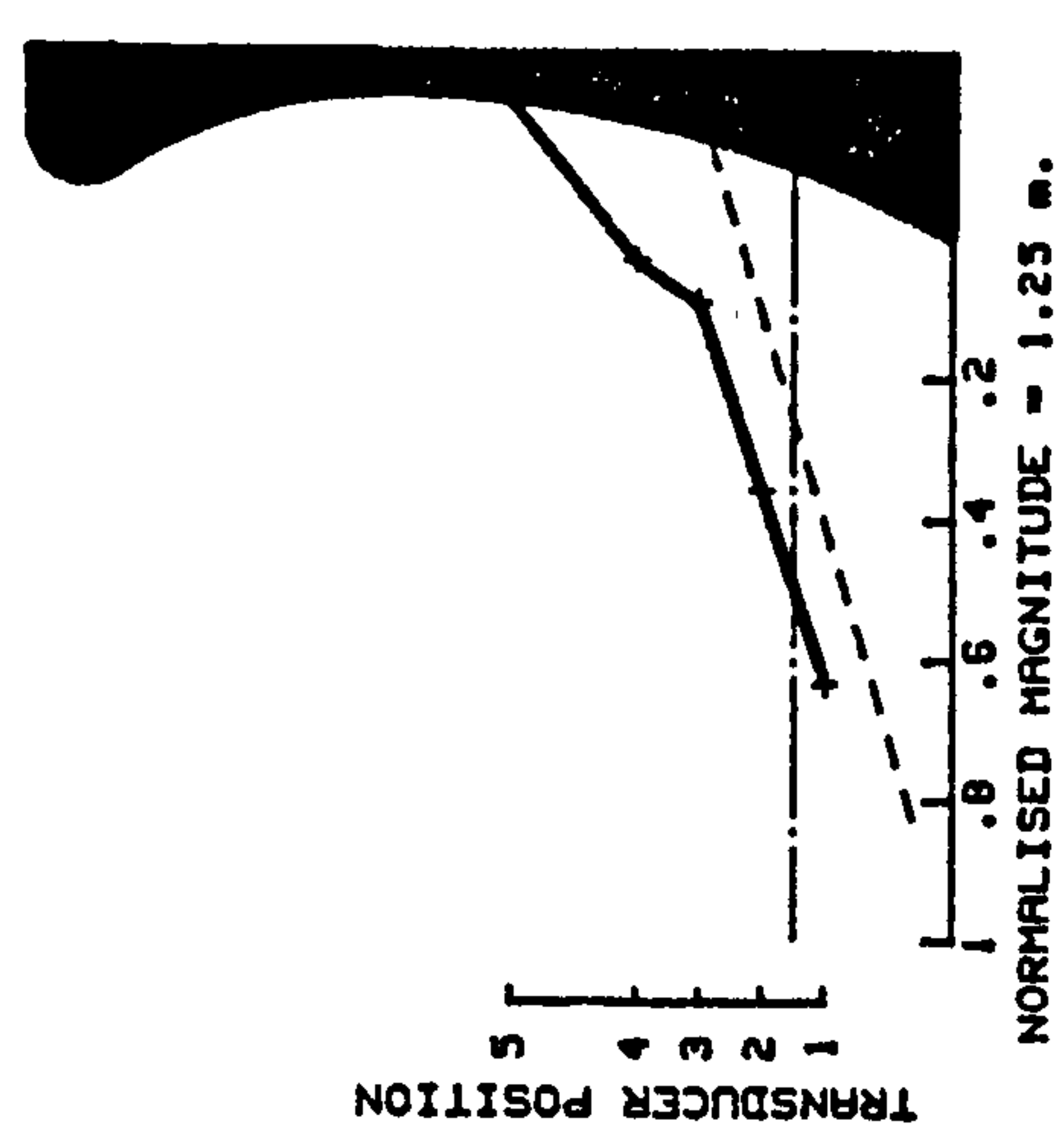
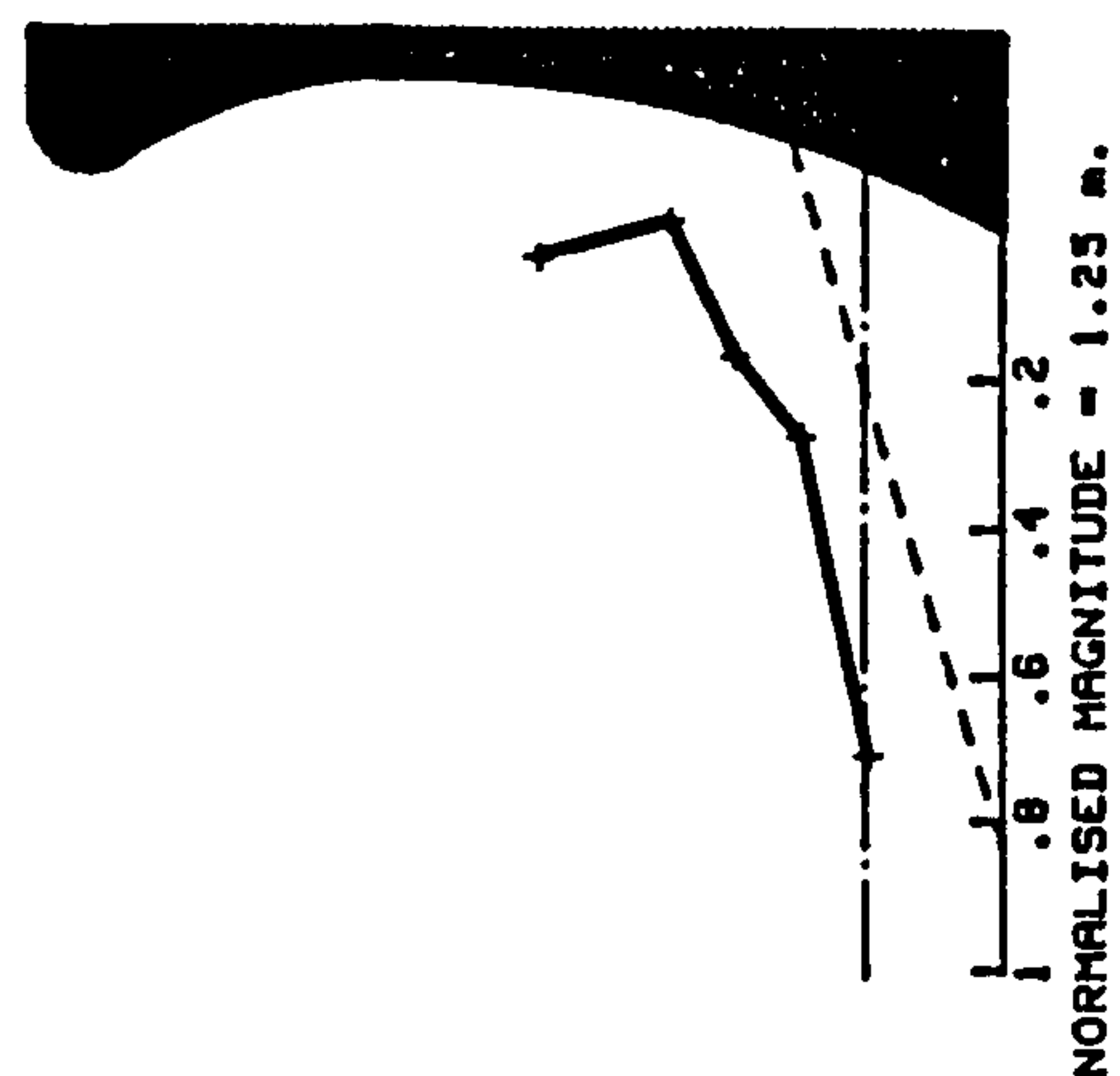
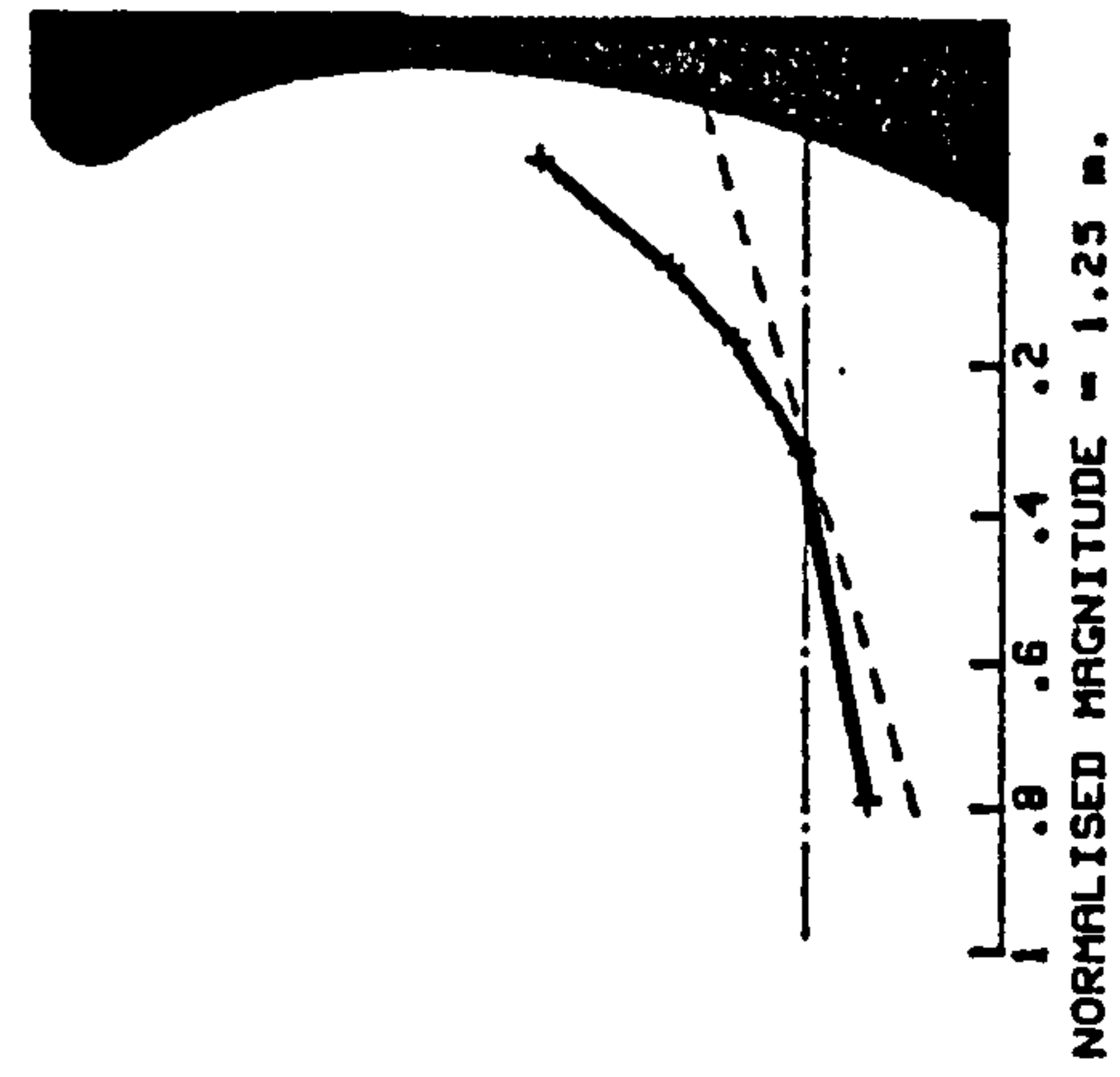
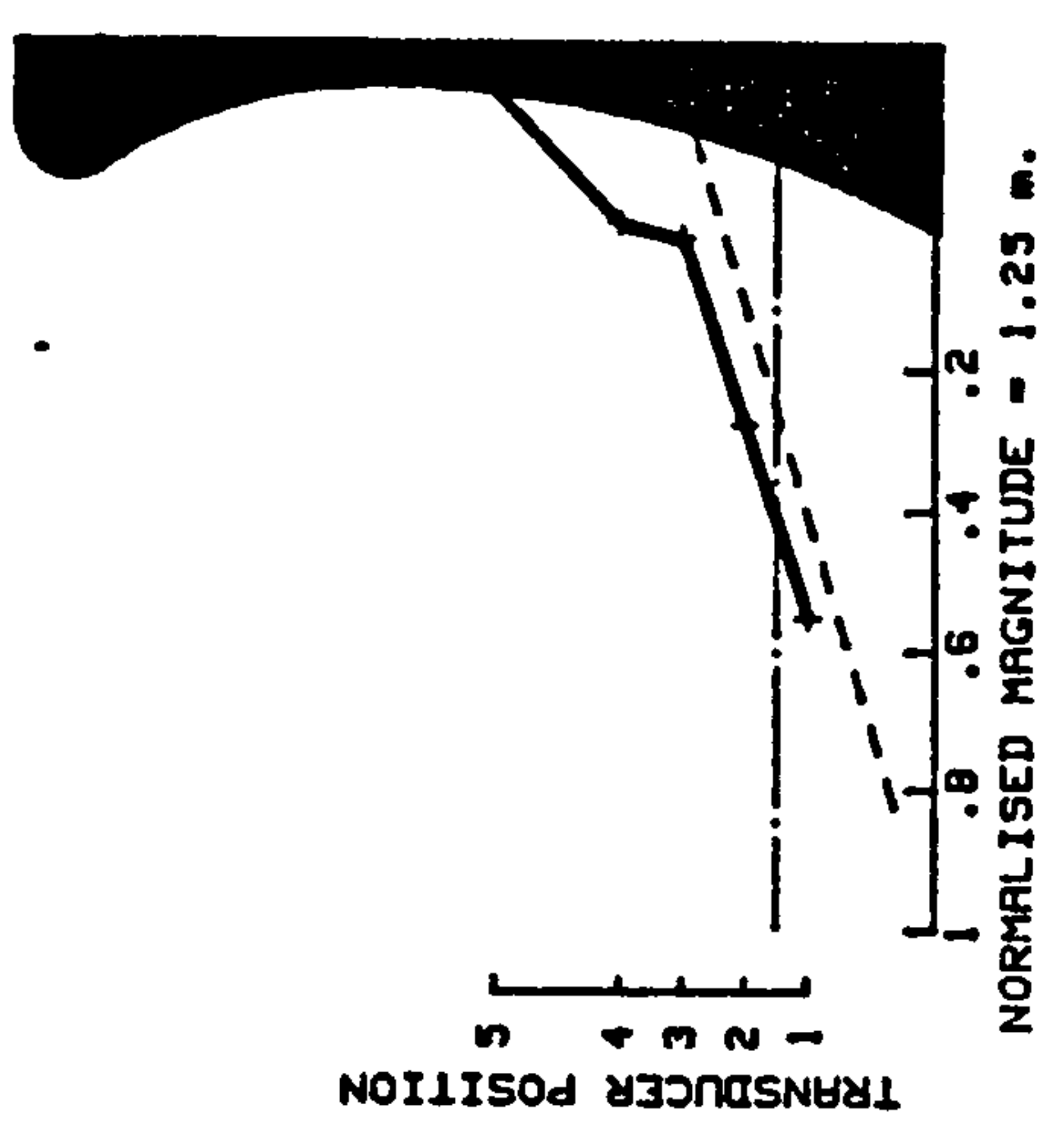
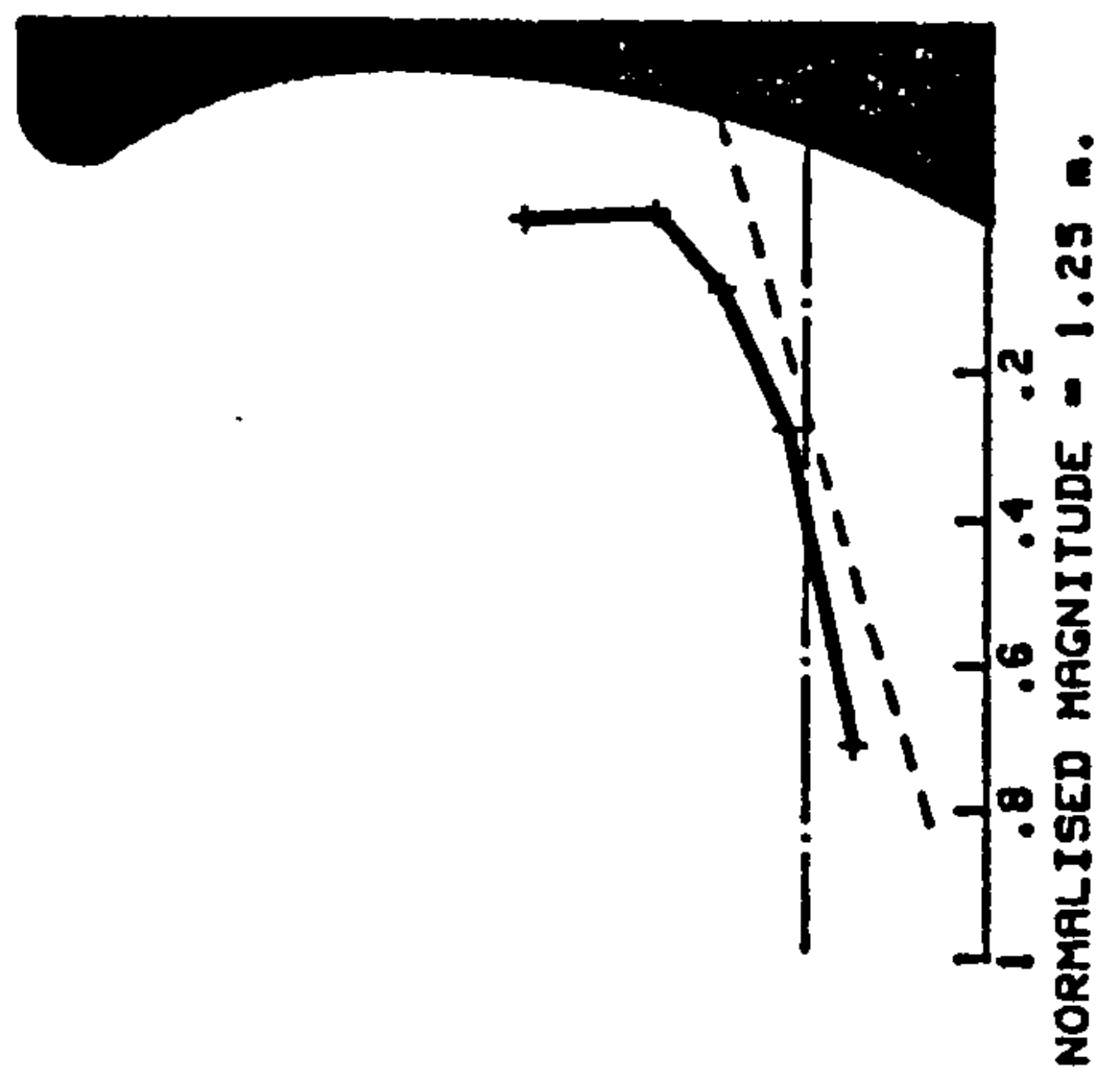
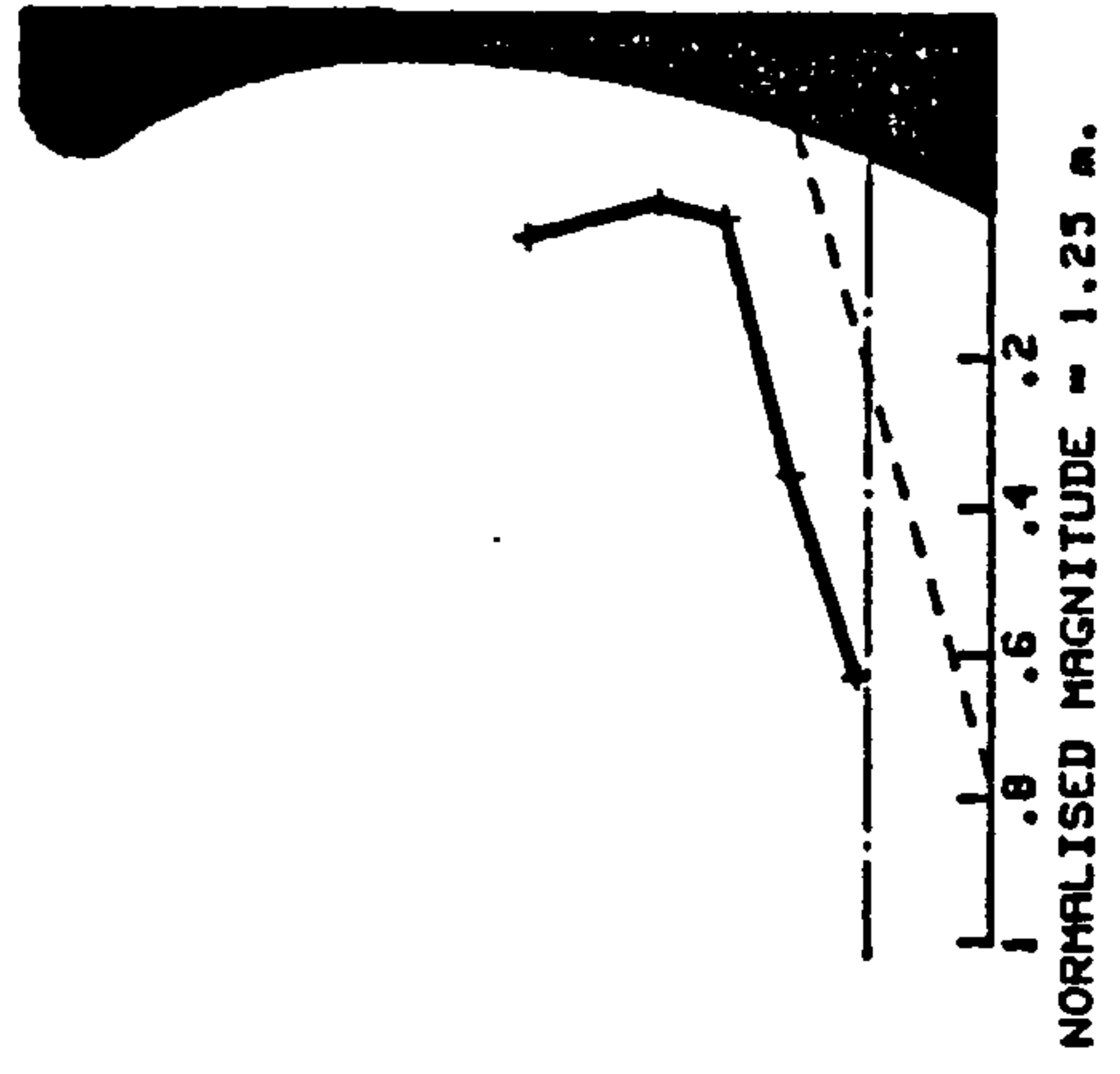


FIG 4.21 TYPICAL SECONDARY PRESSURE DISTRIBUTIONS AT THE SEAWALL

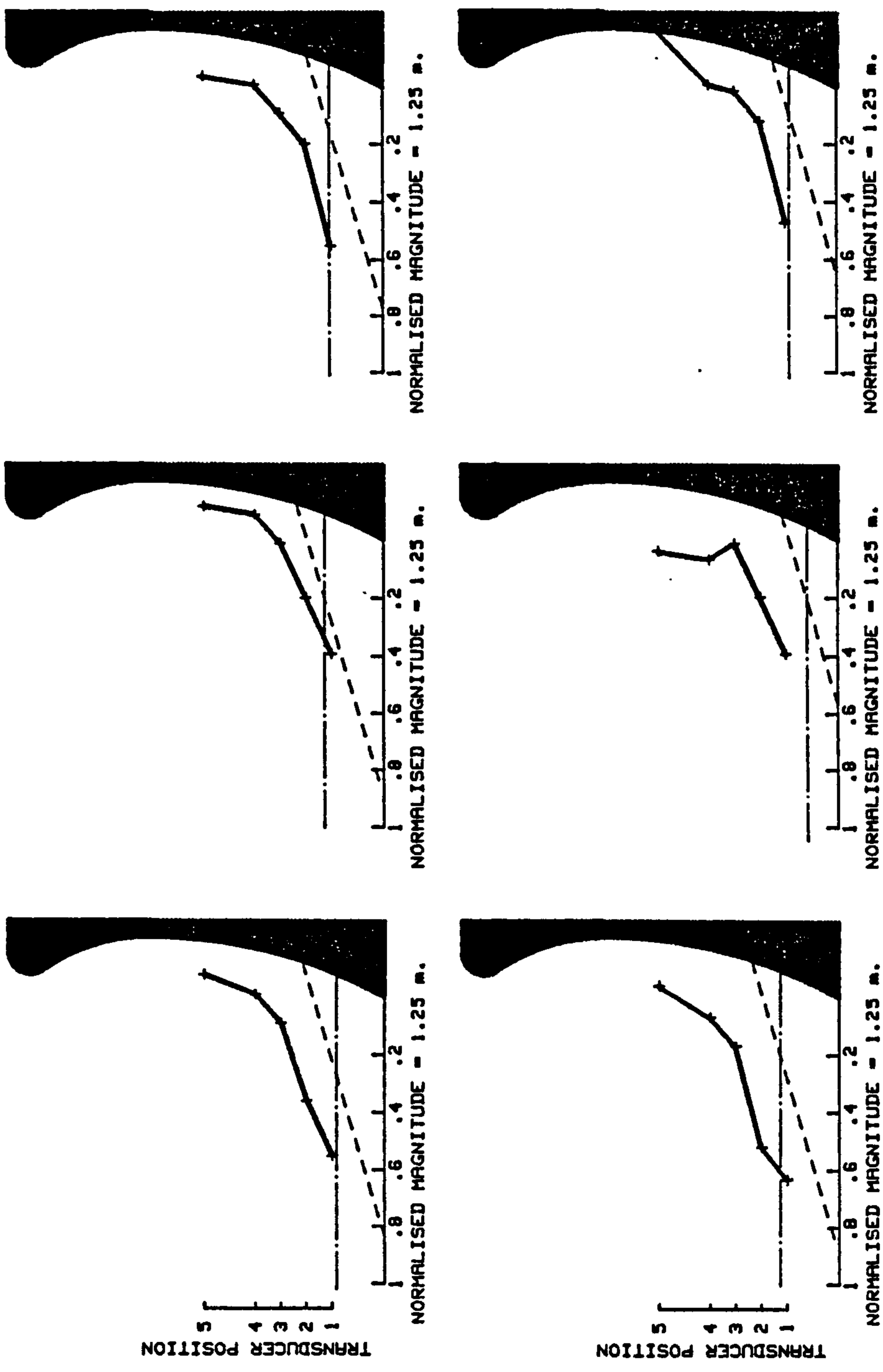
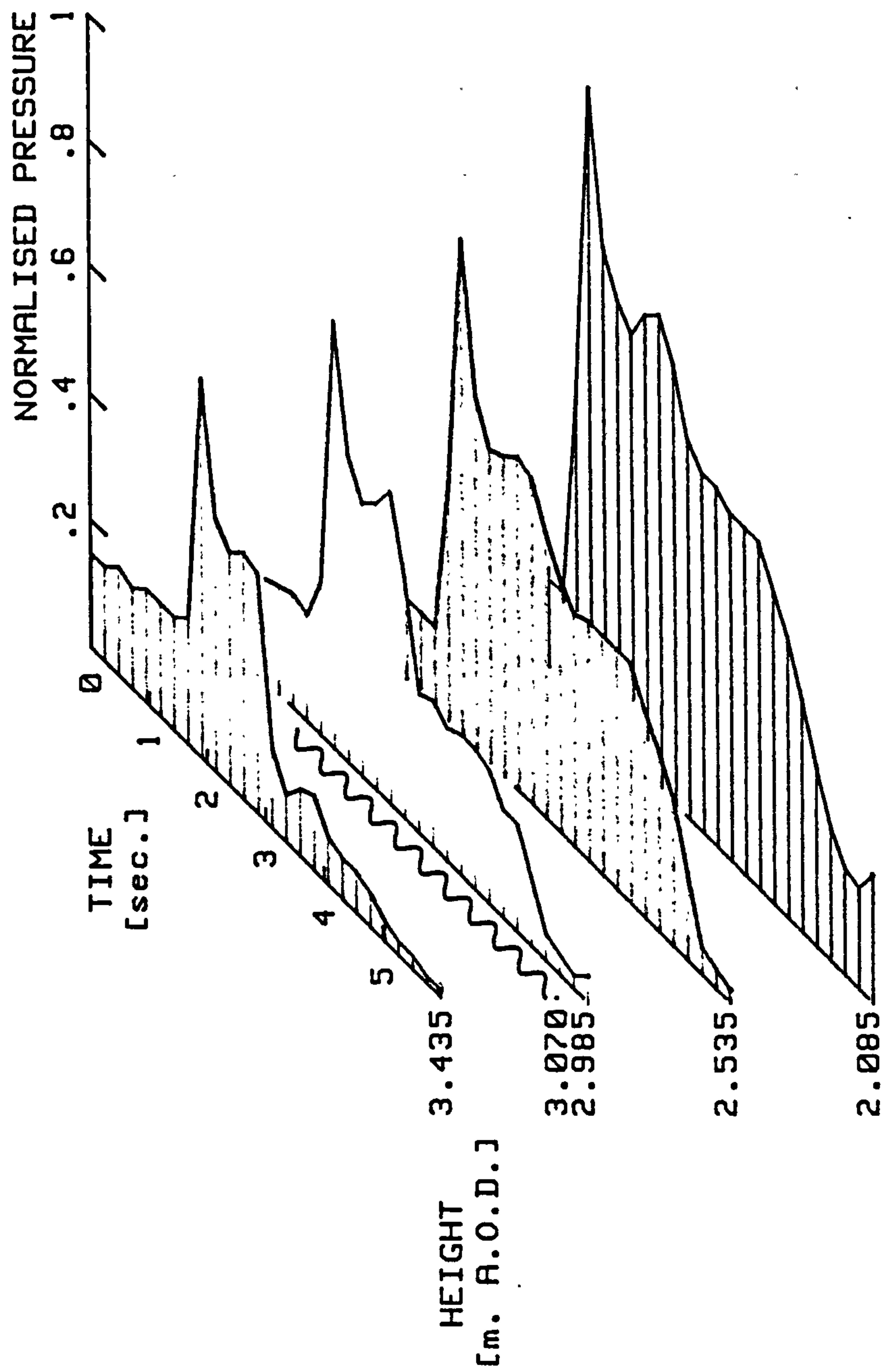


FIG 4.21 TYPICAL SECONDARY PRESSURE DISTRIBUTIONS AT THE SEAWALL



STATIC AND DYNAMIC PRESSURE
NORMALISED MAGNITUDE = 23.75 KN/m²

FIG. 4.22 3-D VARIATION OF IMPACT AND SECONDARY PRESSURE
IN VERTICAL ARRAY.

DATE 29th. March 1982
 TIME 1931 to 2348.

ILFRACOMBE SEAWALL PROJECT

WEATHER W./N.W. winds, gale force 4 to 5; cloudless

TAPE NUMBER 8 (7DS) & 4 (7D)
 TAPE SPEED 0.9375 ins/sec.
 TAPE STOP 1247

TRANSDUCER			AMPLIFIER			TAPE RECORDER			
Number	Position (Level [m.] R.O.D. or Distance [m.] from wall.)	Resistance check	Number	Balance	Gain	Tape Deck	Channel Number	Voltage Scale	Count [ft.]
1	Wall (2.085)	O.K.	1	87	393	7DS	1	.5 1.0	86 542
2	Wall (2.985)	O.K.	2	0	193	7DS	2	1	0
3	Wall (2.985)	O.K.	3	793	220	7DS	3	1 .5	0 187
4	Wall (2.985)	O.K.	4	997	269	7DS	4	1	0
5	Wall (4.335)	O.K.	5	664	109	7DS	5	1	0
11	Beach (5.5)	O.K.	6	486	116	7DS	6	10	0
12	Beach (14.4)	O.K.	7	358	120	7DS	7	1 2	0 150
13	Beach (14.4)	O.K.	8	0	193	7D	1	1	0
Acc	On wall					7D	2	d.c. s/w	645 no rec.

DATE 30th. March 1982
TIME 0740 to 1245

ILFRACOMBE SEAWALL PROJECT

WEATHER Winds picked up, direction N.E.
waves dropped in height. (S.W.L.
= 2 m. below top of mast)

TAPE NUMBER 10 (7DS) & 4 (7D)
TAPE SPEED 0.9375 ins/sec.
TAPE STOP 1807 (7DS) & 1433 (7D)

TRANSDUCER			AMPLIFIER			TAPE RECORDER			
Number	Position (Level [m.] R.O.D. or Distance [m.] from wall.)	Resistance check	Number	Balance	Gain	Tape Deck	Channel Number	Voltage Scale	Count [ft.]
1	Wall (2.085)	O.K.	1	79	393	7DS	1	.5	0
2	Wall (2.985)	O.K.	2	0	193	7DS	2	.5	0
3	Wall (2.985)	O.K.	3	791	220	7DS	3	.5	0
4	Wall (2.985)	O.K.	4	1002	269	7DS	4	.5	0
5	Wall (4.335)	O.K.	5	676	109	7DS	5	1	0
11	Beach (5.5)	O.K.	6	794	116	7DS	6	.5 1.0	43 651
12	Beach (14.4)	O.K.	7	358	120	7DS	7	1 2	108
13	Beach (14.4)	O.K.	8	5	193	7D	3	2	62

DATE 9th. December 1982
 TIME 2200 to 0200

ILFRACOMBE SEAWALL PROJECT

WEATHER S.W./W. winds, gale force 6 to 7; rainy; long period waves

TAPE NUMBER 18 (7DS) & 19 (7D)
 TAPE SPEED 1.875 ins/sec.
 TAPE STOP 2000

TRANSDUCER			AMPLIFIER			TAPE RECORDER			
Number	Position (Level [m.] R.O.D. or Distance [m.] from wall.)	Resistance check	Number	Balance	Gain	Tape Deck	Channel Number	Voltage Scale	Count [ft.]
1	Wall (2.085)	O.K.	1	428	441	7D	1	1	0
2	Wall (2.535)	O.K.	2	451	191	7D	2	1	0
3	Wall (2.985)	O.K.	3	510	206	7D	3	1	0
4	Wall (3.435)	O.K.	4	533	280	7D	4	1	0
5	Wall (4.335)	O.K.	7	520	414	7D 7DS	7 1	1 1	0 0
A	Beach (14.4)	O.K.	8	281	75	7DS	2	5	670
B	Beach (14.4)	O.K.	9	203	203	7DS	3	1	0
Sch	Beach (5.5)					7DS	4	1	0
Acc	On wall					7DS	5	1	0

DATE 10th. December 1982
TIME 1130 to 1530

ILFRACOMBE SEAWALL PROJECT

WEATHER N.W./W. winds; short regular waves with groups of breakers

TAPE NUMBER 9 (7D) & 12 (7DS)
TAPE SPEED 1.875 ins/sec.
TAPE STOP 2260

TRANSDUCER			AMPLIFIER			TAPE RECORDER			
Number	Position (Level [m.] R.O.D. or Distance [m.] from wall.)	Resistance check	Number	Balance	Gain	Tape Deck	Channel Number	Voltage Scale	Count [ft.]
1	Wall (2.085)	O.K.	1	428	441	7D 7DS	1 6	.5 1	10 10
2	Wall (2.535)	O.K.	2	450	191	7D	2	.5	10
3	Wall (2.985)	O.K.	3	508	206	7D	3	.5	10
4	Wall (3.435)	O.K.	4	537	280	7D	4	.5	10
5	Wall (4.335)	O.K.	7	526	414	7D	7	1	10
A	Beach (14.4)	O.K.	8	394	75	7DS	2	1 2.0	10 1848
B	Beach (14.4)	O.K.	9	229	203	7DS	3	1	10
Sch	Beach (5.5)					7D	4	5	10
Acc	On wall					7DS	5	1 5.0	10 200

DATE 10th. December 1982
 TIME 2345 to 0400

ILFRACOMBE SEAWALL PROJECT

WEATHER W. to N.W. wind

TAPE NUMBER 1 (7D)
 TAPE SPEED 1.875 ins/sec.
 TAPE STOP 2403

TRANSDUCER			AMPLIFIER			TAPE RECORDER			
Number	Position (Level [m.] R.O.D. or Distance [m.] from wall.)	Resistance check	Number	Balance	Gain	Tape Deck	Channel Number	Voltage Scale	Count [ft.]
1	Wall (2.085)	O.K.	1	428	441	7D	1	1	0
2	Wall (2.535)	O.K.	2	450	191	7D	2	1	0
3	Wall (2.985)	O.K.	3	506	206	7D	3	1	0
4	Wall (3.435)	O.K.	4	536	280	7D	4	1	0
5	Wall (4.335)	O.K.	7	525	414	7D	7	1	0
Sch	Beach (5.5)					7D	6	5	0

DATE 22nd. March 1983
 TIME 2040 to 0030

ILFRACOMBE SEAWALL PROJECT

WEATHER N.W./W. winds, gale force 5 to 6 (H = 0.8m. T = 9s.)

TAPE NUMBER 13 (7D) & 11 (7DS)
 TAPE SPEED 1.875 ins/sec.
 TAPE STOP 2172 (7D) & 1083 (7D)

TRANSDUCER			AMPLIFIER			TAPE RECORDER			
Number	Position (Level [m.] R.O.D. or Distance [m.] from wall.)	Resistance check	Number	Balance	Gain	Tape Deck	Channel Number	Voltage Scale	Count [ft.]
1	Wall (2.085)	O.K.	1	478	424	7DS 7D	1 7	1 1	0 0
2	Wall (2.535)	O.K.	2	466	151	7DS	2	1	0
3	Wall (2.985)	O.K.	3	516	190	7DS	3	1	0
4	Wall (3.435)	O.K.	4	532	284	7DS	4	1	0
5	Wall (4.335)	O.K.	7	572	432	7DS	7	1	0
A	Beach (14.4)	O.K.	8	unbal.	244	7D	2	1	0
C	Beach (5.5)	O.K.	10	338	346	7D	4	1	0
Sch	Beach (14.4)					7D	5	5	0
Acc	On wall				x 100	7D	6	5	0

DATE 23rd. March 1983
 TIME 0930 to 1355

ILFRACOMBE SEAWALL PROJECT

WEATHER W./S.W. winds; swell
 (H = 0.8m. T = 10s.)

TAPE NUMBER 6 (7D) & 2 (7DS)
 TAPE SPEED 1.875 ins/sec.
 TAPE STOP 2400

TRANSDUCER			AMPLIFIER			TAPE RECORDER			
Number	Position (Level [m.] A.O.D. or Distance [m.] from wall.)	Resistance check	Number	Balance	Gain	Tape Deck	Channel Number	Voltage Scale	Count [ft.]
1	Wall (2.085)	O.K.	1	486	424	7DS 7D	1 7	1 1	100 58
2	Wall (2.535)	O.K.	2	468	151	7DS	2	1	100
3	Wall (2.985)	O.K.	3	516	190	7DS	3	1	100
4	Wall (3.435)	O.K.	4	533	284	7DS	4	1	100
5	Wall (4.335)	O.K.	7	572	432	7DS	7	1	100
A	Beach (14.4)	O.K.	8	556	246	7D	2	1	58
C	Beach (5.5)	O.K.	10	339	343	7D	4	1	58
Sch	Beach (14.4)					7D	5	5	58
Acc	On wall				x 10	7D	6	5	58 1365

DATE 25th. November 1983
 TIME 1800 to 2130

BOVISANDS SEAWALL PROJECT

WEATHER Gale force 6 to 7.
 S.W. wind; strong.

TAPE NUMBER 14 (7DS) & 15 (7D)
 TAPE SPEED 0.9375 ins/sec.
 TAPE STOP 2400

TRANSDUCER			AMPLIFIER			TAPE RECORDER			
Number	Position (Level [m.] R.O.D. or Distance [m.] from wall.)	Resistance check	Number	Balance	Gain	Tape Deck	Channel Number	Voltage Scale	Count [ft.]
1	Wall (0.22)	O.K.	1	486	430	7DS	1	1	0
2	Wall (0.67)	O.K.	2	478	192	7DS	2	1	0
4	Wall (1.57)	O.K.	4	532	287	7DS	4	1	0
5	Wall (2.47)	O.K.	7	584	428	7DS 7D	7 1	1 1	0 0
C	Beach (15.5)	O.K.	10	364	340	7D	4	1	0

TABLE 4.1.1 ILFRACOMBE 30th. March 82	Peak Pressure [KN/m ²]	Rise Time [sec.]	Secondary Pressure [KN/m ²]	Duration [sec.]	IMPULSE = Peak·Rise Time ² x10 ⁻¹ [KNS/m ²]	Rise Time Duration x10 ⁻²	Impact Secondary
	12.2 10.5 21.0 14.0 7.5 16.5 6.6	0.0064 0.012 0.012 0.012 0.006 0.006 0.046	3.2 2.7 2.9 7.0 4.4 6.0 10.0	0.04 0.04 0.04 0.05 0.045 0.26 0.21	0.39 0.63 1.26 0.84 2.23 0.50 1.52	1.56 2.93 2.93 2.35 1.30 0.23 2.14	3.8 3.9 7.2 2.0 1.7 2.8 0.7
	10.0 8.6 6.6 22.5 9.8 8.3 11.0	0.077 0.051 0.038 0.019 0.045 0.045 0.077	8.5 10.8 9.4 14.1 9.0 11.3 12.5	0.11 0.09 0.09 0.07 0.11 0.10 0.21	3.85 2.19 1.25 2.14 2.21 1.87 4.24	6.84 5.54 4.13 2.65 4.00 4.40 3.58	1.2 0.8 0.7 1.6 1.1 0.7 0.9
	9.8 10.6 7.9 6.6 7.9 9.1 6.6	0.040 0.032 0.038 0.051 0.032 0.070 0.083	9.3 12.2 10.8 8.5 5.6 6.6 9.8	0.12 0.14 0.10 0.22 0.13 0.13 0.13	1.96 1.70 1.50 1.68 1.26 3.19 2.74	3.26 2.23 3.71 2.27 2.41 5.26 6.24	1.1 0.9 0.7 0.8 1.4 1.4 0.7

TABLE 4.1.2 ILFRACOMBE 30th. March 82	Peak Pressure [KN/m ²]	Rise Time [sec.]	Secondary Pressure [KN/m ²]	Duration [sec.]	IMPULSE = $\frac{\text{Peak.Rise Time}}{2}$ x10 ⁻¹ [KNS/m ²]	Rise Time Duration x10 ⁻²	Impact Secondary
	8.4	0.077	9.8	0.13	3.23	5.79	0.9
	9.4	0.045	11.8	0.17	2.12	2.59	0.8
	6.6	0.032	7.1	0.08	1.06	3.91	0.9
	11.9	0.064	13.1	0.06	3.81	10.43	0.9
	8.6	0.078	10.5	0.13	3.35	5.87	0.8
	11.4	0.032	14.1	0.12	1.82	2.61	0.8
	9.3	0.064	10.8	0.19	2.98	3.29	0.9
	11.8	0.078	12.7	0.15	0.18	5.08	0.9
	9.4	0.083	11.7	2.28	3.90	3.64	0.8
	11.4	0.032	14.1	0.65	1.82	4.92	0.8
	13.1	0.090	16.4	1.30	5.90	6.92	0.8
	14.0	0.064	14.0	0.78	4.48	8.21	1.0
	15.0	0.064	13.1	1.30	4.80	4.92	1.1
	10.3	0.051	11.3	1.30	2.63	3.92	0.9
	10.8	0.057	12.3	1.76	3.08	3.24	0.9
	8.9	0.057	10.9	1.56	2.54	3.65	0.8
	7.8	0.051	10.2	1.56	1.99	3.27	0.8
	8.8	0.057	12.3	1.56	2.51	3.65	0.7
	6.8	0.038	11.4	1.88	1.29	2.02	0.6
	6.8	0.13	11.8	1.95	4.42	6.67	0.6
	10.5	0.038	12.3	1.69	2.00	2.25	0.9

TABLE 4.1.3 ILFRACOMBE 30th. March 82	Peak Pressure [KN/m ²]	Rise Time [sec.]	Secondary Pressure [KN/m ²]	Duration [sec.]	IMPULSE = Peak·Rise Time ² x10 ⁻¹ [KNS/m ²]	Rise Time Duration x10 ⁻²	Impact Secondary
8.4	0.045	12.6	1.82	1.89	2.47	0.7	
10.1	0.090	12.7	1.43	4.55	6.29	0.8	
10.5	0.102	13.1	1.56	5.36	6.54	0.8	
11.6	0.051	15.1	1.43	2.96	3.57	0.8	
10.6	0.058	11.8	1.30	3.07	4.46	0.9	
11.0	0.064	11.0	1.30	3.52	4.92	1.0	

TABLE 4.2.1 ILFRACOMBE 9th. Dec. 82 Trans. No.		Peak Pressure [KN/m ²]	Rise Time [sec.]	Secondary Pressure [KN/m ²]	Duration [sec.]	IMPULSE = $\frac{\text{Peak} \cdot \text{Rise Time}}{2}$ x10 ⁻¹ [KNs/m ²]	Rise Time Duration x10 ⁻²	Impact Secondary
4.2.1.1	1	12.00	0.06	4.00	1.1	3.6	5.45	3.00
	2	-	-	-	-	-	-	-
	3	-	-	3.00	0.25	-	-	-
	4	-	-	-	-	-	-	-
	5	-	-	-	-	-	-	-
4.2.1.2	1	9.00	0.025	4.00	1.00	1.125	2.5	2.25
	2	-	-	1.00	0.75	-	-	-
	3	-	-	3.00	0.80	-	-	-
	4	-	-	2.00	0.50	-	-	-
	5	-	-	-	-	-	-	-
4.2.1.3	1	12.00	0.0025	5.00	1.5	0.15	0.167	2.4
	2	6.00	0.004	3.00	1.0	0.12	0.40	2.0
	3	-	-	2.00	0.9	-	-	-
	4	-	-	2.00	0.75	-	-	-
	5	-	-	-	-	-	-	-
4.2.1.4	1	34.00	0.006	4.00	1.00	1.02	0.6	8.5
	2	-	-	2.00	0.75	-	-	-
	3	-	-	2.00	0.70	-	-	-
	4	-	-	2.00	0.60	-	-	-
	5	-	-	7.00	1.00	-	-	-

TABLE 4.2.2 ILFRACOMBE 9th. Dec. 82 Trans. No.		Peak Pressure [KN/m ²]	Rise Time [sec.]	Secondary Pressure [KN/m ²]	Duration [sec.]	IMPULSE = $\frac{\text{Peak} \cdot \text{Rise Time}}{2}$ x10 ⁻¹ [KNs/m ²]	Rise Time Duration x10 ⁻²	Impact Secondary
4.2.2.1	1	18.00	0.075	6.00	1.1	6.75	6.82	3.00
	2	10.00	0.035	3.00	0.9	1.75	3.89	3.33
	3	-	-	3.50	0.75	-	-	-
	4	-	-	3.00	0.75	-	-	-
	5	-	-	-	-	-	-	-
4.2.2.2	1	14.00	0.025	4.00	1.15	1.75	2.17	3.5
	2	4.00	0.05	2.00	0.75	1.00	6.67	2.00
	3	-	-	2.00	0.75	-	-	-
	4	-	-	2.00	0.50	-	-	-
	5	-	-	4.00	0.50	-	-	-
4.2.2.3	1	14.00	0.15	6.00	1.2	10.5	12.50	2.33
	2	19.00	0.04	4.00	1.05	3.8	3.81	4.75
	3	7.00	0.10	4.00	1.0	3.5	10.0	1.75
	4	-	-	4.00	1.0	-	-	-
	5	5.00	-	2.00	0.75	-	-	-
4.2.2.4	1	10.00	0.025	10.00	2.0	0.125	1.25	0.1
	2	6.00	0.005	50.00	1.3	0.15	0.385	1.2
	3	-	-	40.00	1.5	-	-	-
	4	-	-	50.00	1.5	-	-	-
	5	-	-	-	-	-	-	-

TABLE 4.2.3 ILFRACOMBE 9th. Dec. 82 Trans. No.		Peak Pressure [KN/m ²]	Rise Time [sec.]	Secondary Pressure [KN/m ²]	Duration [sec.]	IMPULSE = Peak·Rise Time ² x10 ⁻¹ [KNs/m ²]	Rise Time Duration x10 ⁻²	Impact Secondary
4.2.3.1	1	15.0	0.2	6.0	1.5	15.0	13.3	2.5
	2	4.0	0.04	2.0	0.8	0.8	5.0	2.0
	3	-	-	3.0	0.5	-	-	-
	4	-	-	4.0	0.5	-	-	-
	5	-	-	-	-	-	-	-
4.2.3.2	1	10.0	0.06	6.0	1.5	3.0	4.0	1.67
	2	10.0	0.04	4.0	1.0	2.0	4.0	2.5
	3	3.0	0.02	2.0	1.35	0.3	1.48	1.5
	4	-	-	3.0	0.6	-	-	-
	5	1.0	0.03	3.0	0.6	1.5	5.0	3.33
4.2.3.3	1	12.0	0.01	6.0	1.25	0.6	0.8	2.0
	2	-	-	2.5	0.75	-	-	-
	3	-	-	3.0	0.75	-	-	-
	4	-	-	3.0	0.6	-	-	-
	5	-	-	1.5	0.5	-	-	-
4.2.3.4	1	20.0	0.04	7.0	1.7	4.0	2.35	2.86
	2	8.0	0.05	4.0	1.45	2.0	3.45	2.0
	3	-	-	-	0.75	-	-	-
	4	-	-	-	0.6	-	-	-
	5	-	-	-	-	-	-	-

TABLE 4.2.4 ILFRACOMBE 9th. Dec. 82 Trans. No.		Peak Pressure [KN/m ²]	Rise Time [sec.]	Secondary Pressure [KN/m ²]	Duration [sec.]	IMPULSE = Peak·Rise Time ² x10 ⁻¹ [KNs/m ²]	Rise Time Duration x10 ⁻²	Impact Secondary
4.2.4.1	1	11.0	0.025	4.0	0.9	1.375	2.78	2.75
	2	-	-	2.5	0.5	-	-	-
	3	-	-	1.0	0.5	-	-	-
	4	-	-	0.5	0.4	-	-	-
	5	-	-	-	-	-	-	-
4.2.4.2	1	27.0	0.04	4.0	1.25	5.4	3.2	6.75
	2	10.0	0.025	4.0	0.9	1.25	2.78	2.5
	3	5.0	0.025	3.0	0.75	0.625	3.33	1.67
	4	-	-	4.0	0.75	-	-	-
	5	-	-	-	-	-	-	-
4.2.4.3	1	10.0	0.035	4.0	1.25	1.75	2.8	2.5
	2	5.0	0.15	2.0	0.85	3.75	17.6	2.5
	3	1.0	0.015	2.0	0.5	0.075	3.0	0.5
	4	-	-	1.0	0.25	-	-	-
	5	-	-	0.8	0.6	-	-	-
4.2.4.4	1	11.5	0.035	5.0	1.2	2.01	2.92	2.3
	2	9.0	0.015	1.0	0.8	0.675	1.88	9.0
	3	-	-	4.0	0.5	-	-	-
	4	-	-	4.0	0.5	-	-	-
	5	2.0	0.5	3.0	0.35	5.0	143.0	0.67

TABLE 4.2.5 ILFRACOMBE 9th. Dec. 82 Trans- No.		Peak Pressure [KN/m ²]	Rise Time [sec.]	Secondary Pressure [KN/m ²]	Duration [sec.]	IMPULSE = Peak·Rise Time ² x10 ⁻¹ [Kns/m ²]	Rise Time Duration x10 ⁻²	Impact Secondary
4.2.5.1	1	32.0	0.035	6.0	1.35	5.6	2.59	5.33
	2	16.0	0.025	3.0	1.0	2.0	2.5	5.33
	3	-	-	4.0	0.75	-	-	-
	4	-	-	4.0	0.5	-	-	-
	5	1.0	0.005	3.0	0.6	0.25	0.833	0.333
4.2.5.2	1	18.0	0.025	7.0	1.7	2.25	1.47	2.57
	2	2.0	0.0125	4.0	1.1	0.125	1.14	0.5
	3	-	-	2.0	0.75	-	-	-
	4	-	-	3.0	0.6	-	-	-
	5	-	-	-	-	-	-	-
4.2.5.3	1	10.0	0.5	7.0	1.25	25.0	40.0	1.43
	2	4.0	0.25	3.0	1.0	5.0	25.0	1.33
	3	-	-	2.0	0.75	-	-	-
	4	-	-	3.0	0.5	-	-	-
	5	-	-	-	-	-	-	-
4.2.5.4	1	14.0	0.005	5.0	1.25	0.35	0.4	2.8
	2	4.0	0.25	3.0	0.85	5.0	29.4	1.33
	3	-	-	4.0	0.75	-	-	-
	4	-	-	3.0	0.5	-	-	-
	5	-	-	1.0	0.25	-	-	-

TABLE 4.2.6 ILFRACOMBE 9th. Dec. 82 Trans. No.		Peak Pressure [KN/m ²]	Rise Time [sec.]	Secondary Pressure [KN/m ²]	Duration [sec.]	IMPULSE = Peak·Rise Time ² x10 ⁻¹ [KNS/m ²]	Rise Time Duration · x10 ⁻²	Impact Secondary
4.2.6.1	1	16.0	0.07	8.0	1.8	5.6	3.89	2.0
	2	6.0	0.12	6.0	1.0	3.6	12.0	1.0
	3	4.0	0.12	3.0	1.0	2.4	12.0	1.33
	4	4.0	0.25	2.0	0.9	5.0	27.8	2.0
	5	2.0	0.25	1.5	0.75	2.5	33.3	1.33
4.2.6.2	1	30.0	0.035	4.5	1.75	5.25	2.0	6.67
	2	8.0	0.02	3.0	1.0	0.8	2.0	2.67
	3	6.0	0.05	2.0	0.75	1.5	6.67	3.0
	4	4.0	0.12	2.0	0.75	2.4	16.0	2.0
	5	2.0	0.12	2.0	0.65	1.2	18.5	1.0
4.2.6.3	1	12.0	0.2	6.0	1.4	12.0	14.3	2.0
	2	24.0	0.01	4.0	1.0	1.2	1.0	6.0
	3	5.0	0.12	2.0	0.7	3.0	17.1	2.5
	4	4.0	0.07	1.0	0.7	1.4	10.0	4.0
	5	3.0	0.07	1.0	0.6	1.05	11.7	3.0
4.2.6.4	1	16.0	0.05	8.0	1.5	4.0	3.33	2.0
	2	-	-	4.0	1.2	-	-	-
	3	-	-	3.0	0.85	-	-	-
	4	-	-	2.0	0.75	-	-	-
	5	-	-	2.0	0.4	-	-	-

TABLE 4.2.7 ILFRACOMBE 9th. Dec. 82 Trans No.		Peak Pressure [KN/m ²]	Rise Time [sec.]	Secondary Pressure [KN/m ²]	Duration [sec.]	IMPULSE = Peak·Rise Time ² x10 ⁻¹ [KNS/m ²]	Rise Time Duration x10 ⁻²	Impact Secondary
4.2.7.1	1	20.0	0.02	3.0	1.2	2.0	1.67	6.67
	2	-	-	2.0	0.7	-	-	-
	3	-	-	3.0	0.7	-	-	-
	4	-	-	2.0	0.5	-	-	-
	5	-	-	-	-	-	-	-
4.2.7.2	1	40.0	0.01	5.0	1.2	2.0	0.83	8.0
	2	8.0	0.05	2.0	0.5	2.0	10.0	4.0
	3	5.0	0.02	2.0	0.6	0.5	3.33	2.5
	4	4.0	0.07	2.0	0.6	1.4	11.7	2.0
	5	3.0	0.02	1.0	0.5	0.3	4.0	3.0
4.2.7.3	1	45.0	0.06	9.0	1.7	13.5	3.53	5.0
	2	20.0	0.012	4.0	1.2	1.2	1.0	5.0
	3	6.0	0.012	2.0	0.5	0.36	2.4	3.0
	4	5.0	0.005	0.015	0.5	0.125	1.0	3.33
	5	5.0	0.002	1.5	0.55	0.05	0.364	3.33
4.2.7.4	1	30.0	0.015	5.0	1.3	2.34	1.2	6.0
	2	5.0	0.15	3.0	0.9	3.75	16.7	1.67
	3	-	-	2.0	0.7	-	-	-
	4	-	-	2.0	0.4	-	-	-
	5	3.0	0.005	1.0	0.3	0.075	1.67	3.0

TABLE 4.2.8 ILFRACOMBE 9th. Dec. 82		Trans. No.	Peak Pressure [KN/m ²]	Rise Time [sec.]	Secondary Pressure [KN/m ²]	Duration [sec.]	IMPULSE = Peak·Rise Time ² x10 ⁻¹ [KNs/m ²]	Rise Time Duration x10 ⁻²	Impact Secondary
4.2.8.1	1 2 3 4 5	14.0	0.02	3.0	0.9	1.4	2.22	4.67	
		3.0	0.10	1.0	0.45	1.5	22.20	3.0	
		-	-	2.0	0.5	-	-	-	
		-	-	3.0	0.5	-	-	-	
		-	-	-	-	-	-	-	
4.2.8.2	1 2 3 4 5	14.0	0.25	7.0	1.7	17.5	14.7	2.0	
		12.0	0.07	4.0	1.0	4.2	7.0	3.0	
		12.0	0.005	3.0	0.85	0.3	0.588	4.0	
		6.0	0.01	2.0	0.75	0.3	1.33	3.0	
		3.0	0.01	2.0	0.7	0.15	1.43	1.5	
4.2.8.3	1 2 3 4 5	20.0	0.018	10.0	2.0	1.8	0.9	2.0	
		14.0	0.03	6.0	1.4	2.1	2.14	2.33	
		5.0	0.01	4.0	1.4	0.25	0.714	1.25	
		4.0	0.01	3.0	0.6	0.2	1.67	1.33	
		3.0	0.01	1.0	0.5	0.15	2.0	3.0	
4.2.8.4	1 2 3 4 5	24.0	0.02	9.0	1.7	2.4	1.18	2.67	
		20.0	0.07	8.0	1.2	7.0	5.83	2.5	
		-	-	4.0	1.0	-	-	-	
		-	-	3.0	0.7	-	-	-	
		5.0	-	2.0	0.7	-	-	-	

TABLE 4.2.9 ILFRACOMBE 9th. Dec. 82 Trans. No.	Peak Pressure [KN/m ²]	Rise Time [sec.]	Secondary Pressure [KN/m ²]	Duration [sec.]	IMPULSE = Peak·Rise Time ² x10 ⁻¹ [KNS/m ²]	Rise Time Duration x10 ⁻²	Impact Secondary
4.2.9.1	50.0	0.01	10.0	1.8	2.5	0.556	5.0
	10.0	0.01	3.0	1.2	0.5	0.833	3.33
	5.0	0.005	3.0	1.2	0.125	0.417	1.67
	-	-	4.0	0.7	-	-	-
	-	-	3.0	0.5	-	-	-
4.2.9.2	23.0	0.07	9.0	1.6	8.05	4.38	2.56
	26.0	0.005	5.0	1.2	0.65	0.417	5.2
	4.0	0.005	3.0	1.0	0.1	0.5	1.33
	4.0	0.005	2.0	0.7	0.1	0.714	2.0
	4.0	0.01	1.0	0.5	0.2	2.0	4.0
4.2.9.3	16.0	0.05	9.0	1.7	4.0	2.94	1.78
	10.0	0.05	6.0	0.85	2.5	5.88	1.67
	-	-	2.0	0.8	-	-	-
	-	-	2.0	0.75	-	-	-
	-	-	3.0	0.25	-	-	-
4.2.9.4	41.0	0.03	5.0	1.7	6.15	1.76	8.2
	71.0	0.015	7.0	1.5	5.33	1.0	10.1
	30.0	0.0012	3.0	1.3	0.18	0.09	10.0
	3.0	-	3.0	1.25	-	-	-
	-	-	1.0	0.75	-	-	-

TABLE 4.2.10 ILFRACOMBE 9th. Dec. 82 Trans No.	Peak Pressure [KN/m ²]	Rise Time [sec.]	Secondary Pressure [KN/m ²]	Duration [sec.]	IMPULSE = Peak·Rise Time ² x10 ⁻¹ [KNs/m ²]	Rise Time Duration x10 ⁻²	Impact Secondary
4.2.10.1	31.0	0.009	9.0	1.75	1.40	0.51	3.44
	10.0	0.25	6.0	1.25	12.5	20.0	1.67
	3.0	-	3.0	1.00	-	-	-
	-	-	2.5	0.85	-	-	-
	-	-	-	-	-	-	-
4.2.10.2	16.0	0.03	10.0	1.75	2.4	1.71	1.6
	8.0	0.15	5.0	1.40	6.0	10.70	1.6
	-	-	4.0	1.25	-	-	-
	-	-	2.0	1.00	-	-	-
	-	-	3.0	0.70	-	-	-
4.2.10.3	10.0	0.07	11.0	1.80	3.5	3.89	0.91
	18.0	0.02	5.5	1.50	1.8	1.33	3.30
	12.0	0.025	4.0	1.20	1.5	2.08	3.0
	5.0	0.04	3.0	0.75	1.0	5.33	1.67
	-	-	1.8	1.00	-	-	-
4.2.10.4	10.0	0.12	80.0	1.20	6.0	10.0	1.25
	16.0	0.01	50.0	1.00	0.8	1.0	3.20
	-	-	2.0	0.86	-	-	-
	-	-	2.0	0.75	-	-	-
	-	-	-	-	-	-	-

TABLE 4.2.11 ILFRACOMBE 9th. Dec. 82 Trans No.		Peak Pressure [KN/m ²]	Rise Time [sec.]	Secondary Pressure [KN/m ²]	Duration [sec.]	IMPULSE = Peak·Rise Time ² x10 ⁻¹ [KNs/m ²]	Rise Time Duration x10 ⁻²	Impact Secondary
4.2.11.1	1	17.0	0.1	6.0	1.4	8.5	7.14	2.83
	2	18.0	0.025	5.0	1.1	2.25	2.27	3.6
	3	-	-	3.0	0.9	-	-	-
	4	-	-	4.0	0.6	-	-	-
	5	-	-	2.0	0.5	-	-	-
4.2.11.2	1	26.0	0.09	5.0	1.7	11.7	5.29	5.2
	2	21.0	0.005	2.0	1.6	0.525	0.312	10.5
	3	7.0	-	1.2	1.25	-	-	-
	4	-	-	1.0	0.85	-	-	-
	5	-	-	0.5	0.55	-	-	-
4.2.11.3	1	18.0	0.025	10.0	1.85	2.25	1.35	1.80
	2	8.0	0.05	5.0	1.4	2.0	3.57	1.60
	3	-	-	3.0	1.25	-	-	-
	4	-	-	2.0	0.9	-	-	-
	5	-	-	2.5	0.9	-	-	-
4.2.11.4	1	20.0	-	10.0	1.7	-	-	-
	2	12.0	0.06	2.0	1.3	3.6	4.62	6.0
	3	-	-	2.0	1.0	-	-	-
	4	-	-	2.0	0.85	-	-	-
	5	-	-	2.0	0.6	-	-	-

TABLE 4.3.1 ILFRACOMBE 10th. Dec. 82 Trans. No.	Peak Pressure [KN/m ²]	Rise Time [sec.]	Secondary Pressure [KN/m ²]	Duration [sec.]	IMPULSE = $\frac{\text{Peak} \cdot \text{Rise Time}}{2}$ x10 ⁻¹ [KNs/m ²]	Rise Time Duration x10 ⁻²	Impact Secondary
4.3.1.1	12.0	0.048	3.8	0.98	2.88	4.70	3.16
	2.6	0.024	3.3	0.98	0.31	2.45	0.79
	-	-	2.8	0.49	-	-	-
	-	-	-	-	-	-	-
	-	-	-	-	-	-	-
4.3.1.2	13.1	0.072	7.6	0.98	4.72	7.35	1.72
	3.2	0.048	5.2	0.98	0.77	4.90	0.62
	1.8	0.024	4.6	0.98	0.22	2.45	0.39
	-	-	4.2	0.98	-	-	-
	-	-	-	-	-	-	-
4.3.1.3	21.2	0.024	4.4	0.74	2.54	3.24	4.82
	3.5	0.024	4.0	1.22	0.42	1.97	0.88
	2.0	0.024	5.3	0.98	0.24	2.45	0.38
	-	-	3.6	0.98	-	-	-
	-	-	-	-	-	-	-
4.3.1.4	11.8	0.024	3.6	0.74	1.42	3.24	3.28
	2.2	0.048	2.2	0.74	0.53	6.49	1.00
	-	-	1.8	0.37	-	-	-
	-	-	0.6	0.25	-	-	-
	-	-	-	-	-	-	-

TABLE 4.3.2 ILFRACOMBE 10th. Dec. 82 Trans. No.	Peak Pressure [KN/m ²]	Rise Time [sec.]	Secondary Pressure [KN/m ²]	Duration [sec.]	IMPULSE = Peak·Rise Time ² x10 ⁻¹ [KNs/m ²]	Rise Time Duration x10 ⁻²	Impact Secondary
4.3.2.1	10.9	0.048	11.8	1.47	2.62	3.27	0.92
	3.1	0.048	3.1	0.98	0.74	4.90	1.00
	1.8	0.024	3.0	0.74	0.22	3.24	0.60
	-	-	3.1	0.49	-	-	-
	-	-	-	-	-	-	-
4.3.2.2	30.0	0.024	4.8	0.98	3.60	2.45	6.25
	0.2	0.024	4.8	0.98	.02	2.45	-
	0.1	0.024	4.4	0.98	.01	2.45	-
	-	-	3.4	0.98	-	-	-
	-	-	-	-	-	-	-
4.3.2.3	7.6	0.048	3.4	2.94	1.82	1.63	2.38
	7.9	0.024	2.2	1.22	0.95	1.97	3.59
	-	-	1.6	0.74	-	-	-
	-	-	-	-	-	-	-
	-	-	-	-	-	-	-
4.3.2.4	12.4	0.048	5.5	0.98	2.98	4.90	2.25
	3.2	0.024	4.3	0.98	0.38	2.45	0.74
	2.3	0.024	3.4	0.98	0.28	2.45	0.68
	-	-	-	-	-	-	-
	-	-	-	-	-	-	-

TABLE 4.3.3 ILFRACOMBE 10th. Dec. 82 Trans. No.		Peak Pressure [KN/m ²]	Rise Time [sec.]	Secondary Pressure [KN/m ²]	Duration [sec.]	IMPULSE = Peak·Rise Time ² x10 ⁻¹ [KNs/m ²]	Rise Time Duration x10 ⁻²	Impact Secondary
4.3.3.1	1	13.5	0.072	5.1	1.47	4.86	4.90	2.65
	2	12.7	0.048	4.5	0.98	3.05	4.90	2.82
	3	5.1	0.024	4.2	0.98	0.61	2.45	1.21
	4	-	-	-	-	-	-	-
	5	2.8	0.048	3.0	.10	.67	48	0.93
4.3.3.2	1	25.3	0.024	4.0	0.98	3.04	2.45	6.33
	2	-	-	3.4	1.27	-	-	-
	3	-	-	3.4	1.13	-	-	-
	4	-	-	3.3	1.13	-	-	-
	5	3.4	0.024	1.1	0.74	0.41	3.24	3.09
4.3.3.3	1	26.7	0.024	6.4	0.98	3.20	2.45	4.17
	2	3.2	0.048	3.4	0.98	.77	4.90	0.94
	3	-	-	3.2	0.98	-	-	-
	4	-	-	3.1	0.98	-	-	-
	5	-	-	2.9	0.74	-	-	-
4.3.3.4	1	8.7	0.12	11.6	1.47	5.2	8.16	0.75
	2	10.2	0.024	7.0	0.98	1.22	2.45	1.46
	3	0.6	0.072	2.9	0.98	0.22	7.06	0.21
	4	-	-	2.7	0.98	-	-	-
	5	-	-	-	-	-	-	-

TABLE 4.3.4 ILFRACOMBE 10th. Dec. 82 Trans. No.		Peak Pressure [KN/m ²]	Rise Time [sec.]	Secondary Pressure [KN/m ²]	Duration [sec.]	IMPULSE = Peak·Rise Time ² x10 ⁻¹ [Kns/m ²]	Rise Time Duration x10 ⁻²	Impact Secondary
4.3.4.1	1	17.1	0.024	5.3	0.98	2.05	2.45	3.23
	2	-	-	4.1	0.98	-	-	-
	3	2.5	0.024	3.2	0.98	0.30	2.45	0.78
	4	-	-	3.0	0.74	-	-	-
	5	-	-	-	-	-	-	-
4.3.4.2	1	11.0	0.072	9.5	1.52	3.96	4.74	1.16
	2	22.1	0.024	5.4	1.02	2.65	2.35	4.09
	3	-	-	4.7	0.74	-	-	-
	4	-	-	3.0	0.50	-	-	-
	5	-	-	-	-	-	-	-
4.3.4.3	1	15.6	0.024	8.4	1.47	1.87	1.63	1.86
	2	-	-	3.3	0.74	-	-	-
	3	-	-	3.3	0.49	-	-	-
	4	-	-	1.5	0.49	-	-	-
	5	-	-	-	-	-	-	-
4.3.4.4	1	13.13	0.048	4.7	1.23	3.15	0.20	2.79
	2	-	-	3.0	0.74	-	-	-
	3	-	-	1.9	0.74	-	-	-
	4	-	-	1.7	0.50	-	-	-
	5	-	-	-	-	-	-	-

TABLE 4.3.5 ILFRACOMBE 10th. Dec. 82 Trans No.		Peak Pressure [KN/m ²]	Rise Time [sec.]	Secondary Pressure [KN/m ²]	Duration [sec.]	IMPULSE = Peak·Rise Time ² x10 ⁻¹ [Kns/m ²]	Rise Time Duration x10 ⁻²	Impact Secondary
4.3.5.1	1	8.91	0.048	4.2	1.27	2.14	3.78	2.12
	2	23.60	0.048	5.1	0.98	5.66	4.90	4.63
	3	-	-	4.8	0.98	-	-	-
	4	-	-	2.3	0.74	-	-	-
	5	-	-	-	-	-	-	-
4.3.5.2	1	11.3	0.19	10.5	3.53	10.7	5.38	1.08
	2	11.0	0.048	4.4	1.72	0.26	2.79	2.50
	3	-	-	3.7	1.47	-	-	-
	4	-	-	1.3	1.47	-	-	-
	5	-	-	-	-	-	-	-
4.3.5.3	1	30.0	0.048	10.5	1.37	7.20	3.50	2.86
	2	4.8	0.048	7.7	1.23	1.15	3.90	0.62
	3	2.3	0.024	4.5	0.98	0.28	2.45	0.51
	4	-	-	2.2	0.98	-	-	-
	5	2.3	0.012	1.9	0.98	0.28	2.45	1.21
4.3.5.4	1	8.3	0.072	11.3	2.45	2.99	2.94	0.73
	2	4.3	0.072	6.4	0.98	1.55	7.35	0.67
	3	-	-	2.4	0.98	-	-	-
	4	-	-	2.1	0.74	-	-	-
	5	-	-	-	-	-	-	-

TABLE 4.3.6 ILFRACOMBE 10th. Dec. 82 Trans. No.	Peak Pressure [KN/m ²]	Rise Time [sec.]	Secondary Pressure [KN/m ²]	Duration [sec.]	IMPULSE= Peak·Rise Time ² x10 ⁻¹ [KNs/m ²]	Rise Time Duration x10 ⁻²	Impact Secondary
4.3.6.1	23.4	0.10	15.6	1.72	11.7	5.81	1.50
	13.7	0.048	12.7	1.23	3.3	3.90	1.09
	20.1	0.048	8.4	1.23	4.8	3.90	2.39
	1.6	0.024	7.3	0.98	0.19	2.45	0.22
	1.6	0.024	3.0	0.74	0.19	3.24	0.53
4.3.6.2	22.5	0.048	13.5	1.72	5.40	2.79	1.67
	28.4	0.024	8.7	0.98	3.41	2.45	3.26
	3.0	0.024	4.5	0.98	0.36	2.45	0.74
	-	-	1.9	0.74	-	-	-
	2.3	0.024	0.9	0.49	0.28	4.90	1.00
4.3.6.3	15.3	0.10	13.6	3.20	7.7	3.13	1.13
	28.7	0.048	10.2	0.98	6.9	4.90	2.81
	2.6	0.048	3.5	0.74	0.62	6.49	0.74
	-	-	3.0	0.49	-	-	-
	2.0	0.024	2.0	0.49	0.24	4.90	1.0
4.3.6.4	51.0	0.024	6.4	1.23	6.12	0.98	7.97
	45.5	0.024	6.1	0.98	5.46	1.22	7.46
	5.2	0.024	3.7	0.98	0.62	1.22	1.41
	-	-	1.4	0.74	-	-	-
	2.0	0.024	1.0	0.74	0.24	1.62	1.0

TABLE 4.3.7 ILFRACOMBE 10th. Dec. 82 Trans. No.		Peak Pressure [KN/m ²]	Rise Time [sec.]	Secondary Pressure [KN/m ²]	Duration [sec.]	IMPULSE = Peak·Rise Time ² x10 ⁻¹ [Kns/m ²]	Rise Time Duration x10 ⁻²	Impact Secondary
4.3.7.1	1	13.4	0.048	18.8	4.17	3.22	1.15	0.71
	2	8.1	0.048	11.4	2.70	1.94	1.78	0.71
	3	3.5	0.024	7.9	0.98	0.42	2.45	0.44
	4	-	-	4.5	0.74	-	-	-
	5	-	-	3.4	0.74	-	-	-
4.3.7.2	1	16.2	0.380	10.4	4.41	30.78	8.62	1.56
	2	7.2	0.048	10.1	2.94	1.73	1.63	0.71
	3	2.0	0.024	4.6	1.72	0.24	1.4	0.43
	4	1.3	0.024	2.5	0.74	0.16	3.24	0.52
	5	-	-	-	-	-	-	-
4.3.7.3	1	14.3	0.22	16.6	3.43	15.73	6.41	0.86
	2	9.3	0.10	6.8	1.23	4.65	8.13	1.37
	3	2.0	0.048	3.4	0.98	0.48	4.90	0.59
	4	1.0	0.024	2.9	0.98	0.12	2.45	0.34
	5	-	-	-	-	-	-	-
4.3.7.4	1	18.3	0.072	18.3	4.41	6.59	1.63	1.00
	2	25.6	0.048	9.8	1.72	6.14	2.79	2.61
	3	3.0	0.024	3.8	1.23	0.36	1.95	0.79
	4	-	-	3.0	0.74	-	-	-
	5	-	-	1.6	0.49	-	-	-

TABLE 4.3.8 ILFRACOMBE 10th. Dec. 82 Trans. No.	Peak Pressure [KN/m ²]	Rise Time [sec.]	Secondary Pressure [KN/m ²]	Duration [sec.]	IMPULSE = Peak·Rise Time ² x10 ⁻¹ [KNS/m ²]	Rise Time Duration x10 ⁻²	Impact Secondary
4.3.8.1	16.7	0.26	18.4	4.41	21.71	5.90	0.91
	11.4	0.12	8.1	1.96	6.84	6.12	1.40
	1.7	0.024	1.7	0.74	2.04	3.24	1.00
	1.7	0.024	1.7	0.49	2.04	4.90	1.00
	-	-	-	-	-	-	-
4.3.8.2	13.1	0.017	14.9	22.70	1.11	0.75	0.88
	5.7	0.072	7.6	1.5	2.05	4.80	0.75
	2.9	0.048	3.6	0.74	0.70	6.49	0.81
	-	-	2.5	0.74	-	-	-
	-	-	-	-	-	-	-
4.3.8.3	19.7	0.17	19.7	2.45	16.75	6.94	1.00
	10.5	0.048	11.4	1.72	2.52	2.79	1.73
	4.9	0.024	7.3	1.23	0.59	1.95	0.67
	-	-	4.3	0.74	-	-	-
	2.3	0.048	3.9	0.74	0.55	6.49	0.59
4.3.8.4	16.9	0.14	16.9	3.43	11.83	4.08	1.00
	8.8	0.072	9.6	1.23	3.17	5.85	0.92
	4.6	0.024	2.7	0.98	0.19	2.45	0.59
	-	-	1.8	0.98	-	-	-
	-	-	-	-	-	-	-

TABLE 4.3.9 ILFRACOMBE 10th. Dec. 82 Trans. No.	Peak Pressure [KN/m ²]	Rise Time [sec.]	Secondary Pressure [KN/m ²]	Duration [sec.]	IMPULSE = Peak·Rise Time ² x10 ⁻¹ [KNs/m ²]	Rise Time Duration x10 ⁻²	Impact Secondary
4.3.9.1	14.6	0.01	14.6	3.19	0.73	0.31	1.00
	7.0	0.072	7.9	1.23	2.52	5.85	1.86
	4.3	0.024	1.5	0.98	0.52	2.45	2.87
	-	-	0.6	0.98	-	-	-
	-	-	1.2	0.74	-	-	-
4.3.9.2	35.6	0.072	24.7	2.94	12.82	0.12	1.44
	35.0	0.048	16.0	2.45	8.40	1.96	2.19
	10.3	0.048	11.5	1.72	2.47	2.79	0.90
	-	-	8.6	0.98	-	-	-
	2.0	0.024	1.5	0.98	0.24	2.45	1.33
4.3.9.3	22.1	0.43	25.4	4.41	47.50	9.75	0.87
	9.5	0.22	16.9	1.72	10.45	12.79	0.56
	4.7	0.12	13.1	1.23	2.82	9.76	0.36
	5.1	0.024	4.2	0.98	0.61	2.45	1.21
	1.0	0.024	1.7	0.74	0.12	3.24	0.59
4.3.9.4	18.3	0.46	10.7	5.64	42.10	8.16	1.71
	7.1	0.14	2.5	3.68	4.97	3.80	2.84
	2.1	0.024	0.3	0.14	0.25	17.14	7.00
	-	-	-	-	-	-	-
	-	-	-	-	-	-	-

TABLE 4.3.10 ILFRACOMBE 10th. Dec. 82 Trans. No.		Peak Pressure [KN/m ²]	Rise Time [sec.]	Secondary Pressure [KN/m ²]	Duration [sec.]	IMPULSE = Peak·Rise Time ² x10 ⁻¹ [KNs/m ²]	Rise Time Duration x10 ⁻²	Impact Secondary
4.3.10.1	1	13.4	0.10	12.2	2.45	6.70	4.08	1.10
	2	6.3	0.024	3.3	0.98	0.76	2.45	1.91
	3	0.9	0.024	3.2	0.74	0.11	3.24	0.28
	4	-	-	-	-	-	-	-
	5	-	-	-	-	-	-	-
4.3.10.2	1	21.6	0.19	14.4	1.47	20.52	12.93	1.50
	2	16.7	0.024	6.4	0.98	2.00	2.45	2.61
	3	14.1	0.024	4.2	0.98	1.69	2.45	3.36
	4	-	-	3.8	0.98	-	-	-
	5	-	-	1.7	0.98	-	-	-
4.3.10.3	1	14.4	0.38	10.5	3.92	27.36	9.69	1.37
	2	15.8	0.10	3.2	1.23	7.9	8.13	4.94
	3	7.2	0.024	3.3	1.96	0.86	1.22	2.18
	4	-	-	2.7	1.72	-	-	-
	5	-	-	-	-	-	-	-
4.3.10.4	1	30.0	0.12	24.4	2.94	18.00	4.08	1.23
	2	17.1	0.072	13.4	2.94	6.16	2.45	1.28
	3	8.4	0.048	11.3	1.23	2.02	3.90	0.74
	4	2.4	0.024	4.9	0.98	0.29	2.45	0.49
	5	2.1	0.024	3.7	0.98	0.25	2.45	0.57

TABLE 4.3.11 ILFRACOMBE 10th. Dec. 82 Trans No.		Peak Pressure [KN/m ²]	Rise Time [sec.]	Secondary Pressure [KN/m ²]	Duration [sec.]	IMPULSE = Peak·Rise Time ² x10 ⁻¹ [Kns/m ²]	Rise Time Duration x10 ⁻²	Impact Secondary
4.3.11.1	1	24.0	0.29	22.9	3.68	34.80	7.88	1.05
	2	12.2	0.01	12.2	1.72	0.61	0.58	1.00
	3	6.2	0.072	9.8	1.23	2.23	5.85	0.63
	4	3.3	0.48	6.8	0.98	0.79	4.90	0.49
	5	-	-	2.3	0.98	-	-	-
4.3.11.2	1	14.7	0.20	16.2	1.96	14.70	10.20	0.91
	2	10.3	0.096	10.2	1.72	4.94	5.58	1.01
	3	3.4	0.072	3.4	1.23	1.22	5.85	1.00
	4	3.1	0.024	2.3	0.98	0.37	2.45	1.49
	5	2.6	0.024	1.9	0.98	0.31	2.45	1.37
4.3.11.3	1	30.5	0.072	19.1	1.96	10.98	3.67	1.60
	2	34.7	0.048	9.3	1.72	8.33	2.79	3.73
	3	13.8	0.048	4.5	1.47	3.31	3.27	3.07
	4	-	-	3.6	0.74	-	-	-
	5	4.4	0.048	2.6	0.49	1.06	9.80	1.69
4.3.11.4	1	15.3	0.12	16.8	1.96	9.18	6.12	0.61
	2	9.3	0.048	8.4	1.47	2.23	3.27	1.11
	3	-	-	4.5	0.98	-	-	-
	4	-	-	3.4	0.98	-	-	-
	5	-	-	1.8	0.74	-	-	-

TABLE 4.3.12 ILFRACOMBE 10th. Dec. 82 Trans. No.	Peak Pressure [KN/m ²]	Rise Time [sec.]	Secondary Pressure [KN/m ²]	Duration [sec.]	IMPULSE = Peak·Rise Time ² x10 ⁻¹ [KNs/m ²]	Rise Time Duration x10 ⁻²	Impact Secondary
4.3.12.1	49.5	0.12	27.8	1.96	29.70	0.61	1.78
	47.4	0.024	18.9	1.96	5.69	1.22	2.51
	29.7	0.024	12.8	1.47	3.56	1.63	2.32
	17.2	0.024	10.3	1.47	2.06	1.63	1.67
	-	-	8.7	0.98	-	-	-
4.3.12.2	19.1	0.34	12.8	2.45	32.47	13.88	1.49
	13.8	0.19	11.7	2.40	13.11	7.92	1.18
	8.5	0.07	8.5	0.98	0.30	7.14	1.00
	6.7	0.049	3.4	0.74	1.64	6.62	1.97
	2.3	0.024	2.8	0.74	0.28	3.24	0.82
4.3.12.3	23.9	0.24	22.3	3.68	28.68	6.52	1.07
	10.1	0.072	10.1	1.47	3.64	2.45	1.00
	4.3	0.072	7.2	1.23	1.55	2.93	0.60
	-	-	2.3	0.74	-	-	-
	-	-	-	-	-	-	-
4.3.12.4	19.9	0.74	13.3	2.94	73.63	25.17	1.50
	9.8	0.12	12.2	1.72	5.88	6.98	0.92
	7.7	0.12	11.6	1.23	4.62	9.76	0.66
	3.9	0.10	6.8	1.23	1.95	8.13	0.57
	-	-	-	-	-	-	-

TABLE 4.3.13 ILFRACOMBE 10th. Dec. 82 Trans No.	Peak Pressure [KN/m ²]	Rise Time [sec.]	Secondary Pressure [KN/m ²]	Duration [sec.]	IMPULSE = Peak·Rise Time ² x10 ⁻¹ [KNS/m ²]	Rise Time Duration x10 ⁻²	Impact Secondary
4.3.13.1	24.4	0.14	17.1	2.21	17.08	6.33	1.43
	16.9	0.07	9.8	1.96	5.92	3.57	1.72
	7.2	0.024	8.6	1.23	0.86	1.14	0.84
	-	-	4.2	0.76	-	-	-
	-	-	2.2	0.76	-	-	-
4.3.13.2	32.5	0.14	20.3	1.96	22.75	7.14	1.60
	21.1	0.072	14.6	1.72	7.60	4.19	1.45
	11.5	0.012	10.1	1.23	0.69	1.48	1.14
	-	-	4.2	0.76	-	-	-
	-	-	1.4	0.76	-	-	-
4.3.13.3	33.5	0.14	26.0	2.45	23.45	5.71	1.29
	24.7	0.072	15.5	1.72	8.89	4.19	1.59
	16.3	0.048	14.7	1.47	3.91	3.27	1.11
	4.9	0.024	10.5	1.23	0.59	1.95	0.47
	3.0	0.024	3.4	1.23	0.36	1.95	0.88
4.3.13.4	40.5	0.17	30.4	2.45	34.43	6.94	1.33
	25.8	0.07	19.1	1.96	9.03	3.57	1.35
	19.2	0.048	19.1	1.96	4.61	2.45	1.01
	9.2	0.024	23.0	1.96	1.10	1.22	0.40
	2.9	0.024	6.6	0.92	0.35	2.61	0.44

TABLE 4.3.14 ILFRACOMBE 10th. Dec. 82 Trans. No.		Peak Pressure [KN/m ²]	Rise Time [sec.]	Secondary Pressure [KN/m ²]	Duration [sec.]	IMPULSE = Peak·Rise Time ² x10 ⁻¹ [KNS/m ²]	Rise Time Duration x10 ⁻²	Impact Secondary
4.3.14.1	1	40.0	0.14	32.5	2.45	28.00	5.71	1.23
	2	25.0	0.12	14.3	2.45	15.00	4.90	1.75
	3	18.1	0.048	19.9	2.45	4.34	1.96	0.91
	4	10.9	0.024	23.2	2.45	1.31	0.98	0.47
	5	3.3	0.048	4.6	1.23	0.79	3.90	0.72
4.3.14.2	1	30.8	0.17	23.1	2.45	26.18	6.94	1.33
	2	25.0	0.10	16.8	2.45	12.5	4.08	1.49
	3	20.7	0.024	12.7	1.23	2.48	1.95	1.63
	4	19.9	0.048	10.9	1.00	4.78	4.80	1.83
	5	2.7	0.024	3.9	0.98	0.32	2.45	0.69
4.3.14.3	1	29.3	0.24	24.4	3.43	35.16	6.99	1.20
	2	27.6	0.17	23.6	3.43	23.46	4.95	1.16
	3	35.9	0.072	23.0	2.98	12.92	2.41	1.56
	4	20.6	0.048	20.6	1.72	4.94	2.79	1.00
	5	5.6	0.024	7.9	1.23	0.67	1.95	0.71
4.3.14.4	1	34.5	0.31	28.8	2.45	53.47	12.65	1.20
	2	25.6	0.24	20.5	2.45	30.72	9.79	1.25
	3	14.7	0.12	16.8	1.96	8.82	6.12	0.87
	4	10.6	0.072	14.2	1.72	3.82	4.18	0.75
	5	2.4	0.048	4.1	1.72	0.58	2.79	0.58

TABLE 4.3.15 ILFRACOMBE 10th. Dec. 82 Trans No.	Peak Pressure [KN/m ²]	Rise Time [sec.]	Secondary Pressure [KN/m ²]	Duration [sec.]	IMPULSE = Peak·Rise Time ² x10 ⁻¹ [KNs/m ²]	Rise Time Duration x10 ⁻²	Impact Secondary
4.3.15.1	49.2	0.19	32.8	2.45	46.74	7.75	1.50
	35.9	0.048	28.2	2.45	8.62	1.96	1.27
	30.4	0.024	27.2	1.96	3.65	1.22	1.12
	132.7	0.024	26.5	1.96	15.92	1.22	5.01
	2.5	0.024	10.6	1.72	0.30	1.39	0.24
4.3.15.2	37.5	0.38	32.8	3.92	71.25	9.69	1.14
	24.0	0.24	18.4	2.94	28.80	8.16	1.30
	22.1	0.12	16.6	1.96	13.26	6.12	1.33
	14.1	0.072	16.8	1.47	5.08	4.90	0.84
	3.4	0.072	2.8	1.23	1.22	5.85	1.21
4.3.15.3	27.2	0.41	16.7	4.41	55.76	9.30	1.63
	21.4	0.31	12.3	4.41	33.17	7.03	1.74
	17.5	0.19	7.5	3.19	16.62	5.96	2.33
	15.5	0.19	5.8	1.23	14.72	15.45	2.67
	-	-	2.2	0.98	-	-	-
4.3.15.4	59.5	0.13	23.8	1.96	38.67	6.63	2.50
	58.1	0.048	15.5	1.96	13.94	2.45	3.74
	88.6	0.048	13.5	1.47	21.26	3.26	6.56
	78.3	0.024	13.0	1.23	9.40	1.95	6.02
	-	-	3.6	0.98	-	-	-

TABLE 4.3.16 ILFRACOMBE 10th. Dec. 82 Trans No.		Peak Pressure [KN/m ²]	Rise Time [sec.]	Secondary Pressure [KN/m ²]	Duration [sec.]	IMPULSE = $\frac{\text{Peak} \cdot \text{Rise Time}}{2}$ x10 ⁻¹ [KNs/m ²]	Rise Time Duration x10 ⁻²	Impact Secondary
4.3.16.1	1	33.4	0.072	26.7	3.68	12.02	1.96	1.25
	2	61.4	0.048	20.5	3.43	14.74	1.40	2.99
	3	62.1	0.024	17.7	1.96	7.45	1.22	3.51
	4	43.8	0.024	12.9	1.72	5.26	1.39	3.39
	5	3.3	0.024	3.3	1.23	0.40	1.95	1.00
4.3.16.2	1	53.4	0.072	30.0	1.96	19.20	3.67	1.78
	2	49.1	0.024	20.8	1.96	5.89	1.22	2.36
	3	66.6	0.024	15.3	1.96	7.99	1.22	4.35
	4	19.3	0.024	12.9	1.47	2.32	1.63	1.50
	5	4.1	0.024	4.9	0.98	0.49	2.45	0.84
4.3.16.3	1	40.0	0.24	32.5	4.90	48.00	4.90	1.23
	2	35.5	0.14	26.6	4.40	24.85	3.18	1.33
	3	30.5	0.048	19.7	1.96	7.32	2.45	1.55
	4	30.0	0.024	19.0	1.72	3.60	1.39	1.58
	5	2.5	0.024	5.6	0.98	0.30	2.45	0.45
4.3.16.4	1	22.7	0.12	13.7	2.21	13.62	5.43	1.66
	2	23.6	0.12	15.2	1.96	14.16	6.12	1.55
	3	18.7	0.048	12.5	1.47	4.49	3.26	1.50
	4	18.6	0.072	5.4	1.72	6.69	4.19	3.44
	5	-	-	3.1	1.23	-	-	-

TABLE 4.3.17 ILFRACOMBE 10th. Dec. 82 Trans. No.	Peak Pressure [KN/m ²]	Rise Time [sec.]	Secondary Pressure [KN/m ²]	Duration [sec.]	IMPULSE = Peak·Rise Time ² x10 ⁻¹ [KNs/m ²]	Rise Time Duration x10 ⁻²	Impact Secondary
4.3.17.1	25.1	0.14	11.8	1.96	17.57	7.14	2.13
	16.9	0.072	10.1	1.47	6.08	4.90	1.67
	14.1	0.072	9.4	0.98	5.08	7.35	1.50
	-	-	8.8	0.74	-	-	-
	-	-	2.5	0.74	-	-	-
4.3.17.2	31.0	0.17	23.3	2.45	26.35	6.94	1.33
	26.3	0.048	15.0	1.96	6.31	2.45	1.75
	23.4	0.024	12.7	1.72	2.81	1.39	1.84
	15.3	0.024	9.2	1.47	1.84	1.63	1.66
	2.1	0.024	2.7	0.98	0.25	2.45	0.78
4.3.17.3	-	-	31.5	4.86	-	-	-
	-	-	17.9	3.19	-	-	-
	-	-	14.7	1.96	-	-	-
	-	-	10.4	1.47	-	-	-
	-	-	1.4	0.74	-	-	-
4.3.17.4	31.9	0.31	23.7	2.45	49.44	12.65	1.34
	26.3	0.19	16.9	1.96	24.98	9.69	1.56
	23.9	0.072	18.4	1.72	8.60	4.19	1.30
	23.4	0.048	14.9	1.47	5.62	3.26	1.57
	-	-	6.2	0.74	-	-	-

TABLE 4.3.18 ILFRACOMBE 10th. Dec. 82 Trans. No.		Peak Pressure [KN/m ²]	Rise Time [sec.]	Secondary Pressure [KN/m ²]	Duration [sec.]	IMPULSE = Peak·Rise Time ² x10 ⁻¹ [Kns/m ²]	Rise Time Duration x10 ⁻²	Impact Secondary
4.3.18.1	1	-	-	38.0	4.9	-	-	-
	2	-	-	22.5	4.9	-	-	-
	3	-	-	10.8	2.7	-	-	-
	4	7.2	0.024	8.3	2.5	0.86	0.96	0.87
	5	-	-	1.9	1.0	-	-	-
4.3.18.2	1	-	-	28.0	5.9	-	-	-
	2	-	-	23.2	5.9	-	-	-
	3	-	-	11.3	2.0	-	-	-
	4	-	-	7.4	1.2	-	-	-
	5	-	-	2.6	2.0	-	-	-
4.3.18.3	1	-	-	39.5	4.2	-	-	-
	2	-	-	24.9	3.2	-	-	-
	3	-	-	22.8	2.4	-	-	-
	4	-	-	17.8	2.0	-	-	-
	5	3.7	0.024	2.1	1.0	0.44	2.4	1.76
4.3.18.4	1	35.0	0.82	33.0	3.0	143.50	27.33	1.06
	2	22.1	0.072	22.1	2.5	7.96	2.88	1.00
	3	17.5	0.048	20.7	1.7	4.20	2.82	0.84
	4	11.3	0.048	19.7	1.5	2.71	3.20	0.57
	5	2.1	0.024	5.3	1.0	0.25	2.40	0.40

TABLE 4.3.19 ILFRACOMBE 10th. Dec. 82 Trans. No.		Peak Pressure [KN/m ²]	Rise Time [sec.]	Secondary Pressure [KN/m ²]	Duration [sec.]	IMPULSE = Peak·Rise Time ² x10 ⁻¹ [KNS/m ²]	Rise Time Duration x10 ⁻²	Impact Secondary
4.3.19.1	1	40.0	0.096	27.5	1.96	19.20	4.90	1.45
	2	28.0	0.048	20.0	1.96	6.72	2.45	1.40
	3	9.8	0.024	15.0	1.72	1.18	1.39	0.65
	4	-	-	7.5	1.00	-	-	-
	5	-	-	5.0	0.74	-	-	-
4.3.19.2	1	35.6	0.22	24.0	2.45	39.16	8.98	1.48
	2	27.0	0.072	16.9	1.96	9.72	3.67	1.60
	3	19.6	0.024	12.5	1.23	2.35	1.95	1.57
	4	11.8	0.048	10.0	1.23	2.83	3.90	1.18
	5	-	-	3.8	1.00	-	-	-
4.3.19.3	1	35.0	0.10	20.0	1.96	17.50	5.10	1.75
	2	31.1	0.048	12.9	1.96	7.46	2.45	2.41
	3	25.1	0.024	9.2	1.47	3.01	1.63	2.73
	4	14.4	0.072	6.3	0.74	5.18	9.73	2.28
	5	2.0	0.024	3.0	0.74	0.24	3.24	0.67
4.3.19.4	1	60.0	0.19	33.8	2.45	57.00	7.75	1.77
	2	44.5	0.072	20.8	2.45	16.02	2.94	2.14
	3	35.0	0.048	15.0	2.21	8.40	2.17	2.33
	4	30.9	0.048	14.3	1.71	7.42	0.33	2.16
	5	4.0	0.048	7.0	0.98	0.96	4.90	0.57

TABLE 4.3.20 ILFRACOMBE 10th. Dec. 82 Trans. No.		Peak Pressure [KN/m ²]	Rise Time [sec.]	Secondary Pressure [KN/m ²]	Duration [sec.]	IMPULSE = Peak·Rise Time ² x10 ⁻¹ [KNs/m ²]	Rise Time Duration x10 ⁻²	Impact Secondary
4.3.20.1	1	37.5	0.82	26.3	2.45	15.37	33.46	1.42
	2	28.5	0.12	19.6	2.21	17.10	5.43	1.45
	3	20.0	0.048	15.0	1.47	4.80	3.26	1.33
	4	16.2	0.072	14.3	1.47	5.83	4.90	1.13
	5	2.0	0.072	6.0	0.98	0.72	7.35	0.33
4.3.20.2	1	34.6	0.24	23.7	2.45	41.52	9.79	1.46
	2	27.1	0.14	18.6	1.96	18.97	7.14	1.46
	3	26.3	0.048	13.1	1.96	6.31	2.44	2.01
	4	47.7	0.048	10.9	1.72	11.44	2.79	4.38
	5	3.3	0.072	5.9	1.72	1.18	4.19	0.56
4.3.20.3	1	69.5	0.12	30.4	2.94	41.70	4.08	2.29
	2	60.5	0.072	16.1	2.45	21.78	2.94	3.76
	3	88.1	0.072	14.1	1.96	31.72	3.67	6.25
	4	36.6	0.024	8.3	1.23	4.39	1.95	4.41
	5	-	-	3.9	1.23	-	-	-
4.3.20.4	1	34.5	0.19	30.2	2.45	32.77	7.75	1.14
	2	20.2	0.096	20.2	2.45	9.70	3.92	1.00
	3	11.7	0.048	14.1	1.72	2.81	2.79	0.83
	4	5.6	0.048	14.1	1.23	1.34	3.90	0.40
	5	-	-	3.9	1.23	-	-	-

TABLE 4.3.21 ILFRACOMBE 10th. Dec. 82 Trans. No.		Peak Pressure [KN/m ²]	Rise Time [sec.]	Secondary Pressure [KN/m ²]	Duration [sec.]	IMPULSE = Peak·Rise Time ² x10 ⁻¹ [KNS/m ²]	Rise Time Duration x10 ⁻²	Impact Secondary
4.3.21.1	1	28.1	0.14	20.6	1.96	19.67	7.14	1.36
	2	19.7	0.072	12.7	1.96	7.09	3.67	1.55
	3	15.4	0.072	11.5	1.47	5.54	4.90	1.34
	4	-	-	4.2	0.98	-	-	-
	5	-	-	3.1	0.98	-	-	-
4.3.21.2	1	47.5	0.24	38.6	2.94	57.00	8.16	1.23
	2	39.2	0.072	25.5	2.45	14.11	2.94	1.60
	3	30.4	0.024	21.8	1.96	3.65	1.22	1.39
	4	87.0	0.024	15.2	1.72	10.44	1.39	5.72
	5	5.6	0.024	7.9	0.98	0.67	2.45	0.71
4.3.21.3	1	39.0	0.14	24.4	1.72	27.3	8.14	1.60
	2	31.1	0.048	14.2	1.72	7.46	2.79	2.19
	3	24.9	0.024	8.9	1.47	2.99	1.63	2.80
	4	7.6	0.048	7.6	0.98	1.82	4.90	1.00
	5	5.4	0.024	1.7	0.98	0.65	2.45	3.18
4.3.21.4	1	28.0	0.17	30.0	1.96	23.80	8.67	0.93
	2	18.7	0.072	20.1	1.96	6.73	3.67	0.93
	3	6.8	0.048	11.3	1.23	1.63	3.90	0.60
	4	5.0	0.072	5.0	0.98	1.80	7.35	1.00
	5	3.0	0.024	3.8	0.74	0.36	3.24	0.79

TABLE 4.3.22 ILFRACOMBE 10th. Dec. 82 Trans. No.		Peak Pressure [KN/m ²]	Rise Time [sec.]	Secondary Pressure [KN/m ²]	Duration [sec.]	IMPULSE = $\frac{\text{Peak} \cdot \text{Rise Time}}{2}$ x10 ⁻¹ [KNs/m ²]	Rise Time Duration x10 ⁻²	Impact Secondary
4.3.22.1	1	26.7	0.12	22.9	4.41	16.02	2.72	1.16
	2	28.8	0.048	13.3	3.92	6.91	1.22	2.16
	3	39.5	0.024	11.6	1.23	4.74	1.95	3.40
	4	4.3	0.024	8.7	0.98	0.52	2.45	0.49
	5	2.5	0.048	3.1	0.98	0.60	4.90	0.81
4.3.22.2	1	26.3	0.17	18.8	1.96	22.35	8.67	1.40
	2	19.5	0.072	15.0	1.47	7.02	4.90	1.30
	3	7.3	0.072	10.0	0.98	2.62	7.35	0.73
	4	3.6	0.072	3.6	0.98	1.30	4.28	1.00
	5	3.3	0.024	3.3	0.98	0.40	2.45	1.00
4.3.22.3	1	30.9	0.36	30.9	6.62	55.62	5.44	1.00
	2	21.0	0.12	19.5	4.41	12.60	2.72	1.08
	3	13.4	0.048	18.8	1.47	3.22	3.26	0.71
	4	10.9	0.048	13.1	1.23	2.62	3.90	0.83
	5	4.5	0.048	5.4	0.74	1.08	6.49	0.83
4.3.22.4	1	-	-	26.5	3.43	-	-	-
	2	-	-	17.8	3.43	-	-	-
	3	-	-	17.5	2.94	-	-	-
	4	-	-	17.5	1.96	-	-	-
	5	-	-	2.0	1.23	-	-	-

TABLE 4.3.23 ILFRACOMBE 10th. Dec. 82 Trans. No.		Peak Pressure [KN/m ²]	Rise Time [sec.]	Secondary Pressure [KN/m ²]	Duration [sec.]	IMPULSE = Peak·Rise Time ² x10 ⁻¹ [KNS/m ²]	Rise Time Duration x10 ⁻²	Impact Secondary
4.3.23.1	1	-	-	29.5	4.90	-	-	-
	2	-	-	21.6	3.43	-	-	-
	3	4.5	0.048	16.9	3.43	1.08	1.40	0.26
	4	16.3	0.048	5.0	0.74	3.91	6.49	3.26
	5	1.6	0.024	2.7	0.74	0.19	3.24	0.59
4.3.23.2	1	22.9	0.74	19.1	2.45	84.73	30.20	1.20
	2	17.6	0.24	13.2	1.96	21.12	12.24	1.33
	3	10.4	0.10	9.3	1.23	5.20	8.13	1.12
	4	5.8	0.048	5.8	0.98	1.39	4.90	1.00
	5	-	-	5.3	0.98	-	-	-
4.3.23.3	1	-	-	25.8	4.90	-	-	-
	2	13.9	0.14	13.9	1.47	9.73	9.52	1.00
	3	8.9	0.024	12.8	1.23	1.07	1.95	0.69
	4	5.4	0.12	9.7	1.23	3.24	9.76	0.56
	5	-	-	3.3	0.98	-	-	-
4.3.23.4	1	23.6	0.24	13.65	1.96	28.32	1.22	1.73
	2	27.6	0.14	11.50	1.72	19.32	8.14	2.40
	3	13.7	0.072	9.13	1.23	4.93	5.85	1.50
	4	6.7	0.048	6.70	0.98	1.61	4.90	1.00
	5	1.9	0.024	6.70	0.98	0.23	2.45	0.28

TABLE 4.3.24 ILFRACOMBE 10th. Dec. 82 Trans. No.		Peak Pressure [KN/m ²]	Rise Time [sec.]	Secondary Pressure [KN/m ²]	Duration [sec.]	IMPULSE = Peak·Rise Time ² x10 ⁻¹ [KNs/m ²]	Rise Time Duration x10 ⁻²	Impact Secondary
4.3.24.1	1	42.0	1.96	39.4	4.90	411.60	40.00	1.06
	2	34.5	0.10	28.7	2.94	17.25	3.40	1.20
	3	27.4	0.024	23.7	2.94	3.29	0.82	1.16
	4	38.3	0.024	14.1	1.47	4.60	1.63	2.72
	5	3.9	0.048	6.8	0.98	0.94	4.90	0.57
4.3.24.2	1	41.7	0.61	33.4	2.45	127.18	24.89	1.25
	2	34.6	0.10	24.7	2.45	17.30	4.08	1.40
	3	28.5	0.048	21.8	1.23	6.84	3.90	1.31
	4	22.3	0.024	21.9	1.23	2.68	1.95	1.02
	5	2.2	0.024	3.6	0.98	0.26	2.45	0.61
4.3.24.3	1	59.5	0.14	37.2	2.45	41.65	5.71	1.60
	2	21.5	0.10	23.1	2.45	10.75	4.08	0.93
	3	35.3	0.024	19.6	1.96	4.24	1.22	1.80
	4	51.6	0.024	19.2	1.96	6.19	1.22	2.69
	5	4.5	0.024	6.0	1.23	0.54	1.95	0.75
4.3.24.4	1	32.0	0.98	28.8	2.94	156.80	33.33	1.11
	2	22.8	0.19	19.5	2.45	21.66	7.75	1.17
	3	15.3	0.10	18.4	1.47	7.65	6.80	0.83
	4	10.3	0.72	14.4	1.47	3.71	4.90	0.71
	5	5.4	0.24	5.4	0.74	0.65	3.24	1.00

TABLE 4.3.25 ILFRACOMBE 10th. Dec. 82 Trans No.	Peak Pressure [KN/m ²]	Rise Time [sec.]	Secondary Pressure [KN/m ²]	Duration [sec.]	IMPULSE = Peak·Rise Time ² x10 ⁻¹ [KNs/m ²]	Rise Time Duration x10 ⁻²	Impact Secondary
4.3.25.1	33.3	0.17	23.8	1.96	28.31	8.67	1.40
	24.4	0.10	15.0	1.96	12.20	5.10	1.63
	16.6	0.024	14.9	1.47	1.99	1.63	1.11
	12.8	0.072	7.7	1.47	4.61	4.90	1.66
	-	-	4.1	1.23	-	-	-
4.3.25.2	25.1	0.19	27.2	3.68	4.57	5.16	0.92
	21.4	0.12	16.8	2.94	12.84	4.08	1.27
	16.1	0.048	14.0	1.47	3.86	3.27	1.15
	3.8	0.024	10.0	1.23	0.46	1.95	0.38
	-	-	3.0	1.23	-	-	-
4.3.25.3	29.6	0.17	39.5	2.94	25.16	5.78	0.75
	21.4	0.12	24.9	2.45	12.84	4.90	0.86
	15.3	0.048	24.5	2.21	3.67	2.17	0.62
	9.8	0.048	21.4	1.96	2.35	2.45	0.46
	3.3	0.048	6.5	0.74	0.79	6.49	0.51
4.3.25.4	27.2	0.22	34.9	3.43	29.92	6.41	0.78
	17.5	0.048	22.2	3.43	4.20	1.40	0.79
	20.5	0.024	14.9	3.19	2.46	0.75	1.38
	17.2	0.024	10.3	1.47	2.06	1.63	1.67
	3.3	0.024	2.6	1.47	0.40	1.63	1.27

TABLE 4.3.26 ILFRACOMBE 10th. Dec. 82 Trans. No.		Peak Pressure [KN/m ²]	Rise Time [sec.]	Secondary Pressure [KN/m ²]	Duration [sec.]	IMPULSE = Peak·Rise Time ² x10 ⁻¹ [KNS/m ²]	Rise Time Duration x10 ⁻²	Impact Secondary
4.3.26.1	1	27.2	0.24	27.2	3.68	32.64	6.52	1.00
	2	18.6	0.10	15.5	1.96	9.30	5.10	1.20
	3	14.3	0.048	15.1	0.83	3.43	5.78	0.95
	4	3.1	0.024	10.7	1.23	0.37	1.95	0.29
	5	2.6	0.024	3.6	0.74	0.31	3.24	0.72
4.3.26.2	1	35.6	0.36	34.2	2.45	64.08	14.69	1.04
	2	30.6	0.14	22.2	2.45	21.42	5.71	1.38
	3	19.9	0.024	18.6	1.72	2.39	1.40	1.07
	4	18.5	0.024	15.8	1.47	2.22	1.63	1.17
	5	3.9	0.024	8.7	0.98	0.47	2.45	0.45
4.3.26.3	1	57.00	0.17	34.2	2.45	48.45	6.94	1.67
	2	41.70	0.024	19.5	1.96	50.04	1.22	2.14
	3	43.10	0.048	16.6	1.72	10.34	2.79	2.60
	4	26.80	0.048	16.2	1.72	6.43	2.79	1.65
	5	5.40	0.048	4.5	1.72	1.30	2.79	1.20
4.3.26.4	1	34.5	0.29	32.8	2.45	50.03	11.84	1.05
	2	24.8	0.17	28.9	2.45	21.08	6.94	0.86
	3	19.1	0.072	20.6	1.72	6.88	4.19	0.93
	4	12.0	0.048	20.1	1.23	2.88	3.90	0.60
	5	-	-	5.5	0.74	-	-	-

TABLE 4.3.27 ILFRACOMBE 10th. Dec. 82 Trans. No.	Peak Pressure [KN/m ²]	Rise Time [sec.]	Secondary Pressure [KN/m ²]	Duration [sec.]	IMPULSE = Peak·Rise Time		Rise Time Duration x10 ⁻²	Impact Secondary
					$\times 10^{-1}$ [KNs/m ²]	²		
4.3.27.1	42.2	0.14	39.4	2.45	29.54	-	5.71	1.07
	29.3	0.10	29.3	2.45	14.65	-	4.08	1.00
	21.7	0.072	27.6	1.96	7.81	-	3.67	0.79
	15.8	0.024	27.3	1.71	1.90	-	1.40	0.58
	-	-	13.5	1.23	-	-	-	-
4.3.27.2	39.4	0.14	42.2	2.94	27.58	-	4.76	0.93
	25.1	0.072	27.2	2.94	9.04	-	2.45	0.92
	16.5	0.048	23.6	2.45	3.96	-	1.96	0.70
	7.9	0.024	23.6	2.21	0.95	-	1.09	0.33
	-	-	9.3	0.74	-	-	-	-
4.3.27.3	35.0	0.19	32.8	1.96	33.25	-	9.69	1.07
	24.1	0.10	20.6	1.96	12.05	-	5.10	1.17
	14.5	0.072	20.3	1.72	5.22	-	4.19	0.71
	14.6	0.024	16.2	1.23	1.75	-	1.95	0.90
	-	-	4.3	0.74	-	-	-	-
4.3.27.4	40.5	1.23	37.9	4.90	249.08	-	25.10	1.07
	25.8	0.17	24.0	3.68	21.93	-	4.62	1.08
	17.3	0.024	14.8	2.45	2.08	-	0.98	1.17
	14.1	0.048	21.9	1.23	3.38	-	3.90	0.64
	-	-	5.0	0.74	-	-	-	-

TABLE 4.4.1 ILFRACOMBE 22nd. March 83 Trans. No.		Peak Pressure [KN/m ²]	Rise Time [sec.]	Secondary Pressure [KN/m ²]	Duration [sec.]	IMPULSE = Peak·Rise Time ² x10 ⁻¹ [KNs/m ²]	Rise Time Duration x10 ⁻²	Impact Secondary
4.4.1.1	1	-	-	19.0	2.95	-	-	-
	4	-	-	7.2	2.83	-	-	-
	5	-	-	6.3	2.09	-	-	-
4.4.1.2	1	-	-	15.7	1.48	-	-	-
	4	-	-	8.8	1.97	-	-	-
	5	5.25	0.036	7.9	1.97	0.95	1.83	0.7
4.4.1.3	1	7.9	0.036	13.5	2.83	1.42	1.27	0.6
	4	3.4	0.036	3.4	2.21	0.61	1.63	1.0
	5	7.0	0.012	6.0	1.60	0.42	0.75	1.2
4.4.1.4	1	-	-	8.6	2.46	-	-	-
	4	-	-	5.7	1.85	-	-	-
	5	6.1	0.048	6.1	2.21	1.46	2.17	1.0
4.4.1.5	1	10.1	0.036	6.3	1.60	1.82	2.25	1.6
	4	4.5	0.036	4.5	1.48	0.81	2.43	1.0
	5	9.6	0.060	10.3	1.72	2.88	3.49	0.9

TABLE 4.4.2 ILFRACOMBE 22nd. March 83 Trans. No	Peak Pressure [KN/m ²]	Rise Time [sec.]	Secondary Pressure [KN/m ²]	Duration [sec.]	IMPULSE = Peak·Rise Time ² x10 ⁻¹ [KNs/m ²]	Rise Time Duration x10 ⁻²	Impact Secondary
4.4.2.1	15.9	0.012	8.3	1.72	0.95	0.70	1.9
	-	-	2.8	1.85	-	-	-
	2.1	0.012	5.3	1.23	0.13	0.98	0.4
4.4.2.2	13.9	0.012	6.9	1.23	0.83	0.98	2.0
	5.2	0.060	3.8	1.23	1.56	4.88	1.4
	7.0	0.024	5.0	1.23	0.84	1.95	1.4
4.4.2.3	9.0	0.012	13.1	2.71	0.54	0.44	0.7
	4.3	0.048	7.7	1.97	1.03	2.44	0.6
	6.3	0.036	7.5	2.21	1.13	1.63	0.8
4.4.2.4	15.3	0.012	10.9	1.48	0.92	0.81	1.4
	-	-	5.2	1.72	-	-	-
	6.0	0.024	5.0	1.23	0.72	1.95	1.2
4.4.2.5	14.2	0.048	7.7	1.72	3.41	2.79	1.8
	3.3	0.024	3.7	1.60	0.40	1.50	0.9
	6.0	0.012	6.0	1.23	0.36	0.98	1.0

TABLE 4.4.3 ILFRACOMBE 22nd. March 83 Trans. No.	Peak Pressure [KN/m ²]	Rise Time [sec.]	Secondary Pressure [KN/m ²]	Duration [sec.]	IMPULSE = Peak.Rise Time ² x10 ⁻¹ [KNs/m ²]	Rise Time Duration x10 ⁻²	Impact Secondary
4.4.3.1	9.75	0.012	11.4	1.97	0.59	0.61	0.9
	3.56	0.012	6.5	1.85	0.21	0.65	0.5
	3.56	0.024	5.9	1.23	0.43	1.95	0.6
4.4.3.2	38.9	0.012	7.8	1.23	2.33	0.98	5.0
	2.4	0.036	3.3	1.23	0.43	2.93	0.7
	-	-	4.4	0.98	-	-	-
4.4.3.3	6.3	0.024	14.1	1.72	0.76	1.40	0.4
	5.6	0.072	5.6	1.60	2.02	4.50	1.0
	5.5	0.023	5.5	1.60	0.63	1.44	1.0
4.4.3.4	13.6	0.012	9.6	1.48	0.82	0.81	1.4
	-	-	3.2	1.72	-	-	-
	6.7	0.024	3.4	1.48	0.80	1.62	2.0
4.4.3.5	14.3	0.012	13.1	1.23	0.86	0.98	1.1
	5.3	0.036	5.3	1.48	0.95	2.43	1.0
	13.9	0.024	4.6	0.62	1.67	3.87	3.0

TABLE 4.4.4 ILFRACOMBE 22nd. March 83 Trans. No.	Peak Pressure [KN/m ²]	Rise Time [sec.]	Secondary Pressure [KN/m ²]	Duration [sec.]	IMPULSE = Peak·Rise Time ² x10 ⁻¹ [KNs/m ²]	Rise Time Duration x10 ⁻²	Impact Secondary
4.4.4.1	10.9	0.024	12.7	1.72	1.31	1.40	0.9
	4.5	0.024	4.5	1.72	0.54	1.40	1.0
	5.5	0.012	5.5	1.23	0.33	0.98	1.0
4.4.4.2	10.1	0.084	9.8	1.85	4.24	4.54	1.0
	-	-	3.5	1.48	-	-	-
	9.6	0.096	6.2	1.60	4.61	6.00	1.5
4.4.4.3	12.2	0.024	5.6	1.48	1.46	1.62	2.2
	-	-	1.7	1.23	-	-	-
	-	-	4.7	0.98	-	-	-
4.4.4.4	8.0	0.024	12.0	1.23	0.96	1.95	0.7
	2.8	0.024	4.2	1.23	0.34	1.95	0.7
	9.7	0.012	3.7	1.23	0.58	0.98	2.6
4.4.4.5	13.1	0.096	5.6	1.60	6.29	6.00	2.3
	5.0	0.036	6.0	1.85	0.90	1.95	0.8
	3.9	0.012	6.5	1.23	0.23	0.98	0.6

TABLE 4.4.5 ILFRACOMBE 22nd. March 83 Trans. No.	Peak Pressure [KN/m ²]	Rise Time [sec.]	Secondary Pressure [KN/m ²]	Duration [sec.]	IMPULSE = $\frac{\text{Peak} \cdot \text{Rise Time}}{2}$ x10 ⁻¹ [KNs/m ²]	Rise Time Duration x10 ⁻²	Impact Secondary
4.4.5.1	16.5	0.024	14.4	1.72	1.99	1.40	1.1
	2.3	0.024	3.7	1.72	0.28	1.40	0.6
	9.4	0.012	8.1	0.62	0.56	1.94	1.2
4.4.5.2	11.3	0.036	14.1	2.46	2.03	1.46	0.8
	4.8	0.048	3.4	2.21	1.15	2.17	1.4
	9.6	0.012	5.6	0.37	0.58	3.24	1.7
4.4.5.3	10.3	0.180	14.1	2.46	9.27	7.32	0.7
	4.1	0.084	6.9	1.48	1.72	5.68	0.6
	9.4	0.072	5.6	1.48	1.13	4.86	1.7
4.4.5.4	9.8	0.024	13.1	1.23	1.18	1.95	0.7
	2.3	0.012	4.0	1.60	0.14	0.75	0.6
	9.6	0.024	5.3	0.37	1.15	6.49	1.7
4.4.5.5	12.0	0.036	15.3	0.98	2.16	3.67	0.8
	6.0	0.072	5.3	0.98	2.16	7.35	1.1
	12.3	0.084	13.1	0.98	5.17	8.57	0.9

TABLE 4.4.6 ILFRACOMBE 22nd. March 83	Trans No.	Peak Pressure [KN/m ²]	Rise Time [sec.]	Secondary Pressure [KN/m ²]	Duration [sec.]	IMPULSE = $\frac{\text{Peak} \cdot \text{Rise Time}}{2}$ x10 ⁻¹ [KNs/m ²]	Rise Time Duration x10 ⁻²	Impact Secondary
4.4.6.1	1	12.6	0.130	11.6	2.46	8.19	5.28	1.1
	4	7.3	0.060	4.5	1.48	2.19	4.05	1.6
	5	6.8	0.072	8.2	1.72	2.45	4.19	0.8
4.4.6.2	1	21.6	0.012	13.5	1.72	1.30	0.70	1.6
	4	3.4	0.012	4.5	1.72	0.20	0.70	0.8
	5	9.8	0.012	6.1	1.23	0.59	0.98	1.6
4.4.6.3	1	13.5	0.012	14.6	1.23	0.81	0.98	0.9
	4	3.6	0.024	7.1	1.23	0.43	1.95	0.5
	5	9.4	0.012	7.0	0.98	0.56	1.22	1.3
4.4.6.4	1	7.5	0.024	14.1	1.23	0.90	1.95	0.5
	4	2.0	0.024	4.0	1.23	0.24	1.95	0.5
	5	7.3	0.048	4.1	0.98	1.75	4.90	1.8
4.4.6.5	1	13.8	0.084	9.6	1.48	5.80	5.68	1.4
	4	5.0	0.048	5.0	1.23	1.20	3.90	1.0
	5	5.0	0.036	4.3	1.23	0.99	2.93	1.2

TABLE 4.4.7 ILFRACOMBE 22nd. March 83 Trans. No.	Peak Pressure [KN/m ²]	Rise Time [sec.]	Secondary Pressure [KN/m ²]	Duration [sec.]	IMPULSE = Peak·Rise Time ² x10 ⁻¹ [KNS/m ²]	Rise Time Duration x10 ⁻²	Impact Secondary
4.4.7.1	14.3	0.072	8.3	1.23	5.15	5.85	1.7
	6.6	0.060	3.3	1.23	1.98	4.88	2.0
	5.4	0.024	6.7	0.98	0.65	2.45	0.8
4.4.7.2	7.1	0.024	14.2	1.23	0.85	1.95	0.2
	6.6	0.048	3.9	1.23	1.58	3.90	1.7
	8.4	0.048	2.9	1.23	2.02	3.90	2.9
4.4.7.3	-	-	12.2	1.23	-	-	-
	3.2	0.036	1.9	1.23	0.58	2.93	1.7
	8.3	0.120	2.8	1.48	4.98	8.11	3.0
4.4.7.4	12.0	0.072	8.0	1.48	4.32	4.86	1.5
	5.6	0.048	4.7	1.23	1.34	3.90	1.2
	5.0	0.024	4.3	0.86	6.00	2.79	1.2
4.4.7.5	7.3	0.036	18.3	1.72	1.31	2.09	0.4
	4.5	0.048	5.5	1.60	1.08	3.00	0.8
	3.6	0.024	6.3	1.48	0.43	1.62	0.6

TABLE 4.4.8 ILFRACOMBE 22nd. March 83 Trans. No.		Peak Pressure [KN/m ²]	Rise Time [sec.]	Secondary Pressure [KN/m ²]	Duration [sec.]	IMPULSE = $\frac{\text{Peak} \cdot \text{Rise Time}}{2}$ x10 ⁻¹ [KNs/m ²]	Rise Time Duration x10 ⁻²	Impact Secondary
4.4.8.1	1	13.4	0.012	7.2	1.23	0.80	0.98	1.9
	4	2.8	0.024	3.3	1.72	0.34	1.40	0.8
	5	9.6	0.012	6.6	0.98	0.58	1.22	1.5
4.4.8.2	1	14.5	0.060	7.7	1.23	4.35	4.88	1.9
	4	4.8	0.036	4.4	1.48	0.86	2.43	1.1
	5	7.8	0.048	0.56	1.23	1.87	3.90	13.9
4.4.8.3	1	-	-	13.8	2.46	-	-	-
	4	8.0	0.060	3.5	2.2	2.40	2.73	2.3
	5	-	-	13.1	2.2	-	-	-
4.4.8.4	1	15.0	0.072	6.0	1.85	5.40	3.89	2.5
	4	5.6	0.048	3.9	1.85	1.34	2.59	1.4
	5	4.0	0.024	5.5	0.86	0.48	1.29	0.7
4.4.8.5	1	23.0	0.024	11.5	1.48	2.76	1.62	2.0
	4	6.6	0.060	3.9	1.72	1.98	3.49	1.7
	5	2.4	0.012	7.1	0.74	0.14	0.69	0.3

TABLE 4.4.9 ILFRACOMBE 22nd. March 83		Trans. No.	Peak Pressure [KN/m ²]	Rise Time [sec.]	Secondary Pressure [KN/m ²]	Duration [sec.]	IMPULSE = Peak·Rise Time ² x10 ⁻¹ [KNs/m ²]	Rise Time Duration x10 ⁻²	Impact Secondary
4.4.9.1	1	13.0	0.048	8.0	1.50	3.12	3.20	1.6	
	4	5.9	0.060	4.2	1.48	1.77	4.05	1.4	
	5	3.9	0.024	9.7	1.72	0.47	1.40	0.4	

TABLE 4.5.1 ILFRACOMBE 23rd. March 83 Trans. No.	Peak Pressure [KN/m ²]	Rise Time [sec.]	Secondary Pressure [KN/m ²]	Duration [sec.]	IMPULSE = Peak·Rise Time ² x10 ⁻¹ [KNs/m ²]	Rise Time Duration x10 ⁻²	Impact Secondary
4.5.1.1	10.1	0.108	9.3	3.69	5.45	2.93	1.1
	4.7	0.084	5.9	2.70	1.97	3.11	0.8
	9.5	0.048	15.8	1.51	2.28	3.18	0.6
4.5.1.2	12.0	0.024	8.8	2.95	1.44	0.81	1.4
	-	-	7.1	2.95	-	-	-
	3.1	0.012	14.8	1.97	0.19	0.61	0.2
4.5.1.3	13.1	0.012	7.1	3.19	0.79	0.38	1.8
	3.0	0.024	6.0	3.07	0.36	0.78	0.5
	1.6	0.012	10.8	2.09	0.10	0.57	0.1
4.5.1.4	12.45	0.012	9.1	2.95	0.75	0.41	1.4
	4.8	0.036	10.5	2.46	0.86	1.46	0.5
	3.5	0.024	9.3	2.21	0.42	1.09	0.4
4.5.1.5	33.2	0.024	8.3	2.46	3.98	0.98	4.0
	-	-	4.5	2.46	-	-	-
	1.65	0.012	6.2	1.84	0.10	0.65	0.3

TABLE 4.5.2 ILFRACOMBE 23rd.March 83 Trans No.	Peak Pressure [KN/m ²]	Rise Time [sec.]	Secondary Pressure [KN/m ²]	Duration [sec.]	IMPULSE = Peak·Rise Time ² x10 ⁻¹ [Kns/m ²]	Rise Time Duration x10 ⁻²	Impact Secondary
4.5.2.1	66.4	0.024	8.3	2.46	7.97	0.98	8.0
	-	-	4.5	2.46	-	-	-
	-	-	6.2	1.84	-	-	-
4.5.2.2	9.7	0.012	6.5	2.95	0.58	0.41	1.5
	-	-	4.1	2.82	-	-	-
	7.8	0.036	6.0	1.84	1.40	1.96	1.3
4.5.2.3	11.4	0.024	7.3	3.07	1.37	0.78	1.0
	-	-	8.3	2.46	-	-	-
	4.5	0.036	9.0	2.21	0.81	1.63	0.5
4.5.2.4	9.7	0.012	4.1	2.71	0.58	0.44	2.4
	1.4	0.012	2.7	2.71	0.08	0.44	0.5
	2.2	0.024	3.7	1.72	0.26	1.40	0.6
4.5.2.5	9.7	0.012	7.8	2.71	0.58	0.44	1.2
	2.0	0.012	5.2	2.71	1.20	0.44	0.4
	1.5	0.012	4.5	1.72	0.09	0.70	0.3

TABLE 4.5.3 ILFRACOMBE 23rd. March 83 Trans. No.		Peak Pressure [KN/m ²]	Rise Time [sec.]	Secondary Pressure [KN/m ²]	Duration [sec.]	IMPULSE = $\frac{\text{Peak} \cdot \text{Rise Time}}{2}$ x10 ⁻¹ [KNs/m ²]	Rise Time Duration x10 ⁻²	Impact Secondary
4.5.3.1	1	10.8	0.024	12.3	2.71	1.30	0.89	0.88
	4	2.0	0.012	6.2	3.4	0.12	0.35	0.32
	5	5.2	0.012	12.3	2.46	0.31	0.49	4.23
4.5.3.2	1	12.7	0.024	6.9	2.21	1.52	1.09	1.84
	4	-	-	11.4	3.44	-	-	-
	5	-	-	11.6	2.46	-	-	-
4.5.3.3	1	18.5	0.012	9.3	2.21	1.11	0.54	1.99
	4	-	-	4.9	1.72	-	-	-
	5	-	-	5.8	1.23	-	-	-
4.5.3.4	1	6.2	0.024	14.4	2.21	0.74	1.09	0.43
	4	4.3	0.024	6.4	1.72	0.52	1.40	0.67
	5	4.8	0.024	5.5	1.23	0.58	1.95	0.87
4.5.3.5	1	19.3	0.012	8.3	1.97	1.16	0.61	2.33
	4	-	-	3.0	1.6	-	-	-
	5	13.7	0.024	5.0	1.85	1.64	1.30	2.74

TABLE 4.5.4 ILFRACOMBE 23rd. March 83 Trans No.	Peak Pressure [KN/m ²]	Rise Time [sec.]	Secondary Pressure [KN/m ²]	Duration [sec.]	IMPULSE = Peak·Rise Time ² x10 ⁻¹ [KNs/m ²]	Rise Time Duration x10 ⁻²	Impact Secondary
4.5.4.1	-	-	10.6	2.95	-	-	-
	-	-	5.3	3.44	-	-	-
	-	-	10.0	3.44	-	-	-
4.5.4.2	6.5	0.024	12.2	1.85	0.78	1.30	0.53
	1.31	0.012	5.3	1.50	0.08	0.80	0.25
	12.1	0.012	6.7	1.23	0.73	0.98	1.81
4.5.4.3	15.8	0.012	9.0	2.83	0.95	0.42	1.76
	-	-	4.5	2.83	-	-	-
	3.0	0.012	10.5	2.46	0.18	0.49	0.29
4.5.4.4	6.3	0.036	10.8	1.85	1.13	1.95	0.58
	3.8	0.024	4.5	2.46	0.46	0.98	0.84
	1.9	0.012	11.6	2.46	0.11	0.49	0.16
4.5.4.5	21.5	0.012	9.4	1.85	1.29	0.65	2.29
	2.2	0.012	3.4	1.85	0.13	0.65	0.65
	4.4	0.024	5.5	1.85	0.53	1.30	0.80

TABLE 4.5.5 ILFRACOMBE 23rd. March 83 Trans. No.		Peak Pressure [KN/m ²]	Rise Time [sec.]	Secondary Pressure [KN/m ²]	Duration [sec.]	IMPULSE = $\frac{\text{Peak} \cdot \text{Rise Time}}{2}$ x10 ⁻¹ [KNS/m ²]	Rise Time Duration x10 ⁻²	Impact Secondary
4.5.5.1	1	8.1	0.024	10.8	2.21	0.97	1.09	0.8
	4	-	-	5.6	2.09	-	-	-
	5	10.9	0.012	5.47	1.63	0.65	0.74	0.2
4.5.5.2	1	6.6	0.024	14.1	2.21	0.79	1.09	0.5
	4	3.9	0.036	6.2	2.09	0.70	1.72	0.6
	5	2.9	0.012	4.8	1.63	0.17	0.74	0.6
4.5.5.3	1	32.0	0.024	12.0	2.21	3.84	1.09	2.7
	4	3.4	0.024	6.8	2.09	0.41	1.15	0.5
	5	14.4	0.024	9.2	1.72	1.73	1.40	1.6
4.5.5.4	1	13.1	0.024	12.2	2.58	1.57	0.93	1.1
	4	3.6	0.048	4.7	1.97	0.86	2.22	0.8
	5	3.63	0.024	8.2	1.48	0.44	1.62	0.4
4.5.5.5	1	8.8	0.120	13.1	1.97	5.28	6.09	0.7
	4	6.1	0.072	6.1	1.97	2.20	3.65	1.0
	5	4.9	0.048	10.6	1.97	1.18	2.44	0.5

TABLE 4.5.6 ILFRACOMBE 23rd. March 83 Trans. No.	Peak Pressure [KN/m ²]	Rise Time [sec.]	Secondary Pressure [KN/m ²]	Duration [sec.]	IMPACT = Peak·Rise Time ² x10 ⁻¹ [Kns/m ²]	Rise Time Duration x10 ⁻²	Impact Secondary
4.5.6.1	10.7	0.024	15.5	1.72	1.28	1.40	0.7
	1.6	0.012	3.2	1.48	0.10	0.81	0.5
	13.8	0.012	6.1	0.74	0.83	1.62	2.3
4.5.6.2	14.6	0.024	16.9	1.97	1.75	1.22	0.9
	4.2	0.012	10.1	1.97	0.025	0.61	0.4
	21.0	0.024	10.5	1.60	2.52	1.50	2.0
4.5.6.3	8.5	0.036	13.8	2.21	1.53	1.63	0.6
	-	-	5.7	1.97	-	-	-
	9.8	0.012	7.3	2.71	0.59	0.44	1.3
4.5.6.4	10.4	0.048	15.0	2.46	2.50	1.95	0.7
	3.4	0.036	5.5	2.21	0.61	1.63	0.6
	9.5	0.024	7.1	1.97	1.14	1.22	1.3
4.5.6.5	33.5	0.024	8.4	-	4.02	-	4.0
	3.6	0.036	3.6	-	0.65	-	1.0
	13.5	0.024	6.8	-	1.62	-	2.0

TABLE 4.5.7 ILFRACOMBE 23rd. March 83 Trans. No.		Peak Pressure [KN/m ²]	Rise Time [sec.]	Secondary Pressure [KN/m ²]	Duration [sec.]	IMPULSE = Peak·Rise Time ² x10 ⁻¹ [KNS/m ²]	Rise Time Duration x10 ⁻²	Impact Secondary
4.5.7.1	1	24.1	0.012	18.9	2.46	1.45	0.49	1.3
	4	6.5	0.036	8.1	2.46	1.17	1.46	0.8
	5	10.3	0.012	10.3	1.85	0.62	0.65	1.0
4.5.7.2	1	18.9	0.012	13.8	2.21	1.13	0.54	1.4
	4	0.9	0.012	5.7	1.72	0.05	0.70	0.2
	5	8.8	0.012	8.8	1.48	0.53	0.81	1.0
4.5.7.3	1	16.4	0.036	14.2	1.72	2.95	2.09	1.2
	4	2.7	0.024	5.5	1.97	0.32	1.22	0.5
	5	17.1	0.012	8.6	1.23	1.03	0.98	2.0
4.5.7.4	1	11.9	0.060	16.6	1.60	3.57	3.75	0.7
	4	5.3	0.024	7.5	2.21	0.64	1.09	0.7
	5	9.5	0.024	10.6	1.48	1.14	1.62	0.9
4.5.7.5	1	7.5	0.060	15.0	1.23	2.25	4.88	0.5
	4	1.9	0.012	6.8	1.23	0.11	0.98	0.3
	5	6.9	0.024	8.3	1.23	0.83	1.95	0.8

TABLE 4.5.8 ILFRACOMBE 23rd. March 83 Trans. No.		Peak Pressure [KN/m ²]	Rise Time [sec.]	Secondary Pressure [KN/m ²]	Duration [sec.]	IMPULSE = Peak·Rise Time ² x10 ⁻¹ [KNS/m ²]	Rise Time Duration x10 ⁻²	Impact Secondary
4.5.8.1	1	12.5	0.13	15.0	2.46	8.13	5.28	0.8
	4	5.1	0.024	5.6	2.46	0.61	0.98	0.9
	5	5.6	0.048	6.5	1.72	1.34	2.79	0.9
4.5.8.2	1	9.0	0.108	13.0	1.97	4.86	5.48	0.7
	4	4.1	0.036	6.5	1.97	0.74	1.83	0.6
	5	6.8	0.084	9.7	1.48	2.86	5.68	0.7
4.5.8.3	1	9.8	0.084	14.2	2.46	4.12	3.41	0.7
	4	4.1	0.036	5.5	1.97	0.74	1.83	0.7
	5	5.4	0.024	7.8	1.48	0.65	1.62	0.7
4.5.8.4	1	13.13	0.060	17.5	1.85	3.99	3.24	0.8
	4	4.4	0.012	6.3	2.0	0.26	0.60	0.7
	5	9.7	0.024	12.2	1.60	1.16	1.50	0.8
4.5.8.5	1	8.5	0.084	14.9	1.97	3.57	4.26	0.6
	4	4.9	0.084	6.1	2.46	2.06	3.41	0.8
	5	-	-	13.1	0.98	-	-	-

TABLE 4.5.9 ILFRACOMBE 23rd. March 83 Trans. No.		Peak Pressure [KN/m ²]	Rise Time [sec.]	Secondary Pressure [KN/m ²]	Duration [sec.]	IMPULSE = $\frac{\text{Peak} \cdot \text{Rise Time}}{2}$ x10 ⁻¹ [KNs/m ²]	Rise Time Duration x10 ⁻²	Impact Secondary
4.5.9.1	1	9.0	0.012	18.0	2.21	0.54	0.54	0.5
	4	8.3	0.024	6.2	1.97	1.00	1.22	1.3
	5	16.9	0.024	8.4	0.09	2.03	26.67	2.0
4.5.9.2	1	10.9	0.072	15.3	1.97	3.92	3.65	0.7
	4	2.7	0.024	7.4	2.71	0.32	0.89	0.4
	5	5.3	0.036	9.0	1.23	0.95	2.93	0.6
4.5.9.3	1	8.7	0.060	15.3	1.97	2.61	3.05	0.6
	4	6.3	0.084	6.3	2.71	2.65	3.10	1.0
	5	4.4	0.024	8.7	0.74	0.53	3.24	0.5
4.5.9.4	1	10.6	0.108	14.9	2.21	5.72	4.89	0.7
	4	2.7	0.048	6.9	2.83	0.65	1.70	0.4
	5	7.2	0.060	8.3	0.98	2.16	6.12	0.9
4.5.9.5	1	8.5	0.036	14.9	1.85	1.53	1.95	0.6
	4	4.8	0.036	4.1	1.85	0.86	1.95	1.2
	5	5.3	0.012	7.3	2.46	0.32	0.49	0.7

TABLE 4.5.10 ILFRACOMBE 23rd. March 83 Trans. No.		Peak Pressure [KN/m ²]	Rise Time [sec.]	Secondary Pressure [KN/m ²]	Duration [sec.]	IMPULSE = Peak·Rise Time ² x10 ⁻¹ [KNS/m ²]	Rise Time Duration x10 ⁻²	Impact Secondary
4.5.10.1	1	10.1	0.120	14.6	1.97	6.06	6.09	0.7
	4	2.9	0.024	5.6	2.21	0.35	1.09	0.5
	5	7.0	0.048	7.2	0.98	1.68	4.90	1.0
4.5.10.2	1	9.5	0.048	14.3	2.21	2.20	2.17	0.7
	4	-	-	7.6	2.21	-	-	-
	5	5.1	0.012	5.1	1.72	0.31	0.70	1.0
4.5.10.3	1	12.7	0.108	13.9	1.72	6.86	6.28	0.9
	4	3.4	0.072	4.5	2.46	1.22	2.93	0.8
	5	4.2	0.024	8.4	1.23	0.50	1.95	0.5
4.5.10.4	1	12.2	0.072	19.5	1.85	4.39	3.89	0.6
	4	2.4	0.024	12.5	1.85	0.29	1.30	0.2
	5	10.0	0.036	10.0	0.74	1.80	4.86	1.0
4.5.10.5	1	12.0	0.084	15.3	1.72	5.04	4.88	0.8
	4	3.4	0.024	6.9	0.62	0.41	3.87	0.5
	5	9.3	0.036	10.4	0.74	1.67	4.86	0.9

TABLE 4.6.1 BOVISANDS 25th. Nov. 83 Trans. No.	Peak Pressure [KN/m ²]	Rise Time [sec.]	Secondary Pressure [KN/m ²]	Duration [sec.]	IMPULSE = Peak·Rise Time ² x10 ⁻¹ [KNS/m ²]	Rise Time Duration x10 ⁻²	Impact Secondary
4.6.1.1	30.2	0.054	23.7	3.68	8.15	1.47	1.3
	2.4	0.018	3.5	1.84	0.22	0.98	0.7
	15.8	0.054	9.8	3.68	4.27	1.47	1.6
4.6.1.2	28.4	0.072	26.3	2.58	10.22	2.79	1.1
	3.7	0.20	6.6	2.21	3.70	9.05	0.6
	25.8	0.09	11.7	3.31	11.61	2.72	2.2
4.6.1.3	31.1	0.054	25.9	3.68	8.40	1.47	1.2
	3.3	0.144	5.2	2.94	2.38	4.90	0.6
	25.5	0.054	12.7	2.94	6.89	1.84	2.0
4.6.1.4	15.2	0.036	20.3	2.21	2.74	1.63	0.7
	-	-	2.3	1.84	-	-	-
	13.6	0.036	8.5	1.10	2.45	3.27	1.6
4.6.1.5	23.1	0.018	28.2	1.84	2.08	0.98	0.8
	-	-	4.5	3.68	-	-	-
	16.6	0.054	6.5	1.10	4.48	4.91	2.6

TABLE 4.6.2 BOVISANDS 25th. Nov. 83 Trans. No.		Peak Pressure [KN/m ²]	Rise Time [sec.]	Secondary Pressure [KN/m ²]	Duration [sec.]	IMPULSE = $\frac{\text{Peak} \cdot \text{Rise Time}}{2}$ x10 ⁻¹ [KNS/m ²]	Rise Time Duration x10 ⁻²	Impact Secondary
4.6.2.1	1	20.5	0.054	15.4	2.21	5.54	2.44	1.3
	3	4.0	0.090	4.5	1.84	1.80	4.89	0.9
	5	16.6	0.054	8.2	1.84	4.48	2.93	2.0
4.6.2.2	1	21.4	0.036	23.7	2.76	3.85	1.30	0.9
	3	2.3	0.108	3.8	3.31	1.24	3.26	0.6
	5	16.9	0.072	6.4	1.47	6.08	4.90	2.6
4.6.2.3	1	44.6	0.036	28.7	3.13	8.03	1.15	1.6
	3	1.9	0.09	5.6	3.31	0.86	2.72	0.3
	5	29.6	0.036	6.4	3.13	5.33	1.15	4.6
4.6.2.4	1	12.3	0.13	12.9	4.05	8.00	3.21	1.0
	3	-	-	3.0	2.76	-	-	-
	5	6.8	0.14	3.0	3.68	4.76	3.80	2.3
4.6.2.5	1	15.1	0.18	28.0	3.68	13.6	5.00	0.5
	3	-	-	2.5	2.21	-	-	-
	5	6.0	0.09	4.5	2.94	2.70	3.06	1.3

TABLE 4.6.3 BOVISANDS 25th. Nov. 83 Trans. No.		Peak Pressure [KN/m ²]	Rise Time [sec.]	Secondary Pressure [KN/m ²]	Duration [sec.]	IMPULSE = $\frac{\text{Peak} \cdot \text{Rise Time}}{2}$ x10 ⁻¹ [KNs/m ²]	Rise Time Duration x10 ⁻²	Impact Secondary
4.6.3.1	1	12.5	0.018	30.0	3.68	1.13	0.49	0.4
	3	1.9	0.018	6.1	3.68	0.17	0.49	0.3
	5	23.6	0.072	9.1	3.13	8.50	2.30	2.6
4.6.3.2	1	37.5	0.036	22.5	3.31	6.75	1.09	1.7
	3	-	-	2.8	2.58	-	-	-
	5	16.3	0.054	9.1	3.13	4.40	1.73	1.8
4.6.3.3	1	8.3	0.23	11.3	3.31	1.25	0.69	0.7
	3	1.5	0.018	2.3	1.97	0.14	0.91	0.7
	5	2.4	0.072	2.1	2.76	0.86	2.61	1.1
4.6.3.4	1	31.4	0.054	20.9	2.09	8.48	2.58	1.5
	3	-	-	3.4	2.39	-	-	-
	5	12.1	0.09	8.1	3.31	5.45	2.72	1.5
4.6.3.5	1	15.9	0.09	22.31	2.2	7.16	4.09	0.7
	3	-	-	1.9	1.84	-	-	-
	5	4.3	0.11	4.3	3.13	2.37	3.51	1.0

TABLE 4.6.4 BOVISANDS 25th. Nov. 83 Trans. No.		Peak Pressure [KN/m ²]	Rise Time [sec.]	Secondary Pressure [KN/m ²]	Duration [sec.]	IMPULSE = Peak·Rise Time ² x10 ⁻¹ [KNS/m ²]	Rise Time Duration x10 ⁻²	Impact Secondary
4.6.4.1	1	17.2	0.13	18.7	1.84	11.18	7.07	0.9
	3	1.3	0.036	2.5	1.47	0.23	2.45	0.5
	5	6.8	0.13	2.3	3.31	4.42	3.93	3.0
4.6.4.2	1	30.5	0.054	20.3	2.39	8.24	2.26	1.5
	3	-	-	3.4	2.94	-	-	-
	5	11.6	0.14	7.5	2.1	8.12	6.67	1.5
4.6.4.3	1	18.3	0.072	20.3	1.84	6.59	3.91	0.9
	3	-	-	2.2	2.21	-	-	-
	5	9.4	0.036	5.6	3.68	1.69	0.98	1.7
4.6.4.4	1	17.4	0.054	25.2	1.84	4.70	2.93	0.7
	3	4.5	0.13	3.4	2.58	2.93	5.04	1.3
	5	12.8	0.036	7.2	3.13	2.30	1.15	1.8
4.6.4.5	1	9.4	0.018	8.1	2.94	0.85	0.61	1.20
	3	5.8	0.036	7.4	2.94	1.04	1.22	0.8
	5	9.9	0.036	8.6	3.31	1.78	1.09	1.2

TABLE 4.6.5 BOVISANDS 25th. Nov. 83 Trans. No.	Peak Pressure [KN/m ²]	Rise Time [sec.]	Secondary Pressure [KN/m ²]	Duration [sec.]	IMPULSE = Peak·Rise Time ² x10 ⁻¹ [KNS/m ²]	Rise Time Duration x10 ⁻²	Impact Secondary
4.6.5.1	11.3	0.036	10.8	2.76	2.03	1.30	1.1
	1.3	0.018	4.5	2.76	0.12	0.65	0.3
	21.6	0.036	10.8	3.68	3.89	0.98	2.0
4.6.5.2	11.8	0.11	21.9	2.58	6.49	4.26	0.5
	-	-	4.1	3.31	-	-	-
	11.6	0.036	6.5	3.31	2.09	1.09	1.8
4.6.5.3	27.6	0.054	19.7	4.05	7.45	1.33	1.4
	-	-	2.8	3.31	-	-	-
	8.8	0.09	5.3	3.31	3.96	2.72	1.7
4.6.5.4	19.7	0.054	23.6	3.13	5.32	1.73	0.8
	-	-	4.5	3.13	-	-	-
	13.2	0.036	5.9	3.13	2.38	1.15	2.2
4.6.5.5	34.6	0.036	29.6	4.05	6.23	0.89	1.2
	-	-	7.0	4.05	-	-	-
	32.6	0.054	15.2	4.05	8.80	1.33	2.1

TABLE 4.6.6 BOVISANDS 25th. Nov. 83 Trans. No.		Peak Pressure [KN/m ²]	Rise Time [sec.]	Secondary Pressure [KN/m ²]	Duration [sec.]	IMPULSE = Peak·Rise Time ² x10 ⁻¹ [KNs/m ²]	Rise Time Duration x10 ⁻²	Impact Secondary
4.6.6.1	1	14.3	0.09	25.2	3.68	6.44	2.45	0.6
	3	-	-	4.7	3.68	-	-	-
	5	13.2	0.072	7.3	4.23	4.75	1.70	1.8
4.6.6.2	1	15.3	0.09	19.9	4.05	6.89	2.22	0.8
	3	-	-	2.0	3.68	-	-	-
	5	4.4	0.054	4.9	4.05	1.19	1.33	0.9
4.6.6.3	1	15.3	0.11	21.4	3.50	8.42	3.14	0.7
	3	1.5	0.036	2.5	2.58	0.45	1.40	0.6
	5	7.9	0.072	5.3	4.05	2.84	1.78	1.5

TABLE 4.7.1 ILFRACOMBE 23rd Mar. 83	Significant Wave Pressure, P [KN/m ²]	Wave Celerity, C _b [ms ⁻¹]	Wave Height, H _b [m]	Wave Period, T [sec.]	Mean Water Level, d _b [m]	C _b ² [m ² s ⁻²]	H _b /d _b	C _b ² /gd _b	T √g/d _b
4.5.1.3	13.1	4.2	1.0	6.7	1.32	17.64	0.78	1.36	18.3
4.5.1.4	12.5	4.5	0.85	9.0	1.35	20.25	0.63	1.53	24.3
4.5.1.5	33.2	4.6	0.85	7.3	1.35	21.20	0.63	1.6	0.81
4.5.2.1	66.2	4.9	0.50	5.5	1.35	24.0	0.37	1.8	14.8
4.5.2.2	9.7	3.7	0.40	4.5	1.35	13.7	0.30	1.03	12.1
4.5.2.3	11.4	3.7	0.40	4.5	1.35	13.7	0.30	1.03	12.1
4.5.2.4	9.7	3.7	0.40	4.5	1.35	13.7	0.30	1.03	12.1
4.5.2.5	9.7	3.7	0.40	4.5	1.35	13.7	0.30	1.03	12.1
4.5.3.1	10.8	5.66	0.45	4.5	1.5	32.0	0.30	2.18	11.5
4.5.3.4	6.2	3.04	0.80	7.0	1.5	9.2	0.53	0.63	1.8
4.5.3.5	19.3	4.9	0.85	5.5	1.5	24.0	0.57	1.63	14.1
4.5.4.1	10.6	4.9	0.85	5.5	1.5	24.0	0.57	1.63	14.1
4.5.4.2	6.5	3.3	0.70	6.7	1.5	10.9	0.47	0.74	17.1
4.5.4.3	15.8	5.34	0.50	4.3	1.54	28.5	0.33	1.89	10.9
4.5.4.4	6.3	3.52	0.50	4.3	1.54	12.4	0.33	0.82	10.9
4.5.4.5	21.5	4.67	0.90	6.7	1.54	21.8	0.59	1.44	16.9
4.5.5.1	8.1	4.67	0.90	6.7	1.54	21.8	0.59	1.44	16.9
4.5.5.2	6.6	1.76	0.55	7.0	1.6	3.1	0.34	0.20	17.3
4.5.6.1	10.7	3.34	0.65	6.0	1.6	11.2	0.41	0.71	14.9
4.5.6.2	14.6	4.37	0.70	6.7	1.65	19.1	0.42	1.18	16.3
4.5.6.3	8.5	4.56	0.70	6.3	1.65	20.8	0.42	1.28	15.4

TABLE 4.7.2 ILFRACOMBE 23rd Mar. 83	Significant Pressure, P [KN/m ²]	Wave Celerity, C _b [ms ⁻¹]	Wave Height, H _b [m]	Wave Period, T [sec.]	Mean Water Level, d _b [m]	C _b ² [m ² s ⁻²]	H _b /d _b	C _b ² /gd _b	T √g/d _b
4.5.6.4	33.5	5.76	0.85	7.0	1.68	33.2	0.51	2.01	16.9
4.5.7.1	24.1	4.9	0.5	5.5	1.71	24.0	0.29	1.43	13.2
4.5.7.2	18.9	5.39	0.85	6.3	1.71	29.1	0.50	1.73	15.1
4.5.7.3	16.4	5.34	0.85	6.3	1.71	28.5	0.50	1.7	15.1
4.5.7.4	11.9	1.46	-	-	1.77	2.1	-	-	-
4.5.7.5	7.5	5.36	0.45	5.0	1.86	28.7	0.24	1.6	11.5
4.5.8.1	12.5	1.82	1.0	5.5	2.0	3.3	0.5	0.17	12.2
4.5.8.2	9.0	3.73	0.75	6.3	2.0	13.9	0.38	0.71	14.0
4.5.8.3	9.8	5.76	0.70	7.0	2.0	33.2	0.35	1.69	15.5
4.5.8.4	13.3	5.39	0.55	6.0	2.0	29.1	0.41	0.87	13.6
4.5.8.5	8.5	4.24	0.85	6.3	2.1	17.9	0.41	0.25	15.1
4.5.9.1	9.0	2.26	0.85	7.0	2.1	5.1	0.41	0.25	15.1
4.5.9.2	10.9	6.67	0.75	6.3	2.0	44.5	0.38	2.27	14.0
4.5.9.3	8.7	3.49	0.60	6.7	1.97	12.2	0.31	0.63	15.0
4.5.9.4	10.6	2.13	0.65	6.7	1.97	4.5	0.33	0.24	15.0
4.5.10.5	12.0	4.9	0.95	6.3	1.95	24.0	0.49	1.26	14.1
	15.0	4.94	0.42	6.7	1.95	24.4	0.22	1.28	15.0
	15.7	2.59	0.70	7.7	1.95	6.7	0.36	0.35	17.3
	7.9	4.13	0.85	6.3	1.93	17.1	0.44	0.90	14.2

TABLE 4.8.1 ILFRACOMBE 22nd Mar. 83	Significant Pressure, P [KN/m ²]	Wave Celerity, C _b [ms ⁻¹]	Wave Height, H _b [m]	Wave Period, T [sec.]	Mean Water Level, d _b [m]	C _b ² [m ² s ⁻²]	H _b /d _b	C _b ² /gd _b	T √g/d _b
4.4.1.4	8.6	7.28	0.43	7.7	0.45	53.0	0.96	12.0	36.0
4.4.1.5	10.1	2.41	0.57	9.2	0.45	5.8	1.27	1.32	43.0
4.4.2.1	15.9	4.56	0.51	5.5	0.60	20.8	0.85	3.53	22.2
4.4.2.2	13.9	4.29	0.54	5.5	0.60	18.4	0.9	3.13	22.2
4.4.2.3	9.0	4.24	0.53	4.7	0.65	18.0	0.82	2.82	18.3
4.4.2.4	15.3	4.56	0.46	7.3	0.65	20.8	0.71	3.26	28.4
4.4.2.5	14.2	5.39	0.54	6.0	0.65	29.1	0.83	4.56	23.3
4.4.3.1	9.75	4.35	0.51	5.5	0.68	18.9	0.75	2.84	20.9
4.4.3.2	38.9	4.56	0.51	7.0	0.70	20.8	0.73	3.03	26.2
4.4.3.3	6.3	3.8	0.60	6.3	0.70	14.4	0.86	2.1	23.6
4.4.3.4	13.6	4.13	0.57	5.5	0.75	17.1	0.76	2.32	19.9
4.4.3.5	14.3	4.21	0.43	5.1	0.75	17.7	0.57	2.4	18.4
4.4.4.1	10.9	4.23	0.50	4.4	0.78	17.9	0.64	2.34	15.6
4.4.4.2	10.1	4.21	0.65	5.5	0.78	17.7	0.83	2.32	19.5
4.4.4.3	12.2	4.94	0.50	6.7	0.80	24.4	0.63	3.11	23.5
4.4.4.4	8.0	3.93	0.72	7.3	0.85	15.4	0.85	1.85	24.8
4.4.4.5	13.1	5.93	0.46	5.5	0.85	35.2	0.54	4.22	18.7
4.4.5.1	16.5	3.96	0.64	5.5	0.90	15.7	0.71	1.78	18.2
4.4.5.2	11.3	4.24	0.60	6.3	0.95	17.0	0.63	1.93	20.2
4.4.5.3	10.3	4.1	0.50	6.7	0.95	16.8	0.53	1.8	21.5
4.4.5.4	9.8	3.89	0.53	6.0	0.95	15.1	0.56	1.62	19.3

TABLE 4.8.2 ILFRACOMBE 22nd Mar. 83	Significant Pressure, P [KN/m ²]	Wave Celerity, C _H [ms ⁻¹]	Wave Height, H _b [m]	Wave Period, T [sec.]	Mean Water Level, d _b [m]	C _b ² [m ² s ⁻²]	H _b /d _b	C _b ² /gd _b	T √g/d _b
4.4.5.5	12.0	4.21	0.80	7.7	0.95	17.7	0.84	1.9	24.7
4.4.6.1	12.6	4.24	0.77	6.0	0.95	18.0	0.81	1.93	19.3
4.4.6.4	7.5	3.89	0.61	7.0	1.2	15.1	0.51	1.29	20.0
4.4.6.5.	13.8	5.18	0.99	6.7	1.28	26.8	0.77	2.14	18.5
4.4.7.1	14.3	5.39	0.69	6.7	1.30	29.0	0.53	2.28	18.4
4.4.7.2	7.1	5.39	0.86	5.1	1.30	29.1	0.66	2.28	14.0
4.4.7.3	12.2	5.34	0.56	5.5	1.30	28.5	0.43	2.24	15.1
4.4.7.4	12.0	4.29	0.64	5.5	1.32	18.4	0.49	1.42	15.0
4.4.7.5	7.3	4.01	0.57	3.7	1.35	16.1	0.42	1.21	10.0
4.4.8.1	13.4	2.02	0.57	5.5	1.35	4.1	0.42	0.31	14.8
4.4.8.2	14.5	5.66	0.69	8.1	1.35	32.0	0.51	2.42	21.8
4.4.8.3	13.8	5.34	0.61	5.1	1.40	28.5	0.44	2.08	13.5
4.4.8.4	15.0	5.78	0.57	5.1	1.45	33.4	0.39	2.35	13.3
4.4.8.5	23.0	5.8	0.73	5.5	1.45	33.6	0.50	2.36	14.3
4.4.9.1	13.0	5.2	0.81	7.0	1.45	27.0	0.56	1.9	18.2

TABLE 4.9.1 ILFRACOMBE 10th Dec. 82	Significant Pressure, P [KN/m ²]	Wave Celerity, C _b [ms ⁻¹]	Wave Height, H _b [m]	Wave Period, T [sec.]	Mean Water Level, d _b [m]	C _b ² [m ² s ⁻²]	H _b /d _b	C _b ² /gd _b	T √g/d _b
4.3.6.3	15.3	7.2	1.16	4.4	1.2	51.8	0.97	4.4	12.6
4.3.6.4	51.0	7.2	1.00	6.0	1.2	51.8	0.83	4.4	17.2
4.3.7.1	13.4	6.2	1.46	6.3	1.25	38.4	1.17	3.13	17.6
4.3.7.2	16.2	6.2	0.93	4.0	1.28	38.4	0.73	3.06	11.1
4.3.7.3	14.3	-	-	-	-	-	-	-	-
4.3.7.4	18.3	5.5	1.41	5.1	1.3	30.3	1.08	2.37	14.0
4.3.8.1	16.7	4.3	0.79	7.3	1.3	18.5	0.61	1.45	20.1
4.3.8.2	13.1	6.54	1.22	7.0	1.3	42.8	0.99	3.54	19.8
4.3.8.3	19.7	6.39	0.86	4.1	1.33	40.8	0.65	3.13	11.1
4.3.8.4	16.9	6.2	1.03	6.7	1.35	38.4	0.76	2.9	18.1
4.3.9.1	14.6	5.4	1.2	6.7	1.35	29.2	0.89	2.2	18.1
4.3.9.2	35.6	8.3	0.93	6.4	1.35	68.9	0.69	5.2	17.3
4.3.9.3	22.1	-	-	-	-	-	-	-	-
4.3.9.4	18.3	6.2	1.24	6.7	1.40	38.4	0.89	2.8	17.7
4.3.10.1	13.4	4.8	1.04	7.3	1.40	23.0	0.74	1.68	19.3
4.3.10.2	21.6	6.4	1.18	5.5	1.40	40.9	0.84	2.98	14.6
4.3.10.3	14.4	6.39	1.00	5.1	1.40	40.8	0.71	2.97	13.5
4.3.10.4	30.0	5.4	1.08	4.7	1.45	29.2	0.74	2.05	12.2
4.3.11.1	24.0	2.7	0.83	6.0	1.45	7.3	0.57	0.51	15.6
4.3.11.2	14.7	5.6	0.99	5.1	1.45	31.4	0.68	2.2	13.3
4.3.11.3	30.5	6.2	1.20	5.5	1.45	38.4	0.83	2.7	14.3

TABLE 4.9.2 ILFRACOMBE 10th Dec. 82	Significant Pressure, P [KN/m ²]	Wave Celerity, C _b [ms ⁻¹]	Wave Height, H _b [m]	Wave Period, T [sec.]	Mean Water Level, d _b [m]	C _b ² [m ² s ⁻²]	H _b /d _b	C _b ² /gd _b	T √g/d _b
4.3.11.4	15.3	-	-	-	-	-	-	-	-
4.3.12.1	49.5	-	-	-	-	-	-	-	-
4.3.12.2	19.1	6.8	1.34	4.4	1.6	46.2	0.84	2.95	10.9
4.3.12.3	23.9	5.9	1.36	8.5	1.6	34.8	0.85	2.22	21.0
4.3.12.4	19.9	2.7	1.38	6.3	1.6	7.3	0.86	0.46	15.6
4.3.13.1	24.4	2.2	0.71	9.6	1.6	4.84	0.44	0.31	23.8
4.3.13.2	32.5	2.2	0.71	9.6	1.6	4.84	0.44	0.31	23.8
4.3.13.3	33.5	2.8	1.6	5.5	1.8	7.84	0.89	0.44	12.8
4.3.13.4	40.5	5.4	1.4	6.7	1.85	29.2	0.76	1.61	15.4
4.3.14.1	40.0	3.7	0.9	7.0	1.85	13.7	0.49	0.75	16.1
4.3.14.2	30.8	3.7	0.9	7.0	1.85	13.7	0.49	0.75	16.1
4.3.14.3	29.3	4.7	1.37	6.0	2.0	22.1	0.69	1.13	13.3
4.3.14.4	34.5	3.4	1.33	6.0	1.9	11.6	0.7	0.62	13.6
4.3.15.1	49.2	3.4	1.33	6.0	1.9	11.6	0.7	0.62	13.6
4.3.15.2	37.2	7.2	1.42	6.7	1.9	51.8	0.75	2.78	15.2
4.3.15.3	27.2	7.3	1.67	3.7	1.9	53.3	0.88	2.86	8.41
4.3.15.4	59.5	8.7	0.81	4.7	1.9	75.7	0.43	4.06	10.7
4.3.16.1	33.4	3.7	1.22	5.5	1.9	13.7	0.64	0.73	12.5
4.3.16.2	53.4	8.7	2.05	6.0	1.9	75.7	1.08	4.06	13.6
4.3.16.3	40.0	6.2	0.77	5.1	1.8	38.4	0.43	2.18	11.9
4.3.16.4	22.7	-	-	-	-	-	-	-	-

TABLE 4.9.3 ILFRACOMBE 10th Dec. 82	Significant Pressure, P [KN/m ²]	Wave Celerity, C _w [ms ⁻¹]	Wave Height, H _w [m]	Wave Period, T [sec.]	Mean Water Level, d _w [m]	C _b ² [m ² s ⁻²]	H _w /d _w	C _b ² /gd _w	T √g/d _w
4.3.22.3	30.9	6.2	1.73	4.7	1.8	38.4	0.96	2.18	11.0
4.3.22.4	26.5	8.7	1.15	4.7	1.8	75.7	0.64	4.29	11.0
4.3.23.1	29.5	5.4	1.2	6.7	1.8	29.2	0.67	1.65	15.6
4.3.23.2	22.9	6.2	1.25	6.0	1.8	38.4	0.69	2.18	14.0
4.3.23.3	25.8	2.9	1.01	6.0	1.8	8.4	0.56	0.48	14.0
4.3.23.4	23.6	7.9	1.5	4.4	1.8	62.4	0.83	3.53	10.3
4.3.24.1	42.0	2.4	2.0	6.7	1.8	5.8	1.11	0.33	15.6
4.3.24.2	41.7	3.7	0.97	6.3	1.8	13.7	0.54	0.77	14.7
4.3.24.3	59.5	2.9	1.45	5.1	1.95	8.4	0.74	0.44	11.4
4.3.24.4	32.0	6.2	1.09	5.5	1.8	38.4	0.61	2.18	12.8
4.3.25.1	33.3	8.8	1.18	4.7	2.0	77.4	0.59	3.95	10.4
4.3.25.2	25.1	3.1	1.3	6.3	2.0	9.6	0.65	0.49	14.0
4.3.25.3	29.6	3.4	1.39	5.1	2.0	11.6	0.69	0.59	11.3
4.3.25.4	27.2	3.1	2.05	4.8	2.0	9.6	1.02	0.49	10.6
4.3.26.1	27.2	7.2	1.83	7.0	2.0	51.8	0.92	2.64	15.5
4.3.26.2	35.6	8.8	1.82	5.5	2.0	77.4	0.91	3.95	12.2
4.3.26.3	57.0	7.2	1.82	4.7	2.0	51.8	0.91	2.64	10.4
4.3.26.4	34.5	3.6	1.43	7.0	2.0	13.0	0.72	0.66	15.5
4.3.27.1	42.2	3.1	1.03	4.7	2.0	9.6	0.52	0.49	10.4
4.3.27.2	39.4	4.7	1.37	6.0	2.0	22.1	0.69	1.13	13.3
4.3.27.3	35.0	3.4	1.33	6.0	2.0	11.6	0.67	0.59	13.3

CHAPTER FIVE

NUMERICAL ANALYSIS

5.1 INTRODUCTION

In the problem of two dimensional non-linear water waves, one solution that is favoured is the boundary integral equation method. The wave motion is described by the velocity potential as seen under the wave theory section. One of the benefits in applying this method is that non-linear terms are included in the free surface boundary.

The general description of the method is that it provides satisfactory numerical analysis of a non-linear problem. Such a problem is anticipated in the flow of wave motion. The method produces a solution of the free surface propagation bounded by a region. The region defines the free surface as one boundary, and the rigid boundary, which is determined by the configuration of the location under consideration, as the other. The two other boundaries are made up to include the wavelength of the wave motion at a time.

Initially the problem is simplified to one with open boundaries of two-dimensional linear theory⁽³⁸⁾ and further investigation into 3-D problems⁽¹⁵⁰⁾. The majority of work on this method was carried out by Liggett and Liu⁽³⁹⁾ (1982). In 1981, Nakayama and Washizu⁽¹⁵¹⁾ assumed the lateral boundaries to be vertical walls and to confine the flow motion to within a finite domain. Further application of the problem is to include a sloping beach which also becomes one of the imaginary boundaries. This method was carried out with the solitary wave as a disturbance up to non-breaking conditions⁽¹⁵²⁾. The run up of the wave motion was compared to the maximum run up

from the experimental data by Hall and Watts⁽¹⁵³⁾(1953). Another application of the method is to introduce the boundary of a vertical obstruction. The example follows the sloping beach which expresses an interest in the amount of run up a wave train produces. The problem reduces to obtaining the amount of momentum change produced by a travelling wavefront once it reaches a vertical obstruction. This is the basis of the determination of the forces imparted by the waves to the vertical obstruction. As the solution to the problem covers the behaviour under this type of loading, it provides the engineering aspect of the wall.

5.2 REGION

The problem so defined, is solved using Green's identity theorem as its basis. This theory expresses, for a closed boundary problem, the cyclic summation of the velocity potential as a singular variable arranged over the whole of the region. The expression is simplified by equating it to nought. This condition is maintained on the assumption of the flow being irrotational and inviscid. Therefore, Laplace's equation is directly applicable.

A completely defined problem requires that the initial stationary conditions are established. The initial conditions refer to the values of the velocity potential, ϕ and its partial derivatives to the normal along the boundary of the region. These values are applied to Green's identity with a solution that will totally cover the region concerned.

The region is made up of a series of discrete nodes which will define the boundary. The nodes are then considered to be at the ends of line segments at which the velocity potential and its derivatives are assumed to vary linearly.. The joined nodes form linear segments which are used in the evaluation of unknown variables. A line segment represented by its coordinates (ξ_1, η_1) and (ξ_2, η_2) has ends represented by S_1 and S_2 . The local coordinate system of a line segment is used when performing stress calculations. However, the relation of the segment to the adjacent ones for the continuation of the variable evaluation requires the global coordinates. The two are reached through geometrical principles.

The choice of the boundary points taken as nodes implies that the equation of Green's identity is evaluated for every change in the free surface. The singular variable which in turn expresses the contour geometry is changed depending on the number of dimensions in the problem. For a 2-D problem, the value of $\ln r$ is used which is replaced by $1/r$ in a 3-D problem. The value of r is expressed as the distance from an arbitrary point source to consecutive nodal points on the boundary.

The nodal points are used to evaluate the development of the wave flow numerically in terms of time steps. At each time step the region is evaluated to represent the overall 2-D flow. This means that the velocity components are computed at fixed points along a rectangular grid. The grid is replaced by a diagrammatic representation of the velocity components added vectorially. The representation takes the form of an arrow in the direction of the water flow with a magnitude proportional to the combined velocities.

The grid technique is limited by a reduction in spacing necessary to allow for the radius of curvature of the free surface. This problem comes about in the formation of the jet at the wave crest. The radii of curvatures in this area lend towards a limit of instability. A decrease in the spacing involves a relative increase in the number of nodal points N^2 corresponding to a substantial increase in computer time proportional to time used.

5.3 BOUNDARY CONDITIONS

Up to the point of breaking, the numerical method applied assumes no vorticity and an irrotational flow. This limitation allows for the use of velocity potential, a term that satisfies Laplace's equation.

The procedure involves the conversion from an open boundary to a closed boundary problem. From the coordinates of the node making up the free boundary, all points in the region of the (x, y) plane are transferred to the (r, θ) plane. (r, θ) are the polar coordinates in the ζ - plane. The equations of transformation include,

$$r = e^y \quad \text{or} \quad y = \ln r \quad (5.1)$$

$$\theta = -x \quad \text{or} \quad x = -\theta \quad (5.2)$$

This conversion of the physical plane is described as its conformal mapping inside the closed contour in the mapped plane.

Within the closed boundary, the velocity potential function is determined from the boundary values. In the time evolution of the problem, Bernoulli's equation plays a part when applying a pressure to the moving surface. The pressure results from the moving air over the sea surface. The positive aspect of this approach is that the problem is reduced from a two space dimension to one.

Consider the closed contour represented by C and that the motion is periodic in space though not necessarily in time. The values of the boundary conditions, both dynamical and kinematical, are expressed at rates of change of ϕ for the free surface particles as fixed particles.

The governing equations in the process are velocity and velocity potential. The latter is periodic such that $\nabla\phi$ satisfies an exponential decrease with depth. This forms a solution of the velocity components' variation with depth.

At the free surface, the kinematic condition is applied to the dynamical condition. These are given in terms of the material derivatives. The interpretation of this statement is that the horizontal and vertical components of the velocity are obtained from the rate of change of the particles in the surface in the x- and y- direction respectively, that is,

$$\frac{Dx}{Dt} = \frac{\delta\phi}{\delta x} \quad (5.3)$$

$$\frac{Dy}{Dt} = \frac{\delta\phi}{\delta y} \quad \text{at } y = \eta \quad (5.4)$$

These equations combine to give the rate of change of velocity potential following the wave motion of,

$$\frac{D\phi}{Dt} = -p_s - y + \frac{1}{2}(\nabla\phi)^2 \quad (5.5)$$

where p_s is the pressure applied at the surface.

The material derivative implies that the differentiation follows a given particle.

5.4 GOVERNING EQUATIONS

The governing equations are based on the mean or x-averaged horizontal velocity (at some depth, y this value is made equal to zero). This statement is valid for deep water waves. In the case of shallow water waves, the horizontal velocity is important in its measurements, as much as it can be included in the numerical analysis.

The dimensions of all the parameters making up the wave measurements are reduced to non-dimensional values. The mass, length and time parameters are chosen such that density, acceleration due to gravity and wave number, k are made equal to one.

The unit chosen for determining the wave progression numerically reduces to a wavelength equivalent to 2π . The free surface kinematic conditions are satisfied following the path of travel of a given particle. The operational procedure carried out by this statement covers the horizontal and vertical velocities given by the material derivatives of a fixed particle, as mentioned earlier in Airy's Theory in 4.2.3.

5.4.1 The Velocity Potential

The velocity potential has been described in its evaluation from the velocity of particles of either measured or recorded data.

The basis of this interpretation is that the wave is identified along its progression path at two measuring positions a known distance

apart. The value of the data obtained from the field is that the recorded data also includes variations in the asymmetrical profiles.

The kinematic boundary condition assumes particles in the surface to remain in the surface. This assumption provides an option of locating the particles in one wavelength to a second portion of wavelength delayed by a known time increment. The difference in positioning of the particles in both the horizontal and vertical direction divided by the time increment produces the respective velocity components. These components make up the velocity distribution or potential that a wave has in its progression with time. In the approach of using a time delayed amplitude portrait, correction is applied for the phase velocity component. The correction covers the x-direction component. This step is justified as an equivalent to the moving reference frame.

The value of the velocity potential is given as discrete values at the nodal points, by taking the numerical integration for the values of the velocity components (Gaussian four point integration). The significance of this deviation has been to produce a standard method by which the potential for velocity in the wave motion is interpreted. It also gives the potential a numerical value from which the basis of the behaviour and development of the free water surface may be defined.

The appraisal of this solution has been found through the application of varying extents to which the forward wave is measured from the original one. This produces corresponding values of velocity components.

The resultant curve fitting of the velocity components shows periodic tendencies. Also, for equal changes in time intervals, the velocity components vary at different proportions. The larger the time interval, the more pronounced is the magnitude of the velocity component. The reason for the different proportion is explained by the periodic nature of the velocity in time. Also, to produce accurate representations of the velocity components, the relative displacement has to be calculated in the limit the increment Δt , tends to nought. In consequence to this observation, the velocity potential follows the same pattern as the component velocity, establishing a predicted unknown value.

The setting up of a wave potential from the separate records is summarised in the following discussion. The use of a moving reference frame plays a significant part in the proceeding of the numerical analysis. It has to be deducted from resulting particle displacements in the x-direction. From two wave profiles separated by a time increment, the particle location in both determines the variation in velocity along the surface. The related equations for the velocity components are,

$$\frac{x_{2n} - x_{1n}}{\Delta T} = u_n \quad (5.6)$$

$$\frac{Y_{2n} - Y_{1n}}{\Delta T} = v_n \quad \text{where } n = 1, 2, 3\dots \quad (5.7)$$

The dynamic free surface is used in determining the pressure distribution in terms of the rate of change of potential and velocity components of the particles (see Bernouilli's equation in section 4.2.2).

5.5 STATIONARY INITIAL CONDITIONS

The problem starts to unfold when the initial conditions are given at $t = t_0$ for the velocity potential everywhere inside the boundary. The values of the potential partial derivatives with respect to tangential s , and normal n , directions are required at nodal points of the boundary. The boundary region values are derived once the contour variables at the nodes are known.

However, the problem arises when the values of ϕ and its partial derivative with respect to the normal are not totally known as initial conditions. The method chosen to solve the unknown quantities is to consider Green's identity around the boundary area, S ,

$$\int_S \left(\phi \frac{\delta}{\delta r} (\ln r) - \ln r \frac{\delta \phi}{\delta n} \right) ds = 0 \quad (5.8)$$

The values of the unknowns are then found by performing the above equation in turn using the number of points P_i as origins for the $\ln r$ term. The points P_i become nodal points on line segments. From the rotation of the nodal points all the values of ϕ , $\delta\phi/\delta n$ are then obtained.

One idea is held that the free surface is reduced to its projected nodal points on the mean level⁽³⁸⁾. In the calculation with P_i established, moving around the boundary, the above equation is written in a number of coefficients in terms of the unknown $\delta\phi/\delta n$, ϕ .

Solving for all nodal points the final condition is one of a matrix equation given by,

$$[R] \{\phi^{k+1}\} = [Q] \left\{ \begin{array}{c} (\delta\phi)^{k+1} \\ \delta n \end{array} \right\} \quad (5.9)$$

The factor to bear in mind in this calculation is that R and Q are square matrices and they depend on the configuration of the boundaries. This shows how the development of the free surface is being formed by constantly including its profile together with the driving force in terms of hydrodynamic parameters.

5.6 INDEPENDENT VARIABLES

In free surface calculations, the objective is to derive from the free surface boundary conditions, a relation between ϕ and $\delta\phi/\delta n$ at the free surface nodal points. A method opted for by Liu and Liggett⁽¹⁵⁴⁾(1983) defines arbitrary axes x_* , y_* which apply to each nodal point. The direction, γ is specific to the direction the node moves from one time step to another. The value of y from the x -axis denotes the free surface profile, η . This value is modified from the rotated coordinate system whose origin is situated on the x -axis (See Fig. 5.1).

The modified boundary condition equations become, for β being the angle the free surface makes with the horizontal axis,

$$\frac{\delta\eta_*}{\delta t} = \frac{1}{\cos(\beta-\gamma)} \frac{\delta\phi}{\delta n} \quad \text{on } y_* = \eta_* \quad (5.10)$$

$$\left(\frac{\delta\phi}{\delta t}\right)_{x_*} = - (x_* \sin \gamma + \eta_* \cos \gamma) - \frac{1}{2} \left[\left(\frac{\delta\phi}{\delta s}\right)^2 - 2 \tan(\beta-\gamma) \frac{\delta\phi}{\delta n} \frac{\delta\phi}{\delta s} - \left(\frac{\delta\phi}{\delta n}\right)^2 \right] \quad \text{on } y_* = \eta_* \quad (5.11)$$

The last equation gives the rate of change of potential for a given x_* value. Also if $\gamma = 0$, the nodal point moves in the vertical y direction. This statement provides a check on the derived equation from the original boundary conditions.

5.6.1 Time Stepping Procedure

Finite difference forms of the last two equations, produce, for a time step of Δt between two levels of k and $k+1$ in the time domain, the equation,

$$\eta_*^{k+1} = \eta_*^k + \Delta t \left[\frac{1-\theta_1}{\cos(\beta^k-\gamma)} \left(\frac{\delta\phi}{\delta n} \right)^k + \frac{\theta_1}{\cos(\beta^{k+1}-\gamma)} \left(\frac{\delta\phi}{\delta n} \right)^{k+1} \right] \quad (5.12)$$

Also,

$$\phi^{k+1} = \phi^k - \Delta t \{ A + 0.5 (1-\theta_3) B + 0.5 \theta_3 C \} \quad (5.13)$$

where,

$$A = x_* \sin \gamma + \cos \gamma [(1-\theta_2) \eta_*^k + \theta_2 \eta_*^{k+1}] \quad (5.14)$$

$$B = \left[\left(\frac{\delta\phi}{\delta s} \right)^k \right]^2 - 2 \tan(\beta^k-\gamma) \left(\frac{\delta\phi}{\delta n} \right)^k \left(\frac{\delta\phi}{\delta s} \right)^k - \left[\left(\frac{\delta\phi}{\delta n} \right)^k \right]^2 \quad (5.15)$$

$$C = \left[\left(\frac{\delta\phi}{\delta s} \right)^{k+1} \right]^2 - 2 \tan(\beta^{k+1}-\gamma) \left(\frac{\delta\phi}{\delta n} \right)^{k+1} \left(\frac{\delta\phi}{\delta s} \right)^{k+1} - \left[\left(\frac{\delta\phi}{\delta n} \right)^{k+1} \right]^2 \quad (5.16)$$

The similarities between the coefficients B and C result in working the terms out separately and combining under one equation. The values of θ_1 , θ_2 , and θ_3 , are weighting factors chosen as 0.5. The other main point is that B and C each contain second order terms — introducing the factor of non-linearity.

The way to overcome this difficulty is to introduce estimate values of the unknown terms. This value is used in the one part of the non-linear term, therefore reducing the equation to linearity. For completeness of the problem, the values obtained from these separate

identities become the new estimates while increasing the iterative step by one. The iteration stops until the last obtained value differs from the estimate value by an acceptable difference.

The values from the iterated parts of the equation are substituted into the parent equation to extract a value of the velocity potential and its derivatives in the (k+1)th. time step. The simplification of the equation in terms of the unknowns becomes,

$$\phi^{k+1} + a \left(\frac{\delta\phi}{\delta n} \right)^{k+1} + b \left(\frac{\delta\phi}{\delta s} \right)^{k+1} = r \quad (5.17)$$

The values of a, b, r consist of terms that either have been estimated in the (k+1) time step, or have previously been known from the k th. time step. The result of the rotated coordinate system is reverted to the original system with γ tending to zero, that is,

$$\eta_*^k \cos \gamma = \eta \quad (5.18)$$

and,

$$x_* \sin \gamma \rightarrow 0 \quad \text{as } \gamma \rightarrow 0 \quad (5.19)$$

The above equation (5.17) is made up of three unknowns. By central difference methods, the value of $(\delta\phi/\delta s)$ at a nodal point is given in terms of the potential velocity at two adjacent nodal points, in the proportion of the line segment lengths joining the points, that is,

$$\left(\frac{\delta\phi}{\delta s} \right)_j = \frac{1}{l_j l_{j-1}^2 + l_{j-1} l_j^2} [l_{j-1}^2 \phi_{j+1} + (l_j^2 - l_{j-1}^2) \phi_j - l_j^2 \phi_{j-1}] \quad (5.20)$$

This substitution reduces the equation to having two unknowns. The accuracy of the substitution is maintained because $(\delta\phi/\delta s)$ terms have low values which could be calculated by ignoring higher order terms.

5.6.2 Values Of Coefficients

The values of the coefficient of the (k+1)th time stepping series of unknowns are:-

$$a = \frac{(\Delta t)^2 \theta_1 \theta_2 \cos \gamma}{\cos(\beta^{k+1} - \gamma)} - (\Delta t) \theta_3 \left[\left[\frac{\delta \bar{\phi}}{\delta n} \right]^{k+1} + \tan(\beta^{k+1} - \gamma) \left[\frac{\delta \bar{\phi}}{\delta s} \right]^{k+1} \right] \quad (5.21)$$

$$b = (\Delta t) \theta_3 \left[\left[\frac{\delta \phi}{\delta s} \right]^{k+1} - \tan(\beta^{k+1} - \gamma) \left[\frac{\delta \phi}{\delta n} \right]^{k+1} \right] \quad (5.22)$$

$$r = \phi^k - (\Delta t) \eta^k - \frac{(\Delta t)^2 (1 - \theta_1) \theta_2 \cos \gamma}{\cos(\beta^k - \gamma)} \left[\frac{\delta \phi}{\delta n} \right]^k$$

$$\frac{-\Delta t}{2} (1 - \theta_3) R_1 + \frac{\Delta t}{2} R_2 \quad (5.23)$$

where

$$R_1 = \left[\left[\frac{\delta \phi}{\delta s} \right]^k \right]^2 - \left[\left[\frac{\delta \phi}{\delta n} \right]^k \right]^2 - 2 \tan(\beta^k - \gamma) \left[\frac{\delta \phi}{\delta s} \right]^k \left[\frac{\delta \phi}{\delta n} \right]^k \quad (5.24)$$

$$R_2 = \left[\left[\frac{\delta \bar{\phi}}{\delta s} \right]^{k+1} \right]^2 + \left[\left[\frac{\delta \bar{\phi}}{\delta n} \right]^{k+1} \right]^2 + 2 \tan(\beta^{k+1} - \gamma) \left[\frac{\delta \bar{\phi}}{\delta s} \right]^{k+1} \left[\frac{\delta \bar{\phi}}{\delta n} \right]^{k+1} \quad (5.25)$$

5.7 SMOOTHING CHARACTERISTICS

The evaluation of the wave profile development by numerical analysis, is subject to its specific type of accuracy. The measure of accuracy is carried out in a number of ways, each one involved with a wavelength to cover the periodic nature of the output.

The partial derivative of the potential velocity with respect to the normal component is evaluated over the whole contour, C. For each time step this function is calculated with the view that the expected value should vanish, that is,

$$\int_C \frac{\delta\phi}{\delta n} ds = 0 \quad (5.26)$$

Another physical criterion is that the mean value of the surface elevation should tend to zero. The evaluation of this term is directly applicable to the nature of the problem intended and is given by,

$$\frac{1}{2\pi} \int_0^{2\pi} \eta dx = \frac{1}{2\pi} \int_0^{2\pi} (\ln r) d\theta \quad (5.27)$$

In conjunction with this value, other relevant determining terms are:-

$$\text{Potential Energy, P.E.} = \frac{1}{2\pi} \int_0^{2\pi} \frac{\eta^2}{2} dx \quad (5.28)$$

$$\text{Kinetic Energy, K.E.} = \frac{1}{2\pi} \int_0^{2\pi} \int_{-d}^{\eta} \frac{1}{2} (\nabla\phi)^2 dx dy$$

$$= \frac{1}{4\pi} \int_C \phi \frac{\delta\phi}{\delta n} \delta s \quad (5.29)$$

The value of the energy component calculations is that for no input value of energy in the waveform, the total energy, E, that is,

$$E = P.E. + K.E. \quad (5.30)$$

remains a constant.

The accuracy of the solution is measured by one of the above mentioned methods, quoting the number of decimal places that are valid for accuracy.

5.7.1 Smoothing The Instability

The solution of the wave profile after a number of time stepping processes invariably produces a saw toothed appearance. The effect of this appearance is that the resultant nodal points appear above and below the expected line of continuity.

This form of instability is inevitable in the numerical analysis of this type. Once started, the rate of growth per unit time step is found to be independent of the number of time steps. The reason for the instability occurring is due to physical effects besides the rounding errors. The physical effect is assimilated to the growth of short gravity waves suppressed by longer wave compression of the crest ⁽¹⁵⁵⁾.

Instabilities of this type are removed by approximating a polynomial that passes through the nodal points, leaving alternate points of either side of the smooth curve. For a mean curve of the second degree, the smoothing characteristic is obtained as the mean curve summed to another polynomial which reduces the given nodal points by a number of units. The latter polynomial is one of an oscillating nature in the opposing sense to the variations of the nodal output from the numerical analysis. For a given period of oscillation, the nodal points are reduced or increased depending on which side of the mean curve they are found. A suitable solution was found to work with five points centered about a nodal point. The smoothing function of the curve with a mean parabolic curve is given by the equation,

$$\bar{f}_j = \frac{1}{16} (-f_{j-2} + 4f_{j-1} + 10f_j + 4f_{j+1} - f_{j+2}) \quad (5.31)$$

where j represents the centre node.

5.8 CONVERGENCE OF SOLUTION FOR ITERATIVE STEPS

In a specific example, the free surface nodal movements are restricted to the vertical direction. This condition allows $\gamma = 0$. In carrying out this solution, the inclusion of estimate values involves a number of iterations. The objective of doing iterations is that convergence is achieved to produce a solution. The estimate values, therefore, have to be of a realistic magnitude, maintaining the right order throughout the governing equations.

The determining factor of the convergence criterion is the termination of the iteration process. For this objective, the boundary condition at the surface gives a good measure of when to stop the iteration. The ratio of the $(i-1)$ th iterated value to the i th iterated value of the free water surface is calculated for each node, such that,

$$\max = \left| 1 - \frac{\eta_j^{(i-1)}}{\eta_j^i} \right| < e \quad \text{for } j = 1, 2, 3 \dots N_f \quad (5.32)$$

where e is the allowable error difference. This is an arbitrary value depending on the approximation of the results required. A good indication is to give this error-bound a value having an order of magnitude of two degrees less than the expected result. The number of runs expected to produce a result is also to be kept to a minimum.

5.9 VARIATIONS ON THE BOUNDARY CONDITIONS

i) Unsteady Surface Flow

The direct application of a free surface flow is to determine the failure surface due to wave height instability or depth reduction of a free surface. The stationary initial values are established for a given free surface.

Equations of equilibrium include non-linear terms which are identified and eliminated by the equivalent estimated values. These values are inserted at a lower level of the time stepping routine. By the means of these estimates the unknowns are output at a higher level of iteration within the same time step. The final solution produced from a given number of iterative steps is obtained from updated values of the potential and the free surface. This solution ensures that the original equations are maintained and from which the new values in the following time steps are iterated.

ii) Breaking Waves

In numerical analysis, breaking waves are seen as agents for the transfer of horizontal momentum from wind generated waves to water surface movements.

The basic assumptions of free surface flow remain valid to the point when the wave breaks. As in previously mentioned wave theories, an irrotational and inviscid fluid, is assumed with Laplace's equation governing the motion.

5.9.1 Asymmetry

The important factor in wave profiles at the breaking phase of the development of its progression is the asymmetry. This parameter comes into force either as a result of the advanced numerical analysis or a result of the measurements of the wave profile. These measurements are of various extents of breaking of the wave. As a result the trough ahead of a breaking wave takes up a characteristic shape.

The consequence to this observation is that breaking criteria cannot be formulated solely by wave steepness, S . This is because for a steepness kept constant, the crest front steepness shape shows different forms of asymmetry. In order to express the asymmetry and steepness of a transient near a breaking wave more accurately the datum level must be established ⁽¹⁵⁶⁾.

The datum for analysis of field measurements made from fixed measuring devices is defined as the mean water level over a twenty minute recording period with proper corrections for tide. Three parameters are also described to give a quantitative assessment of waves up to the point of breaking. These are:-

- i) crest-front steepness
- ii) vertical asymmetrical factor
- iii) horizontal asymmetrical factor

The crest-front steepness is defined as the ratio of the maximum wave crest height to the length of water ahead of this point and above water

$$\xi = \frac{\eta'}{L'} \quad (5.33)$$

The vertical asymmetrical factor is defined as the ratio of the crest length before the maximum value, to the crest length ahead of the maximum crest height value, such that,

$$\lambda = \frac{L''}{L'} \quad (5.34)$$

The horizontal asymmetrical value is defined as the ratio of the maximum crest height value to the overall wave height,

$$\mu = \frac{\eta'}{H} \quad (5.35)$$

As can be seen from the illustration (Fig. 5.2) the determining terms of the crest elevation are given above the datum while L' and L'' are horizontal distances relative to zero crossing points.

In the design of fixed structures, the value of crest elevation becomes more meaningful than an amplitude value. This value incorporates the steepness and asymmetry of large proportions. As the extent of breaking is the reason for the largest forces exerted on the structure, this discussion is inkeeping with the expected behaviour of a fully developed sea wave.

A rough guide to the description of a sea state in terms of wave height is:-

slight	H = 0.5	to	1.25m
moderate	H = 1.25	to	2.50m
rough	H = 2.50	to	4.00m

(World Meteorological Organisation 1974)

When the wave crest steepness is high and combined with low wave heights, the sea is said to be choppy. When the wave crest steepness is not too high but combined with high wave heights, the sea describes as a heavy swell. These types of sea are not as disastrous as a combination of a high crest elevation with high wave heights. This is termed as a very rough sea consisting of severe breaking waves.

5.10 NUMERICAL RESULTS FROM A FULLY DEVELOPED SEA STATE

The numerical method is extended to apply to non-stationary breaking waves. At this level of operation, the output has to be further checked with the dynamic boundary conditions. The significant points covered by this dynamical condition are that:-

- i) the rate of change of total energy is equal to the pressure P_s at the free surface acting over a given area and given in the form of work done.
- ii) The rate of change of momentum in the x-direction is equal to the total horizontal force acting on the fluid at the free surface.

These conditions express a meaning of the distance moved by the wave particles as the work done by them. In this case, the particles are providing a means of dissipation of energy with time for a non-stationary wave. The result of this happening produces a horizontal force linked to the rate of change of momentum, creating impacts by a breaking wave on an obstruction.

The other associated condition experienced by the breaking wave phenomena is that the flux of fluid, or rate of change of power, through the free surface remains at a low insignificant value.

5.10.1 Induced Pressures To A Progressive Wave

The reason for the application of external forces to the free water surface is to assimilate the air-water interface. It also provides a way of advancing the condition of asymmetry in the wave profile by induced instability. The result is that the wavefront is assimilated to a breaking wave profile.

In producing the asymmetrical profile, a pressure is applied to the rear of the crest elevation. The pressure was based on variable distribution as is expected in an elevated structure with the maximum imposed at the highest point. The pressure was applied to that part of the wave above datum level, at which it was given null magnitude. The consequence of this wave type required that the trough section be adjusted for continuity. The case of applying a parabolic curve to the crest elevation gave a result of a plunging type of breaker. The inclusion of this profile into numerical analysis routine produced an advanced specimen to be taken to further time stepping stages.

The development of the wave involves further steepening of the wavefront from an asymmetrical wave. A smooth jet of fluid is ejected from the wave crest and hits the forward face of the wave. In the formation of this plunging type of breaker, a shallow wave produces a quicker and larger jet than a deep water wave would.

Velocities and accelerations as the breaking wave develops are determined to accomplish the aim of applying the numerical analysis exercise. These component values are referred to basic values of phase velocity and acceleration due to gravity for comparative reasons.

While the horizontal velocities outweigh the phase velocities, the accelerations along the wave crest are of the same order as g (or as much as $g/2$). However, on the forward face of the breaker the particles' acceleration is increasing in the direction approaching the crest tip.

After the wavefront becomes vertical, the particles entering the jet do so from the forward face of the wave. Maximum velocities of up to 1.5 times the phase velocity, and accelerations of up to $3g$ have been measured in the wave's front face. The front of the jet falls freely with vertical acceleration reaching a value of g ; this represents a thin layer of fluid with constant pressure on both sides. These accelerations are considered large in relation to the maximum acceleration detected in a progressive wave which is given as $0.5g$, where g represents the acceleration due to gravity.

The dynamic pressure distribution within the wave profile is identified relative to the reference $g\eta$ and is represented in vectors divided by the density of the fluid, that is,

$$\frac{p}{\rho} = g\eta \quad (5.36)$$

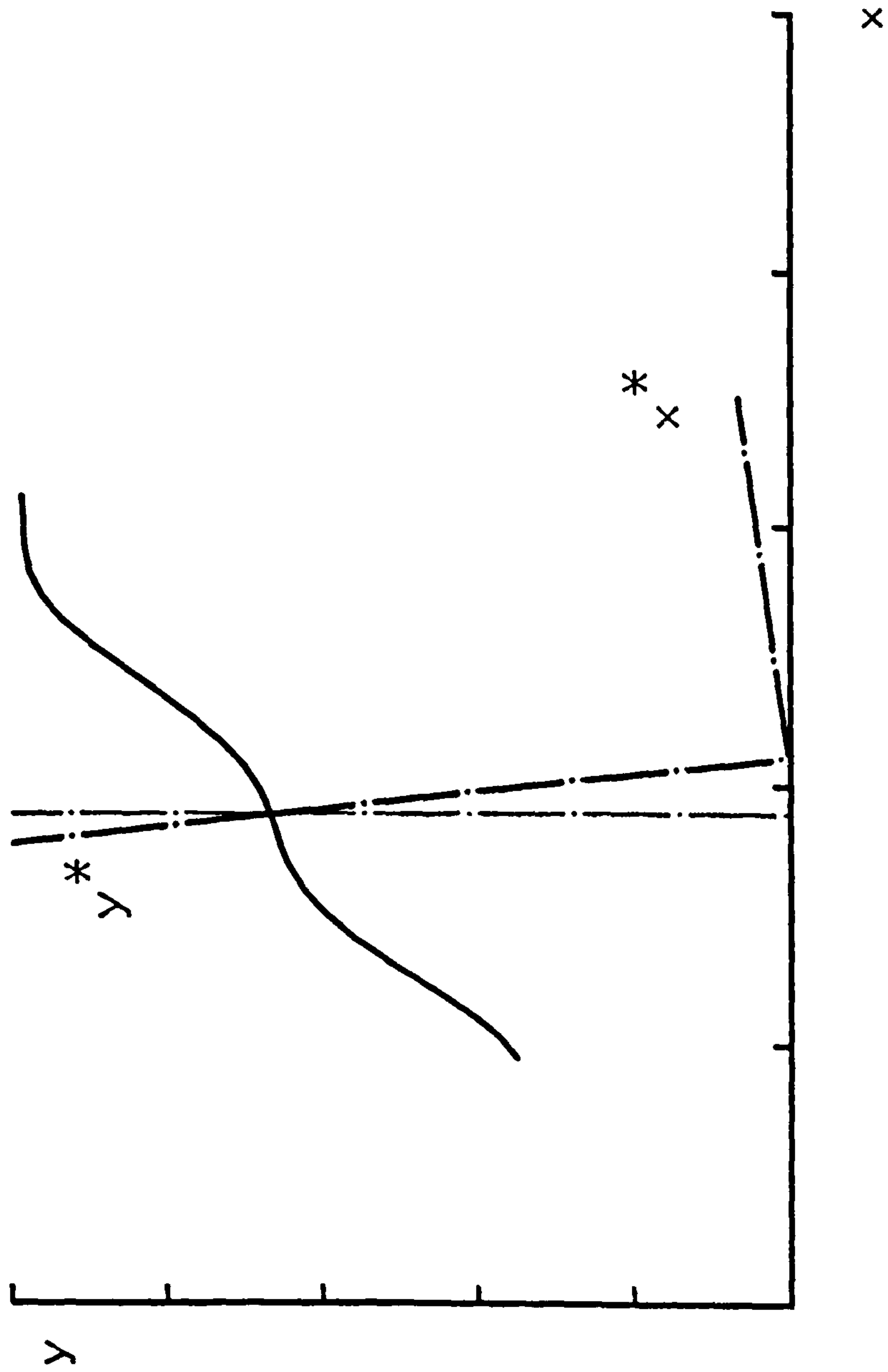


FIG 5.1 ARBITRARY AXES FOR NODAL POINTS ON FREE WATER SURFACE

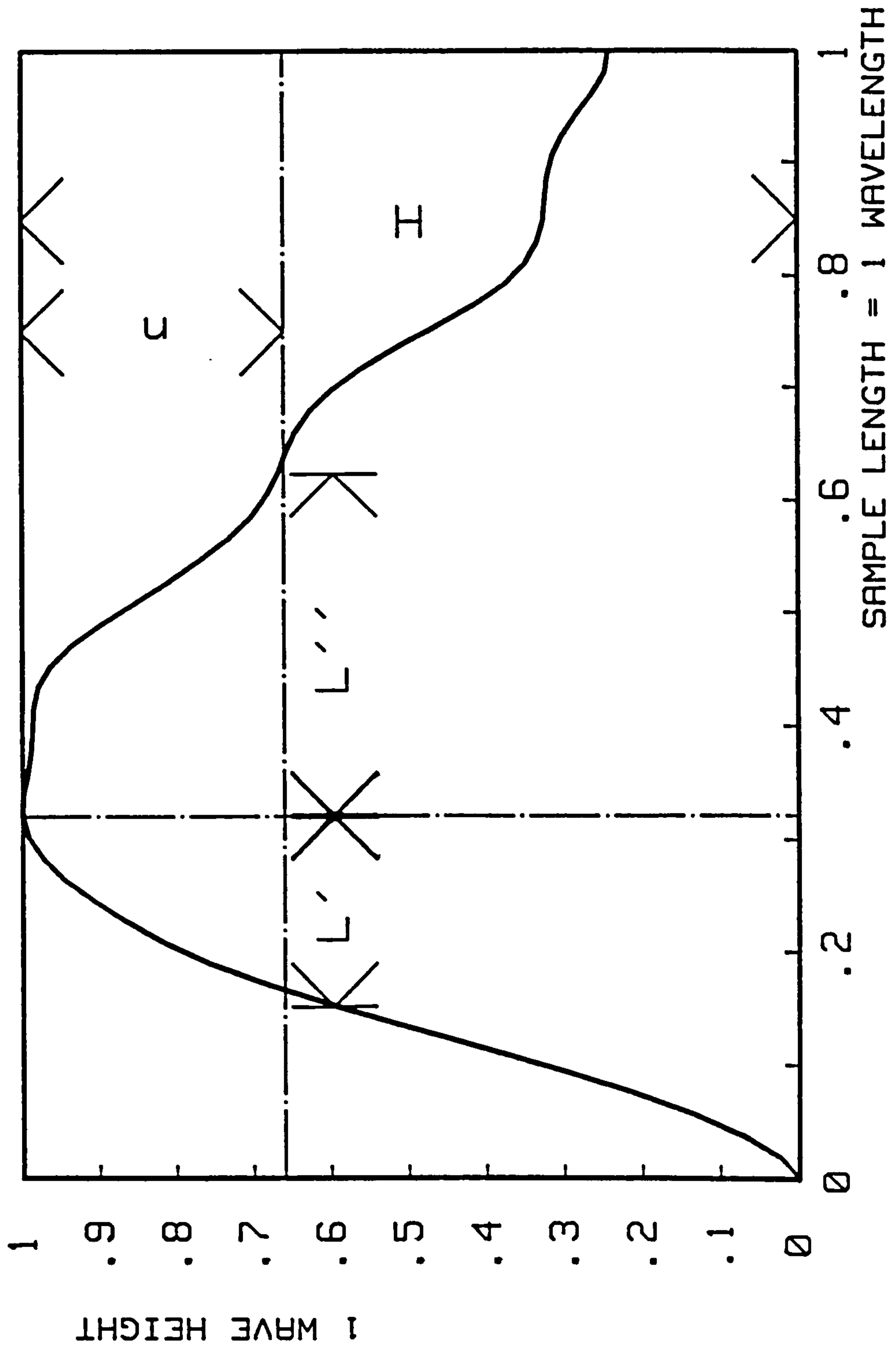


FIG 5.2 · STEEPNESS AND ASYMMETRICAL FACTORS OF A PROGRESSIVE WAVE

DISCUSSION

DISCUSSION

In reviewing the readings collected at Ilfracombe and Bovisand it is to be noted that most of the readings come from Ilfracombe, and they can be seen in Tables 4.1.1 - 4.1.3; 4.2.1 - 4.2.11; 4.3.1 - 4.3.27; 4.4.1 - 4.4.9 and 4.5.1 - 4.5.10, and compared with Bovisand values found in Table 4.6.1 to 4.6.6. The readings record pressure distribution measurements on 290 occasions at Ilfracombe and 28 occasions at Bovisand. Of the 290 data recording sessions at Ilfracombe, 80 of them gave a relative pressure distribution made up of 4 transducers or more.

The main features of the first site at Ilfracombe formed the basis of assessing the favourable conditions required when choosing the second site. The readings of the impact pressures at the second site at Bovisand can be seen to be more intense than those of the first, as for instance those in tables 4.6.2 and 4.6.5, when compared to 4.3.24 and 4.3.25 showing the same order of peak dynamic pressure values. As can be seen from the description in section 2.1 and 2.1.2, the main point in favour of the second site was the difference in the foreshore. At the Bovisand site, amount of rock outcrops were insignificant when compared to the Ilfracombe site. These outcrops at Ilfracombe helped the energy dissipation by providing obstacles to the wind generated waves. The additional advantage under consideration for the choice of a new site was the direction of the prevailing

winds. Fig. 2.18(a) shows the wind distribution over the period when measurements were taken at Ilfracombe given in terms of leeward wind direction, but this condition occurred less frequently than could be hoped for. For this reason, as explained in 2.1.2, a site facing the prevailing south westerly winds would give a higher probability of obtaining bad weather conditions and waves at the site. This condition made the Bovisand site far better suited than Ilfracombe one. It also meant that the chances of setting up the experiment in a stormy weather environment and matching it with large tidal ranges occurred more often. The most significant improvement in choosing the second site showed in the nature of the sea bed profile which was of a more consistent nature. This is documented in section 2.1 and 2.1.2, and substantiated by Plates XIV and XIII. Variations in the sea bed profile, by providing the necessary depth reduction, were a key factor to the formation of the breaking waves. The choice of the measuring zone in the second site was further enhanced by the sudden rise in the rock formation. This asset relating to the second site provided the additional benefit for further accentuating the process for the breaking of waves. The compatibility of the main direction of wave approach shown in Fig. 4.9 with wind direction is seen when referred to the typical wind rose of Fig. 2.18(a). The representative of this wind data obtained from a local source is identified as a leeward wind direction for a person positioned on the point of origin equivalent to the location for which the data is taken, or the sea wall, in this case. The second site also had the advantage

of ease of access, and in addition the instrumentation station was much closer to the pressure transducers.

The bulk of the readings came from Ilfracombe, (See Table 4.1.1 to 4.5.10 inclusive) and were compared to the data from Bovisand (Tables 4.6.1 to 4.6.6 inclusive). The Bovisand data was more consistent in terms of regular occurrence of marked impact pressure formation represented by the average rise times ranging from 30 to 70 ms. These values were grouped in terms of impulse range and plotted on the graphs shown in Fig. 4.20a to 4.20d. The data expressed in Fig. 4.20d was indicative of the measurements obtained from the initial recordings that were analysed, and for this reason may not be as accurate as the later values.

Within the impulse range of 2.5 to 8 KN m⁻² sec. are included impact pressures of 88 KN/m² with measured rise times of 70ms, and these are grouped together in Fig. 4.20a. These values, for the same impulse range, showed an improvement on those obtained by P. Blackmore, expressed in Fig. 4.20e. In the latter case, as explained on page 14, pressures of 45 to 49 KN/m² for 1m wave height were recorded at the site at Seaford. However, for Ilfracombe, recorded maxima pressures of 88KN/m² show a threefold increase over these pressures when compared to the value of 27KN/m², recorded by P. Blackmore. This marked improvement over the previous pressure values is not accompanied by any dramatic change in the rise time measurements. Of the data recorded in the tables on page 313 to 385, the unexpected magnitude of entry 4.3.15 of 133KN/m²

is not felt to be correct but is included for completeness of results. The difference in the recently acquired sets of data over the previous results is thought to be due to a cleaner water volume. This aspect of air entrainment is at present under investigation. In the case of air entrained in the water volume, a reduction in rise time would be expected. One of the main items of interest to the engineer is that, as shown by these measurements, particularly at the first site, a breaking wave is seen to bring about a rise in water level, as explained in section 4.8. In these circumstances, the rise in water level implies a proportional increase in pressure and therefore an increase in load acting on the wall. An increase in wave reflection also produces an enhanced wave pressure as well as a scouring effect in the seabed zone of the structure.

A characteristic vertical pressure distribution for Ilfracombe may be obtained from the recorded impacts of 4.3.14.3, 4.3.16.1, 4.3.16.2, 4.3.23.4, 4.3.24.1, 4.3.24.3, and 4.3.25.4, which include simultaneous measurements from all levels on the face of the wall (See Fig. 6.1). By representing the results in this way, the maximum pressures are related to the location of pressure measurement in terms of the measured mean water level. For this plot, non-dimensionalising the parameters was used. For this purpose, the maximum pressures are divided by the equivalent hydrostatic pressure expected from the measured breaking wave heights. The level from which this pressure is calculated is taken from the hypothetical mean water level. The presented results for impact pressures show that the distribution peaks at the mean water level for 60% of the Ilfracombe values. The gradual decrease of the maximum pressures

below the level of the peak pressure distribution contrasts with the more rapid reduction above this level of reference. The explanation for this difference is probably due to the additional component of the hydrostatic pressure acting below the mean water level. This type of spatial distribution was first suggested by Minikin⁽¹³⁸⁾ (See Fig. 4.18).

In a number of laboratory based experiments, M.S. Kirgoz⁽¹⁴⁰⁾ deduced similar results when he applied different beach slopes to relate various maximum impact pressures obtained at different levels of his model. The comparison of the current field experiments with Kirgoz's results shows a similar vertical pressure distribution acting mainly at the mean water level. The vertical spatial distribution particular to these results is one with a reduction on either side of the peak value. The distribution plotted with P. Blackmore's results has given marked changes around the mean water level, and for the practical results quotes a linear dynamic pressure component to be added to the hydrostatic pressure resulting from a breaking wave height reaching the wall. The additional feature in this set of results is that the more detailed arrangement of vertical measurements shows the peakier profile of the distribution detected with a wave breaking at the wall. The maximum pressure associated with this peak value is quoted in B.S. 6439 deduced from Minikin's work, also referred to in the Shore Protection Manual⁽¹⁵⁸⁾, and can be calculated from the equation,

$$p_m = 101 \frac{H_b}{L_b} \rho g d_b \left(1 + \frac{d_b}{d_s} \right) \quad [\text{in KN/m}^2] \quad (6.1)$$

where d_s is the depth of the mean water level at a wavelength L from the obstruction.

The value obtained from this equation is compatible with the results obtained from this research and is of the order of 50KN/m^2 for a 1m wave height.

The peak value of the distribution may be approximated by a linear variation of this calculated peak value acting from the mean water level to the crest of the breaking wave. This simplified type of dynamic pressure distribution becomes a practical solution for the design of the seawall, subject to breaking wave conditions. The other factor to consider at this stage is that this pressure only occurs over a very short time and over the local area of impact, and should not be considered to have an overall static effect on the design of the structure. Having said this, the condition of maximum pressure reached cannot be ignored especially in its dynamic action on modular elements as constituents of the overall structure.

Wave characteristics were determined from suitable wave forms recorded from beach transducers close to the pressure measurements on the seawall. The detailed information obtained from this data is extracted from one continuous sample, as shown in Fig. 3.1(a), subject to having adequate signal-to-noise compatibility. Initial tests for stationarity and ergodicity are carried out to qualify the random data before any analysis is carried out, as described in 3.4. This phase follows the rational vetting of parts of the signal that are extraneous to those producing the measurements for which the data is collected. The data extracted from a waveform signal took the form of either general statistical values to cover

the whole recording for which it was taken, or, more specifically, to identify the individual characteristics of waves that are directly related to impact pressure measurements on the seawall, as are recorded in table 4.7.1 to 4.9.3 inclusive.

The value of the measurements obtained digitally is initially compared to the observations taken on site with the help of a graduated wave mast (see Plate VI) and recorded on the site notes (pages 305 - 312). This approach has given a basis to refer to when verifying the order of the more accurate measurements obtained by analysis. With enough practice, the main parameters of the wave characteristics have been obtained to 10% of the visually measured values. This agreement shows that such a basic method of wave detection proves adequate for preliminary engineering purposes.

The conversion of analogue recorded information to the digital equivalent produces the required measurements after applying the appropriate or purposely designed software. The initial information obtained from a continuous signal consists of the sequential extraction of the wave height and wave period of each recorded wave. This data is then processed to produce a standard statistical equivalent diagram of the representative significant wave height and wave period as given in Fig. 3.6 with a maximum wave height of 1.1m and a period of 5 sec. In the process involved to achieve these results it is best to provide a relatively smooth signal and pass it through the steps shown in the flow diagram of Fig. 4.7, necessary for the organisation of digital information. These methods involved are applied to the signal in the time domain. By applying

an analysis in the frequency domain, the results obtained help to verify the previous results, as the characteristic frequency of 0.12 Hz shown in Fig. 3.12. The statistical values representing the random sea state are also given a theoretical significance by calculating the probability distribution of the wave height. The distributions so produced, indirectly give the mean measured value of the wave height as well as the predicted extreme wave height suitable for design purposes. (See Fig. 2.16).

The other main measurements obtained in carrying out the time series analysis were individual wave characteristics directly relating to particular pressure measurements on the sea wall. These take the form of the individual wave height and period as well as the mean water level over a short sample of record, (2½ minutes of real time recording) (as recorded in Tables 4.7.1 - 4.9.3 inclusive). The value of the mean water level is checked with the tidal water level recorded for the day. The other significant measurement obtained for individual characteristic is the mean velocity and direction of approach. These values are based on the measured time differences obtained between pairs of strategically placed beach transducers. The summation of the wave velocity and direction can be seen in Fig. 4.9 which coincides with the general wind direction recorded for the site.

The individual waveform characteristics are used to correlate the measurements with theoretical values. The comparison is carried out by calculating the theoretical free surface profile that complies with the given parameters and comparing it with a measured profile.

The Stokes' wave is based on the steepness and water depth to wavelength ratio, while the Cnoidal wave is based on Ursell's number. Both cases apply to shallow water conditions and governed by their respective limitations (See sections 4.2.4 and 4.2.5). The comparison of the experimental data (Fig. 6.2) to the two types of theoretical waveform bears a similarity among the three. This example shows how, relative to the complexity required, the choice of theoretical approach may be applied to design wave parameters to deduce the time dependent parameters throughout the area subject to wave action.

The analysis of the secondary pressure takes the form of a distribution. This distribution is approximated by that of a triangular form and follows the hydrostatic mean water level pressure pattern. Its magnitude is compared to the equivalent hydrostatic pressure of twice the breaking wave height positioned at the mean water level (See Fig. 4.21). These values, on average, show a twofold increase over the mean water hydrostatic pressure. The other point of interest is that the secondary pressure acts over a prolonged duration of up to 20% of the period of the wave as seen in recorded pressures of 4.2.10.2 and 4.2.10.0 (wave period measured as 7.8 sec.) These values are for beach slopes of greater than 1:40. This secondary pressure should be given priority over the impact pressure when designing a coastal defence structure because it occurs over a longer duration and over a larger area.

The understood mechanism of generated secondary pressure is that when the body of water approaches the wall after impact, water

dispersion occurs in all directions but mostly in the vertical direction (section 4.10). The increase in pressure is, therefore, due to an additional head of water sustained by the mass of water at the point of impact. The duration for which the action takes place is a result of the time the water movement takes to reach the peak of its climb and down again. This observation holds as long as no overtopping is involved when some water is subject to find itself over the top of the wall. The effect of air entrained in the volume of water is to reduce the rise time of an impact pressure. This results in producing a pressure distribution similar to one after an impact has occurred, that is, nearing a secondary pressure distribution.

The variation of the peak impact pressure with velocity has been plotted in terms of their equivalent head of water in Fig. 4.12. Out of the 140 values, recorded and examined, the data falls into three groups with 3% of the data discarded for non-conformity reasons. The three groups may be generalised by a common equation of,

$$p_m = k\rho u_b^2$$

with the value of constant, k, for each of the three groups given as,

$$\begin{aligned} k &= 0.38 \text{ for } 40\% \text{ of the data values with a } 2\% \text{ scatter} \\ k &= 0.83 \text{ for } 33\% \text{ of the data values with a } 2\% \text{ scatter} \\ k &> 1.75 \text{ for } 21\% \text{ of the data values with a } 2\% \text{ scatter} \end{aligned}$$

The significance of these three bands is due to the differences between pressures recorded from non-breaking waves and impact pressures due to breaking waves. The increase in value of the constant, k recorded above, is compatible with the degree of adversity connected

with progressive stages of breaking wave formation. The above values show that with direct impact due to breaking waves, the impact pressures are directly proportional to the square of the velocity, as k is approximately equal to one. The relationship is reduced by a factor of half when applied to non-breaking waves; this particular relationship allows a 25% overestimate over the measured values. The more adverse impact pressures support a higher coefficient of proportionality of up to a value of two. However, this relationship only covers a fifth of the measurements to give a significant representation of extreme impact pressure formation.

From the numerous examples of pressure measurements at the wall, some of the more outstanding ones were due to waveforms approaching limiting steepness. This type of waveform produced a condition of breaking and therefore a cause for the more significant change in momentum. The data values plotted as steepness to water depth against wavelength show how they fall within the limiting boundary condition in Fig. 4.13. These values include 8% of the 140 values which fall outside this boundary and is due to an overestimate of the steepness value. This plot shows how the data values conform with expression 4.73 for limiting steepness.

The values tabulated throughout this study form a representation of impacts and secondary pressures with their relationship to wave characteristics. The process of design cannot be complete if extreme conditions for design waves were not known. The method adopted to reach this aim is by prediction of the extreme values. The prediction of extreme values is carried out by extrapolation of the data set shown on the Rayleigh distribution curve (Shown in Fig. 2.16).

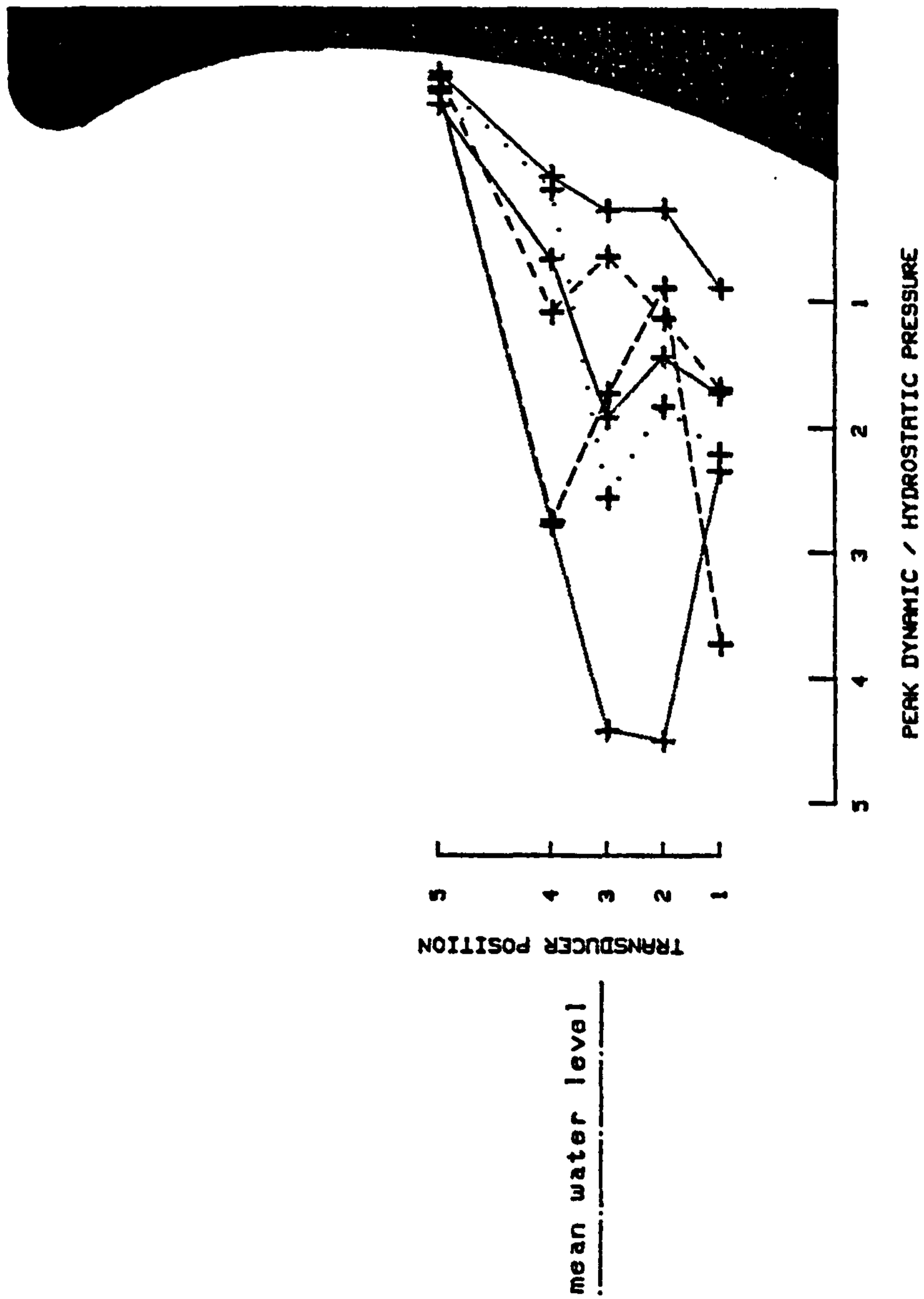
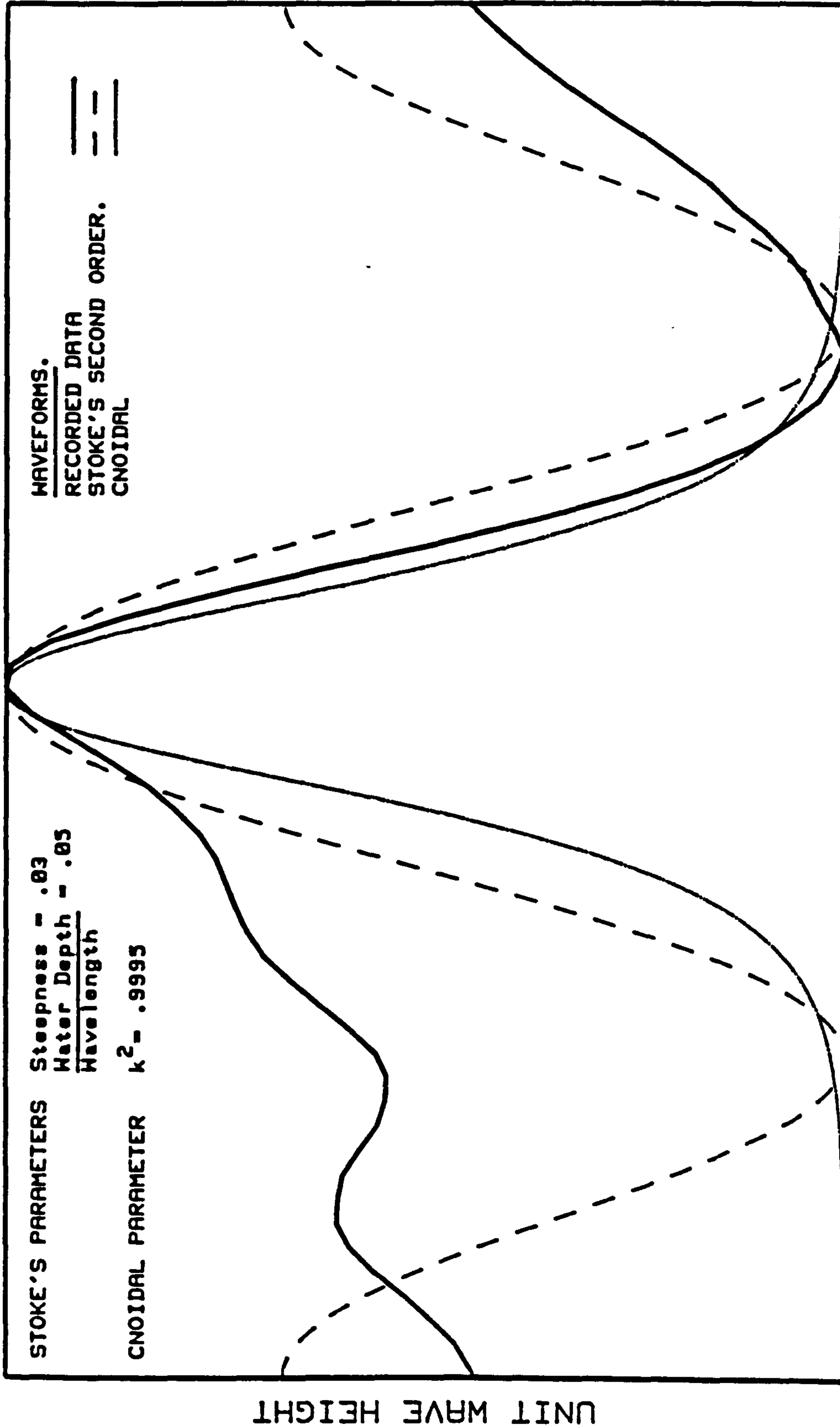


FIG 6.1 TYPICAL IMPACT PRESSURE DISTRIBUTIONS AT THE SEAWALL



UNIT WAVELENGTH
 FIG 6.2 COMPARISON OF TYPICAL EXPERIMENTAL TO THEORETICAL
 WAVEFORM (for 10th December 1982. at ILFRACOMBE)

CONCLUSION

From the discussion of the results obtained in this research, it has been seen that the impact pressures are of a dynamic nature occurring over a short time only and are associated with waves breaking at the sea wall. The distribution, representing the impact pressure action at the sea wall, peaks at the mean water level acting over the local area of impact.

The secondary pressures have taken the form of a triangular distribution acting at the sea wall. These pressures are more important for design because of the time duration and a larger area of contact.

A good correlation between the measured values and shallow water theories has been achieved. This enables the determination of time dependent parameters from design wave parameters for situations that favour shallow water conditions.

SUGGESTIONS FOR FURTHER RESEARCH

Following the work on impact and second peak pressure distributions acting on the seawall, it would be useful to extend the work into the armouring of sea defences. The sea defences falling within this category are grouped as having side slopes that are less steep than the two examined in this work. This type of sea defence is also chosen when a breakwater is required.

The design side slope is a function of the type of armouring unit used for its construction, in terms of its size and shape. A substitute for quarrystone, when not readily available is the introduction of concrete armouring units. The concrete units provide an improved stability coefficient value, as a basic design parameter towards the breakwater's safety. Units of less than 20 tonnes which are not placed by land based equipment are not required to be reinforced, and therefore provide a cost effective solution. A suggested type of armouring unit is the Cob. This precast concrete unit takes the form of a hollowed out cuboid with the interstices reaching each of the six faces of this platonic solid.

An assessment into the behaviour of this unit as part of a sea defence is suggested in terms of various aspects of wave environmental loading. One factor to be considered is how this type of sea defence behaves in terms of impact, and more important, second peak pressure distribution. Further, whether the packing density and indeed, solid to void ratio, have a reducing effect on the peak pressures and second peak pressure magnitude around the mean water level. Other factors involved in producing a stable structure

include the constituents of the layered placement as are the interlocking friction and packing density of the random or organised units.

A study into the permeability of the core and underlayer of this type of structure is also essential to provide a more detailed understanding towards the stability and safety of this class of sea defence.

REFERENCES

REFERENCES

1. TUCKER, M.J. Simple Measurements of Wave Records. The Docks and Harbour Authority , Vol. 42, Nov. 1961.
2. DRAPER, L. The Analysis and Presentation of Wave Data — A Plea For Uniformity. Proc. of 10th Conf. on Coastal Eng. Tokyo ASCE, 1966.
3. ARTHUR, R.S. Variability in Direction of Wave Travel. Ocean Surface Waves, Ann. N.Y. Acad, Sci. Vol. 51, 1949.
4. ISAACS, J.D.
CHINN, A.J. Preliminary Report on the Mark II Wave Direction Recorder and Indicator. Tech. Rpt. No. Hel 116 - 290, Inst. of Eng. Res. Univ. of Calif. Berkeley 1948.
5. HALL, J.V. The Rayleigh Disk as a Wave Direction Indicator. Tech. Memo No. 18, Beach Erosion Board, U.S. Army Corps of Engineers, July 1950.
6. SNODGRASS, F.E. Wave Measurements. Cn. IX — Oceanographic Instrumentation. National Research Council, Pub. No. 309, 1952.
7. KIM, Y.Y.
SIMONS, L.H. Sea State Measurements From Pressure Records. Int. Symp. on Ocean Wave Measurement and Analysis. A.S.C.E. Waves, 1974.
8. STOKES, G.G. On the Theory of Oscillatory Waves. Trans. Camb. Phil Soc. Vol 8, 1847. Math. Phys. Papers Vol. 1, Camb. Univ. Press, 1880.
9. DE, S.C. Contribution to the Theory of Stokes Waves. Proc. Camb. Phil. Soc. Vol 51, 1955.

10. CHAPPELEAR, J.E. On the Theory of the Highest Waves.
U.S. Army Corps of Engineers, Beach Erosion Board, Tech. Memo No. 116, 1959.
11. SCHWARTZ, L.W. Computer Extension and Analytical Continuation of Stokes' Expansion for Gravity Waves.
J.F.M. Vol. 62, 1974
12. BOUSSINESQ, J. Theorie De L'Intumescence Liquide, Appelee Onde Solitaire Ou De Translation Se Propageant Dans un Canal Rectangulaire.
Comptes Rendus Acad. Sci. Paris, Vol. 72, 1871.
13. RUSSELL J.S. Report on Waves. 14th Meeting, Brit. Assoc. Adv. Sci. 1844.
14. KORTEWEG, J.G.
DE VRIES, G. On the Change of Form of Long Waves Advancing in a Rectangular Canal, and on a New Type of Long Stationary Wave.
Phil. Mag. 5th series Vol. 39, 1895.
15. LAITONE, E.V. The Second Approximation to Cnoidal and Solitary Waves. J.F.M. Vol. 9, 1961.
16. FRIEDRICHS, K.O. On the Derivation of the Shallow Water Theory, Appendix to the "The Formation of Breakers and Bores" by J.J. Stoker.
Comm. Pure Appl. Math. Vol. 1, 1948.
17. FENTON, J.D. A Higher Order Cnoidal Wave Theory.
J.F.M. Vol. 94, 1979.
18. URSELL, F. Surface Waves on Deep Water in the Presence of a Submerged Circular Cylinder.
I. Proc. Camb. Phil. Soc. Vol. 46, 1956.

19. LONGUET HIGGINS, M.S. Recent Developments in the Study of
Breaking Waves. Proc. 15th Eng.
Conf. Honolulu, Vol. I, 1976.

20. COKELET, E.D. Breaking Waves. Nature, Vol. 267, 1977.

21. PEREGRINE, D.H. Mechanics of Breaking Waves — A Review
of Euromech 192. Pitman, London, 1979.

22. GALVIN, C.J. Breaker Type Classification on Three
Laboratory Beaches. J. Geophys. Res.
Vol. 73, 1968.

23. TENAUD, R.
 GRAILLOT, A. Ouvrages de Protection dans la Zone
de Deferlement des Houles — La Houille
Blanche. Vol. 718, 1975.

24. WEGGEL, J.R. Maximum Breaker Height For Design.
Proc. 13th Coastal Eng. Conf. Vancouver
Vol. 1, 1972.

25. GALVIN, C.J. Breaker Travel and Choice of Design Wave
Height. J. Waterways, Harbours and Coastal
Eng. Div. A.S.C.E. Vol. 95, No. WW2, 1969.

26. GODA, Y. A Synthesis of Breaker Indices.
Trans. Jap. Soc. Civ. Eng. Vol. 2, 1970.

27. GAILLARD, D.D. Wave Action in Relation to Engineering
Structures. U.S. Army Corps of
Engineers, 1904, (reprint, 1935).

28. HIROI, I. The Force and Power of Waves.
The Engineer, 1920.

29. MOLITOR, D.A. Wave Pressure on Seawalls and Breakwaters.
Trans. A.S.C.E. Vol. 100, 1935.

30. LUIGGI, L. Correspondence on Improvement of the Port of Valparaiso. Proc. I.C.E. Vol. 214, 1922.
31. ROUVILLE, M.
BESSION, P.
PETRY, P. Etat Actueles des Etudes Internationales sur les Efforts dus aux Lambs Annales de Pont et Chaussees 108(2), 1938.
32. COT, P.D. Le Laboratoire du Havre pour la Measuer des Efforts dus aux Lambs. 1953.. Proc. 5th Conf. Coastal Eng. Sept. 1974.
33. MURAKI, Y. Field Observations of Wave Pressures, Wave Runup and Oscillation of Breakwater. Proc. 10th Conf. Coastal Eng. Vol. 1, 1966.
34. MILLER, R.L.
LEVERETTE, S.
O'SULLIVAN, J.
TOCHKO, J. Full Measurements of Impact Measurements in Surf. Proc. 14th Conf. of Coastal Eng. Vol. 3, 1974.
35. MARCHI, E.
RAITERI, E.
SCARSI, G.
STURA, S. Storm Wave Pressures on the Breakwater of Genoa Harbour. 16th Int. Assn. for Hydraulic Research, Vol. 1, 1975.
36. BLACKMORE, P. The Evaluation of Wave Forces on Seawalls. Ph.D. Thesis, Plymouth Polytechnic, 1982.
37. LARRAS, J. Le Deferlement des Lames sur les Jetees Verticales. Annals des Ponts et Chaussees, Vol. 107, 1937.
38. KIRKGOZ, M.S. Secondary Pressures of Waves Breaking on Seawalls. Jnl. of Waterway, Port and Coastal and Ocean Engineering. A.S.C.E. Vol. 109 No. 4, 1983.

39. LONGUET HIGGINS, M.S. The Deformation of Steep Surface Waves
COKELET, E.D. on Water. I A Numerical Method of
 Computation. Proc. Roy. Soc. Sev. A.
 Vol. 350, 1976.
40. SALMON, J.R. An Integral Equation Method for Linear
LIU, P.L.F. Water Waves. J. Hydr. Div. A.S.C.E.
LIGGETT, J.A. 12 (HY 12) 1980.
41. LIGGETT, J.A. The Boundary Integral Equation Method
LIU, P.L.F. for Porous Media Flow. George Allen
 and Unwin, England, 1982.
42. Manual Steel Designers' Manual. Constructional
 Steel Research and Development Organisation.
 Crosby, Lockwood, Staples, London.
 4th Edition, Metric.
43. BITNER-GREGERSON, E.M. Local Properties of Seawaves Derived From
GRAN, S. a Wave Record. Applied Ocean Research,
 Vol, 5 No. 4, 1983.
44. TIMOSHENKO S. Strength of Materials, Part II.
 Advanced Theory and Problems, 1976. Ed. Krieger.
45. Manual B.S.S.M. Strain Measurement Reference Book.
 British Society of Strain Measurement -
 Prepared by J. Pople, 1979.
46. ZAVERI, K. Measurements of Lowest Vibration Levels.
 Bruel & Kjaer, Tech. Rev. No. 1, 1970.
47. Technical Report Severn Tidal Power. Hydraulics Research
 Station, Oct. 1981.

48. Technical Report Severn Tidal Power. Hydraulics Research Station, Two-dimensional Water Movements Model. Report No. Ex. 985, 1981.
49. BASCO, D.R. Surfzone Currents. Coastal Engineering, 7, 1983.
50. LONGUET HIGGINS, M.S. On the Statistical Distribution of the Height of Sea Waves. J. Mar. Res. 11, No. 3, 1952.
51. HORIKAWA, K. Coastal Engineering - An Introduction to Ocean Engineering. University of Tokyo Press, 1978.
52. BRETSCHNEIDER, C.L. Wave Variability and Wave Spectra for Wind Generated Gravity Waves. U.S. Army Corps of Engineers, Beach Erosion Board, Tech. Memo No. 118, 1959.
53. HASSELMANN, K. On the Non-linear Energy Transfer in a Gravity Wave Spectrum. J. Fl. Mechanics, 15, (part 2 and part 3), 1963.
54. HOUMB, D.G. On the Statistical Properties of 115
OVERNIK, T. Records from the Norwegian Continental Shelf. Div. of Port and Ocean Engineering, The University of Trondheim, The Norwegian Inst. of Tech. 1977.
55. PIERSON, W.J. On the Motions of Ships in Confused Seas.
ST. DENIS, M. Trans. Sname, Vol. 61, 1953.
56. LONGUET HIGGINS, M.S. Observations of the Directional Spectrum
CARTWRIGHT, D.E. of Sea Waves Using the Motions of a
SMITH, N.D. Floating Buoy. Ocean Wave Spectra,
Prentice-Hall, Englewood Cliffs,
New Jersey, 1961.

57. IPPEN, A.T. Estuary and Coastline Hydrodynamics.
McGraw Hill Book Company, 1966.
58. RESIO, D.T. The Estimation of Wind-Wave Generation
In a Discrete Spectral Model.
J. of Phy. Ocean, Vol. II, 1980.
59. AHRENS, J.P. Wave Runup on Idealised Structures.
Coastal Structures, A.S.C.E. 1983.
60. THOMPSON, E.F. Prediction of Wave Height in Shallow Water.
VINCENT, C.L. Coastal Structures, A.S.C.E. 1983.
61. MYNETT, A.E. West Breakwater — Sines, Wave Climatology.
de VOOGT, W.J.P. Coastal Structures, A.S.C.E. 1983.
SCHMELTZ, E.J.
62. MITSUYASU, H. Directional Spectra of Ocean Waves in
Generation Area. Proc. of a Conf. on
Directional Wave Spectra Applications,
A.S.C.E. 1982.
63. MUSUDA, A. 1) On the Dispersion Relation of Random
KUO, Y.Y. Gravity Waves. Part I, Theoretical
MITSUYASU, H. Framework, J. Fluid Mech, 92, 1979.
2) Experimental Study on the Phase Velocity
of Wind Waves, Part 2, Ocean Waves.
Rep. Res. Inst. Appl. Mech. Kyushu Univer.
84, 1979.
64. LONGUET-HIGGINS, M.S. Radiation Stresses in Water Waves; A Physical
STEWART, R.W. Discussion With Applications. Deep Sea
Res, II, 1964.
65. SAND, S.E. Short and Long Wave Directional Spectra.
Proc. Conf. on Directional Wave Spectra
Applications. A.S.C.E. 1982.

66. ATKINS, (R & D). Dynamics of Marine Structures — Methods of Calculating the Dynamic Response of Fixed Structures Subject to Wave and Current Action. C.I.R.I.A. Underwater Engineering Group, Report UR 8, 2nd Ed.
67. ISAACSON, M. de St. Q. The Viscous Damping of Cnoidal Waves. J. Fluid Mech, 75, 1976.
68. SKOVGAARD, O.
PETERSEN, H.M. Refraction of Cnoidal Waves. Coastal Engineering, 1, 1977.
69. DUNSIGER, A.D.
COCHRANE, N.A.
VETTU, W.J. Seabed Characteristics From Broad Band Acoustic Echosounding With Scattering Models. I.E.E.E. Trans. of Ocean Eng. Vol. OE, 6, NO. 3, July 1981.
70. JOHNSTON, J.W. Engineering Aspects of Diffraction and Wave Refraction. Proc. A.S.C.E. 118, 1953.
71. GODA, Y.
SUZUKI, Y. Estimation of Incident and Reflected Waves in Random Wave Experiments. Proc. of the 15th Conf. on Coastal Engineering, A.S.C.E. 1976.
72. MANSARD, E.P.D
FUNKE, E.R. The Measurement of Incident and Reflected Spectra Using a Least Square Method. Proc. of the 17th Conf. on Coastal Eng. A.S.C.E. 1979.
73. AHRENS, J.P. Unpublished Irregular Wave Reflection Data. U.S. Army Corps of Engineers, Coastal Engineering Research Centre, Fort Belvoir, Va. 1980.

74. SEELIG, W.N. Wave Refraction from Coastal Structures.
Proc. of Coastal Structures, A.S.C.E. 1983.
75. FRANCIS, J.R.D. Fluid Mechanics for Engineering Students.
Edward Arnold, 4th Ed. Pub. 1979.
76. SEELIG, W.N. Estimation of Wave Reflection and Energy
AHRENS, J.P. Dissipation Coefficients for Beaches,
Revetments and Breakwaters.
U.S. Army, Corps of Engineers, Coastal Eng.
Research Centre, Fort Belvoir, Va. Feb. 1981.
77. WATNABE Instruction Manual For Multicorder Model
MC 6720 Series.
78. Manuals H.P. 7470A Plotter Manuals No.
90002 - Operator's Manual.
90001 - Interfacing and Program Manual.
79. Manual Gould OS 4200 Manual Part No. 450351
80. BENDAT, J.S. Random Data: Analysis and Measurement
PIERSOL, A.G. Procedures. Wiley, Interscience, 1971.
81. Technical Notes Hewlett-Packard, Part No. 06940 - 90010
82. Technical Notes Hewlett-Packard, Part No. 69336B - 90007
83. Technical Notes Hewlett-Packard, Part No. 69602 - 90001
84. Technical Notes Hewlett-Packard, Part No. 69422 - 90001
85. Technical Notes Hewlett-Packard, Part No. 5952 - 4076
Product Note 6940B-1, Scanning with the
6940B.

86. LYNN, P.A. An Introduction to the Analysis and Processing of Signals. The Macmillan Press Ltd. 2nd Edition, 1982.
87. Journal Recursive Digital Filters with Linear Phase Characteristics. Computer J. 15, 1973.
88. Technical Note Electronic Filter System EF3 Technical Handbook, No. 1842. Barr and Stroud, 1978.
89. OPPENHEIM, A.P.
SCHAFFER, R.W. Digital Signal Processing. Prentice-Hall, Englewood Cliffs, N.J. 1975.
90. BINGHAM, C.
GODFREY, M.D.
TUKEY, J.W. Modern Techniques of Power Spectrum Estimation. Trans. I.E.E.E. Audio and Electroacoustics, AV-15, June 1946.
91. WELCH, P.D. The Use of Fast Fourier Transform For the Estimation of Power Spectra: A Method Based on Time Averaging Over Short Modified Periodograms. I.E.E.E. Trans. on Audio and Electroacoustics, Vol. AU-15, 1967.
92. Manuals Hewlett-Packard Basic Operating Manual 9826 - 90000.
93. Manuals Hewlett-Packard Basic Interfacing Techniques 9826 90020
94. ROBINSON E.A. Physical Applications of Stationary Time Series. 1980. Charles Griffin and Co. Ltd.
95. BORGMAN, L.E.
CHAPPELEAR, J.E. The Use of Stokes-Struik Approximation for Waves of Finite Height. Proc. 6th Conf. on Coastal Engineering, Gainsville and Miami Beach, 1958.

96. TSUCHIYA, Y.
YAMAGUCHI, M. Some Considerations on Water Particle Velocities of Finite Amplitude Wave Theories. Coastal Engineering in Japan, Vol. 15, 1972.
97. SCHWARTZ, L.W.
VANDEN-BROECK, J.M. Numerical Solution of the Exact Equations For Capillary-Gravity Waves. J.F.M. Vol. 95, No. 1, 1979.
98. PEREGRINE, D.H. Equations for Water Waves and the Approximation Behind Them. In, Waves on Beaches and Resulting Sediment Transport. Ed. R.E. Meyer, Academic Press, New York, 1972.
99. PHILLIPS, O.M. The Dynamics of the Upper Ocean. Cambridge Univ. Press, 2nd Ed. 1977.
100. KINSMAN, B. Wind Waves. Prentice-Hall, Englewood Cliffs, N.J. 1965.
101. EBBESMEYER, C.C. Fifth Order Stokes Wave Profiles. J. Waterways, Harbours and Coastal Eng. A.S.C.E. Vol. 100, No. WW3, 1974.
102. STOKER, J.J. Water Waves. Interscience, New York, 1957.
103. WIEGEL, R.L.
MASCH, F.D. Cnoidal Waves: Tables of Functions. Berkeley Calif. The Engineering Foundation Council on Wave Research, 1961.
104. ABRAMOWITZ, M.
STEGUN, I.A. Handbook of Mathematical Functions. Dover, N. York, 1965.
105. MUNK, W.H. The Solitary Wave Theory and its Application to Surf Problems. Annals New York Acad. Sci. Vol 51, 1949.

106. DEAN, R.G. Stream Function Representation of Non-Linear Ocean Waves. J. Geophys. Res. Vol.70,1965.
107. WIEGEL, R.L. Oceanographical Engineering. Prentice-Hall, Fluid Mechanics Series, Englewood Cliffs, N.J. 1964.
108. BEAUCHAMP, K.G.
YUEN, C.K. Data Acquisition For Signal Analysis. George Allen and Unwin, London, 1980.
109. FORRISTALL, G.Z. Kinematics of Directionally Spread Waves. Proc. of the Conf. on Directional Wave Spectra Applications, Calif. A.S.C.E. 1981.
110. DRAPER, L. Derivation of a 'Design Wave' from Instrumental Measurements of Sea Waves. Proc. Inst. Civil Eng. Vol. 26, 1963.
111. MICHE, R. Movements Ondulatoires Des Mers En Profondeur Constante on Decroissante. Annals des Ponts et Chaussees, 1944.
112. IRRIBARREN, R.C.
NOGALES, C. Talud Limite Entre La Rotura Y La Reflexion de las Olas. Rev. Obras Publicas (Madrid), Feb. 1950.
113. MUNK, W.H.
WIMBUSH, M. A Rule of Thumb for Wave Breaking over Sloping Beaches. Oceans, 9, 1969.
114. CARRIER, G.F.
GREENSPAN, H.P. Water Waves of Finite Amplitude on a Sloping Beach. J. Fluid Mech. 4, 1957.
115. LONGUET-HIGGINS, M.S.
FENTON, J.D. On the Mass, Momentum, Energy and Circulation of a Solitary Wave, II. Proc. Roy. Soc. Set A, Vol. 340, 1974.

116. LONGUET-HIGGINS, M.S. Theory of the Almost High Wave: The
FOX, M.J.H. Inner Solution. J.F.M. Vol. 80, 1977.
117. HEDGES, T.S. Wave Breaking and Runup. Dept. of Civil
Eng. Univ. of Liverpool, March 1981.
118. HASSELMANN, D.E. Directional Wave Spectra Observed During
DUNCKEL, M. JONSWAP 1973. J. Phy. Oceanog. Vol.1,
EWING, J.A. No. 8, 1980.
119. Report Committee, I. Environmental Conditions.
Proc. 7th, Int. Ships Structures Congress,
Paris, Vol. 1, 1979.
120. Report Handbook on Wave Analysis and Forecasting.
Rep. 446, W.M.O. 1976.
121. BARBER, N.F. Finding the Direction of Travel of Sea Waves.
Nature, Dec. 4th Vol. 1, 1954.
122. PANIKER, N.N. Determination of Directional Spectra of
Ocean Waves From Gage Arrays. Tech.
Rep. Hel. 1-18, Univ. of Calif. Berkeley,
Aug. 1971.
123. MOBAREK, I.E. Directional Spectra of Laboratory Wind Waves.
J. of Waterways and Harbours Div. A.S.C.E.
Vol. 91, no. WW3, 1965.
124. FAN, S.S. Diffraction of Wind Waves. Tech. Rep.
Hel. 1-10, Hydraulic Eng. Lab. Univ. of
Calif. Berkeley, Oct. 1968.

125. MUNK, W.H.
MILLER, G.R.
SNODGRASS, F.E.
BARBER, N.F. Directional Recording of Swells From Distant Storms. Roy. Soc. of London Philos. Transactions, Series A, Vol. 2555, No. 1062, 1963.
126. KARLSSON, T. Refraction of Continuous Ocean Wave Spectra. J. of Waterways and Harbours Div. A.S.C.E. Vol. 95, No. WW4, 1969.
127. BREEDING, J.E. Group Velocity and Wave Refraction. Trans. American Geophys. Union, Vol. 50, No. 11, 1969.
128. HASSELMANN, K. On the Spectral Dissipation of Ocean Waves Due to White Capping. Hamburg Heft. 3, 1973.
129. BRETSCHNEIDER, H. Die Auswirkungen Von Oberflachen Kraften Im Wasserbaulichen Verjuchswesen Die Bautechnik. Heft 4, 1965.
130. FUHRBOTER, A. Airentainment and Energy Dissipation in Breakers. Proc. XIIth Coastal Eng. Cong. Washington, 1970.
131. LONGUET-HIGGINS, M.S. The Statistical Analysis of a Random Moving Surface. Phil. Trans. Roy. Soc. Set. A, Vol. 249, 1957.
132. BRETSCHNEIDER, C.L. Investigation of the Statistics of Wave Heights - Discussion. J. Waterways and Harbours Division, A.S.C.E. No. WW1, 1964.
133. BRETSCHNEIDER, C.L. Chapter 3, on Estuary and Coastline Hydrodynamics. Ed. A.T. Ippen, Pub. Mc Graw Hill, 1966.

134. HEDGES, T.S. Wave Forces on Rigid Vertical Walls.
Dept. of Civil Eng. Univ. of Liverpool,
Mar. 1981.
135. HAYASHI, T. Pressure of the Breaker Against a
HATTORI, M. Vertical Wall. Coastal Eng. in Japan,
Vol. 1, 1958.
136. VON KARMAN, Th. The Impact of Seaplane Floats During Landing.
Tech. Note No. 321, National Advisory
Committee for Aeronautics, Washington, 1929.
137. GIBSON, F.W. Measurement of the Effect of Air Bubbles
on the Speed of Sound in Water. J.
Acoustical Society of America. Vol. 48,
No. 5, 1970.
138. MINIKIN, R.R. Wind Waves and Maritime Structures.
Charles Griffin and Co. 1963.
139. NEGAI, K. Runs of Maxima of the Irregular Sea.
Coastal Eng. in Japan, Vol. 16, 1973.
140. KIRKGOZ, M.S. Shock Pressures of Breaking Waves on
Vertical Walls. J. of the Waterway, Port,
Coastal and Ocean Division, A.S.C.E. Vol.
108, No. WW1, 1982.
141. MILLER, R.L. Field Measurements of Impact Pressures
LEVERETTE, S. In Surf. Proc. 14th Coastal Eng. Conf.
O'SULLIVAN, J. A.S.C.E. 1974.
TOCHKO, J.
THERIAULT, K.

142. SARGEANT, H.L.
TIMME, R.C. Wave Heights Expressed in Engineering Terminology. Int. Symp. on Ocean Wave Measurement and Analysis, A.S.C.E. 1974.
143. LIN, Y.K. Probability Theory of Structural Dynamics. McGraw-Hill
144. THOMPSON, W.C. Period by the Wave Group Method. A.S.C.E. Proc. 13th Coastal Eng. Cong. Chap. 8, 1972.
145. PUTZ, R.R. Statistical Distribution for Ocean Waves. Amer. Geoph. Union, Trans. 33,5. 1952.
146. EWING, J.A. The Distribution of Wave Heights and Periods in Ocean Waves. Roy. Met. Soc. Quar. Jour. 80, 1973.
147. SMITH, R.C. Ocean Swell Groups from Wave Record Analysis. M.S. Thesis. Naval Postgraduate School, Monterey, Calif, 1974.
148. PIERSON, W.J.
NEWMANN, G.
JAMES, R.W. Practical Methods for Forecasting Ocean Waves. H.O. pub. 603, 284p. 1955.
149. DONELAN, M.
LONGUET-HIGGINS, M.S.
TURNER, J.S. Periodicity in Whitecaps. Nature 239, 1972.
150. LENNON, G.P.
LIU, P.L.F.
LIGGETT, J.A. Boundary Integral Solutions of Water Wave Problems. J. Hyd. Div. A.S.C.E. 108, (Hy. 8) 1982.

151. NAKAYAMA, T.
WASHIZU, U. Boundary Element Method Applied to the Analysis of Two-dimensional Non-linear Sloshing Problems. Int. J. Numerical Methods, Eng. 17(11), 1981.
152. STREET, R.L.
CAMFIELD, F.E. Observation and Experiments on Solitary Wave Deformation. Proc. 10th Conf. Coastal Eng. 1966.
153. HALL, J.V.
WATTS, G.M. Lab. Investigation of the Vertical Rise of Solitary Waves on Impermeable Slopes. U.S. Army Corps of Engineers, Beach Erosion Board, Tech. Memo No. 33, 1953.
154. LIU, P.L.F.
LIGGETT, J.A. Boundary Integral Equation Solutions for Solitary Wave Generation, Propagation, and Runup. Coastal Eng, 7, 1983.
155. LONGUET-HIGGINS, M.S. Mass Transport in the Boundary Layer at a Free Oscillating Surface. J. Fluid Mech. 8, 1960.
156. KJELDEN, S.P. Design Waves - for Laboratory Testing of Ship Models for Stability. Seminar on the Norwegian "Ships in Rough Seas" (SIS) project (Conf.) 1982.
157. GUNTHER, H.
ROSENTHAL, W. Hindcast of Seastate During MARSEN 79. Abstr. First Inst. Conf. Meteor. and Air/Sea Interaction of the Coastal Zone. Am. Meteorol. Soc. The Hague, 1982.
158. Manual Shore Protection Manual. U.S. Army Coastal Engineering Research Center. Dept. of Army Corps of Engineers. 1984.